TRACER STUDIES IN THE SOLID STATE

-

SELF-DIFFUSION IN AROMATIC SOLIDS

ProQuest LLC.
789 East Eisenhower Parkway
P.O. Box 1346
Ann Arbor, MI 48106 – 1346

Tracer Studies in the Solid State - Self-Diffusion in Aromatic Solids.

Thesis

submitted for the degree of

Doctor of Philosophy

of the

University of Glasgow

by

David James White, B.Sc.

October, 1965.

ABSTRACT

Naphthalene and Anthracene were purified and single crystals of the materials grown by the Bridgmann-Stockbarger method. Self-diffusion coefficients were measured by a tracer-sectioning technique in pure and doped single crystals of naphthalene, in polycrystalline naphthalene, and in monocrystals of anthracene. Additional measurements on monocrystals of naphthalene were made by a surface-decrease method. From the variation of diffusion coefficient with temperature the activation energies of diffusion and the Arrhenius pre-exponential factors were calculated.

Self-diffusion in both naphthalene and anthracene was found to be an extrinsic process, the diffusion coefficient at a particular temperature decreasing with increasing perfection of the crystal. Annealing was found to reduce the diffusion coefficient. For a particular grade of crystal, the diffusion coefficient, D, varied with absolute temperature, T, according to the Arrhenius relationship

$$D = D_o \exp(-E/RT),$$

where E is the activation energy for diffusion, D_o the pre-exponential or frequency factor, and R the Ideal Gas constant. For annealed single crystals of naphthalene E was found to be 34.9kcal. per mole, and D_o 2.8×10^{11} $cm^2.sec.^{-1}$ For highly pure, doubly annealed naphthalene crystals E was 42.7kcal. per mole, and D_o 2.5×10^{15} $cm^2.sec.^{-1}$ The Arrhenius parameters were also measured in other grades of crystal. D_o and E were smaller in doped crystals than in pure crystals. The Arrhenius parameters in polycrystals of naphthalene were measured.

Diffusion measurements in naphthalene were made perpendicular to the "ab" plane and parallel to the "a" and "b" axes of the crystal.

Diffusion anisotropy was not detected.

Measurements of diffusion perpendicular to the cleavage plane of anthracene gave $E = 60$kcal. per mole and $D_o = 5 \times 10^{16}$ cm.^{2}sec.$^{-1}$ The diffusion coefficient at a given temperature was found to decrease with increased perfection of the crystal.

The results are discussed with particular reference to the extrinsic nature of the diffusion process and to the high values of the Arrhenius parameters. Comparisons are made with previous measurements on molecular solids. It is suggested that diffusion in naphthalene and anthracene occurs by a co-operative mechanism involving disordered regions of the lattice.

This is one of the few studies in which diffusion in molecular solids has been measured by a direct means. It is the first in which the diffusion process is recognised as extrinsic.

ACKNOWLEDGEMENTS.

The author wishes to express his sincere gratitude to Dr. J.N. Sherwood without whose help and encouragement this work would not have been completed. His thanks are also due to Professors P.L. Pauson and M. Gordon for Laboratory facilities in the Chemistry Department of the University of Strathclyde, and to the Scientific Research Council for a maintenance grant. He is indebted to Miss Nora McKechan for typing the thesis and assisting with the diagrams. Finally, the author wishes to record his appreciation of the help and inspiration he received from his wife and family during the course of this work.

CONTENTS.

LIST OF FIGURES

PART I. - INTRODUCTION.

INTRODUCTION

Radioactive Tracer Studies on Solids.

Tracer studies in the solid state have been carried out on very many substances and have contributed greatly to our understanding of the structure of solids and the mechanisms of processes occuring in the solid state. One of the most rewarding techniques has been that of the direct observation of diffusion by measuring the penetration of an isotopically labelled solid into a matrix of the same, but unlabelled solid. Assuming that the labelled and unlabelled materials are identical, the information so obtained may be treated as information about a solid moving within itself, viz. self-diffusion. Many such studies have been carried out on metals, ionic solids, and valence solids, but very few indeed on molecular solids, and up until very recently there was only one published report of a direct study on an organic solid. This was by Sherwood and Thomson on Anthracene.[1] Very recently Labes and his co-workers have published another diffusion study on the same solid.[2] The work reported in this thesis was initiated to extend tracer studies further into this field in the hope of obtaining experimental results which would throw some light on the defect structure of organic solids.

The Defect Solid State and Diffusion.

Defects in solids are defined as irregularities in the otherwise regular, three-dimensional array of particles of which solids are ideally composed. Irregularities could occur in various ways, for example, a site in the array which ought to be occupied may, in fact, be vacant thus creating a "hole" in the lattice. On the other hand, a position which ought not to be filled, such as an interstitial position, may contain a particle. Vacant

sites and "interstitials" are known as "point defects" and are the well-known Schottky and Frenkel defects.[3] The simple picture becomes complicated[3] due to such phenomena as the interaction of point defects with each other or with foreign particles or with gross defects. The point defects may also be associated with electric charge or may distort the surrounding lattice. Other complications may also arise.

It is the existence of point defects which is believed to be responsible for bulk diffusion in solids. In the case of interstitials, the particle is envisaged as moving from one interstitial position to another, or as a particle on a lattice site moving into an interstitial position and the interstitial particle moving into the vacated site. In the case of vacancies, a particle on a neighbouring site moves into the vacancy filling the vacant site but creating a new vacancy in the position it has just left. Thus defects and particles move through the lattice giving rise to the phenomenon of diffusion. The defects through which diffusion occurs may be intrinsic to the solid under consideration or their presence may be due to a non-intrinsic property of the lattice such as the presence of impurities. Where both types of defect occur it is usually possible to distinguish between the intrinsic and the extrinsic regions of diffusion.

Diffusion has been postulated to occur by other mechanisms also, e.g. by the co-operative rotation of rings of particles (Zener's ring mechanism), or by the "crowdion" mechanism, or even by simple interchange between two neighbouring particles. The energy required for diffusion to occur is closely dependent on the mechanism by which it occurs.

As well as defects occuring at particular single positions in the lattice, faults associated with many lattice positions may arise.[3] Typical of such faults are edge and screw dislocations in which lattice sites are displaced with respect to each other in a line extending through many

lattice points. Such faults extend in one dimension and are called "line dislocations". In addition, surfaces - both external and internal - may be considered as two dimensional defects. It is believed that diffusion can occur down line dislocations and over surfaces far more rapidly than through the lattice. The activation energy for surface diffusion is generally less than that for dislocation diffusion, which in turn is less than the energy required for movement through the lattice.

Other Properties Associated with Defects.

The study of defects is of great importance for the understanding of the bulk properties of solids. The strengths of materials, their plastic flow, their brittleness, their conductivities, and many other properties are governed to a large extent by the defects present in the materials. The presence of defects should also have an effect on such properties as crystal density, thermal expansion, specific heat, elastic modulus, and so on, and all of these have received attention in the past with varying degrees of success. The metals, in particular, have been thoroughly investigated.

Conductivity in ionic solids must also be closely related to diffusion since the current is carried by the diffusing particles. In addition the requirement of overall electrical neutrality in the solid implies that the numbers of cationic and anionic defects are not independent. The experimental work[3] on ionic solids has been dominated by these facts. The controlled introduction of aliovalent ions in order to change the balance between cationic and anionic defects and so alter the electrical properties of the solid has been a powerful tool in the elucidation of the defect structure and its associated properties. This is closely bound up with the work on non-stoichiometric solids.

Compared with the joint studies of conductivity and diffusion in ionic solids and the application of the Nernst-Einstein equation which relates them, the study of diffusion as an adjunct to the study of solid state chemical

reactions is very much neglected. However, some workers[4,5] have made attempts to relate the kinetics of solid state reactions to the diffusion process with at least some success.

Until fairly recently few diffusion measurements had been made on valence crystals. However, with the great increase in interest in semiconductors arising out of the commercial exploitation of the transistor a great number of diffusion and conductivity studies[6] have been carried out on semiconducting solids, particularly germanium and doped germenium. The p- or n- nature of a semiconductor may be altered at will by the controlled introduction of aliovalent impurities and the diffusion process has been used to introduce such impurities. The measurement of diffusion coefficients has led to a greater understanding, not only of inorganic semiconductors, but of all solids and the processes occuring within them.

Since very few diffusion studies have been made on molecular solids it is not surprising that the relationships between diffusion and other properties have not been developed very far. However the conductivity of organic solids has arroused considerable interest[7,8] and reference has been made to diffusion in some conductivity papers.[8] The importance of these solids as scintillators is an obvious source of interest. Photo-conductivity, dark conductivity, and semiconductivity have all been measured.[7] The semiconducting properties are likely to receive increasir attention in the future.

The polymerisation[9] of organic substances in the solid state is an interesting development into which an understanding of diffusion in molecular solids gives additional insight. A joint study of lattice and dislocation diffusion in a polymerisable solid would undoubtedly contribute a great deal to our understanding of organic solids.

The great variety of shapes and sizes formed in organic substances makes them very much different from metals, salts or valence solids

in which the particles may be considered as spheres at least to a first approximation. Organic molecules are seldom spherical. The forces holding organic solids together are those usually called van der Waals forces. The name conceals a great variety of forces about which we know little but which are weak and non-directional. The consequences of these two facts - that organic molecules come in all shapes and sizes and are held together by weak, non-directional forces - have been investigated by many workers, notably by Kitaigorodskii[10] and his school. The consequences are far-reaching. Kitaigorodskii considers that the structure of these solids is controlled almost exclusively by the rule of closest packing, i.e. that the molecular shapes pack into that structure which gives the maximum density, the "bumps" in one molecule fitting into the "hollows" in its neighbours. The "co-ordination number" of a molecule in such a structure is found by geometry to be almost always twelve, i.e. each molecule is in contact with twelve neighbours: six of these neighbours are coplanar with the molecule under consideration. The crystalline structure and density of organic solids is, therefore, according to Kitaigorodskii, predictable from molecular shape alone. The theory has been extended[11] to cover impurities in organic solids with interesting conclusions about the sub-structure of organic solid solutions.

It would be a most remarkable fact if the peculiar structure of organic solids were not reflected in their defect structure and in diffusion studies on the solids. As a corollary it would be expected that an increased understanding of diffusion will give an increased understanding of the organic crystalline state.

The low symmetry of organic structures may give rise to diffusion anisotropy. Such anisotropy has been found in a few non-molecular substances. Conductivity anisotropy has been reported[12] in organic

solids and is expected from theoretical considerations.[12] Labes has reported slight diffusion anisotropy in anthracene.

The Measurement of Diffusion.

The earliest measurements of diffusion were made by diffusing one substance into another and measuring the depth of penetration in a given time at a known temperature. Roberts-Austen's measurements[12] of the diffusion of gold into lead is a classic example. The method is still one of the best for measuring interdiffusion but is, of course, not applicable to self-diffusion.

In self-diffusion the movement of a substance within itself is being studied, and hence direct measurements are strictly impossible. However making the approximation that different isotopes of the same substance are physically and chemically indistinguishable, the interdiffusion of isotopic varieties may be interpreted as self-diffusion, and hence self-diffusion may be measured directly. Isotopic species are, of course, not identical and isotope effects have been reported in diffusion studies.[13] Nevertheless, as long as the ratio of the masses of the interdiffusing isotopic species is close to unity and given that the isotope effect is within the accuracy of diffusion measurements (as it usually is) it would be pedantic at this stage in our knowledge of diffusion to distinguish between self-diffusion and isotope interdiffusion for the vast majority of cases. Therefore, in most studies, including the one reported in this thesis, the tracer technique may be taken as a direct measurement of self-diffusion.

One of the advantages of a direct method is that there is no ambiguity about what is being measured. In the tracer-sectioning technique[14] the concentration of a labelled species is measured at a known penetration after a known time. Thus a penetration profile may be built up. Ambiguity arises only after this point when the profile has to be interprete

either mathematically or in the light of some theory. In indirect methods, such as N.M.R. measurements, uncertainty about interpretation arises much earlier. Hence, despite the many advantages an indirect study may have, a direct study by the tracer-sectioning technique is intrinsically more certain. This was the chief reason for the adoption of the tracer-sectioning method as the principle technique used in this thesis. The method also has the very great advantage that it can detect the simultaneous occurance of more than one transport process. This was done in the case of anthracene.[1,2]

Autoradiography[14] is another direct method capable of detecting concurrent processes. In this method a radioactively labelled material is allowed to diffuse into an unlabelled specimen and the specimen is then cut in some appropriate way to reveal the depth of penetration of the tracer when put in contact with photographic paper. The method has been used on a great many metallic and inorganic solids.

If a radioactive material is deposited on the surface of a solid and diffuses into it, then the activity as measured at the surface should decrease. From a knowledge of the rate of decrease of surface activity and the absorption coefficient of the solid for the emitted rays, information can be gained about diffusion into the solid. The method has been used widely ever since Steigman, Shockley, and Nix[15] used it to measure self-diffusion in copper. The technique is used in this thesis as a check on the tracer-sectioning method.

The decrease in activity of a radioactive vapour or gas in contact with a solid may also give information about solid state diffusion.[16,17] Alternatively, the increase in activity of an initially inactive vapour or gas when in contact with an active solid may be used.[18] The solid may be in contact with its own vapour (e.g. solid cyclohexane with cyclohexane vapour)[17] or with some other gas (e.g. solid sodium chloride with

chlorine gas[10]). The isotopic composition of the vapour phase changes due to exchange at the surface of the solid followed by diffusion of the exchanged particles into the solid. The method can be used to measure very low diffusion coefficients.[18]

Of the methods used to measure diffusion without utilising isotopes, the most important is the nuclear magnetic resonance technique.[19,20] A simplified picture of how diffusion affects the width of the nuclear magnetic resonance line is the following[19,21]. The local magnetic field at the site of each atomic nucleus is acted upon by the field of neighbouring nuclei. The interactions are both intra- and inter-molecular. If there is no motion in the solid the fields will be static and will differ from one nucleus to another depending on position. A broad resonance line will result. If there is motion in the solid the magnetic fields will be averaged out and the N.M.R. line-width will narrow. Thus, if the width of a resonance line is measured as a function of temperature and the width narrows at a particular temperature this may be taken as indicative of the onset of motion at that temperature. The motion need not be translational; rotational motion will also result in narrowing of the line. If the molecule undergoes completely free rotation that part of the local magnetic field due to intramolecular interactions will average out to zero and the residual line width will, therefore, be due to intermolecular interactions. If at a higher temperature the line-width should narrow further, it would have to be concluded that this intermolecular interaction was averaging out. This could occur only if motions approximating to the intermolecular distance were taking place. Such motions would constitute diffusion through the lattice.

The N.M.R. technique has been used to detect diffusion and to measure its energy of activation in many substances, in organic solids[22,23] notably by Andrew.[19] The results obtained sometimes agree with

those obtained by other methods, sometimes they do not.[19,24,25] The method is undoubtedly a very powerful one but the discrepancies between it and other methods require an explanation.

An interesting technique to detect diffusion has been used in the case of solid benzene[26] and other materials.[27] It is to create and trap free radicals in the solid by irradiation at reduced temperatures. When the temperature is raised to a value at which diffusion can occur the radicals move through the lattice and anihilate each other, the decrease in concentration of the radicals being measured by an electron spin resonance (E.S.R.) method.

Other even less direct methods of measuring diffusion are possible. For example, the rate of annealing out of quenched-in defects[28] or irradiation-induced defects[29] can be measured. Many properties may be used as a measure of the rate of annealing out e.g. conductivity or hardness[29] measurements. Such methods have been used on metals and interpreted in terms of diffusion. Spectroscopic methods have been used[30] to measure interdiffusion.

Once a set of diffusion results is obtained, whether it be a diffusion profile or some other less direct measurement, it must be interpreted in a meaningful way. This usually takes the form of a mathematical treatment of the experimental figures to give the diffusion coefficient of the system under study. The variation of the diffusion coefficient with temperature is also of interest since from it can be deduced the activation energy and other parameters of the diffusion process.

The Mathematical Treatment of Diffusion.

The mathematics of diffusion were first treated by Fick.[14,31] For the uni-dimensional case, diffusion along the x direction may be considered as occurring because of the existence along that axis of a concentration gradient dc/dx. Hence the quantity of diffusing substance

passing in unit time through any given unit plane at right angles to the diffusion direction is proportional to dc/dx. This quantity, J, is called the flux. Putting in a proportionality constant, D, we may write

$$J = -D \frac{dc}{dx}, \qquad \text{Eqn.1.1}$$

which is Fick's first equation and defines the diffusion coefficient, D. The negative sign arises because diffusion occurs down the gradient and not up it. More correctly the driving force is the gradient of chemical potential, but in the case of self-diffusion the concentration (c) gradient may be used, or it may be used to a first approximation in other cases.

The flux through a second plane a distance dx from the first is J + dJ/dx, where dJ/dx is the rate of change of flux along the x direction. From equation 1.1 we obtain the second flux:

$$J + \frac{dJ}{dx} = -D\frac{dc}{dx} - D \frac{d^2c}{dx^2}, \qquad \text{Eqn.1.2}$$

assuming D is invariant. The quantity of material accumulating in unit time between the two planes dx apart is the difference between these fluxes (i.e. material remaining between the planes equals the material entering the first plane minus the material leaving the second plane). Hence the rate of accumulation dc/dt is given by equation 1.2 minus equation 1.1 viz.

$$\frac{dc}{dt} = \frac{-dJ}{dx},$$

or

$$\frac{dc}{dt} = D\frac{d^2c}{dx^2} \qquad \text{Eqn.1.3}$$

where t refers to time and D is constant. All the above differentials are partial. Equation 1.3 is Fick's second equation. The assumption of constant D is true for self-diffusion but not necessarily otherwise.

Since it is concentration which is measured it is necessary to make equation 1.3 explicit in C. However, there is no general solution of

Fick's second equation, the solution depending on the boundary conditions chosen. It has, however, been solved[31,32,33] for all important experimental boundary conditions. A discussion of the final choice of solution will be left until after the experimental procedure has been described. The units of D are cm^2 per sec.

Deviations from Fick's laws are reported from time to time.[1,34-36] These are detected when the diffusion profile fails to give a linear plot when treated in the way which seems appropriate to the system under study. The most frequently reported deviations consist of either a plot which gives two linear portions instead of one, or a plot which shows an upward hook at small penetrations in an otherwise linear profile. Anthracene[1] exhibited both anomalies.

Where a doubly linear plot is obtained the investigators have postulated that two processes are occurring simultaneously[1]. When treated separately both diffusion processes obey Fick's laws. In Anthracene one of the processes was very rapid and the authors suggested that it was due to rapid diffusion down dislocation pipes or along block walls in the crystal. This interpretation has received strong support from other diffusion studies and also from conductivity work[2]. However, the energy of the process has never been measured and conclusive evidence is lacking.

The occurrence of an anomalous upward hook is frequently reported[1,3] but has received no satisfactory explanation. In the case of Anthracene it was only the first point in the profile which was high, but in other cases the depth affected by the hook is considerable.[36] Workers have ignored the hook and treated the remainder of the profile as being due to the diffusion process, with satisfactory results. However, some doubts remain, and it has been suggested[37] that the existence of the hook contravenes the boundary conditions of the mathematical analysis and so leads to erroneous values of the diffusion coefficient. A method for

"correcting" for the presence of an initial upward hook has been suggested.[37] One proposed[38] cause of the hook is that diffusion in the near-surface layer differs from diffusion in the bulk.

The use of polycrystalline specimens is a frequent source of anomalous behaviour[39,40] so that diffusion measurements are best carried out on single crystals.

Diffusion is an activated rate process, and like other such activated processes it would be expected to be a function of temperature and to conform to a simple Arrhenius-type of relationship. This is generally found to be the case.[31,33] The Arrhenius equation for diffusion is usually written in the form

$$D = D_o \exp\left(\frac{-E}{RT}\right), \qquad \text{Eqn. 1.4}$$

where D is the diffusion coefficient at T°K., R is the Ideal Gas constant, and E is the activation energy for diffusion. The pre-exponential factor, D_o is also called the frequency factor. The values of E and D_o are characteristic of a given system and are intimately connected with the mechanism of diffusion.

Taking logarithms to the base 10 of equation 1.4 gives

$$\log D = -\frac{E}{2.303RT} + \log D_o , \qquad \text{Eqn. 1.5}$$

hence a plot of log D against 1/T should be a straight line of slope $-E/2.303R$ and intercept $\log D_o$. Hence the parameters E and D_o can be found by measuring D as a function of temperature.

The activation energy, E, for diffusion is an important property of the solid since it is dependent on the mechanism of diffusion. For example, in the intrinsic vacancy diffusion process E should be related to the sum of the energy for the creation of a vacancy and the energy to move a neighbouring particle into the vacancy.[41] This rather simplified picture has been developed by many workers, notably by Rice and his co-workers[42,43]

who have developed a dynamical theory of diffusion closely related to the activated state theory but which makes explicit allowance for most processes likely to contribute to the activation energy. Processes likely to contribute include the enthalpy of formation of a vacancy, the translational energy of the diffusing particle, the energy required to move aside any particle hindering the translation, and energy changes required for readjustments to the surrounding lattice. It would be possible to add other terms or to break down those terms further, but in our present state of knowledge this does not appear justified.[43] Estimates[42] of the relative importance of the contributing terms have been made for a simple model, but the conclusions reached are unlikely to be applicable to organic solids.

Zener, Le Claire,[44] and others have made theoretical calculations of the values expected for the activation energy for various mechanisms. Comparison of the experimental value with the calculated values allows in principle a choice to be made between the various postulated mechanisms. Unfortunately, a clear-cut choice cannot always be made. Theoretical calculations of E in inert gas solids have been made[43,46] and agree reasonably well with experiment.[47]

Various empirical relationships[47] have been found between E and other physical constants. For example, the relationship

$$E = 35\ T_m, \qquad \text{Eqn. 1.6}$$

where T_m is the melting-point, has been found to hold quite well for face-centred cubic (f.c.c.) metals, but not for other metals. The relationship

$$E = 16.5\ L_f, \qquad \text{Eqn. 1.7}$$

where L_f is the latent heat of fusion, holds for f.c.c. and body-centred cubic (b.c.c.) metals, and also for phosphorus which is a molecular crystal.

It is often found that the activation energy for diffusion is approximately equal to the latent heat of sublimation (or to the lattice energy[31]). In indirect studies on molecular crystals this has been found to hold for some solids, including cyclohexane[19] and phosphorus[40]. However, although the tracer-sectioning and N.M.R. results on phosphorus[39,40] agree reasonably well, the results on cyclohexane do not. The tracer-sectioning results[24] on cyclohexane give E as twice the latent heat of sublimation (L_s). The activation energy was also found to be approximately twice L_s for Anthracene[1], Argon[48], Xenon[49], and hydrogen[25]. (Although Lobes[2] found E to be approximately equal to L_s in his study of Anthracene.) Clearly, further experiments are required to resolve this position and to explain the discrepancies between the tracer-sectioning results and the N.M.R. results.

The Arrhenius pre-exponential factor, D_o, has received theoretical treatment also[31,44] but is somewhat less amenable to treatment[47] than E. However, it can be shown[50] from rate theory that the diffusion coefficient should be given by

$$D = a^2 \gamma \nu \exp\left(\frac{-\Delta G}{RT}\right), \qquad \text{Eqn. 1.8}$$

where a is the unit cell dimension or jump distance, ν is the jump frequency (i.e. the number of times per second the particle attempts to surmount the potential barrier between lattice sites), and ΔG is the isothermal work required for the formation of a vacancy plus that required to move the particle to the top of its potential barrier. Substituting

$$\Delta G = \Delta H - T\Delta S$$

and equating ΔH with the Arrhenius activation energy, E, we obtain

$$D = \gamma a^2 \nu \exp\left(\frac{\Delta S}{R}\right) \exp\left(\frac{-E}{RT}\right) \qquad \text{Eqn. 1.9}$$

from which comparison with the Arrhenius equation (1.4) gives

$$D_o = \gamma a^2 \nu \exp\left(\frac{\Delta S}{R}\right) \qquad \text{Eqn. 1.10}$$

A similar equation may be deduced from probability considerations[50]. More sophisticated treatments are also available[6,42]. In any case, the numerical value of D_o is a sensitive function of the entropy of activation, S.

In principle it is possible to compare the experimental value of the entropy of activation as found from equation 1.10 with that calculated from possible diffusion mechanisms[47]. In practice the entropy would not be expected to deviate very far from the entropy of melting and D_o would not be expected to differ from unity by more than one, or perhaps two orders of magnitude. These expectations are usually borne out in practice[31].

However, there are more than a few cases[31] where D_o differs from unity by many powers of ten, in some cases to give an extremely small value of D_o and in others to give very large values of D_o. Anthracene and cyclohexane[24] fall into the latter category and give D_o equal to 6.5×10^{10} and 6.3×10^{6} respectively, which from equation 1.10 give entropies of activation equal to about six times the entropy of melting in the case of anthracene and nineteen times the entropy of melting in the case of cyclohexane.

Theory is not adequate to explain these high values but it has been suggested that a high entropy factor and a high D_o could arise due to pre-melting effects[1;39] or to large-scale loosening of the lattice round vacancies[1]. High pre-exponential factors have also been reported in phosphorus[39] and sulphur[51]. The experimental values of D_o found in inert gas solids[48,49] are several orders of magnitude larger than expected from theory[45-47]. It would be of interest to see if high frequency factors are a feature of diffusion in molecular solids.

It is seen, therefore, that the Arrhenius parameters, E and D_o, found in anthracene and cyclohexane do not fit very well into current theories. This is not really surprising since organic solids differ so much from the spherical solids treated in most diffusion theories.

Despite the almost universal applicability of the Arrhenius equation to diffusion processes there are some reported results where it is claimed that diffusion is "non-Arrhenius", i.e. does not satisfy a simple Arrhenius equation. In these cases the plot of equation 1.5 does not yield a straight line. As in other rate processes[52] the non-Arrhenius behaviour could be due either to the activation energy being a function of temperature or to the frequency factor being a function of temperature. In fact, however, only a very few cases[53,54] are attributed to these. The majority of cases where a simple Arrhenius equation is not satisfied are explained as being caused by the existence of two diffusion processes, one predominant at lower temperatures and the other at higher temperatures.[39,51] These can usually be resolved and are found separately to obey Arrhenius relations.

Thus, the mathematical treatment of diffusion results allows the diffusion coefficient, D, to be measured, and from its variation with temperature the Arrhenius parameters, E and D_o, can be calculated. From these an insight into the mechanism of diffusion may be obtained. The results obtained from the few molecular solids so far studied leave many questions unanswered.

Scope of the Present Work.

The results obtained on organic solids by previous workers indicates that both the activation energies for diffusion and the frequency factors are higher than anticipated. In addition, a secondary diffusion process was found in anthracene. Further data are required to confirm or deny these findings.

The best hope of increasing our understanding of these problems appeared to lie in an investigation of diffusion in aromatic hydrocarbons. Not only have the structures of hydrocarbons been investigated thoroughly

but many conductivity measurements and other studies have been carried out on them. In addition aromatic hydrocarbons are readily available. No complications, such as hydrogen bonding, arise.

It was decided, therefore, to attempt to measure diffusion in solid aromatic hydrocarbons - naphthalene in particular - using tracer techniques. Diffusion anisotropy would also be looked for. Before the diffusion studies proper could be carried out, a procedure had to be devised for growing single crystals of the pure material and also of the doped material, since diffusion studies on doped crystals may throw some light on the secondary process attributed in anthracene to rapid movement down dislocations. The growth of single crystals requires methods of obtaining the materials in very high purity.

Thus, the work of this project was, firstly, to obtain hydrocarbons in a state of high purity; secondly to grow large, single crystals of the material; and thirdly, to carry out diffusion studies on the material. This work and other subsidiary studies are the subject matter of this thesis.

PART II. - EXPERIMENTAL

A. Purification of Materials

B. Crystal Growth

C. Measurement of Diffusion Coefficients.

A. PURIFICATION OF MATERIALS

(i) Introduction.

Purification of materials is one of the oldest problems in chemistry. It takes on an added importance in the solid state since the presence of even small amounts of impurities is known to affect solid properties; thus, the presence of even a few parts per million of impurity can affect profoundly the semiconducting properties of germanium, and even one part per million of impurity may influence the spectrum of organic crystals.[55]

In diffusion studies, also, the presence of impurities is known to have a profound affect. The best known examples are in the alterations additives produce in the extrinsic region of diffusion of very many substances.[33] The intrinsic region of diffusion may also be affected.[14,56] If the fast diffusion process found in anthracene[1] and other materials[57,58] is, indeed, due to the presence of dislocations or block walls, then impurities should have an effect on that process.

In growing single crystals, the purity of the starting materials has an affect on the quality of crystals produced. It is not possible, in the great majority of cases, to incorporate large proportions of foreign molecules or ions into a crystal lattice.[59,60] Even with small amounts of impurity in the melt crystal growth becomes difficult.[59]

When an impurity is incorporated into a crystal it may be present either at a lattice site, or an interstitial site, or it may be in a site adjacent to a line defect or a block wall.[8,11,61] It may be precipitated along dislocations or in block walls. The presence of impurities may increase both the number of dislocations in a crystal and the number of sub-boundaries in the solid. All these possibilities will affect the growth

properties of the crystal and may have an effect on its diffusion properties.

There are many techniques available for purifying substances.[62-64] Some, like distillation, are very old; others, like chromatography and zone-refining, have been developed much more recently. The techniques used in this work were crystallisation, sublimation, distillation, and zone-refining. The latter method was the chief one used and will be described in detail; crystallisation, sublimation and distillation are old established processes requiring little explanation here, and will be described briefly in the experimental details.

In zone-refining, a molten zone of material is passed repeatedly down a rod of the same substance. The impurities in the solid move with the molten zone and so become concentrated at the bottom of the rod. A few impurities move in the reverse direction and so collect at the top. The result is that the bulk of the material is purified.

The method is similar to fractional crystallisation from the melt.[65] It can be applied to any substance which can be melted without decomposition and in which the impurities have different solubilities in the liquid and solid phases.[65] It can give substances of exceptionally high purity.

Zone-refining[66] has been applied to metals, other inorganic substances, semiconductors, and more recently to organic substances.[62,67,68]

Consider a solid in equilibrium with its melt. If c_s is the concentration of a given impurity in the solid phase and c_l the concentration in the liquid phase, then the equilibrium distribution coefficient, k_o, is defined by

$$k_o = \frac{c_s}{c_l}$$

The solubility in the liquid is usually greater than that in the solid and so k_o is less than unity and the impurity tends to be rejected by the solid. If k_o is greater than 1, the impurity will tend to accumulate in the solid.

In practice equilibrium conditions are not achieved, in which case the effective distribution coefficient, k, is used. A relationship between k and k_o has been derived by Burton, Prim and Slichter.[69]

When a molten zone passes down a solid bar the leading edge of the zone is continuously melting material into the zone, whereas the retreating edge is continuously solidifying, i.e. crystallising material out from the melt. If k is less then 1, the material crystallising out will contain less impurity than the melt. When the molten zone reaches the bottom of the bar and heating is stopped, the zone at the bottom of the bar will solidify and will contain a higher concentration of impurities than the rest of the rod.

If instead of switching off at the bottom of the bar, the heater is returned quickly to the top of the bar (so quickly that it melts no material while moving upwards) and then moves slowly down the bar again causing another molten zone to traverse the bar, further purification of the bar will result and more impurities will collect in the final zone at the bottom. By repeating this process many times very high purities can be obtained.

In practice more than one heater can be used so that several molten zones can be passed simultaneously. There must always be solid material between the zones.

Attempts[67] have been made to zone-refine organic compounds in horizontal tubes. However, it was found that the melt flowed back through fissures in the solid contaminating the purified material. For the same reason passing the molten zone upwards is not satisfactory. Refining speeds of 10 to 50 mm. per hour have been recommended[67,70] for organic substances, and designs for automatic refiners have been published.[67,71,72]

The requirement for the present work was for highly pure

naphthalene and anthracene for crystal growth. It was decided to build an automatic zone-refiner which would be of general use in the laboratory and which would be capable of purifying up to kilogram quantities of material. The apparatus which was built is a modification of a reported refiner,[67] the new features being that it operates with one motor only (instead of two) and incorporates an automatic clutch and rapid return by means of a counter-poise. It is described in the following section.

(ii) The Zone-Refining Apparatus.

The apparatus consists essentially of a heater which surrounds a tube containing a cast rod of the material being refined. The heater melts a narrow band of the material and moves slowly down the rod, material melting into the molten zone at the bottom (leading) edge of the heater and crystallising out at the top (retreating) edge. When the heater reaches the bottom of the rod it returns quickly to the top and another, slow, downward traverse is made. This process is repeated as often as desired.

More than one heater may be used in the apparatus. In this case several molten zones traverse the rod simultaneously. The return mechanism is adjusted so that a reciprocating motion is obtained. By this reciprocating mechanism the speed of zone-refining is increased two, three, etc. times depending on whether two or three, etc. heaters are used.

The limit to the number of heaters is reached when a solid band cannot be maintained satisfactorily between the molten zones.

The heaters consist of nichrome resistance tape wound on glass formers. The formers are made of short (about 1½ to 2 in.) lengths of glass tubing of internal diameter just large enough to allow the heater to move easily over the tube containing the material for refining. The nichrome tape is wound to give a heating band 1 cm. long and with a resistance of about 60 ohms. The temperature is controlled by a

2 amp. "variac". Where more than one heater is used the heaters are connected in series.

One of the problems encountered was keeping the molten zones small. As the heater moved down the tube the zone lengthened to an unacceptable size. It was attempted to overcome this by winding a cooling coil round the tube just above the heater, the coil moving in company with it. The coil was initially cooled with water but this was found not to be completely satisfactory. The water coil was replaced by a copper coil perforated on the inside edge. Compressed air was blown through the perforated tube giving very satisfactory cooling and reducing the zone size to one inch or less.

When the heater with its attached cooling coil reaches the end of its traverse a stop attached to the lowering cord activates a microswitch which decouples the lowering mechanism from the heater. The heater is counterpoised by means of a weight which, when the heater is decoupled, falls under gravity rotating the cord and restoring the heater to the starting position. When it has fallen the correct distance the counterpoise activates a second microswitch which re-couples the heaters to the lowering mechanism. This cycle repeats itself automatically as long as the apparatus is switched on.

A diagram of the de-coupling mechanism and the circuit of the apparatus is shown in Fig.2.1.1. The cord carrying the heaters and the counterpoise passes round the pulley which is driven, via the drive shaft and clutch head shown, by a "Parvalux" motor (1 r.p.m. geared down to 1 r.p.h.) The drive speed is controlled by a "Simmerstat" switch. At the end of a traverse, microswitch N.O. operates de-clutching the drive and allowing the heaters to return to the "start" position when microswitch N.C. opens cutting the current to the solenoid and so re-clutching the drive and starting another traverse. The numbering in

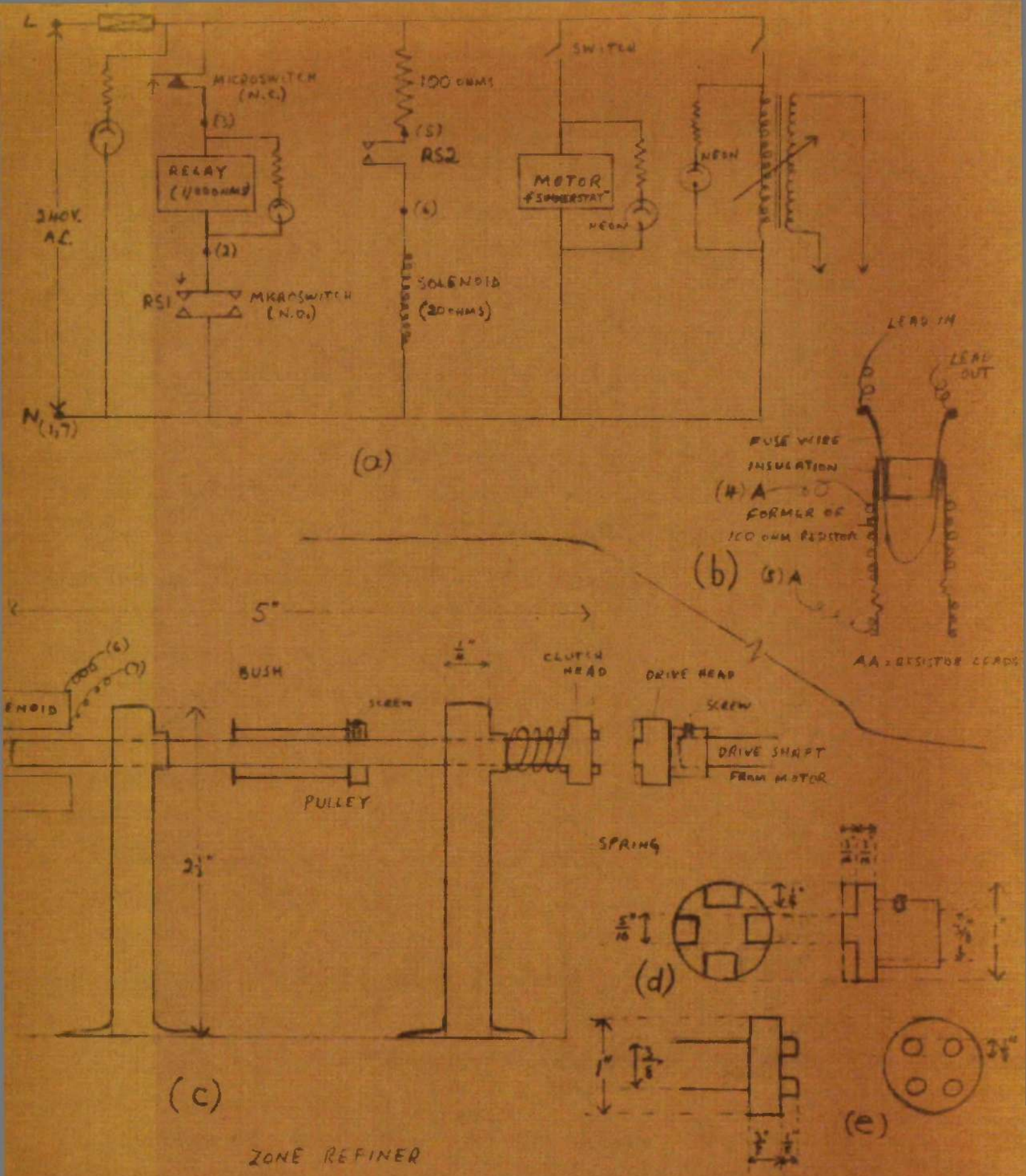

ZONE REFINER

(a) Circuit ; (b) Detail of fuse

(c) Clutch ; (d) Detail of drive head ; (e) Detail of clutch head

Fig. 2.1.1: Circuit and Clutch for Zone-Refiner.

the sketch refers to the wiring positions in the junction blocks and are numbered correspondingly in the apparatus itself.

Fig. 2.1.1 (b) shows a fuse built into the apparatus to prevent damage to the solenoid and clutch if the heaters or clutch should stick or otherwise fail to return to the starting position and so fail to deactivate the solenoid. If it fails to be deactivated the solenoid burns out. To prevent this the input to the apparatus passes through a loop of fuse-wire inserted into the glass former of the 100 ohm resistor in the solenoid circuit. If the solenoid fails to turn off after about 30 secs. of activation the 100 ohm resistor heats up, melts the fuse-wire and so cuts the input to the whole apparatus. This safety device was found to be very effective.

The apparatus described has been used to zone-refine up to kilogram quantities of naphthalene, benzoic acid, and camphene. In these cases two heaters were used. Anthracene has also been refined but in smaller quantities and using only one heater.

(iii) Purification of Naphthalene.

Naphthalene (molecular weight grade B.D.H., Ltd.) was packed into the zone-refining tube and melted by heating the tube. The tube was packed until full when the naphthalene was molten, the material was allowed to solidify and more naphthalene added to fill the space left due to the contraction on solidification.

The packed tube was mounted on the zone-refiner and two heaters and cooling coils fitted into place. The current to the heaters was switched on and adjusted to as low a value as practicable while maintaining the zones molten. The drive was then switched on and the material left until zone-refined.

Naphthalene, anthracene, and other organic substances have large expansivities and also expand greatly on melting. This leads to stresses

being set up inside the zone-refining tubes in the region of the molten zone with the consequent risk of the tubes cracking or even shattering explosively if the stresses are very large. A considerable amount of trouble was caused by this. If ordinary glass tubes (20-25 mm. bore) were used for zone-refining shattering of the tube always occurred. Even with thick (2 mm.) walled glass tubing shattering sometimes occurred. Nevertheless, with care (and luck) naphthalene could be zone-refined in thick-walled glass tubing and one lot was successfully refined using glass tubing with 24 mm. bore and 2 mm. thick walls.

Risk of breakage appeared to decrease if the bottom of the zone-refining tube was left open. One lot of naphthalene was successfully refined in an open tube, the stresses in the tube being at least partially relieved by extrusion of several inches of solid out of the bottom of the tube during the zone-refining. However, the method was not full-proof and breakages still occurred.

The open tube mthod suggested that if refining were carried out in a tube treated to prevent the solid adhering to the walls, most of the stresses inside the tube would be relieved by movement of the solid up the tube. Siliconising of the walls seemed a promising method of preventing adhesion to the glass. However, despite siliconising the glass with trimethylchlorosilane the refining tubes continued to shatter and glass was abandoned as a material in which to zone-refine large amounts of naphthalene. Exactly the same problem was found with benzoic acid.[73] Camphene, however, zone-refined satisfactorily in wide-bore glass tubes.[74] This is probably because camphene is a plastic crystal[26] and takes up stress readily by plastic deformation. Naphthalene, anthracene, and benzoic acid can be zone-refined safely in thick walled glass tubing of about half inch bore.

Naphthalene was refined successfully in a copper tube of one inch

bore. The tube was cleaned with dilute nitric acid, water, and acetone before packing with naphthalene. The zone-refined material was slightly contaminated with copper but on greaseless distillation into the crystal growth vessel (see section II B of this thesis) gave beautiful white material which gave excellent single crystals. It was felt, however, that this was still not quite satisfactory. Eventually a "teflon" tube (one inch bore) was used for zone-refining. This was perfectly satisfactory as long as the temperature of the heater was kept low.

(iv) Purification of Anthracene.

Anthracene obtained commercially, even so-called "Reagent Grade" anthracene, is very impure. Zone-refining of this material without initial purification seemed unpromising. It was decided, therefore, to carry out an initial purification by sublimation in vacuo.

A further complication arises in that anthracene is easily oxidised and so could not be melted in the presence of air and could not be zone-refined in an unsealed tube. It was decided to refine anthracene in thick-walled glass tubing and reduce the risk of shattering by using smaller amounts of anthracene and narrower tubes with only one heater on the refiner.

To achieve this, and to prevent the anthracene being exposed to the air from the beginning of the sublimation to completion of single crystal growth it was decided to sublime, zone-refine, and fill the crystal growing vessel in one closed piece of apparatus.

The purification apparatus is shown in Fig. 2.1.2. It is made entirely of glass and consists of three glass sausages, A, B, and C, a crystal growing vessel E, and a zone-refining tube, D. The latter is made of $\frac{1}{2}$ inch bore G.V.F. glass piping. ~~Almost~~ About 150g. blue-fluorescent anthracene was placed in A via tube F, tube F was sealed off, and the apparatus attached to a vacuum-line by means of the ball and

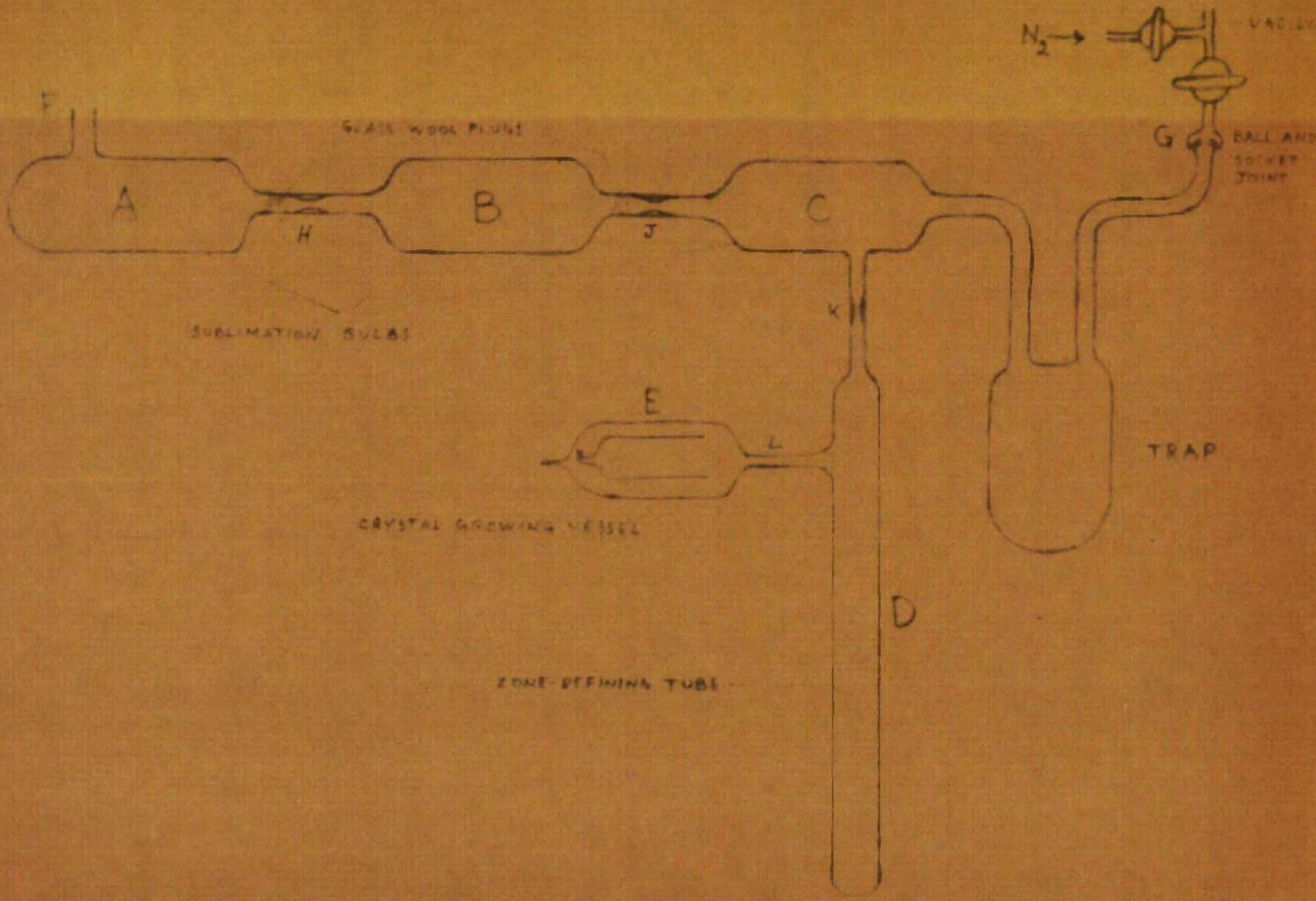

FIG. 21.2 : APPARATUS FOR PURIFYING ANTHRACENE

socket joint at G. The trap was cooled with liquid nitrogen to prevent any volatile material contaminating the vacuum-line, and the apparatus evacuated to approximately 0.003 mm.Hg pressure. A heating tape was wrapped round A and the material slowly sublimed into B. Tube A was removed by sealing off at the constriction H. The procedure was repeated, this time subliming the anthracene from B into C and sealing off at J. Pumping was continued throughout the double sublimation.

About half an atmosphere of "white-spot" nitrogen (scrubbed by bubbling through Fieser's solution and concentrated sulphuric acid) was admitted to the apparatus and the anthracene melted using the heating tape. The material was prevented from running into the zone-refining tube by a plug of anthracene which had solidified at K. When the anthracene was molten, tube D was heated by a flame, the plug at K finally being melted thus allowing the molten anthracene to run into tube D. The zone-refining tube was sealed off at K.

The tube was set in place on the zone-refining apparatus and one heater and cooling coil fitted round the tube. The stops for operating the microswitches were adjusted on the cord to give the correct path length, the current to the heater set to the minimum value which would maintain a molten zone, and the material left to zone-refine.

When zone-refining was complete the tube was inverted and the top inch or so of material melted and allowed to run down the tube past the entrance to E. The remaining pure material (assumed to be three-quarters of the remainder) was melted and allowed to flow into the crystal growing tube, E. The bottom quarter of material in D was not used since this part contained the impurities.

After the pure anthracene was in E, the tube was sealed off at L in such a way as to leave a glass hook on E. The material in E was then melted making sure that the capillary was properly filled, and E

suspended by its glass hook in the top half of the crystal growing furnace.

An improved version of the above method was to start with anthracene which had been recrystallised once from glacial acetic acid and activated charcoal, once from pure glacial acetic acid, and once from toluene before packing into the purification apparatus shown in Fig. 2.1.2. Only one sublimation was carried out in this case. The nitrogen used was purified by bubbling through alkaline pyrogallol, concentrated sulphuric acid, and passing over freshly reduced copper turnings at 500° C.

(v) Analysis of Purified Naphthalene

Many methods[62] are available for the analysis of hydrocarbons but at the concentrations likely to be found in zone-refined material few of the methods will be useful. The impurities commonly present in crude naphthalene have been identified[75] and this offers a lead since particular impurities can be looked for. Comparison of the ultra-violet spectra of the zone-refined naphthalene with the published spectra[76] of the expected impurities shows that none of the impurities is present in detectable amounts, even when saturated solutions of the material in ethanol or hexane are examined. From the extinction coefficients of peaks outside the naphthalene absorbing region the maximum possible concentration present can be calculated on the assumption that an absorbance of 0.02 would be detected. This calculation indicates that the concentration of anthracene is less than about ½ part per million (p.p.m.). It is known that zone-refining quickly reduces anthracene in naphthalene to less than 1 p.p.m. Other impurities likely to be present have u.v. spectra which overlap with that of naphthalene.

Thus u.v. spectroscopy indicates that anthracene is not present in excess of ½ p.p.m., but otherwise is not useful at the small concentrations any impurities will be present at.

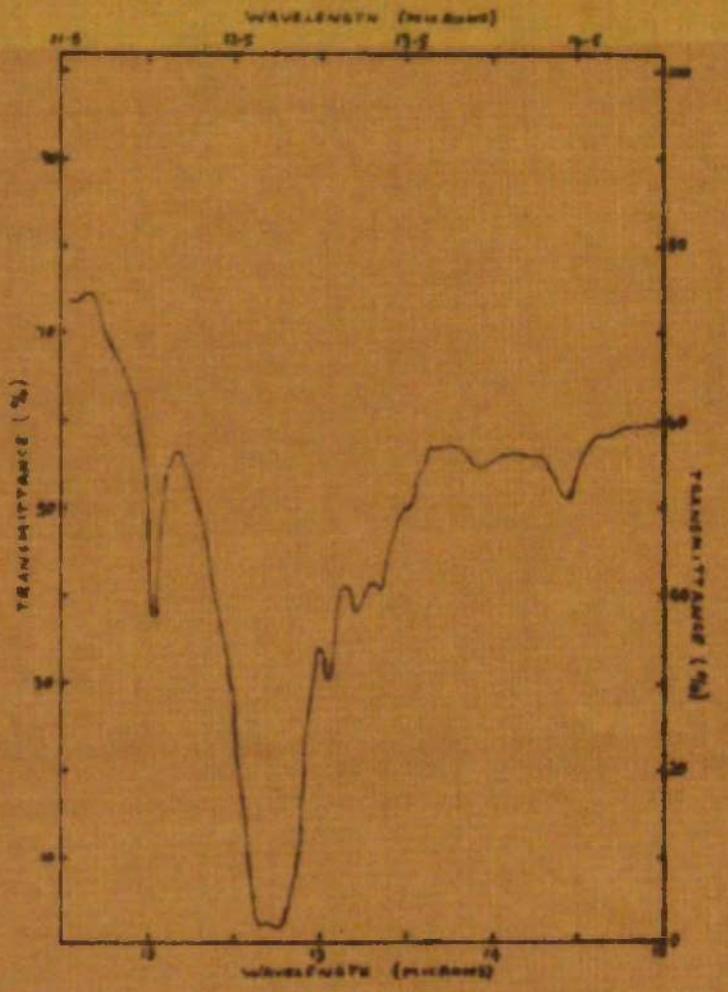

(a) Reagent Grade

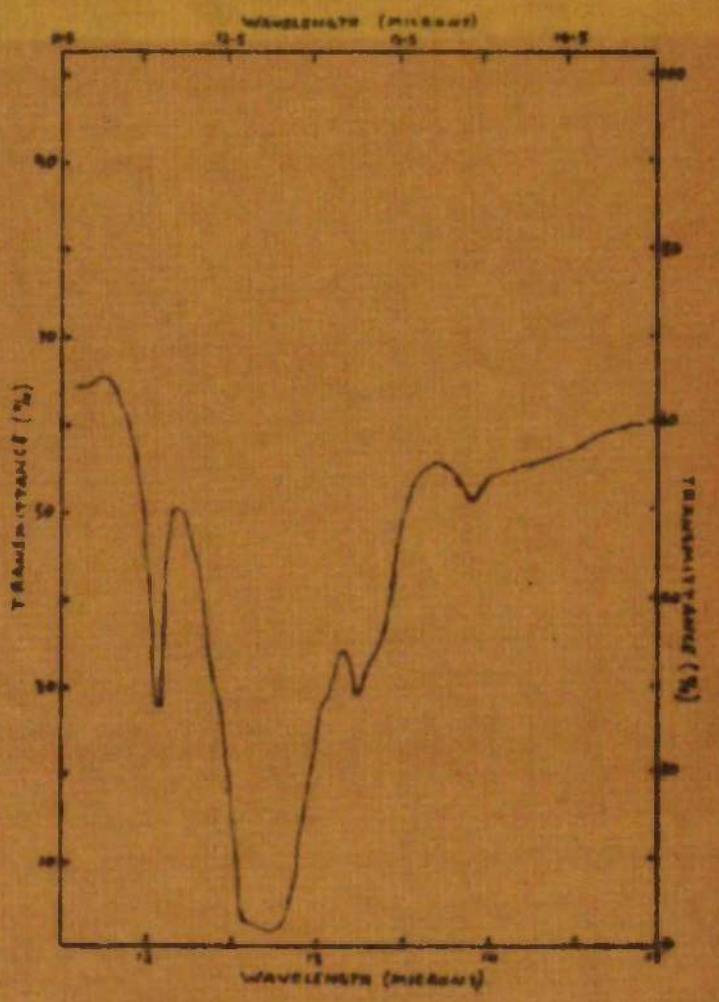

(b) Zone - Refined

Fig. 2.1.3: Infra-Red Spectra of Naphthalene.

Comparison of the infra-red spectra of B.D.H. naphthalene and zone-refined naphthalene shows that some peaks present in the former are absent in the latter. The relevent part of the spectrum is shown in Fig.2.1.3. However, the impurity or impurities giving rise to the peaks at 13.15, 13.45, and 14.50 microns could not be identified and so maximum impurity limits cannot be calculated for them.

It is known that the impurities commonly present in naphthalene readily zone-refine out, with the possible exception of the methyl naphthalenes.[77] The methyl naphthalenes have a strong i.r. absorption. This peak was absent in the spectrum of zone-refined naphthalene.

Zone-refined naphthalene was examined by thin-layer chromatography (t.l.c.) and gas-liquid chromatography (g.l.c.). T.l.c. failed to show any impurity. Both petroleum ether and chloroform were tried as solvent, and the plates were examined under u.v. light and by iodising. G.l.c. was equally negative.

Melting curves and freezing curves[78] can indicate the presence of small amounts of impurity and give a measure of their concentration. The freezing curves of samples of naphthalene were taken and it was found that the method readily detected differences of purity between them. The sample was melted in a small tube which was stirred automatically and enclosed in a vessel with a vacuum jacket to reduce the cooling rate. The vessel was thermostatted at 78°C. The temperature of the naphthalene was measured with a thermistor calibrated against a platinum resistance thermometer. The method readily detected impurity differences along a zone-refined bar, but in the pure part of the bar reproducible curves were difficult to obtain probably because the impurity concentration was at the limit of detection or less than it.

(vi) Analysis of Doped Naphthalene Crystals.

Several doped naphthalene crystals were grown (see Section II B.)

Anthracene doped crystals were analysed by u.v. spectrometry. Anthracene has three strong absorptions at 338,355, and 375 millimicrons with which the naphthalene peaks do not overlap even with a very large excess of naphthalene (see Fig. 2.1.4). Standard solutions of anthracene in excess naphthalene were made in cyclohexane and a calibration curve drawn for the three peaks (Fig. 2.1.5). Excellent straight lines up to absorbances of unity and passing through the origin were obtained. The doped crystals were analysed by dissolving weighed samples of the crystals in a known volume of cyclohexane and taking their u.v. spectra. The anthracene contents of the samples were calculated from the calibration curves.

The 2-methyl naphthalene doped and indole doped crystals were not analysed.

Details of materials zone-refined and analysed are given for each crystal grown from them in the crystal growing section (II B.).

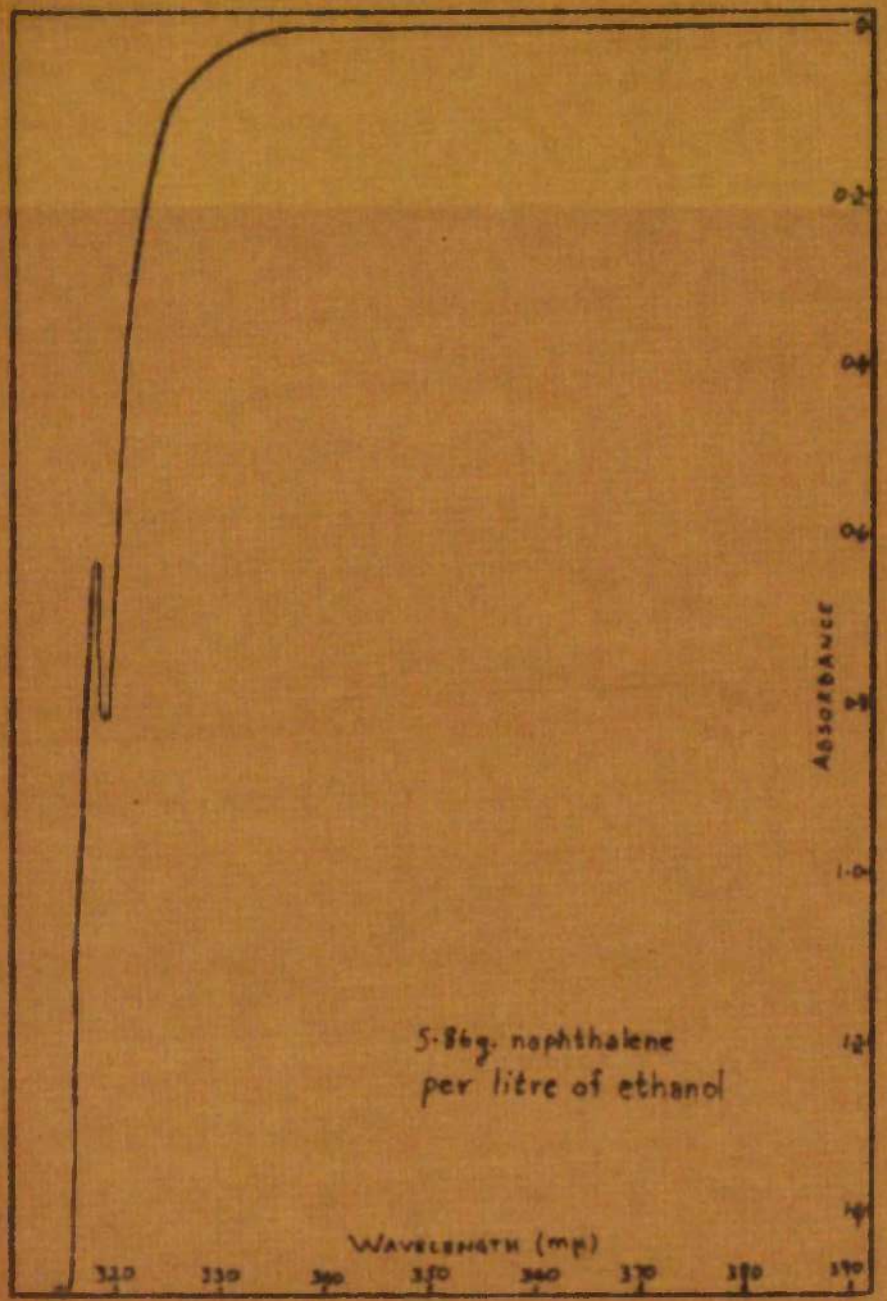

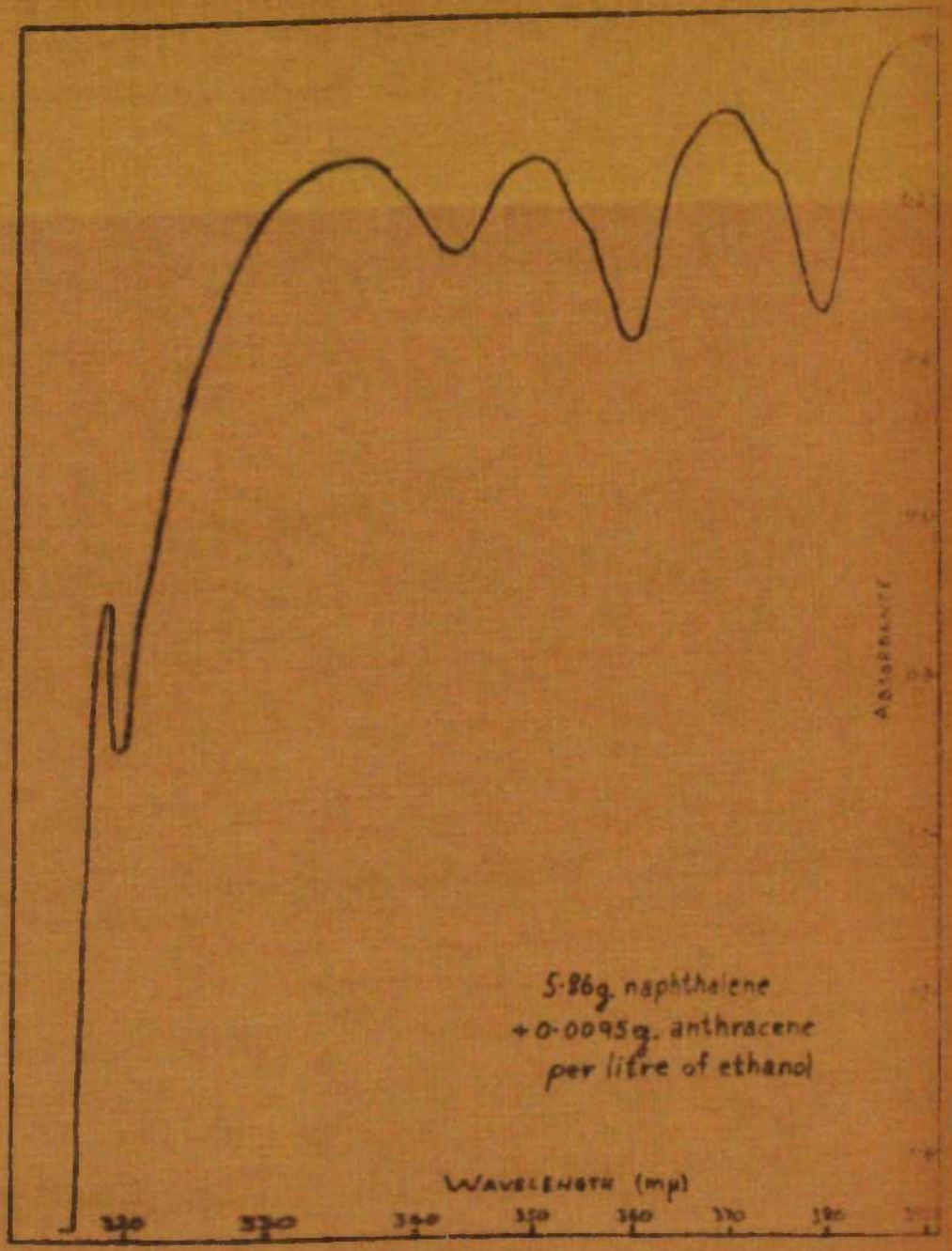

Fig.21.4: U.V. Spectra of Naphthalene and Anthracene

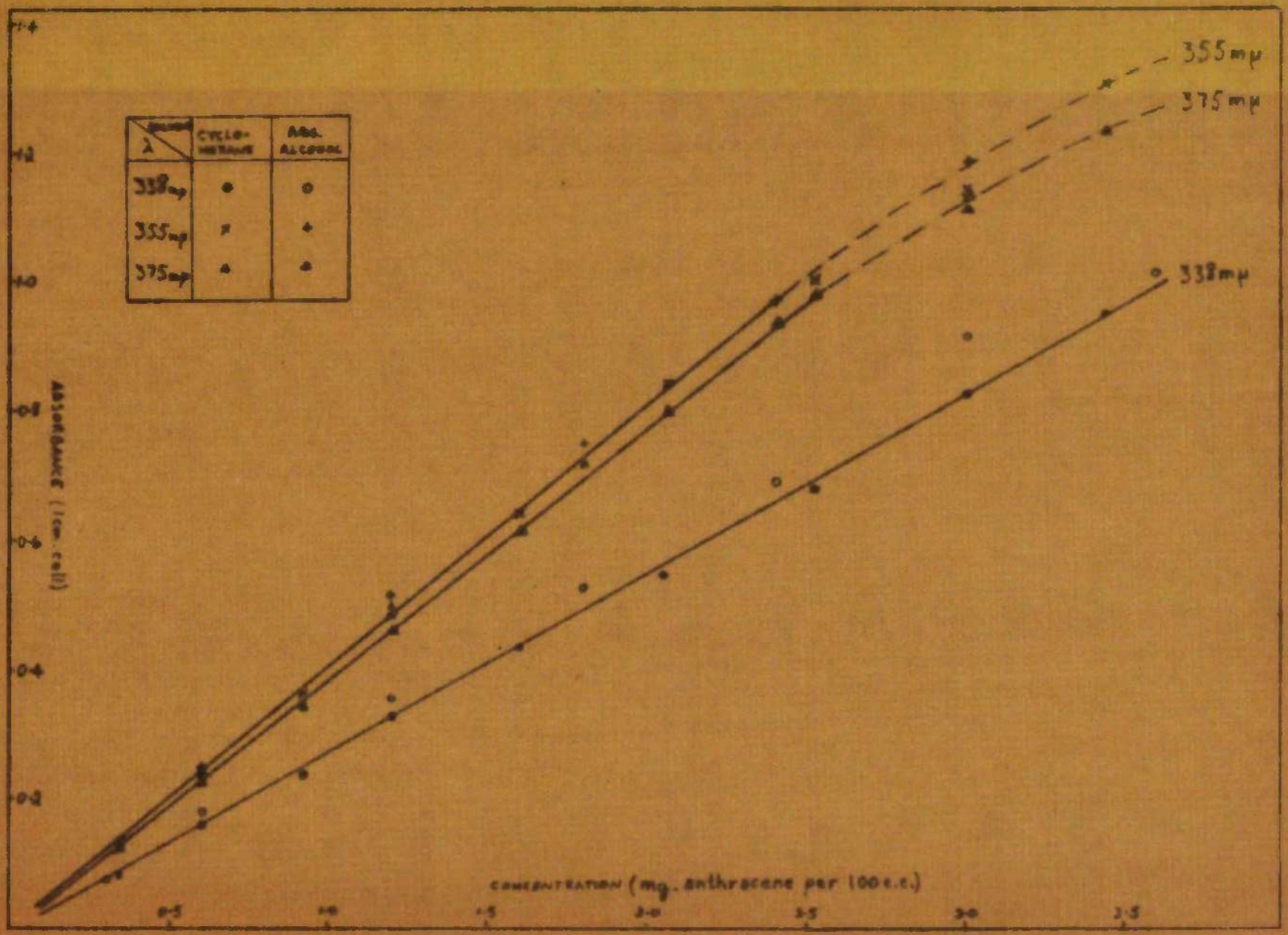

Fig. 2.1.5: Determination of Small Amounts of Anthracene

B CRYSTAL GROWING

(i) Introduction.

Single crystals can be grown in many ways, the commonest methods being growth from solution, from the melt, and from the vapour. It is also possible to grow monocrystals in the solid state by the annealing of crystal aggregates.[79] With crystal aggregates of plastic, organic materials, monocrystals of good quality and of almost any desired size can be obtained by annealing. In this laboratory large crystals of pivalic acid, cyclohexane, etc., have been grown from the solid state. The method, however, is not suitable for growing large crystals of anisotropic materials such as naphthalene.

Growth of crystals from the vapour phase has been used to obtain monocrystals of many substances and Sloan has used the method for growing single crystals of organic materials.[80]

Crystal growth from solution is the commonest method of obtaining single crystals and has been investigated thoroughly.[81,82] The method has the advantage that a high temperature is not required so that if the material decomposes at elevated temperatures or has a solid state transition between the melting-point and the required temperature it can still be grown by the method. It has, however, the serious objection that the crystal will contain occluded mother-liquor. This was felt to be so serious a disadvantage as to make it undesirable to use solution-grown crystals for the diffusion experiments. However, some crystals were grown and it was found that reasonably large crystals of naphthalene could be obtained easily from solution. The ease of growth of the crystal and its habit depended on both the solvent used and the purity of the naphthalene, e.g. B.D.H.

"molecular-weight" naphthalene grows from spectroscopic grade cyclohexane as plates, but zone-refined naphthalene grows as rods from the same solvent.

Growth from the melt can be used to obtain crystals of any material which does not decompose on melting. The method has been used to prepare crystals of very many substances, e.g. silicon iron, aluminium, alkali halides, anthracene, naphthalene, acetic acid, ice, cyclohexane, etc. The method has proved to be of considerable importance and several techniques have been developed. No one method has proved better than another, the method adopted for a particular substance depending on the properties of the material and the inclinations of the experimenter.

The chief methods of growing from the melt are:-

(a) The Bridgmann-Stockbarger method,

(b) The Kyropoulos method, and

(c) The zone-melting technique.

In the zone-melting or zone-refining technique[83] purification of the material can be combined with growth of a single crystal of the substance. By the repeated passage of several molten zones through a sample of the material contained in a glass tube the material is zone-refined and, with suitable substances, the purified material forms a single crystal inside the tube. In this laboratory single crystals about 1 cm. diameter and 4 to 6 inches long have been grown of plastic organic solids by the zone-refining method. The crystals contain vapour bubbles but these are easily removed by reversing the direction of motion of the final pass.[84]

With non-cubic organic crystals growth of single crystals by the zone-melting method is much more difficult due to the anisotropy and brittleness of the crystals and their tendency to crack during heating or cooling. In this laboratory it was observed that zone-refining of naphthalene and benzoic acid even in large (30 mm.) diameter tubes gave fairly large

single crystals of the substances. Those tended to crack on further cooling and broke up still further by mechanical shock on removing from the glass tubes. The crystals were, in any case, of very poor quality.

The commonest methods of growth from the melt are the Bridgmann-Stockbarger method and the Kyropoulos method. In both methods the molten material is contained in a crucible, solidification being brought about under controlled conditions either with or without a seed crystal. In the former method crucibles have been devised to initiate growth from seeds produced within the vessel.

In the Bridgmann-Stockbarger method[85,86] the closed vessel or crucible containing the substance is placed in a furnace the temperature of which is above the melting-point of the material at the top of the furnace but below the melting-point at the bottom of the furnace. The crucible containing the molten material is lowered slowly down the furnace and as the tip of the vessel passes through the melting-point isotherm crystallization occurs at the bottom of the crucible. Continued lowering of the vessel results in the melt becoming entirely solidified and, if lowering is slow enough and other conditions correct, the solid produced is monocrystalline.

The furnace used must be of high heat stability so that the melting-point isotherm does not move up or down the furnace while the crystal is growing (growth may take several days or even weeks). The temperature gradient in the neighbourhood of the melting-point should be steep to give good results. Many designs of furnace have been made to achieve these ends.[87,88]

To obtain a sharp temperature gradient at the melting-point and to keep the isotherm stable it is necessary to have a baffle inside the furnace with a hole in it just large enough to allow the crucible to pass through. The controls of the furnace are adjusted so that the melting-point isotherm is at the baffle. A sketch of the system is shown in Fig. 2.2.1 (a).

The shape of the temperature gradient recommended by Stockbarger[86]

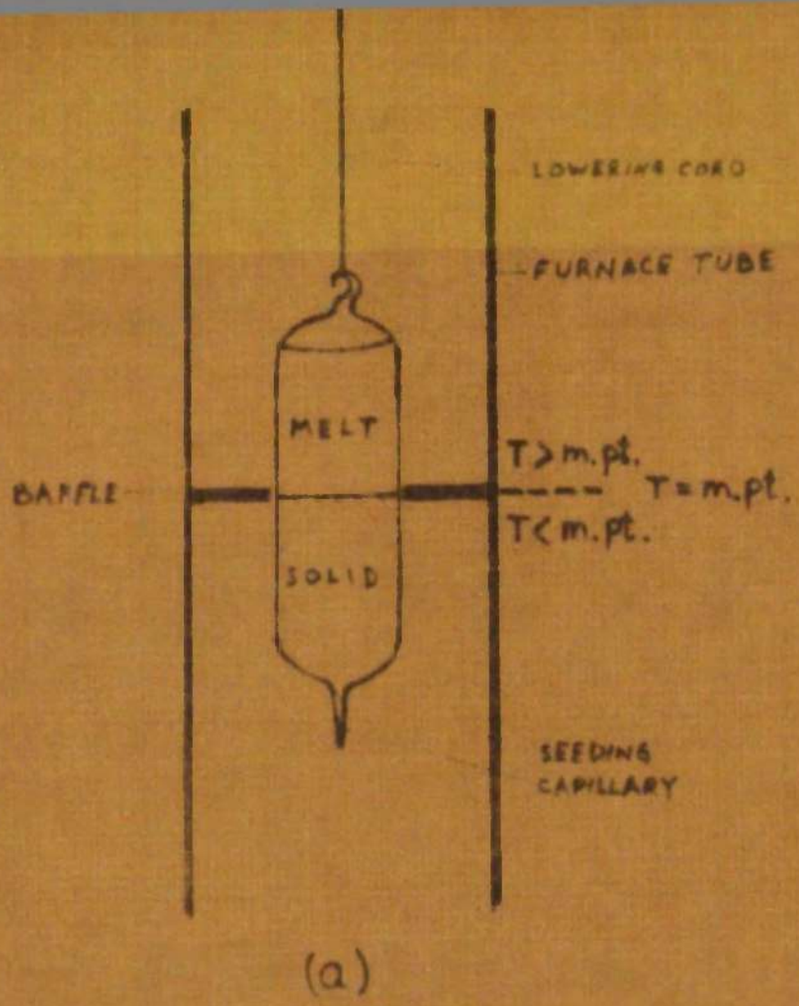

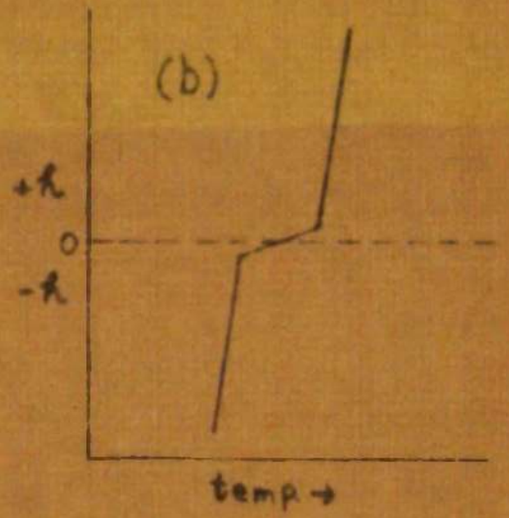

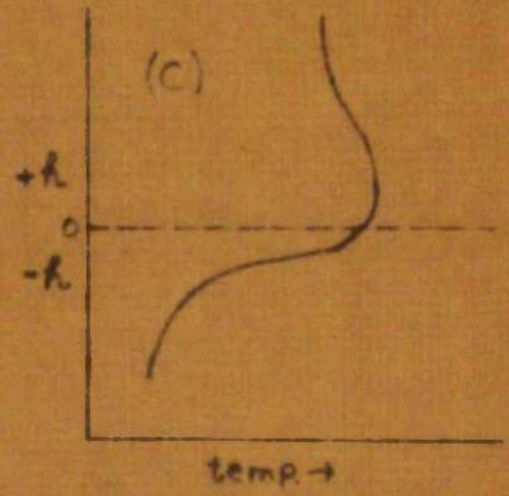

(a) Principle of Operation
(b) Stockbarger's Gradient
(c) Stepanov and Vasileva's Gradient
h = distance from baffle

FIG.2.2.1: THE BRIDGMAN-STOCKBARGER METHOD

is shown in Fig. 2.2.1 (b). Stepanov and Vasileva[89] found that the performance of their furnace improved and that they could increase the growth rate of their crystals if the temperature gradient in the lower part of the furnace was steeper than that recommended by Stockbarger. These authors recommend a gradient shaped as in Fig. 2.2.1 (c).

With gradients below the baffle as sharp as those recommended by Stepanov and Vasileva shattering may occur in some crystals due to rapid cooling and in all cases the physical perfection of the grown crystal will be less the quicker the cooling.[90] On the other hand it has been found impossible to grow some crystals with too slow a gradient below the baffle[89] so that some compromise gradient must be found by trial and error. The kinds of imperfection likely to be introduced by using Stepanov and Vasileva's method are internal stresses which can be eliminated by subsequent annealing and slow cooling after the crystal growing process is complete.[89]

The initiation of crystallisation is of great importance in both the Bridgmann-Stockbarger method and the Kyropoulos method. In the latter initiation is usually by means of a prepared seed; in the former it may be by means of a prepared seed[91] but more usually crystallisation is initiated from a seed itself grown within the crucible. If this is not done correctly the material solidifies as a polycrystalline mass instead of a monocrystal.

Some of the designs of vessels for crystal growth by the Bridgmann-Stockbarger method are shown in Fig. 2.2.2. The principle of operation of all these tubes is similar. Nucleation is initiated at the tip of the capillary by cooling, this usually being achieved by placing the crucible in the furnace with the tip of the capillary just below the baffle. Hence, a small number of crystals are present in the capillary tip which grow on lowering the vessel. One of the crystals is usually more favourably oriented for growth than the others and grows in preference to the others so as to fill the capillary by the time the junction with the

main growth tube has reached the baffle. There will thus be a single seed initiating growth in the main vessel.

Type (a) vessel in Fig. 2.2.2 was used by Tammann[92,93] and type (b) by Bridgmann.[85] Sherwood[94] grew crystals of anthracene in a vessel shaped as (c) in Fig. 2.2.2. Polycrystalline material grows in the outer vessel, some growing into the capillary. The bends in the capillary lead to the elimination of all but the most favourably oriented seed. Hence the material in the inner vessel is seeded by a single crystal. The method gives more certain results than the simple capillary designs (a) and (b).

The orientation of the crystal within the growth tube depends on various factors particularly the orientation of the seed and the rate of growth.

The rate of growth of the crystal is governed by the rate at which the vessel is lowered through the baffle. If the rate of lowering is very slow the crystal will grow in any direction depending on the orientation of the seed. However, if the rate is increased the crystal may be unable to grow in those crystallographic directions whose rates of growth are small. Hence fast growth rates will encourage growth along axes which can grow rapidly and discourage growth along axes which can grow only slowly. If lowering is too fast the crystal growth may be unable to keep pace with the movement of the temperature gradient, spurious nucleation will occur and a polycrystal result.

In growth of Stilbene crystals[95] in a vessel of type (d) in Fig.2.2.2, Scott and co-workers found that orientation of the crystal depended on the angle of the limb of the zig-zag capillary adjacent to the tip of the conical baffle in the vessel. A similar effect was found by the present writer in growing naphthalene in a vessel of type (f) and by Sherwood[94] in growing anthracene crystals. The present writer found that the cleavage plane in naphthalene grew vertically if the limb of the capillary

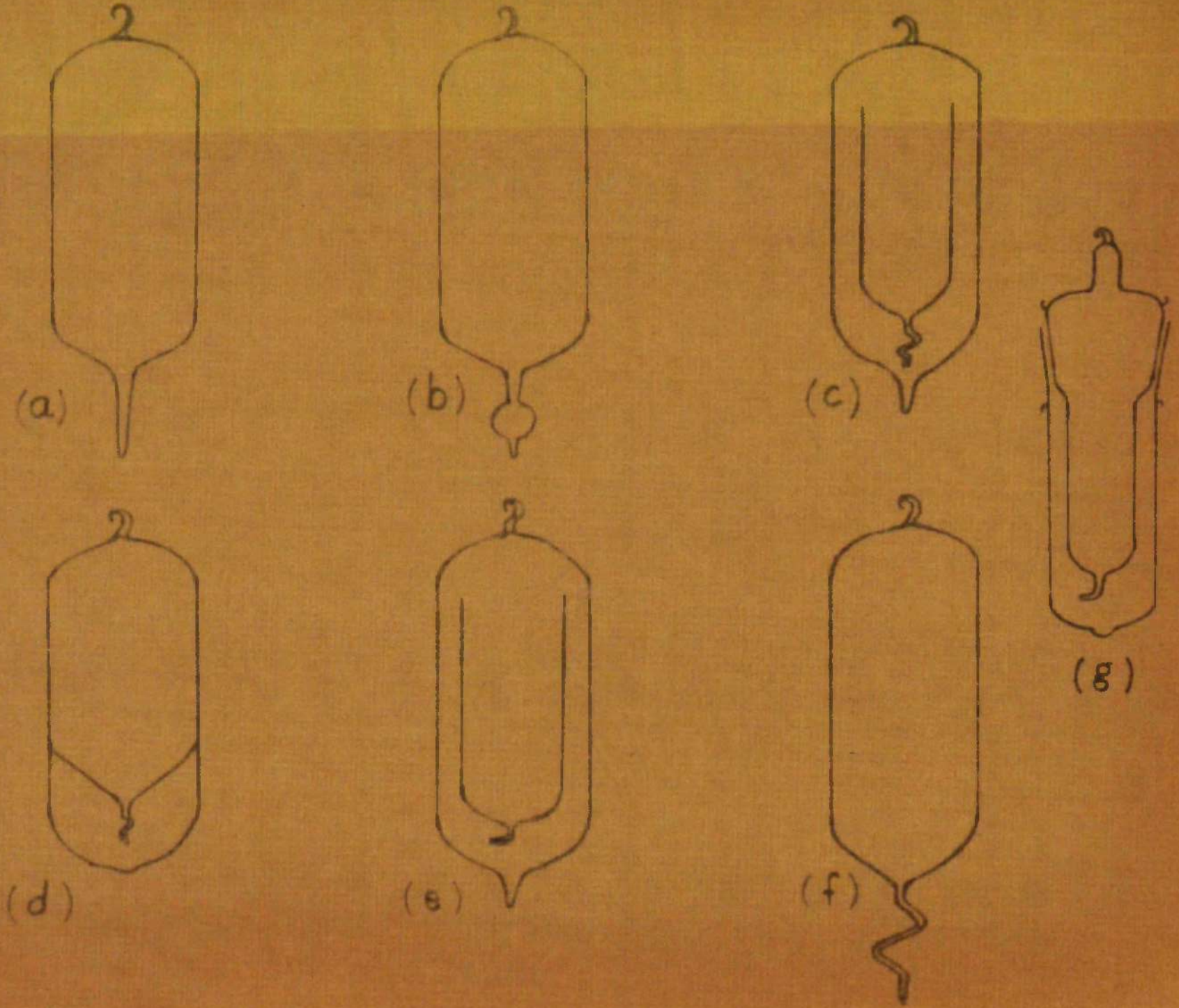

FIG.22.2 : CRYSTAL GROWTH VESSELS

entered the growth vessel vertically. The angle of the cleavage plane could be altered by altering the angle at which the capillary entered the vessel. It was found that the cleavage plane could not be tilted more than by about 60°. However, Sherwood[94] was able to tilt the angle of the cleavage plane of anthracene through 90° by using a vessel shaped like (e) in Fig. 2.2.2. Crystals grown in this vessel cleaved horizontally. Type (g) is an adaptation of (e).

An adaptation of the Bridgmann-Stockbarger method is to keep the vessel stationary and move the temperature gradient by reducing the input to the furnace in a controlled manner.

The Bridgmann-Stockbarger technique has been used for growing monocrystals of very many substances. One of the advantages of the method is that it can be used to grow crystals of a pre-determined shape. However, since the crystal is grown in a vessel it suffers from the disadvantage of having to remove the crystal from the vessel, a process which frequently leads to breakages. Cooling within the vessel usually produces stresses within the crystal but these can normally be removed by annealing after removal from the vessel.

Crystals can also be grown from the melt by means of the Kyropoulos or Crystal Pulling Method.[96] The material is melted in a crucible and a seed crystal attached to a shaft is dipped into the centre of the molten surface. A small amount of the seed is allowed to melt and then the shaft is raised slowly. If temperature and pull rate are adjusted correctly a single crystal is "pulled" from the melt. Stirring may be achieved by rotating the shaft.

The method has been used for growing single crystals of metals, salts, and semiconductors.

The requirements of the present work was for large single crystals of volatile organic solids. Other investigators[88,93,97] have found growth

from the melt an excellent method for obtaining such crystals, and, since the materials used are volatile, growth in a closed vessel seemed the most promising method. For these reasons, and for the reasons outlined in the discussion above, it was decided to try to grow large monocrystals by the Bridgmann-Stockbarger method, using a furnace with stationary isotherms and lowering the melt down the temperature gradient. It was decided to contain the melt in a closed, glass vessel, and to attempt to produce the seed crystal in situ.

(ii) Growth of Naphthalene Crystals.

A diagram of the crystal growing furnace is shown in Fig. 2.2.3. The furnace consists of a refractory tube, 2 ft. long, with an internal diameter of 12 cm. It is wound with nichrome resistance wire, there being five leads (A to F) into the windings to enable the furnace to be heated non-uniformly. The windings and tube are coated with alundum cement. Thermal insulation is by means of a dense asbestos "blanket" wrapped round the outside of the coated tube, which is then placed inside an 18 in. diameter can and packed round with glass fibre and asbestos.

The tube is closed top and bottom by "Sindanyo" plugs, readily removable, and half-way down the inside of the tube is a half-inch thick asbestos baffle. The baffle and the top "Sindanyo" plug are pierced to take a glass tube of 39 mm. diameter, as shown in the figure. The baffle and plug fit tightly round the tube. The top plug has a small hole to allow a "Sunvic" control thermostat (type TS1) to be inserted. The whole apparatus is surmounted by a glass bell-jar, 14 in. high, which holds the glass tube in place and also allows samples to be viewed by pulling the growth vessel up into the jar, but not completely out of the furnace. The glass tube is closed at the top by a stopper carrying a narrower diameter glass tube. Through this small tube passes the "cord" holding the vessel in place.

A diagram of the circuit used to heat the crystal growing furnace is

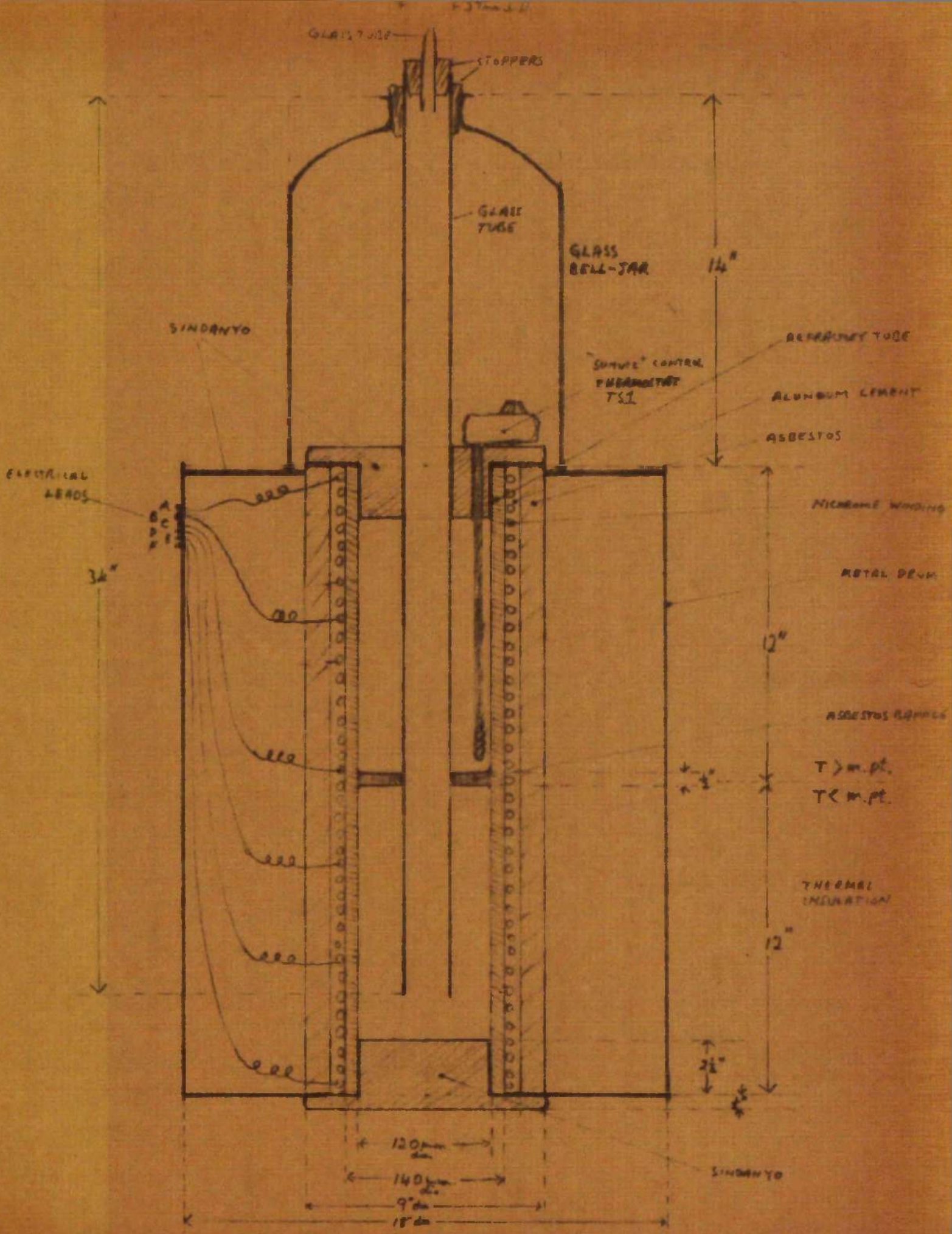

Fig. 2.2.3: Crystal Growing Furnace.

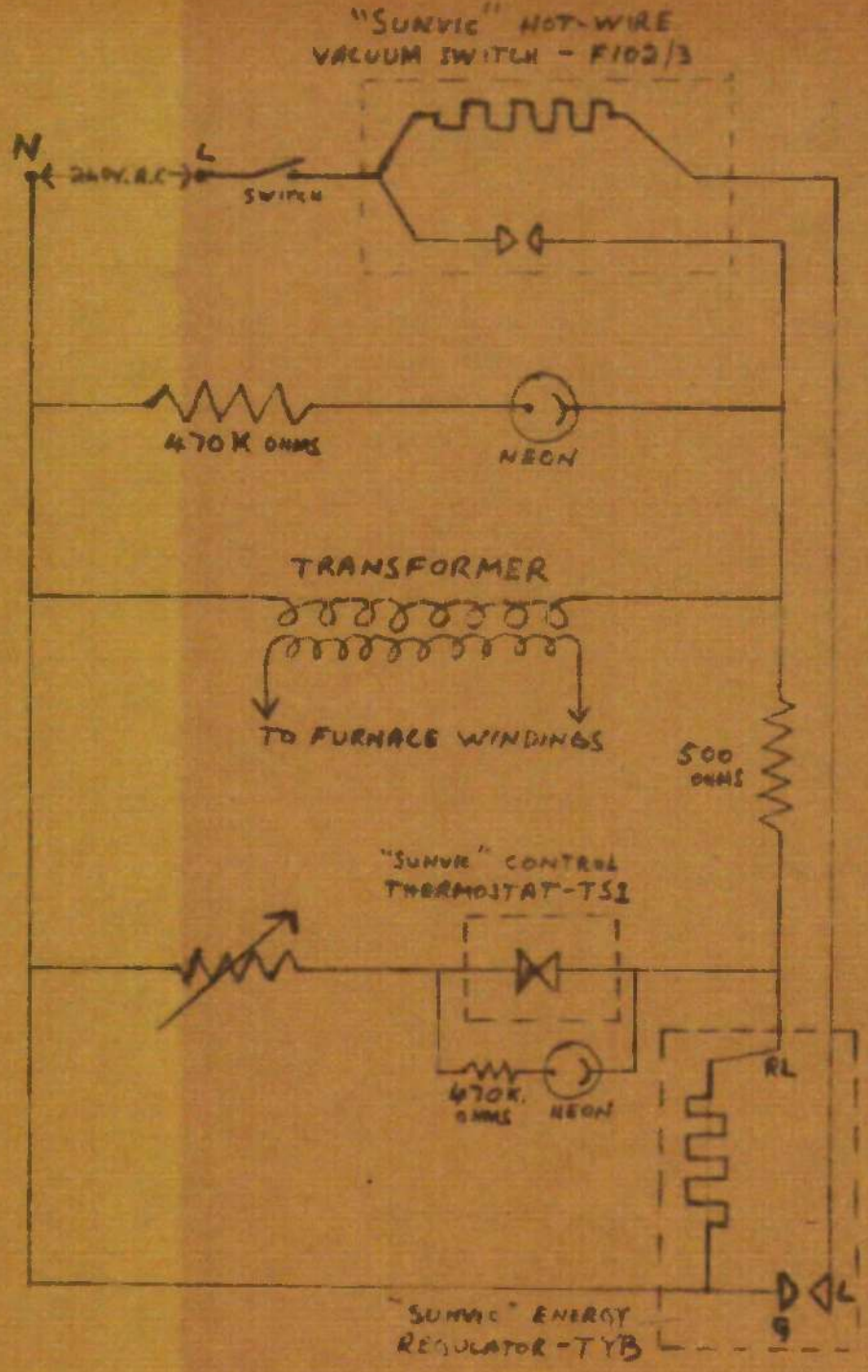

(a)

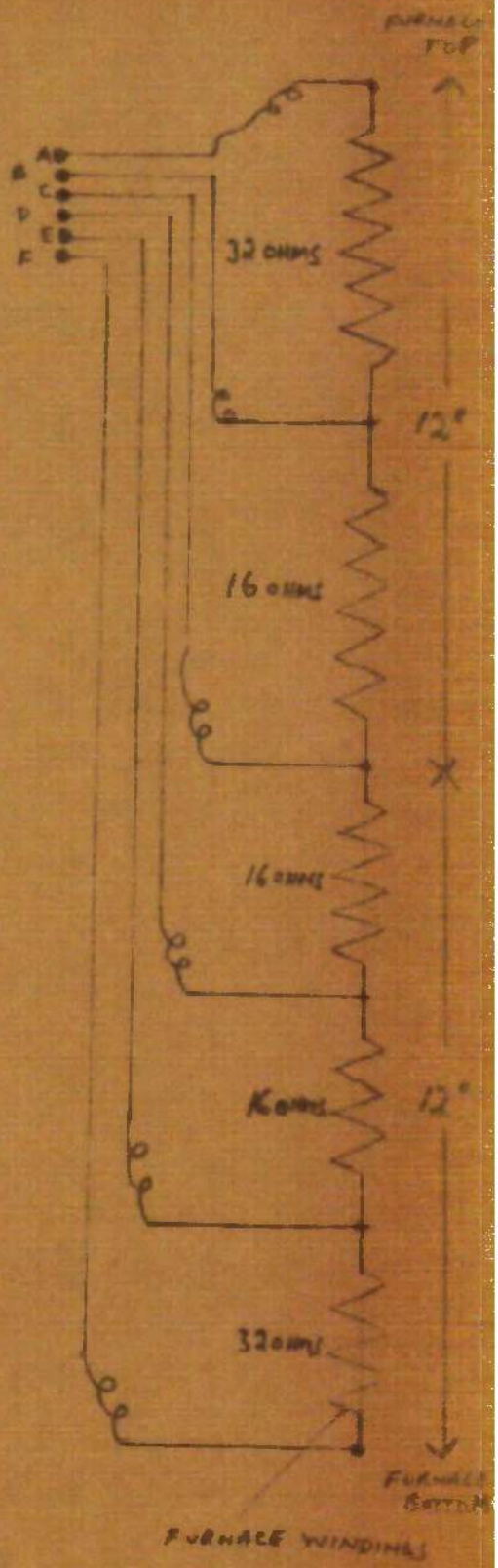

(b)

(a) Diagram of circuit
(b) Diagram of furnace windings

Fig. 2.24 - Crystal-Growing Furnace - Circuit.

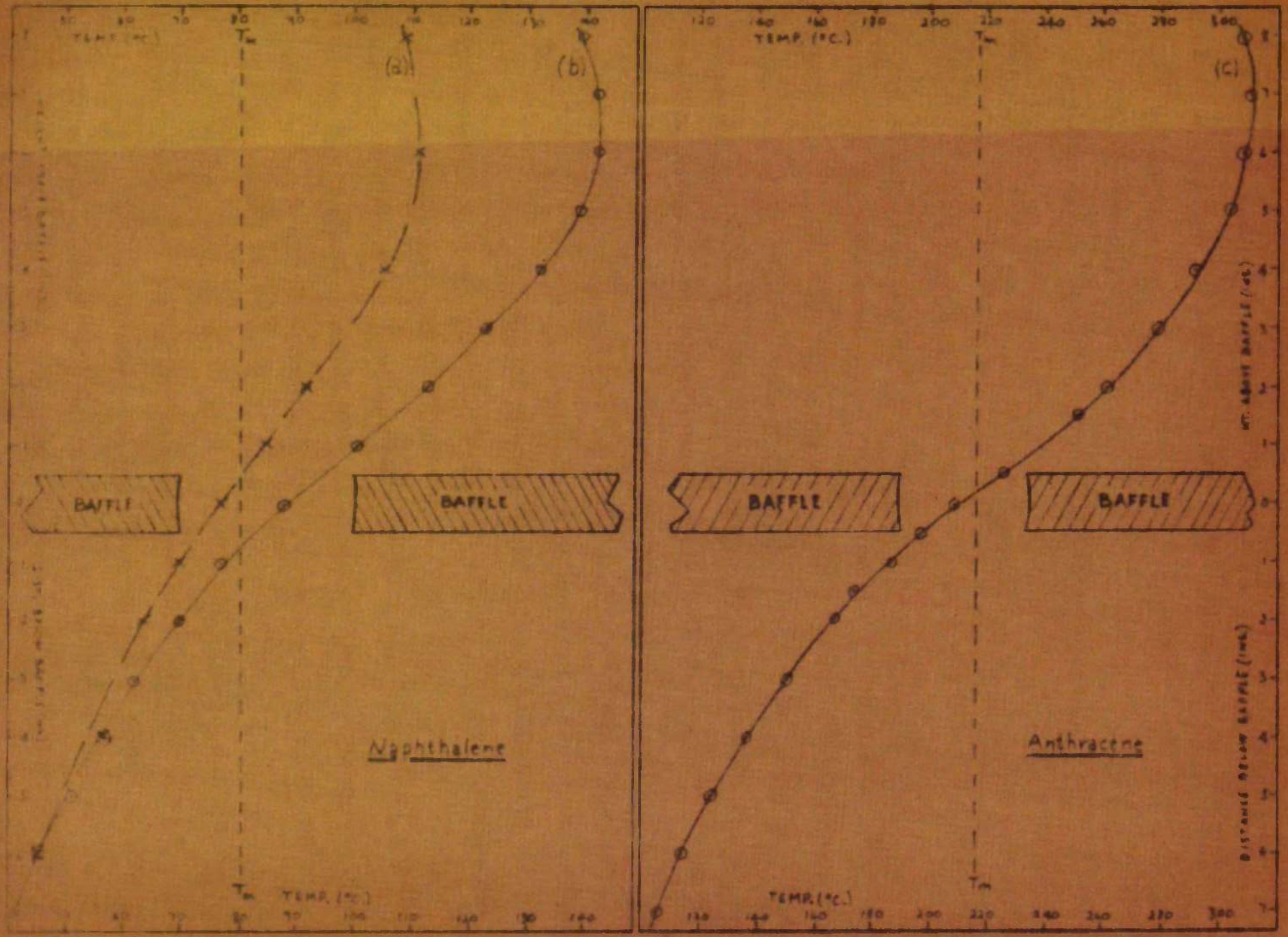

Fig. 2.2.5: Temperature Gradients in Furnace

shown in Fig. 2.2.4. The temperature setting in the furnace is controlled by means of a "Sunvic" energy regulator (type TYE) and a control thermostat (type TE1), the latter being inserted into the furnace as shown in Fig. 2.2.3. A first, rough control is obtained by selecting from the various voltage outputs of the transformer. The output of the transformer is fed into the furnace windings at appropriate points (A to F, Fig. 2.2.4). A wide variety of temperatures and temperature gradients is possible by means of these controls and also by varying the input points and short-circuiting various sections of the furnace windings. Examples of the gradients obtained are shown in Fig. 2.2.5.

The above furnace was rather massive and suffered from the disadvantage that it required a long time to heat up and stabilize, and hence a long time to obtain the correct isotherm across the baffle by altering the controls. However, this was more than compensated for by its high thermal stability and, once set, no alteration in temperature at the baffle was observable over several weeks or even months. This very high stability is believed by the writer to have been responsible, more than any other single factor, for the success in growing large good quality monocrystals.

The crystal-growing vessel used for growing single crystals of naphthalene was of type (f) in Fig. 2.2.2. It was constructed of glass tubing of external diameter 32 mm. The length of the vessel varied from vessel to vessel. The capillary at the bottom, by means of which the seed was formed in situ, was of 2 mm. internal diameter, the zig-zag tube being about 3 cm. long from the base of the main tube to the tip of the capillary.

Filling the vessel was done either directly (i.e. packing the material into it by hand) or by greaseless distillation of the material into the growth vessel. The greaseless distillation was carried out by placing the naphthalene in flask B (Fig. 2.2.6), sealing the tube C onto a vacuum-line and evacuating the apparatus. A few cm. pressure of "white-spot"

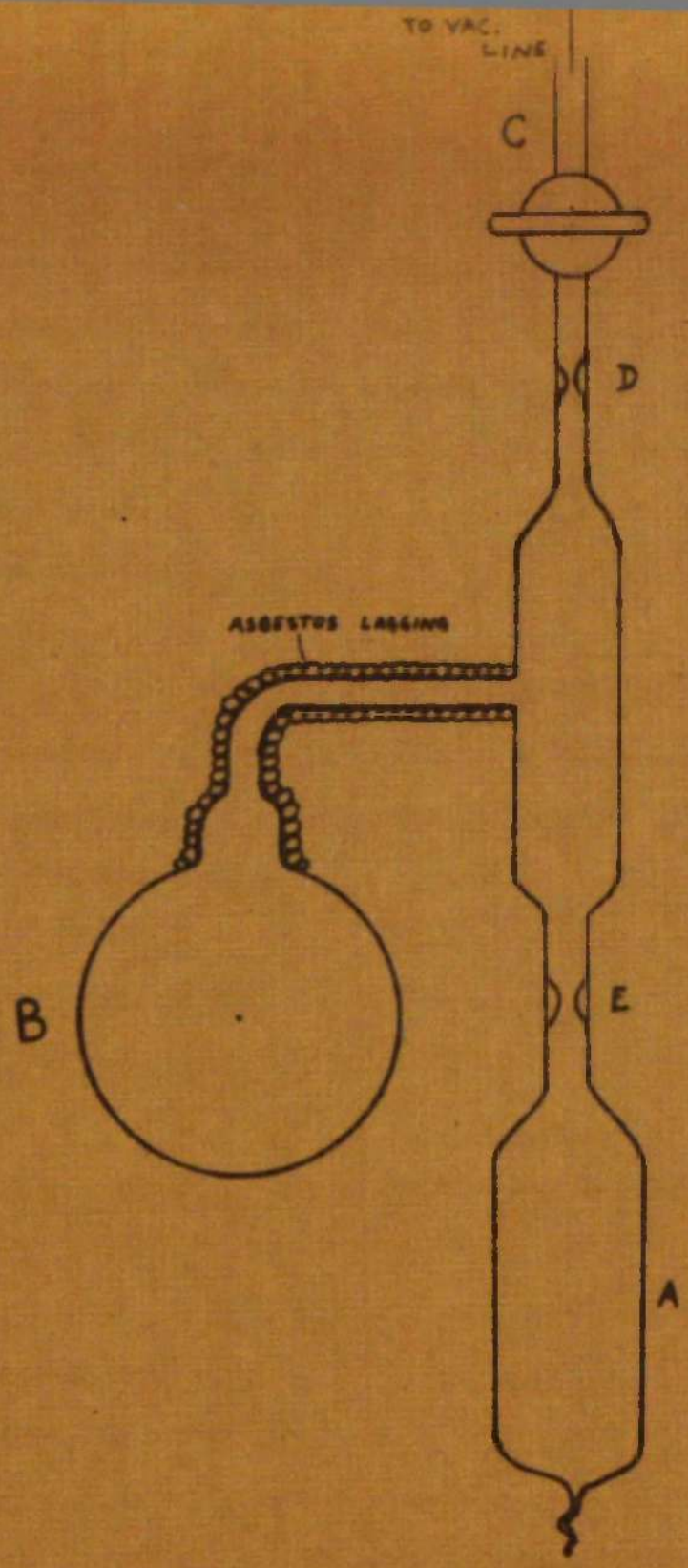

Fig. 2.2.6: Greaseless Distillation of Naphthalene.

nitrogen was admitted via tube C and the naphthalene melted. The material was allowed to solidify and the apparatus then re-evacuated. This was repeated, the procedure serving to "de-gas" the naphthalene. After the degassing, the apparatus was evacuated, a few cm. pressure of nitrogen added and the vessel sealed off at D.

The naphthalene was subsequently distilled into the crystal growing vessel A, and when most of it had distilled over, the crystal growing vessel was sealed off at E. No air was allowed into the vessel during the distillation or the sealing off. The sealing off was carried out in such a way as to form a glass hook at the top of the vessel.

The naphthalene was then melted, particular care being taken that the capillary was properly filled, the vessel attached to the lowering cord by means of its glass hook, and suspended in the upper part of the furnace with only the tip of the capillary protruding below the baffle. The vessel remained in that position for 24 hours to ensure that the naphthalene was completely molten except for the material in the tip of the capillary which formed a small crystal aggregate. At the end of this period the lowering motor was switched on.

Lowering the vessel was carried out by means of a "Sangamo Weston" motor, speed 3 revolutions per day. The lowering cord was wound round the spindle of the motor. The rate of lowering could be altered by changing the diameter of the spindle. The usual rate of lowering was 4.8 cm. per day, and this gave excellent results.

That part of the cord which entered the furnace was made of stranded copper wire, the remainder was of thread.

When the "Sangamo" motor is switched on, the vessel, suspended by its cord, is slowly lowered down the furnace, the melt solidifying as it passes through the melting point isotherm at the baffle and enters the lower part of the furnace. The material in the capillary solidifies first,

and as lowering proceeds one of the crystals in the polycrystalline mass at the tip of the capillary outgrows the others and by the time the bottom of the main growth tube has reached the baffle the whole diameter of the capillary is filled by one seed. This seed grows into the main vessel and initiates growth there. If spurious seeding does not occur during subsequent lowering of the vessel, a large single crystal results.

Many excellent crystals of naphthalene were grown by this method. Table 2.1 gives details of the crystal boules grown. The temperature gradients used are shown in Fig. 2.2.5.

In addition to crystals grown in the furnace described here, naphthalene crystals were also grown in a furnace designed and built by Sherwood.[66] The furnace used in this particular case is shown in the Table.[a]

(iii) Growth of Doped Crystals of Naphthalene.

In growing doped crystals, the required quantity of "dope" was placed in the crystal growing vessel, A (Fig. 2.2.6) prior to sealing tube C onto the vacuum line. The naphthalene was then distilled into the vessel as described above and the crystal grown as before.

The organic crystal lattice will not dissolve an unlimited proportion of foreign material.[59,60] Indeed, it is usually only very small quantities of impurities which can be grown into a crystal, and if it is attempted to incorporate too much foreign material, a polycrystalline mass results. Some of the attempts made in the present work failed because an excessive amount of "dope" was present in the melt. In other cases, growth resulted in the vessel containing, not one monocrystal, but several. These pieces were large enough to be used. Where only very small amounts of dope were added, good monocrystals were obtained.

A summary of the doped crystals grown is given in Table 2.1

(iv) Growth of Anthracene Crystals.

The anthracene was purified and the crystal growing vessel filled

as described in section II A of this thesis. The growth vessel used was type (c) (Fig. 2.2.2); the temperature gradient in the furnace was as shown in Fig. 2.2.5 (c).

Anthracene crystals were also grown in vessels of type (g). This is a modification of type (e) in which the purified material is placed in the inner tube only. The outer tube may be filled by any convenient material e.g. impure anthracene or silicone oil. The inner and outer vessels fit together by means of a ground glass joint. The capillary in the inner vessel is sealed. Use of this vessel effects a great saving in pure anthracene.

(v) Annealing of Crystal Boules.

Where a crystal boule was annealed the crystal growing vessel was left in place until it had reached the bottom of the furnace. The temperature there was about 40°C. in the case of naphthalene. The vessel was then removed and placed in a Dewar flask containing water at 40° and left to cool to room temperature.

While this procedure prevented cracking of the crystal boule due to too rapid cooling it was felt that it was not an entirely satisfactory method of annealing. The temperature gradient in the furnace is too sharp to anneal satisfactorily and the growth vessel fits too closely to the crystal and may cause strain even on slow cooling. Therefore, the crystals were re-annealed by removing them from the growth vessel, placing in a larger glass vessel, and annealing for 7 days at 75 - 78°C. (Naphthalene melts at 80°). The temperature was then reduced to about 55° over another 7 days and thereafter cooled to room-temperature in about 2 days.

Table 2.1: Single Crystals Grown.

(a) Crystals of Pure Naphthalene.

Boule A: Scintillation grade naphthalene without further purification. Grown in furnace (1) at 1mm. per hour. The resulting monocrystal was of poor quality.

Boule B: As for A.

Boule C: As for A.

Boule D: As for A. Somewhat better quality.

Boule E: Scintillation grade naphthalene without further purification. Grown in furnace (2) at 2 mm. per hour. Quite good quality crystal.

Boule F: B.D.H. Molecular weight naphthalene. Distilled into growth vessel. Grown in furnace (1) at 1 mm. per hour. Quite good quality.

Boule G: Scintillation grade naphthalene. Distilled. Grown in furnace (2) at 2 mm. per hour. Annealed in furnace for several days. Crystal was of very good appearance.

Boule H: As for G. Crystal of very good appearance.

Boule I: Scintillation grade naphthalene. Distilled. Grown in furnace (2) at 2 mm. per hour. Annealed. The crystal was of very good appearance.

Boule J: B.D.H. Molecular weight naphthalene. Greaseless distillation. Grown in furnace (2) at 2 mm. per hour. Annealed. The crystal was of excellent appearance.

Boule K: B.D.H. M. Wt. naphthalene. Zone-refined in glass tube (10 passes). Greaseless distillation. Grown in furnace (2) at 2 mm. per hour. Crystal of good appearance but some contamination and had several vapour tubes.

Boule L: B.D.H. M. Wt. naphthalene. Zone-refined in "teflon" tube (20 passes). Greaseless distillation. Grown in furnace (2)

at 2 mm. per hour. Part of the crystal annealed. The crystal was of excellent appearance. Boules L and M were the best crystals grown.

Boule M: As for L but not annealed.

Boule N: B.D.H. M. Wt. naphthalene without further purification. Grown in furnace (2) at 4 mm. per hour. Gave several large monocrystalline fragments of poor appearance.

Boule O: As for N.

(b) Doped Crystals of Naphthalene.

Boule AD1: Scintillation grade naphthalene without further purification. 5% anthracene added. Grown in furnace (2) at 2 mm. per hour. Gave a polycrystalline mass even in the capillary tube of the growth vessel.

Boule AD2: Scintillation grade naphthalene. Greaseless distillation. 0.5% anthracene added. Grown in furnace (2) at 2 mm. per hour. Gave one large monocrystal of poor appearance plus several fragments. Analysis showed that the crystal contained 30p.p.m anthracene near the bottom and 86p.p.m. near the top. Scrapings from the top surface contained 1% anthracene.

Boule AD3: As for AD2 but 0.1% anthracene added. Gave a good monocrystal except for about 1 mm. at the top surface. Analysis showed that the crystal contained 2p.p.m. anthracene near the bottom and 46p.p.m. near the top. Scrapings from the upper surface contained 0.3% anthracene.

Boule MD: B.D.H. M. Wt. naphthalene. Greaseless distillation. 0.1% 2-methyl naphthalene added. Grown in furnace (2) at 2 mm. per hour. Gave a good monocrystal, slightly darker in colour than usual.

Boule ID: B.D.H. M. Wt. naphthalene. Greaseless distillation. 0.5%

indole added. Grown in furnace (2) at 2 mm. per hour. Gave two monocrystals. Rather brown in appearance.

(c) Crystals of Pure Anthracene.

Boule An1: Blue -fluorescent anthracene. Sublimated twice. Zone-refined (12 passes at 1½ ins. per hour and 6 passes at 0.75 ins. per hour.) Grown in vessel of type (e) (Fig. 2.2.2). Grown in furnace (2) at 2 mm. per hour. Gave a fairly good monocrystal but not water white (very slightly yellow).

Boule An2: Blue-fluorescent anthracene. Crystallised twice from glacial acetic acid and once from toluene. Grown in vessel of type (g) (Fig. 2.2.2) with silicone fluid in the outer vessel. Grown in furnace (2) at 2 mm. per hour. The bottom half was a monocrystal with the remainder polycrystalline.

Boule An3: Blue-fluorescent anthracene. Crystallised twice from acetic acid and once from toluene. Sublimated once. Zone-refined (12 passes at 1½ ins. per hour). Grown in vessel of type (e) (Fig. 2.2.2). Grown in furnace (2) at 2 mm. per hour. Gave a fairly good monocrystal with a little polycrystalline material near the top. Crystal distinctly yellow.

Notes.

(a) Furnace (1) is the crystal growing furnace described in ref. 80. Furnace (2) is the furnace described in this thesis.

(b) Annealing procedure is described in Chap. (v) above.

(c) Greaseless distillation is described in Chap. (ii) above.

(d) All the naphthalene crystals were grown in vessels of type (f) in Fig. 2.2.2.

C MEASUREMENT OF DIFFUSION COEFFICIENTS

(i) Introduction.

Methods of measuring diffusion coefficients are discussed in Part I of this thesis. It was wished to measure diffusion by a direct method using a tracer technique. The principle method employed was the tracer-sectioning technique but some runs were carried out using the surface-decrease method.

This programme required the preparation of radioactive tracers, their deposition on prepared faces of the crystals to be studied, and, after diffusion was complete, the crystal had to be sectioned and the activity of each slice counted.

In the surface-decrease method an apparatus had to be designed to count the surface activity of the crystal while it was held at the experimental temperature.

Additional experiments were carried out to discover the effect, if any, of annealing, and also to try to elucidate the phenomenon of the diffusion "tail".

(ii) Radioactive Tracers.

Since the materials studied were hydrocarbons, only isotopes of carbon and hydrogen could be used. The isotopes used were carbon-14 and tritium (H^3). Details of these tracers are given in Table 2.3.1. Both are weak beta-emitters, tritium being very weak. Both have very long half-lives and so decay corrections are not required.

Table 2.3.1: Tritium and Carbon-14.

	Half-Life (Years)	Millistoms Per Curie	Beta Particle Mean MeV	$E_{max.}$ (MeV)
Tritium	12.5	0.035	0.0057	0.0185
Carbon-14	5568	15.4	0.049	0.155

1. The material used for most of the diffusion runs was naphthalene-1-C14, which was purchased from the Radiochemical Centre, Amersham, in vials containing 0.05 mc. (3.2mg.). The vials were chilled, opened, and 122mg. inactive naphthalene added and the whole dissolved in about 2c.c. toluene or acetone. The material was transferred to a stoppered bottle and the solvent allowed to evaporate. When not in use the bottle was stored at -20°C., as were the other tracers used.

The activity of this material was 0.4 microcurie per mg. It was used for Diffusion Runs 1 to 29, for the diffusion runs parallel to the "a" and "b" axes, and for runs on doped naphthalene and polycrystalline compacts. For runs from 30 onwards and for the "tail" experiments, tracer of four times this activity was used.

2. It has been reported[98] that proton movement may occur in aromatic hydrocarbons. If such movement does take place the diffusion coefficient as measured by naphthalene-1-C14 may differ from the apparent diffusivity found using a hydrogen isotope. To test this, a few diffusion experiments were carried out using tritiated naphthalene as tracer.

Tritiated naphthalene can be made either by synthesis, in which case the material is labelled at a known position, or by exchange, in which case the substance is labelled generally. Exchange can be either with tritium gas or tritiated water. The method[99] used was that of exchange with tritiated water in the presence of a Lewis acid.

0.2g. naphthalene were melted in a glass tube with 1g. anhydrous aluminium chloride and 0.1c.c. (2mc.) THO added. The tube was chilled in liquid nitrogen, evacuated, and sealed. The sealed tube was heated at 100°C. for 40 hours, broken open, and its contents extracted with methylene chloride. The methylene chloride solution was washed successively with water (several times), dilute potassium hydroxide solution, dilute sulphuric acid, and again several times with water. Anhydrous calcium chloride was added and the solution left to dry over-

night. The dry solution was filtered and evaporated, the residue being transferred to a sublimation vessel and sublimed in vacuo. 0.16g. naphthalene was recovered. The activity of this material was found to be 0.103 microcurie per mg.

The active naphthalene was redissolved in methylene chloride, and the washing, drying, and sublimation procedure repeated twice. The activity of the recovered naphthalene was found to be 0.110 microcurie per mg. This is close enough to the first figure to show that the activity is due to naphthalene and not to traces of tritiated water.

Although the activity of the material recovered was disappointingly low, it was high enough to be used in deciding whether diffusivities obtained using this material as tracer were the same or different from those obtained using naphthalene-1-C14.

3. Anthracene. The tracer used in the anthracene studies was anthracene-9-C14, made by Sherwood and Thomson[1] when these workers were measuring diffusion in anthracene. It was resublimed before use. Its activity was 0.6 microcurie per mg.

(iii) Preparation of Crystals for Diffusion Experiments.

In most of the experiments using the tracer-sectioning method and in all of the experiments using the surface-decrease method, diffusion was studied perpendicular to the (001) plane (also called the "ab" plane). In both naphthalene and anthracene this is the cleavage plane and so is readily found.

The crystal for use in a diffusion run was cleaved from a single-crystal boule using a sharp blade. The crystal was cut into a disc approximately 5 mm. thick and 12 mm. in diameter, the two flat faces of the disc being ab planes. The ab face on which radioactive tracer was to be deposited was prepared further either by grinding with carborundum and polishing on a toluene-wet tissue (the polishing method) or by mounting the crystal on the microtome with its cleavage face parallel to the

blade and removing slices from the face until it was perfectly flat. The last slices to be removed were always 1 micron thick (the microtome method). Use of the microtome is described later.

Crystal faces prepared by both these methods were found to be satisfactory for diffusion runs and the method of face preparation did not affect the result (see later). However, preparation by the polishing method occasionally left the face slightly convex instead of flat and such crystals had to be rejected.

Diffusion runs 1 to 14, runs on boule N, the surface-decrease experiments, the anthracene studies, and the "tail" experiments were carried out on crystals prepared by the polishing method. Runs from 14 onwards and those parallel to the "a" and "b" axes were carried out on crystals prepared by microtoming, as were those using tritiated naphthalene as tracer.

For most of the crystals this was all the preparation required. However, some crystals were "specially annealed" before diffusion. These crystals were prepared by the microtome method but, before depositing radioactive material on their propared faces, they were enclosed in a small brass vessel (the same type as was used for the diffusion anneals, q.v.)and immersed in a thermostat where they were annealed to remove any strain, which might have been introduced by the crystal preparation. All "specially annealed" crystals were from a boule which had been annealed after growth and so were effectively twice annealed. The temperature, time, and cooling rate for the "special anneal" were the same as for the first anneal (see Section II B). No further mechanical work was done on these crystals until diffusion was complete.

(iv) Preparation of Crystals for Runs not Perpendicular to the Cleavage Plane.

It was wished to carry out some diffusion experiments on naphthalene in directions other than perpendicular to the cleavage (ab) plane. This

required the various crystallographic axes to be identified and a rapid method of doing this was found.

It was observed that when naphthalene is cleaved the cleavage surface obtained is never perfect but contains a series of parallel lines or steps whose direction bears no relation to the direction of movement of the blade used for cleaving the crystal. It was deduced that these steps always lie parallel to the same crystallographic direction on the ab face. In addition it was found that double refraction vanishes in a direction parallel to the steps, i.e., if a cross is viewed normally through the cleavage face and the crystal rotated in the ab plane the two images of one arm of the cross coincide when the arm is parallel to the steps on the cleavage plane. The steps must, therefore, lie in an optic axial plane. Plane "ac" is such a plane in naphthalene,[100] and so the steps must be parallel to the a-axis. The b-axis is at right angles to the a-axis in the ab-plane.

If the cleavage flake is rotated until one arm of the cross is parallel to the steps and the flake is then tilted, a position can be found in which double refraction vanishes for both arms of the cross. The line of sight is then parallel to the c-axis.

The positions of the a- and b-axes were confirmed as follows: For a Laue photograph the symmetry of the naphthalene crystal is 2/m, i.e., a mirror plane perpendicular to a diad[10] axis. Hence, a photograph taken with the X-ray beam parallel to the b-axis should show a diad axis of symmetry, and one taken with the beam parallel to the a-axis should show a mirror plane. Two specimens were cut from a crystal boule, one of which, it was predicted, would have an "ac" plane and the other a "bc" plane. A Laue photograph of the first specimen taken with the beam parallel to the predicted b-axis and normal to the ac-plane showed a diad axis of symmetry, and a photograph taken of the second specimen with the beam parallel to the predicted a-axis and normal to the bc plane

showed a mirror plane, thus confirming the directions of the a- and b-axes

The author wishes to record his appreciation of the help he obtained in this crystallographic work from Mr. T.S. Wylie of the Nat. Phil. Department and Mr. J.D. Wilson of the Mining Department, both of the University of Strathclyde.

Crystals were cut from a boule to give a plane at right angles to the cleavage plane and parallel to the steps on the cleavage surface. The resulting plane is normal to the b-axis and such crystals were used for experiments in which diffusion was parallel to the b-axis.

Other crystals were cut to give a plane at right angles to both the cleavage surface and the cleavage steps. The resulting plane is normal to the a-axis and such crystals were used for experiments in which diffusion was parallel to the a-axis.

The boule was cut with a toluene-wet thread and the resulting faces prepared by microtoming prior to the diffusion experiments.

(v) Preparation of Polycrystalline Compacts.

Some diffusion experiments were carried out on polycrystalline compacts of naphthalene. The compacts were made by compressing crystalline naphthalene in a die with a $\frac{3}{4}$ in. diameter plunger. Satisfactory compacts were obtained by compressing 1g. of naphthalene under a load of 4 tons applied for 10 secs. The surface on which active naphthalene was to be deposited was polished on toluene-wet tissue.

(vi) Deposition of Radioactive Material on the Specimens.

Radioactive material can be deposited on the prepared faces of the crystals either from a solution or a suspension of the material or by a vapour deposition method. Deposition from solution or suspension gives an uneven deposit and may corrode the prepared face but where diffusion penetration is deep the method is satisfactory. Where penetration is expected to be small a vapour deposition method is better since it does

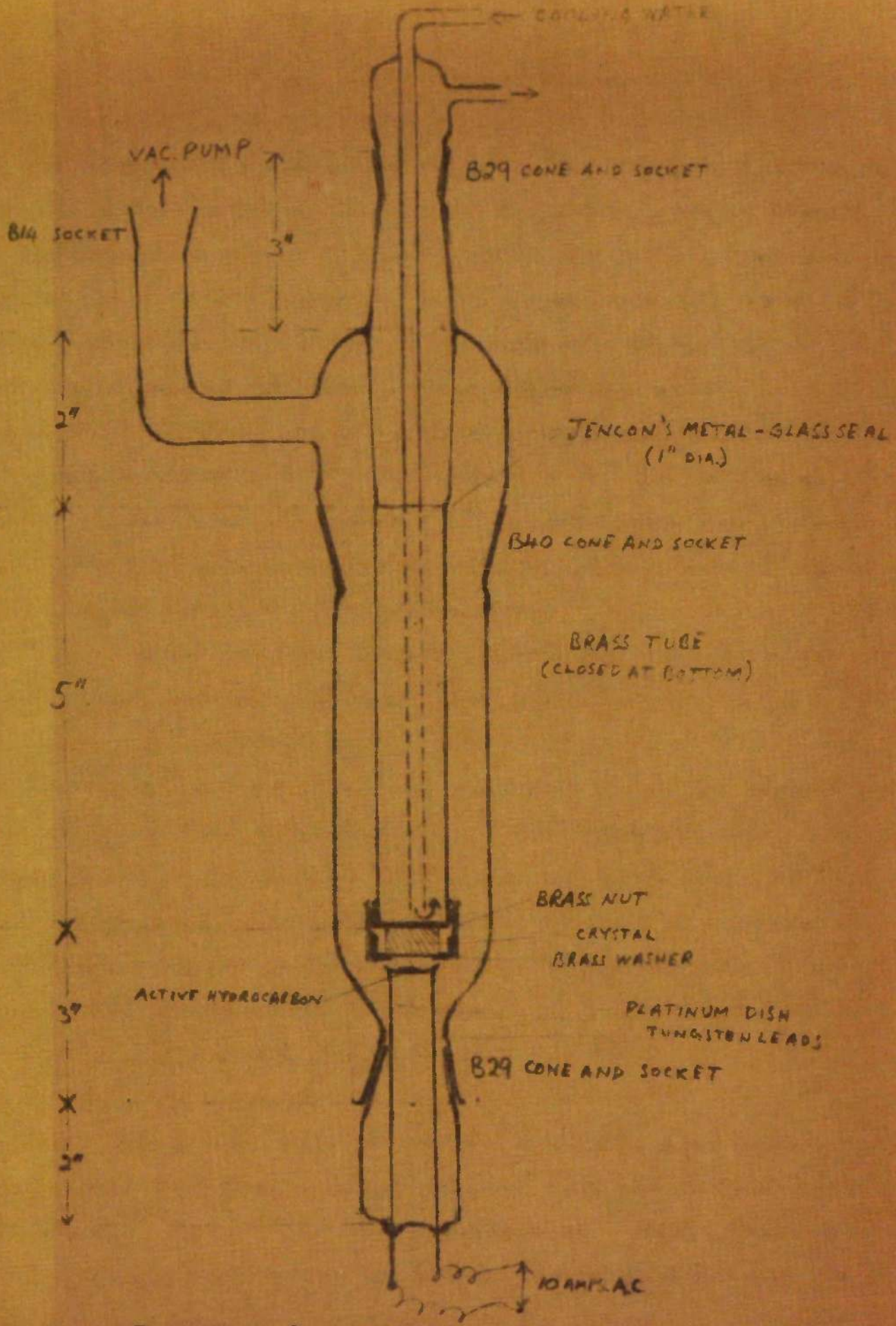

Fig.2.3.1: Deposition Apparatus.

not corrode the prepared face and gives an even, epitaxial layer of the radioactive hydrocarbon on the crystal. A vapour deposition method was used for most of the results reported here.

A diagram of the deposition apparatus is shown in Fig. 2.3.1. It is made of glass except for the closed brass tube and the brass nut which holds the crystal in place. The crystal, with its prepared face downwards is placed in the brass nut which is screwed into place at the base of the closed brass tube. Some radioactive hydrocarbon (1-2mg.) is placed in the platinum dish and the apparatus assembled. Cooling water is passed for 15 mins. and the apparatus evacuated to approximately 0.003 mm. Hg pressure. The radioactive material is flashed onto the prepared crystal face by passing a 10 amp. current through the platinum dish. The apparatus is restored to atmospheric pressure and the crystal with its radioactive deposit removed.

The depositer is approximately 25% efficient for naphthalene and 10% efficient for anthracene. It can be calculated that the active deposits are from 2 to 6 microns thick.

The vapour deposition method was used for all the naphthalene work except the "tail" experiments. In the latter deposition was from acetone solution. In the first anthracene run deposition was by the vapour method but in subsequent runs the tracer was deposited on the prepared face from a fine suspension of active anthracene in a saturated solution of active anthracene in acetone. In these cases the deposit was from 5 to 15 microns thick.

(vii) Diffusion Anneals.

The crystals with their radioactive deposits were enclosed in an air-and water-tight brass vessel, 19 mm. internal diameter with internal length 30mm. They were held in position by a light spring and prevented from coming into contact with the brass vessel by small mica discs. The vessel was immersed in a thermostat at the required experimental temper-

ature for the required time. At the end of the diffusion anneal the brass vessel was removed from the thermostat, allowed to cool, and the crystals removed and sectioned.

Where more than one crystal was enclosed in a vessel the crystals were placed in pairs with their active faces in contact.

For the naphthalene experiments the diffusion anneals were carried out in a water or glycerine thermostat controlled to $\pm$ 0.01C°. The anthracene diffusion anneals were carried out in an air thermostat controlled to $\pm$ 0.1C°. by a Resistance Thermometer Controller, Type RT2. The thermometers used were calibrated against N.P.L. standardised thermometers. Heating up and cooling down times were small compared with the anneal times and were not corrected for.

(viii) Sectioning the Crystals.

At the end of the diffusion anneal the crystals were sectioned using a Beck Sledge-Base Microtome. With this instrument the specimen moves vertically with the blade stationary during a cut. At the completion of one cutting movement the blade moves a pre-set distance towards the specimen in preparation for the next slice. The microtome can be set to give slices of nominal thicknesses from 1 to 15 microns. The instrument has been calibrated and found to give single slices accurate to $\pm$ 5% of the nominal setting, with the accumulative error over 25 slices not greater than 2%.[73,101]

The blade of the microtome can be set at various angles and the crystals are very difficult to cut if the correct blade angle is not used. A nominal blade angle setting of 15 was found to give the smoothest cutting.

Before slicing, the crystal was lined up accurately with the blade so that the sections were removed parallel to the prepared face and so normal to the diffusion direction. This was done by attaching a piece of paraffin wax of about the same dimensions as the crystal onto an adjustible chuck and placing the chuck in the jaws of the microtome. The wax

was sectioned on the microtome until it gave a smooth face after each slice. A small plane mirror was attached to the smooth face with its back flat against the face. A light with cross-wires was reflected from the mirror, focussed onto a piece of paper attached to a screen, and the position of the cross-wires on the paper marked. This procedure was repeated until the cross-wires reflected to the same position each time. The mirror and wax were removed and the crystal to be sectioned attached by its inactive face to the chuck (using black wax or paraffin wax) and the chuck replaced on the microtome ensuring that neither the microtome nor the light were moved in the process. The active surface of the crystal was outwards and to it was attached the small plane mirror. The chuck was then adjusted to bring the reflection of the cross-wires to the marked position. The prepared face of the crystal was then parallel to the face made in the paraffin wax by the microtome blade and so slices removed from the crystal were accurately parallel to the prepared face.

It can be shown that with the light 1 metre from the mirror and the reflected cross-wires an equal distance away, an error in lining up of 1 degree will move the reflected cross-wires 3.5 cm. from the marked position.

Before the crystal was attached to the chuck the sides of the crystal were cut off with a sharp blade. This was to remove any activity which may have diffused over the surface of the crystal and down its sides.

After lining the crystal up with the microtome the blade was brought up to touch the face of the crystal to ensure that the first section was the correct thickness. This was achieved by turning a fine screw on the microtome which brought the blade towards the specimen, moving the crystal down each time until the blade was in a position where the active face of the crystal was scratched evenly when it passed over the blade. The blade was then in the zero position and the crystal ready for

sectioning. Slices of the desired thickness were removed by rotating the handle of the microtome.

As each section was cut it was removed from the microtome blade and placed in a half-dram vial and the vial stoppered. After each slice the face and sides of the crystal were dusted lightly with a piece of paper tissue and the blade cleaned with a toluene-wet tissue. When enough slices were collected each slice was weighed on a microbalance, washed into a scintillation vial with 1-2 c.c. toluene, 10 c.c. scintillator solution added, and its activity measured. In this way the activity was found at known depths in the crystal.

With anthracene crystals 5 micron sections could be removed very smoothly. These were placed directly in the scintillator vial without weighing. Table 2.3.2 shows the weights of 5 micron slices taken from inactive anthracene crystals. Where slice thicknesses greater than 5 microns were required for anthracene these were removed as multiples of 5 microns by placing the required number of 5 micron slices in the same scintillator vial.

Table 2.3.2: Weights of Anthracene Sections.

Experiment 1		Experiment 2	
Section	Weight (mg.)	Section	Weight (mg.)
1	0.340	1	0.832
2	0.345	3	0.827
3	0.347	5	0.824
4	0.345	7	0.825
5	0.350	9	0.820
6	0.351	11	0.824

(ix) Measuring the Radioactivities of the Sections.

In all cases where the tracer-sectioning technique was employed activities were measured by scintillation counting. A general purpose scintillator was used. This was made up by dissolving 3 g. 2,5-diphenyloxazole (PPO) and 0.1 g. 1,4-bis-(2-(5-phenyl-oxazolyl)-benzene (POPOP) in 1 litre of scintillation-grade toluene. 10 c.c. of

scintillator were used for each count.

A block diagram of the counting equipment used is shown in Fig. 2.3.2. It consists of a scintillation counter (photomultiplier) with an amplifier and an E.H.T. supply. The output from the scintillation counter is fed into a linear pulse amplifier and from thence into a pulse-height selector by which the energy and distribution range of the pulses to be counted are selected. The selected pulses are fed into a scaler which counts them and with which is incorporated an automatic timer.

Various counting set-ups were used, the two arrangements most used being shown in Fig. 2.3.2. The scintillation vial with its active sample was placed in the scintillation counter, the optimum E.H.T., amplification (gain), pulse-height (threshold), and gate-width selected and the count rate determined. A "background" count was obtained by counting a vial containing scintillator but no sample. Wherever possible 10,000 counts were taken for each sample giving a standard deviation of 1%.

The count rate - number of counts observed divided by the time of observation - was calculated in counts per second (c.p.s.).

If R_t is the count rate observed for the sample (including background), and R_B is the count rate for background alone, then the count rate (R_s) for the sample alone is

$$R_s = R_t - R_B$$

The counting error (standard deviation) may be calculated from (Poisson Distribution):

$$S_s = (S_t^2 + S_B^2)^{\frac{1}{2}},$$

where

$$S = \left(\frac{R}{t}\right)^{\frac{1}{2}}$$

R and the subscripts have the same meaning as before, t is the time of observation in secs., and s is the standard deviation. The counting

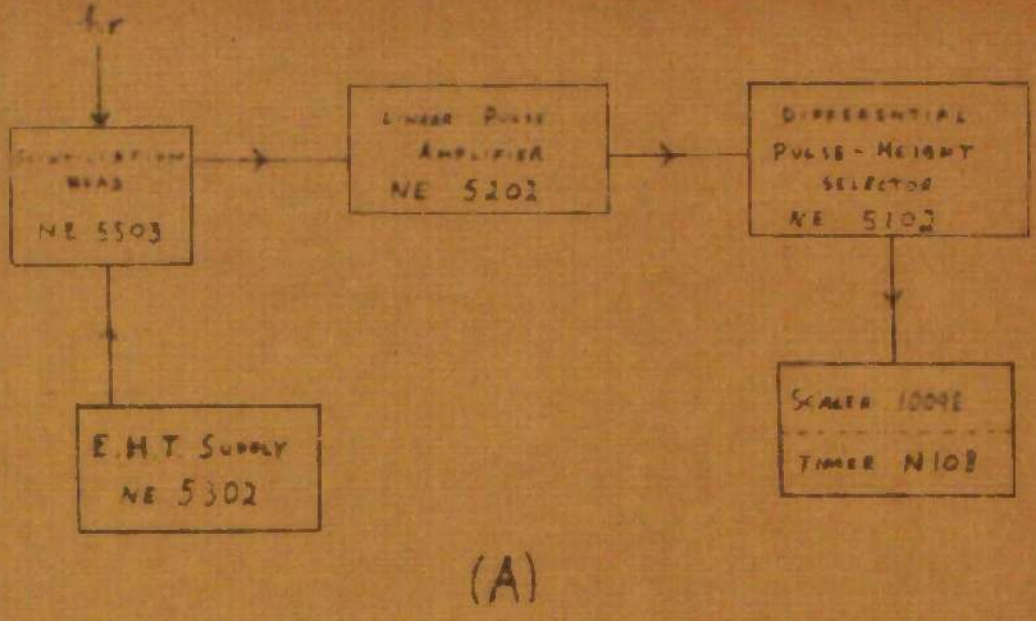

(A)

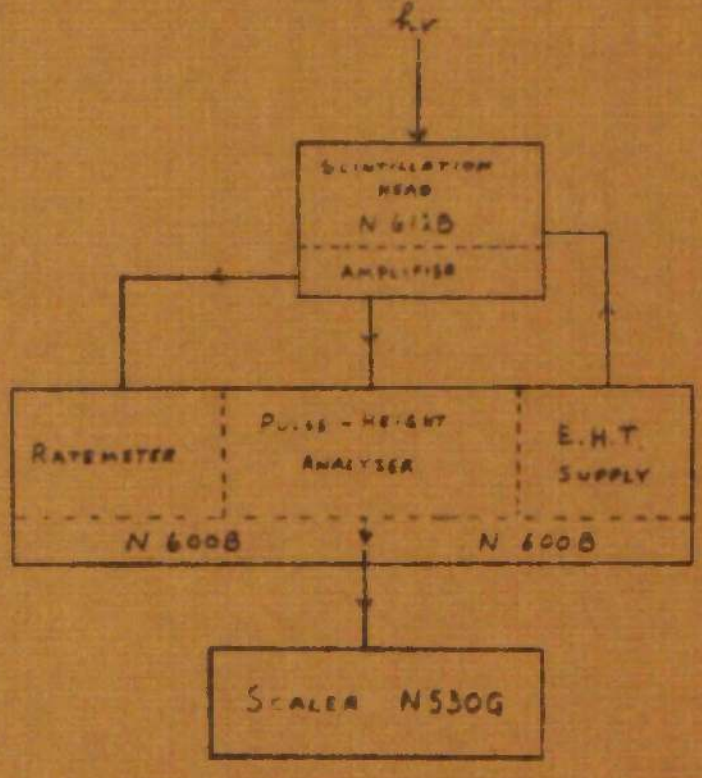

(B)

Fig. 2.3.2: Block Diagram of Counting Equipment

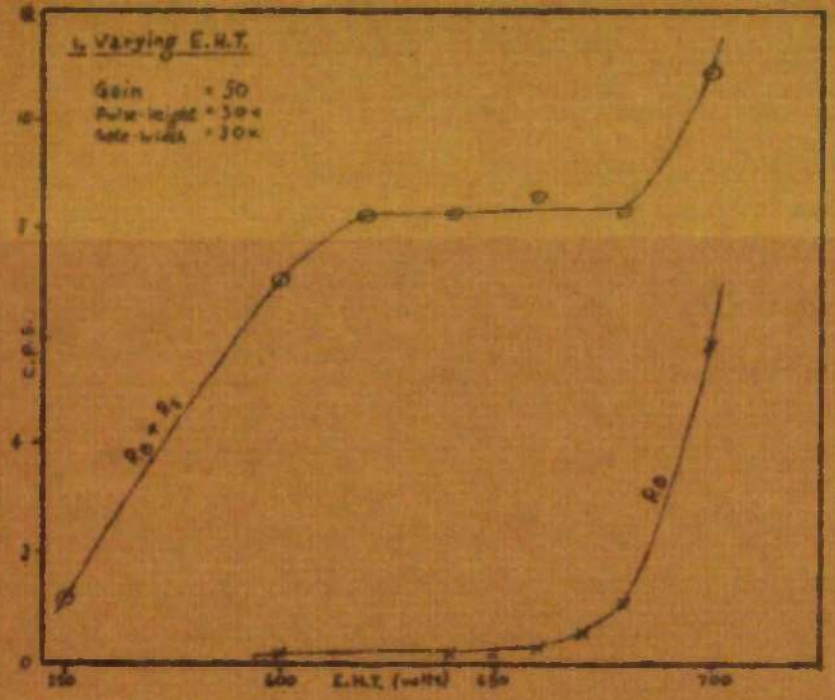

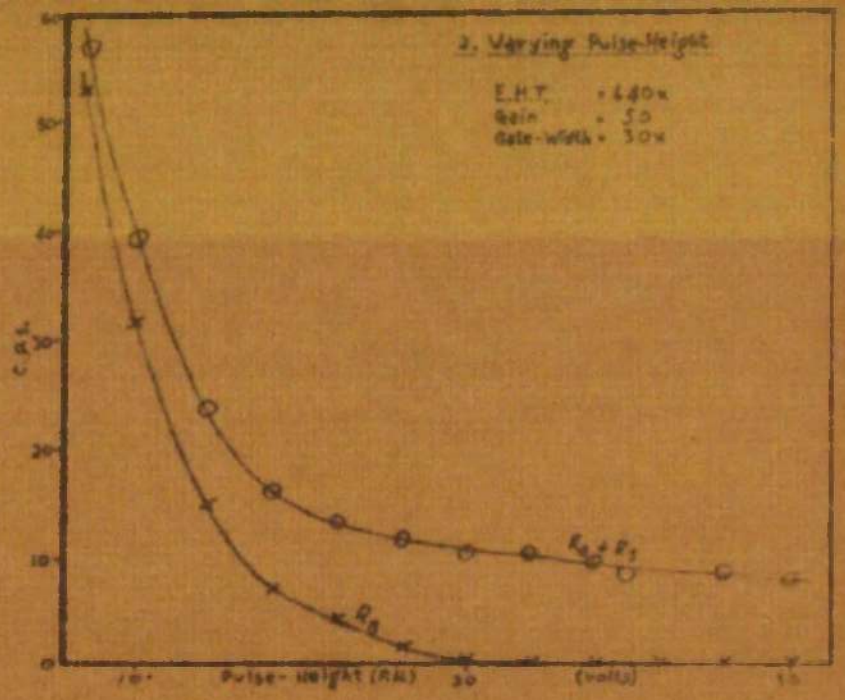

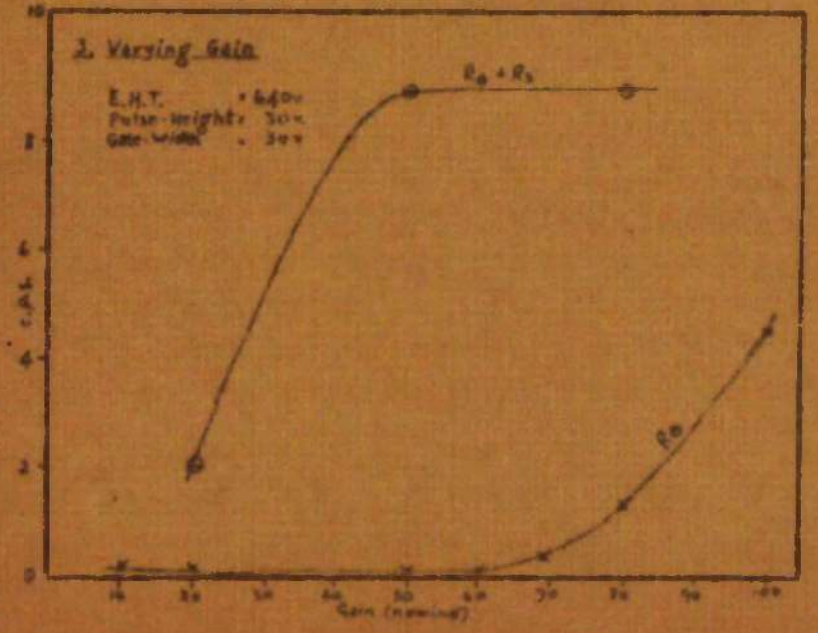

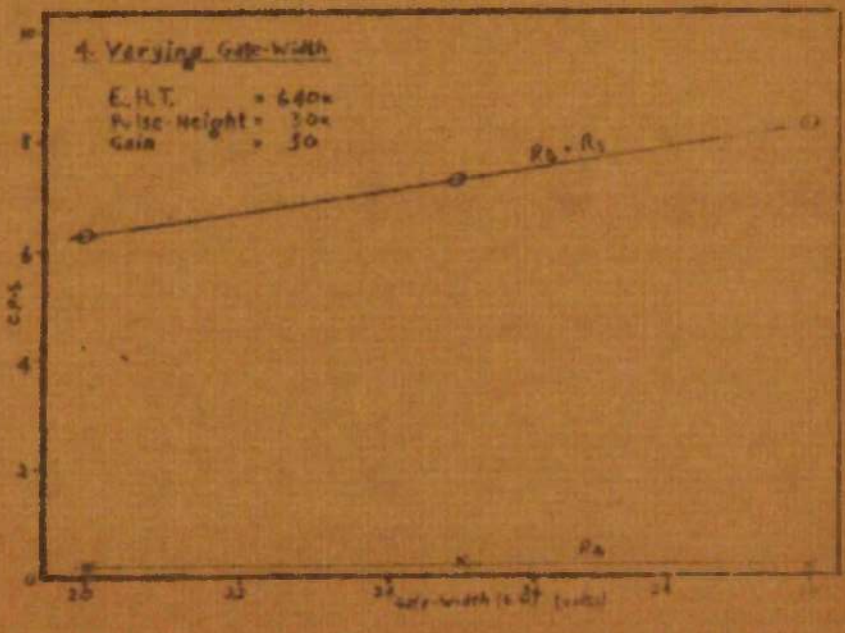

Fig.2.3.3(a): Scintillation Counting Conditions - Equipment A

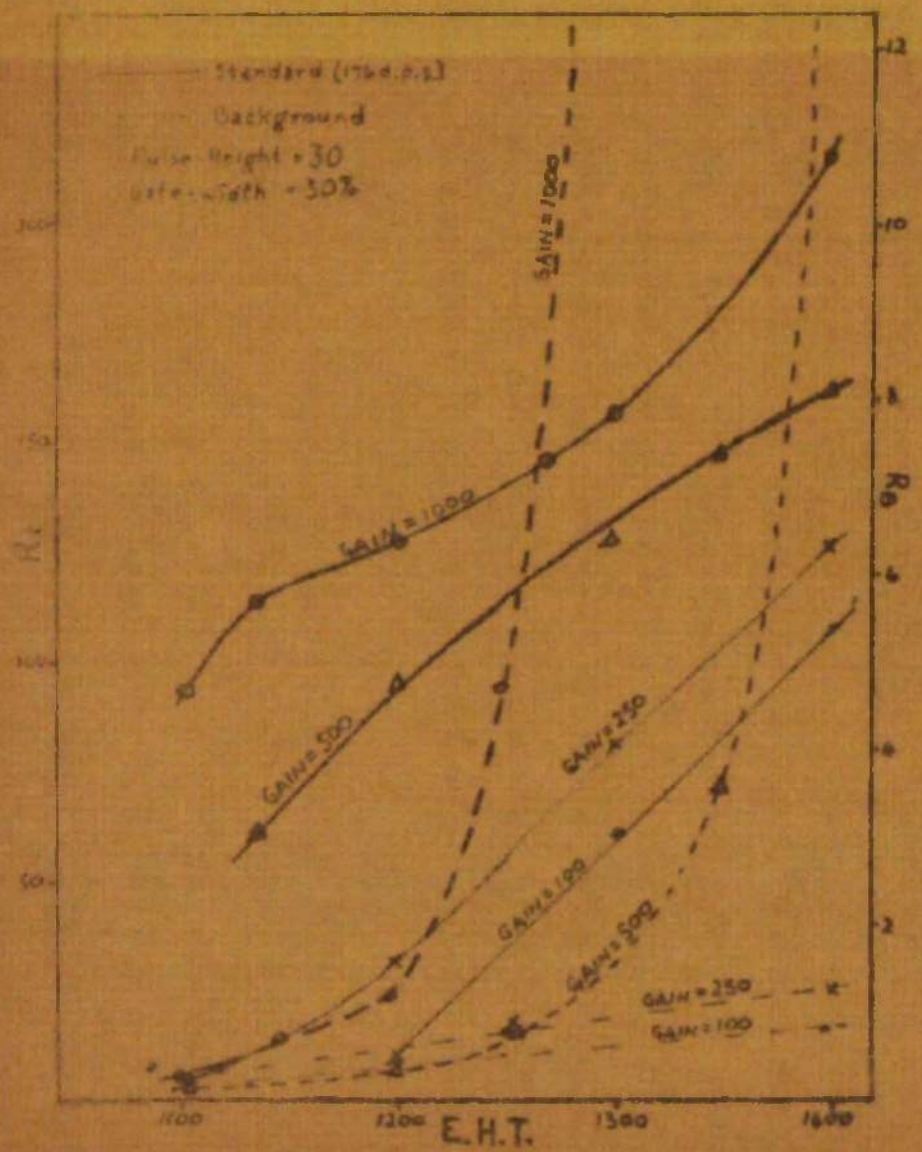

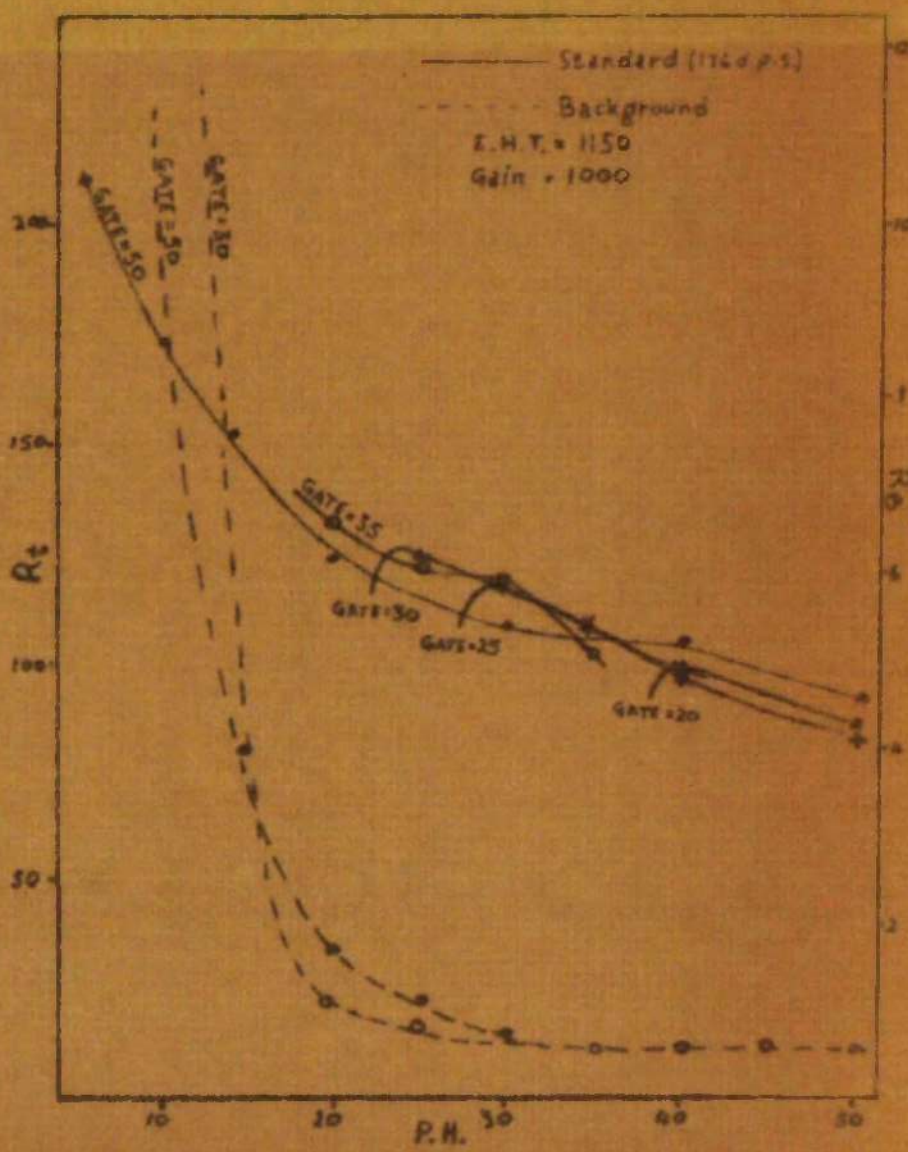

Fig. 2.3.3(b): Scintillation Counting Conditions - Equipment B

errors are not quoted in full in the Tables of Results but a typical calculation is given in the Appendix.

The specific activity (A) was obtained by dividing R_s by the weight of sample in the vial. A is quoted in c.p.s. per mg. For the anthracene results, where the sections were not weighed, A is quoted in c.p.s. per 5 microns.

(x) Counting Conditions.

The optimum conditions for counting were determined by making standard solutions of hexadecane-1-C14 and observing the variations in standard and background counts as the variables in the counting equipment were changed. These variables are the H.T. (E.H.T.) supply, the gain, the pulse-height (P.H.), and the gate-width (G.W.). This was done several times during the course of the work and the optimum conditions for counting found in each case. Examples of the graphs obtained are shown in Fig. 2.3.3 for the equipment shown in Fig. 2.3.2.

The performance of a counter may be characterised by the efficiency, E, where

$$E = R_s / r,$$

R_s being the count rate of a standard of disintegration rate r. E should be as high as possible. For weak samples, where R_s is about 1, the optimum conditions are those where R^2s/R_B (or E^2/R_B) is a maximum. In the present work it was required to count samples varying from fairly high activities to very low activities in the same experiment so that in practice a compromise had to be made between maximising E and maximising R_s^2/R_B.

The conditions used following the analysis of the curves shown in Fig. 2.3.3 were: Equipment A: E.H.T. = 640 volts, Gain = 50 (nominal), P.H. = 30, G.W. = 30. This gives a background count of 0.15 c.p.s. and a counting efficiency of 50%. E^2/R_B = 16,700. Equipment B: E.H.T. = 1150 volts, Gain = 1,000, P.H. = 30, G.W. = 25. This gives a background of 0.6 c.p.s. and a counting

efficiency of 66%, with $E^2/R_{Bi} = 7,260$.

As well as finding the best counting conditions it was necessary to find if the following had any effect on the count rate:

(a) The volume of scintillator used. This is shown in Table 2.3.3. It is seen that scintillator volume has no effect between volumes of 2 and 20 c.c.

Table 2.3.3: Effect of Scintillator Solution Volume.

Total Volume of Scintillator c.c.	Activity c.p.s.	Total Volume of Scintillator c.c.	Activity c.p.s.
1	28.69 ± 0.29	8	29.30 ± 0.29
2	29.82 ± 0.30	9	29.39 ± 0.29
3	29.90 ± 0.30	10	29.56 ± 0.29
4	29.80 ± 0.30	11	29.44 ± 0.29
5	29.36 ± 0.29	12	29.51 ± 0.29
6	29.34 ± 0.29	15	29.48 ± 0.29
7	29.45 ± 0.29	20	29.30 ± 0.29

(b) Effect of time. A sample may change its count slightly from day to day. This was observed frequently but did not always occur. The effect is probably due to small fluctuations in the counting equipment. To overcome this all samples concerned with a particular experiment were counted on the same day.

(c) Effect of scintillator vial. It is possible that a count may vary depending on which vial contains the sample. Table 2.3.4. shows the counts obtained from ten different vials containing 10 c.c. scintillator each but no sample. It is seen that there are small differences between vials. While the differences are insignificant for most counts, they become important for very small counts such as those found in the "tail" experiments.

Table 2.3.4: Effect of Scintillator Vial.

Vial No.	Activity c.p.s.	Vial No.	Activity c.p.s.
1	1.07±0.02	6	1.28±0.02
2	1.08±0.03	7	0.99±0.03
3	1.09±0.03	8	1.12±0.02
4	1.15±0.04	9	1.03±0.02
5	1.16±0.04	10	1.10±0.02

Average = 1.07; Range = 0.99 to 1.28

(d) Effect of dilution of scintillator. Since small amounts of toluene were used to wash the samples into the scintillation vials the effect of small additions of toluene to the scintillator had to be discovered. Table 2.3.5 shows counts obtained from a sample containing 10 c.c. of scintillator with small amounts of toluene added. It is seen that there is no significant effect.

Table 2.3.5: Effect of Dilution by Toluene.

Total Vol. of Toluene added (c.c.)	Activity (c.p.s.)	Total Vol. of Toluene added (c.c.)	Activity (c.p.s.)
Nil	24.25±0.14	5.0	24.40±0.44
1.0	24.42±0.45	6.5	24.41±0.45
2.0	24.50±0.45	10.0	24.10±0.44
4.0	24.35±0.44	12.0	22.55±0.24

(e) Possible "quenching" by naphthalene. There is a possibility that the addition of naphthalene to the scintillator quenches it. However, Table 2.3.6, shows that naphthalene has no quenching effect on the count.

Table 2.3.6: "Quenching" Effect of Naphthalene.

Experiment 1

Total Wt. of naphthalene present (g.)	Activity (c.p.s.)

Experiment 2.

Total Wt. of naphthalene present (g.)	Activity (c.p.s.)

See over.

Experiment 1		Experiment 2	
Total Wt. of naphthalene present (g.)	Activity (c.p.s.)	Total Wt. of naphthalene present (g.)	Activity (c.p.s.)
Nil	34.33±0.31	Nil	36.42±0.36
0.0004	35.01±0.34	0.070	36.24±0.36
0.0014	34.66±0.31	0.241	36.64±0.37
0.0111	34.48±0.41	0.516	36.45±0.36
0.0334	34.27±0.41	0.888	36.37±0.36
0.0764	34.71±0.41	1.213	36.79±0.37

(f) Possible "quenching" by anthracene. Table 2.3.7 shows the effect of anthracene on the count-rate. Crystalline anthracene was used in the first experiment and zone-refined anthracene in the second experiment.

Table 2.3.7: Quenching by Anthracene.

Total Wt. of Anthracene present (mg.)	Activity (c.p.s.)	Total Wt. of Anthracene present (mg.)	Activity (c.p.s.)
Experiment 1		Experiment 2	
Nil	29.20±0.23	Nil	33.15±0.26
0.605	29.00±0.37	0.378	33.15±0.33
1.040	28.42±0.52	1.159	30.67±0.32
2.264	27.38±0.25	2.065	28.74±0.26
3.281	26.26±0.40	2.534	27.48±0.26
5.763	23.80±0.14	4.488	26.19±0.26
7.003	22.90±0.42		
9.559	20.87±0.27		

Quenching is quite marked. However, for the diffusion runs - where very small quantities are counted and the same amount of anthracene is present in each case - no correction is required. Where slice thicknesses were varied in a particular experiment the count-rate was corrected for differences in quenching between slices.

(xi) Surface-Decrease Measurements.

In this technique a thin deposit of active material is placed on a plane surface of the crystal and the decrease of surface activity with time is measured.

The apparatus constructed is shown in Fig. 2.3.4. It consists of a thin-windowed Geiger-Muller tube contained in a cylindrical brass vessel, the leads of the G.-M. tube passing out of the vessel through a brass pipe. The crystal is placed in the brass crystal holder with its active deposit upwards. A thin film of mica is placed over the active surface to prevent losses by evaporation, and the cap screwed into place. The crystal holder is assembled and screwed into position in the brass vessel by means of the matching threads. The end of the G.-M. tube is held against the holder by the spring. All external threads are made water-tight with "threadseal" teflon tape.

When assembled the apparatus is immersed in a thermostat maintained at the desired temperature ($\pm 0.01°C$), and the leads connected to a scaler type N529D via a probe unit. Count-rates are taken at intervals and so surface activity measured as a function of time.

An E.H.T. of 500 volts was used for the G.-M. tube (one-third of the way along the plateau). A background count was taken either before the experiment was started or after its completion.

The crystals used in the experiments were prepared by polishing as described in (iii) above and the radioactive deposits made by the vapour deposition method (section (vi) above).

All diffusion measurements by the surface-decrease method were made perpendicular to the "ab" plane in single crystals of naphthalene.

(xii) Annealing Experiments.

These experiments were carried out to attempt a quantitative determination of the affect of annealing the crystals. It had previously been found that the diffusion coefficient of an annealed crystal was smaller

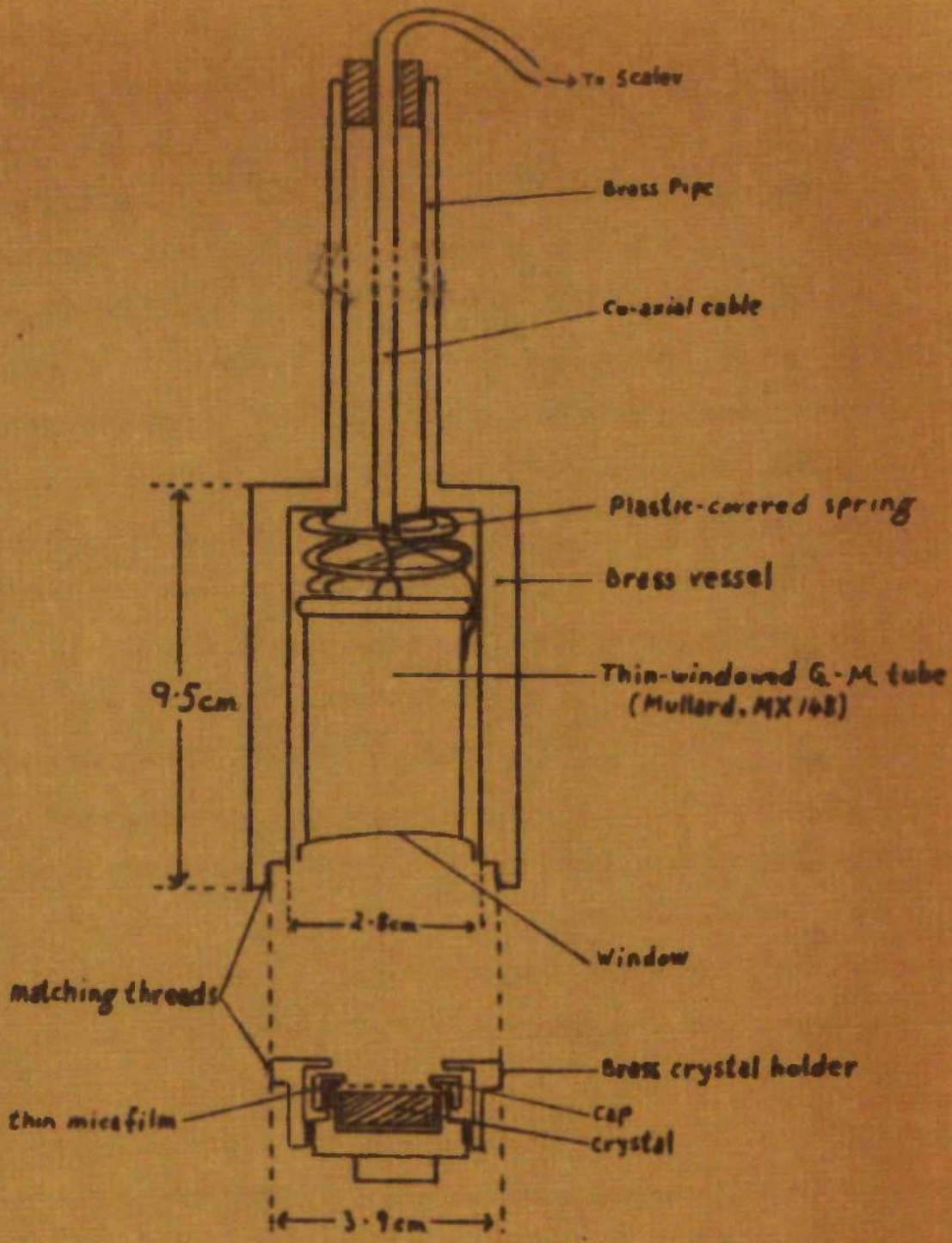

Fig. 2.3.4: Surface-Decrease Apparatus.

than that of the same crystal unannealed. The method used for measuring the diffusion coefficients was exactly as described above for the tracer-sectioning experiments, however, the annealing treatment prior to the diffusion anneal was varied.

Several crystals from the same naphthalene boule were prepared by the polishing method, enclosed (without active deposits) in a brass vessel, and the vessel immersed in the thermostat at a temperature close to the melting-point. This temperature is described in the results as the annealing temperature, T_a. Crystals were removed from the thermostat at varying times so that several crystals were obtained from the same boule, the crystals having been annealed at T_a for differing annealing times, t_a. When the last crystal had been removed, radioactive deposits were placed on them, and their diffusion coefficients measured at a lower temperature, T_d (the "diffusion temperature"). In all cases diffusion was measured perpendicular to the "ab" plane.

(xiii) "Tail" Experiments.

Typical diffusion "tails" were found in many of the diffusion runs described in this thesis. However, the activity in the tail region was so low that the counts were of doubtful significance. Several experiments were carried out on naphthalene to try to measure the activity of the tail more accurately. In these experiments the crystals were prepared by the polishing method as for a normal experiment in which diffusion was to be measured perpendicular to the cleavage plane. Radioactive naphthalene was deposited from acetone solution on the prepared faces and the crystals enclosed in a glass tube and immersed in a thermostat at the required temperature for the diffusion anneal. At the end of the diffusion time the crystals were removed and all surfaces cut away with a scalpel to a depth greater than the probable bulk diffusion penetration. The remainder of the crystals were washed with toluene to remove any active fragments, crushed, weighed into scintillation vials, and their

activities determined.

By this method a very much larger weight of crystal was obtained than in sectioning, and hence a better estimate of the tail activity could be made on the assumption that the tail activity is levelled throughout the crystal by rapid diffusion along short-circuiting paths. The results are discussed later in the thesis.

(xiv) Sources of Error.

Most sources of error, such as deposit thickness, quenching effects, etc., have already been dealt with. Of the possible sources of error not yet discussed the most important are (a) unevenness of the deposit, (b) losses of activity during the diffusion anneal, and (c) the possibility of contamination of sections during microtoming of the crystal.

(a) Unevenness of the Radioactive Deposit.

Microscopic examination of deposits made by the vapour deposition method showed that the material was deposited in a thin, even disc of diameter equal to that of the hole in the brass washer of the deposition apparatus (Fig. 2.3.1). "Whiskers" were observed growing out from the deposit but were few in number. Since the diameter of the crystal was greater than the diameter of the hole in the brass washer, there was always a small area of the prepared face not covered by the circular deposit. Deposits made from solution or suspension were also thin but were less even than those made by the vapour method.

The only likely source of error in the deposits made by both methods appears to be that due to incomplete coverage of the prepared surface. This problem has been discussed in several diffusion studies, notably by Tannhauser[107] who shows that it is not necessary for the diffusing species to be deposited evenly over the entire surface and that the error introduced by non-uniform coverage is zero.

(b) Losses of Activity.

Active material could be lost from the diffusion face by surface

diffusion round the crystal or by evaporation during the diffusion anneal. After a diffusion anneal the edges and back of the crystal were always active. Table 2.3.8 shows the activities found on the diffusion surface, the edges, and back of various crystals used in diffusion runs. The activities are quoted in c.p.s. per sq. cm. of surface. The background count (R_B) is given for comparison.

Table 2.3.8: Surface Activity after the Diffusion Anneal.

Run	Diff. Surface Activity (c.p.s./cm.^{2})	Back Surface Activity (c.p.s./cm.^{2})	Edges Activity (c.p.s./cm.^{2})	R_B (c.p.s.)
17B	212.3	9.4	41.7	0.2
A1	43.6	11.7	40.3	0.4
D2	61.0	30.7	53.6	0.7
D3	138.6	10.3	40.1	0.2
D6	325.7	14.6	82.0	0.6

It is seen that considerable activity is present on the edges and back of the crystals. However, it is possible that active material reaches the surfaces, not by diffusion from the deposit or by evaporation and re-deposition on the other surfaces, but during the deposition itself. The crystal does not fit tightly into the brass nut of the depositer and so it is possible that active material escapes through the washer and reaches the back and sides of the crystal. To test this a deposit was made on a crystal and the deposition surface, the back, and the edges of the crystal removed immediately and tested for activity. The activities found are shown in Table 2.3.9.

Table 2.3.9: Surface Activity after Deposition.

On the prepared (deposition) surface---------- 59.1 c.p.s./cm.^{2}
On the back surface---------- 23.0 c.p.s./cm.^{2}
On the edges---------- 21.2 c.p.s./cm.^{2}

Thus much of the activity on the edge and back found after a diffusion

anneal is there before diffusion commences.

To find how much active material reached the surfaces during a diffusion anneal, a deposit was made on a crystal, the edges and back of the crystal cut away to eliminate activity reaching them during the deposition, and the crystal with its active deposit enclosed in a brass vessel and immersed in a thermostat at 78.4 °C. for 70 hours. The surfaces of the crystal were then removed and their activities and the activity of the remainder of the crystal determined. The inside of the vessel was washed out with toluene and the activity of the washings measured. The result of the experiment is shown in Table 2.3.10.

Table 2.3.10: Activity Losses at 78.4 °C.

	Count per unit area (c.p.s./cm.^{2})	Absolute Count (c.p.s.)	Count as fraction of total count %
Diff. surface:	1090	305.2	88.0
Back surface:	19.7	5.5	1.6
Edges:	27.7	16.6	4.8
Remainder of Xtal:	-	3.8	1.1
Washings:	-	15.6	4.5

It is seen that the diffusion surface is far more active than any of the other surfaces. However, there are some losses. Allowing for the activity in the remainder of the crystal and assuming that the edges and back are active to the same level, the losses by evaporation and surface diffusion are about 10%. However, most of the losses will be from the "whiskers", which offer a very large surface area, and in addition the experiment is rather a severe test (1.6° below the melting-point for almost 3 days) where evaporative losses will be at a maximum. The losses in the diffusion experiments themselves will usually be less.

That gross losses of activity from the surface do not occur can also be shown by taking counts with a thin-windowed G.-M. tube before and after the diffusion anneal. Examples likely to give losses greater than average are given in Table 2.3.11.

Table 2.3.11: Surface Counts before and After Diffusion.

	(a)	(b)	(c)	(d)
Count before diffusion anneal (c.p.s.):	336	200	1214	310
Count after 65 hrs. at 74.9°C. (c.p.s.):	210	170	-	-
Count after 356 hrs. at 78.2°C. (c.p.s.):	-	-	900	280

The agreement of the diffusion coefficients obtained by the surface-decrease method with those obtained by the tracer-sectioning technique is also good evidence that large activity losses do not occur.

Any error in the tracer-sectioning method which might be caused by the active edges was eliminated by cutting away the edges of the crystal before sectioning.

(c) Contamination.

Great care was taken during the sectioning of the crystals that slices should not contaminate each other. However, since it would require only an extremely small amount of contamination from the first slice to give significant increases in the counts of subsequent slices, experiments were carried out to ensure that such contamination did not occur. These experiments also served to check that the lining-up technique was efficient, and to discover if appreciable diffusion takes place at room temperature.

Three crystals from naphthalene boule N were prepared by the polishing method and active naphthalene deposited from acetone solution on the prepared faces. The crystals were stored in a glass bottle at room

temperature. After varying times the crystals were removed, lined-up on the microtome and sectioned as for an ordinary diffusion run. Table 2.3.12 gives the activities of the first to the fifth sections of these crystals. All sections were 5 microns thick. R_B is the background count, R_s the slice count minus R_B, and t is the time elapsing between deposition of active material on the surface and microtoming of the crystal.

Table 2.3.12: Room Temperature Experiments.

Expt. No.	RT1	RT2	RT3
R_B (c.p.s.)	1.18±0.01	1.25±0.02	1.29±0.02
t	24 hours	17 days	8.4 weeks
Slice	R_s (c.p.s.)	R_s (c.p.s.)	R_s (c.p.s.)
1	328.0±1.2	25.8±0.3	93.3±0.9
2	4.60±0.06	0.39±0.04	3.07±0.04
3	0.50±0.02	0.02±0.05	1.96±0.03
4	0.33±0.02	Nil±0.05	1.49±0.02
5	0.40±0.02	0.07±0.04	1.51±0.02

These experiments show that (a) contamination does not extend beyond the second, or at most the third, slice; (b) the lining-up technique is excellent; and (c) measurable diffusion does not take place at room temperature even after 2 months.

PART III. -- RESULTS.

RESULTS

(i) Introduction.

The results for the tracer-sectioning experiments on naphthalene are given in Tables 3.1 to 3.6 and plotted in the Figures numbered correspondingly. Surface-decrease results are shown in Table 3.7 and Fig. 3.7. Anthracene results are dealt with after naphthalene.

In the Tables and Figures, A is the specific activity in counts per second per milligram, or, in the anthracene results where sections were not weighed, A is in c.p.s. per 5 micron slice. The distance, d, from the active deposit is taken as the distance from the centre of the section to the active surface.[102,103] The distance, d, is quoted in microns and d^2 in square microns. The other Tables and Figures are explained in the appropriate places.

Table 3.1 Naphthalene - Diffusion Perpendicular To "ab" Plane.

(Tracer-sectioning method, using Naphthalene-1-C14 as tracer)

Run	t(hrs.)	Slice	d	A	d^2	logA
1 A	48.0	8,9	120.0	5.06	14,400	0.704
		11	157.5	3.44	24,800	0.537
		12	172.5	3.30	29,750	0.519
		13	187.5	2.46	35,160	0.391
		14	202.5	1.98	41,020	0.297
		16	232.5	1.41	54,050	0.149
		17	247.5	1.07	61,270	0.029
		18	262.5	0.91	68,900	$\bar{0}.959$ -0.041
2 A	72.0	1	7.5	206.5	56	2.315
		3	37.5	421.5	1410	2.625
		5	67.5	261.2	4560	2.417
		7	97.5	83.9	9510	1.924
		10	142.5	21.7	20,300	1.337
		11	157.5	17.6	24,800	1.246
		12	172.5	6.07	29,750	0.783
		14	202.5	3.02	41,020	0.480
3	69.67	3,4	45	25.6	2,025	1.408
		7,8	105	41.1	11,025	1.614
		9,10	135	18.1	18,025	1.258
		11,12	165	7.03	27,225	0.847
		13,14	195	8.40	38,025	0.924
		17,18	255	1.50	65,025	0.172
4	26.17	2	22.5	340.4	506	2.532
		6	82.5	140.0	6,808	2.146
		8	112.5	92.5	12,660	1.966
		10	142.5	20.3	20,310	1.308
		14	202.5	16.6	41,020	1.221
		15	217.5	19.6	47,320	1.293
		17	247.5	18.1	61,270	1.258
		18	262.5	13.4	68,900	1.128
		22	322.5	11.1	104,000	1.045
6	146.5	4	52.5	56.8	2,757	1.754
		6	82.5	39.5	6,808	1.596
		8	112.5	18.6	12,660	1.270
		10	142.5	7.43	20,310	0.871

Table 3.1 (cont/d.)

Run	Δ(hrs.)	Slice	d	A	d^2	logA
7 A	119.08	1	7.5	33.1	56	1.519
		2	22.5	18.3	506	1.262
		3	37.5	5.69	1,406	0.755
		4	52.5	2.12	2,757	0.327
		5	67.5	2.39	4,556	0.378
		6	82.5	2.69	6,808	0.430
7 B	119.08	1	7.5	101.4	56	2.006
		2	22.5	36.6	506	1.564
		3	37.5	3.40	1,406	0.531
		4	52.5	2.46	2,757	0.390
		5	67.5	3.23	4,556	0.509
8	41.0	1	5	368.8	25	2.567
		3	25	182.4	625	2.261
		4	35	136.2	1,225	2.134
		5	45	122.1	2,025	2.087
		6	55	60.0	3,025	1.778
		7	65	26.8	4,225	1.428
		8	75	7.26	5,625	0.861
		10	95	0.81	9,025	-0.092
9	48.0	1	5	628.3	25	2.798
		2	15	631.6	225	2.800
		3	25	275.0	625	2.439
		4	35	92.4	1,225	1.966
		5	45	7.57	2,025	0.879
		6	55	0.37	3,025	-0.432
		7	65	0.20	4,225	-0.699
		8	75	0.40	5,625	-0.398
11 A	20.0	2	15	25.7	225	1.410
		3	25	11.4	625	1.057
		4	35	1.55	1,225	0.190
		6	55	0.22	3,025	-0.66
		7	65	(0.11)	4,225	(-0.92)
		9	85	(0.05)	7,225	(-1.7)

Table 3.1 (cont/d.)

Run	t (hrs.)	Slice	d	A	d^2	logA
11 B	20.0	1	5	17.39	25	1.240
		2	15	8.98	225	0.953
		3	25	4.49	625	0.652
		4	35	1.50	1,225	0.176
		5	45	1.08	2,025	0.033
		7	65	1.33	4,225	0.124
		8	75	0.97	5,625	-0.013
12 A	48.0	1	5	3.36	25	0.527
		2	15	1.40	225	0.147
		3	25	1.00	625	-0.002
		4	35	0.49	1,225	-0.312
12 B	48.0	1	5	518.1	25	2.714
		2	15	168.0	225	2.225
		3	25	53.8	625	1.731
		4	35	26.1	1,225	1.416
		5	45	8.33	2,025	0.921
		6	55	2.11	3,025	0.325
		7	65	0.43	4,225	-0.366
		8	75	0.18	5,625	-0.752
14	96.0	1	5	105.3	25	2.022
		2	15	14.09	225	1.149
		3	25	5.30	625	0.724
		4	35	2.13	1,225	0.328
		5	45	0.95	2,025	-0.022
		6	55	0.63	3,025	-0.201
		7	65	0.57	4,225	-0.244
15 A	65.0	1	5	17.64	25	1.247
		3	25	6.61	625	0.820
		4	35	1.93	1,225	0.286
		5	45	0.38	2,025	-0.420
15 C	65.0	3	25	7.96	625	0.901
		4	35	4.33	1,225	0.637
		5	45	4.50	2,025	0.653
		6	55	2.85	3,025	0.455
		7	65	2.17	4,225	0.337
		8	75	0.71	5,625	-0.149
		9	85	0.23	7,225	-0.638

Table 3.1 (cont/d.)

Run	t (hrs.)	Slice	d	A	d^2	logA
16 C	89.0	7	65	139.8	4,225	2.146.
		8	75	44.31	5,625	1.647
		9	85	9.11	7,225	0.960
		10	95	2.17	9,025	0.337
		11	105	0.30	11,025	-0.523
		13	125	0.27	15,625	-0.569
		14	135	0.31	18,225	-0.509
17 A	449.0	1	5	162.4	25	2.212
		2	15	243.0	225	2.386
		3	25	113.1	625	2.054
		4	35	7.39	1,225	0.869
		5	45	1.70	2,025	0.230
		6	55	1.88	3,025	0.274
		7	65	1.59	4,225	0.201
		8	75	1.16	5,625	0.065
		9	85	1.16	7,225	0.065
		10	95	0.71	9,025	-0.149
17 B	449.0	1	5	366.3	25	2.564
		2	15	172.3	225	2.236
		3	25	31.20	625	1.494
		4	35	2.32	1,225	0.366
		5	45	0.59	2,025	-0.229
		6	55	0.38	3,025	-0.420
		7	65	0.47	4,225	-0.328
		8	75	0.43	5,625	-0.366
		9	85	0.42	7,225	-0.377
		10	95	0.37	9,025	-0.432
18	546.17	2	15	400.8	225	2.603
		4	35	242.5	1,225	2,385
		5	45	166.2	2,025	2.221
		6	55	83.22	3,025	1.920
19 A	113.0	1	5	153.2	25	2.185
		2	15	122.4	225	2.088
		3	25	22.20	625	1.346
		4	35	9.56	1,225	0.981
		5	45	1.85	2,025	0.267
		6	55	0.20	3,025	-0.699

Table 3.1 (cont/d.)

Run	t(hrs.)	Slice	d	Δ	d^2	logΔ
19 B	113.0	3	25	4.42	625	0.645
		4	35	4.93	1,225	0.693
		5	45	3.81	2,025	0.581
		6	55	1.79	3,025	0.253
		7	65	1.63	4,225	0.212
20 A	396.0	1	5	17.8	25	1.251
		2	15	1.20	225	0.080
		3	25	0.04	625	-1.398
20 B	396.0	1	5	191.5	25	2.282
		2	15	39.27	225	1.594
		3	25	1.34	625	0.127
21	556.0	1	2.5	6.03	6.25	0.780
		2	7.5	3.75	56.25	0.574
		3	12.5	3.17	156	0.501
		4	17.5	2.03	306	0.308
		5	22.5	1.15	506	0.061
		6	27.5	0.91	756	-0.186
		7	32.5	0.71	1,056	-0.487
		8	37.5	0.13	1,406	-0.886
22 A	46.0	1	5	90.61	25	1.957
		2	15	73.78	225	1.868
		3	25	64.14	625	1.807
		4	35	25.32	1,225	1.403
		5	45	3.74	2,025	0.573
		6	55	0.65	3,025	-0.187
		7	65	0.32	4,225	-0.495
		8	75	(0.11)	5,625	(-0.959)
22 B	46.0	1	5	161.1	25	2.207
		2	15	144.7	225	2.161
		3	25	100.3	625	2.001
		4	35	48.09	1,225	1.682
		5	45	16.30	2,025	1.212
		6	55	2.59	3,025	0.413
		7	65	0.66	4,225	-0.180

Table 3.1 (cont/d).

Run	t (hrs.)	Slice	d	A	d^2	logA
23	336.0	1	5	389.0	25	2.590
		2	15	209.5	225	2.321
		3	25	115.2	625	2.062.
		4	35	63.24	1,225	1.801
		5	45	27.61	2,025	1.441
		6	55	9.18	3,025	0.963
		7	65	2.16	4,225	0.335
		8	75	0.61	5,625	-0.215
26 A	63.1	1	5	4.70	25	0.672
		2	15	3.03	225	0.481
		3	25	0.92	625	-0.030
		4	35	0.31	1,225	-0.510
		5	45	0.07	2,025	-0.150
27	113.0	1	3	4.24	9	0.627
		2	8.5	2.54	72.25	0.405
		3	13.5	1.49	182.3	0.173
		4	18.5	0.88	342	-0.055
		5	23.5	0.45	552	-0.347
29	65.0	1	5	571.5	25	2.757
		2	12.5	23.2	156	1.366
		3	17.5	9.66	306	0.985
		4	22.5	3.84	506	0.584
		5	27.5	2.85	756	0.455
		6	32.5	2.71	1,056	0.433
		7	37.5	2.16	1,406	0.335
		8	42.5	1.96	1,806	0.292
		9	47.5	1.74	2,256	0.241
		10	52.5	1.68	2,756	0.225
30 A	356.0	1	2.5	1,400.	6.25	3.15
		2	7.5	42.0	56	1.623
		3	12.5	59.4	156	1.774
		4	17.5	12.5	306	1.097
		5	22.5	21.7	506	1.337
		6	27.5	4.94	756	0.694
		7	32.5	7.68	1,056	0.885
		8	37.5	4.83	1,406	0.684
		9	42.5	2.55	1,806	0.407
		10	47.5	1.71	2,256	0.233
		11	52.5	1.26	2,756	0.100
		12	57.5	0.59	3,306	-0.229

Table 3.1 (cont/d.)

Run	t (hrs.)	Slice	d	Δ	d^2	logΔ
30B	356.0	1	2.5	4,772	6.25	3.679
		2	7.5	502	56	2.701
		3	12.5	343	156	2.535
		4	17.5	247	306	2.393
		5	22.5	157.6	506	2.198
		6	27.5	112.1	756	2.050
		7	32.5	44.5	1,056	1.648
		8	37.5	15.3	1,406	1.185
		9	42.5	3.55	1,806	0.550
		10	47.5	0.70	2,256	-0.155
		11	52.5	1.04	2,756	0.017
		12	57.5	0.58	3,306	-0.237
31	21.5	1	2.5	900	6.25	2.954
		2	7.5	14.8	56	1.170
		6	27.5	4.24	756	0.627
		7	32.5	3.16	1,056	0.500
		10	47.5	0.27	2,256	-0.569
		12	57.5	0.06	3,306	-1.222
32	70.0	1	2.5	480.8	6.25	2.682
		2	7.5	446.8	56	2.650
		3	12.5	304.9	156	2.484
		4	17.5	258.6	306	2.413
		5	22.5	164.4	506	2.216
		6	27.5	78.4	756	1.894
		7	32.5	53.6	1,056	1.729
		8	37.5	35.1	1,406	1.545
		9	42.5	10.4	1,806	1.017
		10	47.5	6.11	2,256	0.786
		11	52.5	3.41	2,756	0.533
		12	57.5	2.96	3,306	0.471
		13	62.5	2.10	3,906	0.322
		14	67.5	2.07	4,556	0.316
		15	72.5	2.04	5,256	0.310
33C	360.0	1	2.5	552.1	6.25	2.742
		2	7.5	261.3	56	2.417
		3	12.5	181.9	156	2.260
		4	17.5	102.8	306	2.012
		5	22.5	72.8	506	1.862
		6	27.5	31.7	756	1.501
		7	32.5	8.97	1,056	0.953
		8	37.5	3.30	1,406	0.519
		9	42.5	0.86	1,806	-0.065
		10	47.5	0.22	2,256	(-0.658)

Table 3.1 (cont/d.)

Run	t (hrs.)	Slice	d	Δ	d^2	log Δ
33A	306.0	1	5	10.74	25	1.031
		2	15	10.14	225	1.006
		3	25	9.55	625	0.980
		4	35	7.96	1225	0.901
		5	45	6.12	2,025	0.787
		6	55	4.90	3,025	0.690
		7	65	3.48	4,225	0.542
		8	75	2.12	5,625	0.324
		9	85	1.45	7,225	0.161
		10	95	0.84	9,025	-0.076
		11	105	0.50	11,025	-0.301
		12	115	0.25	13,225	-0.620
33B	360.0	1	5	16.98	25	1.230
		2	15	12.82	225	1.108
		3	25	11.97	625	1.078
		4	35	9.77	1,225	0.990
		5	45	8.05	2,025	0.906
		6	55	6.62	3,025	0.821
		7	65	5.26	4,225	0.721
		8	75	3.44	5,625	0.537
		9	85	2.55	7,225	0.407
		10	95	1.42	9,025	0.152
		11	105	0.93	11,025	-0.031
		12	115	0.54	13,225	-0.268
33D	360.0	1	2.5	38.82	6	1.589
		2	7.5	37.58	56	1.575
		3	12.5	35.32	156	1.548
		4	17.5	31.55	306	1.499
		5	22.5	27.23	506	1.435
		6	27.5	22.49	756	1.352
		7	32.5	17.86	1,056	1.252
		8	37.5	13.80	1,406	1.140
		9	42.5	10.19	1,806	1.008
		10	47.5	7.21	2,256	0.858
		11	52.5	5.02	2,756	0.701
		12	57.5	3.64	3,306	0.561
		13	62.5	1.91	3,906	0.281
		14	67.5	1.26	4,556	0.100
		15	72.5	0.76	5,256	-0.119

Table 3.1 (cont/d.)

Run	t (hrs.)	Slice	d	A	d^2	log A
34	119.2	1	2.5	42.70	6	1.630
		2	7.5	16.54	56	1.219
		3	12.5	2.13	156	0.328
		4	17.5	0.08	306	-1.097
35	346.1	1	5	8.72	25	0.941
		2	15	7.13	225	0.853
		3	25	5.00	625	0.699
		4	35	2.65	1,225	0.423
		5	45	1.21	2,025	0.083
		6	55	0.52	3,025	-0.284

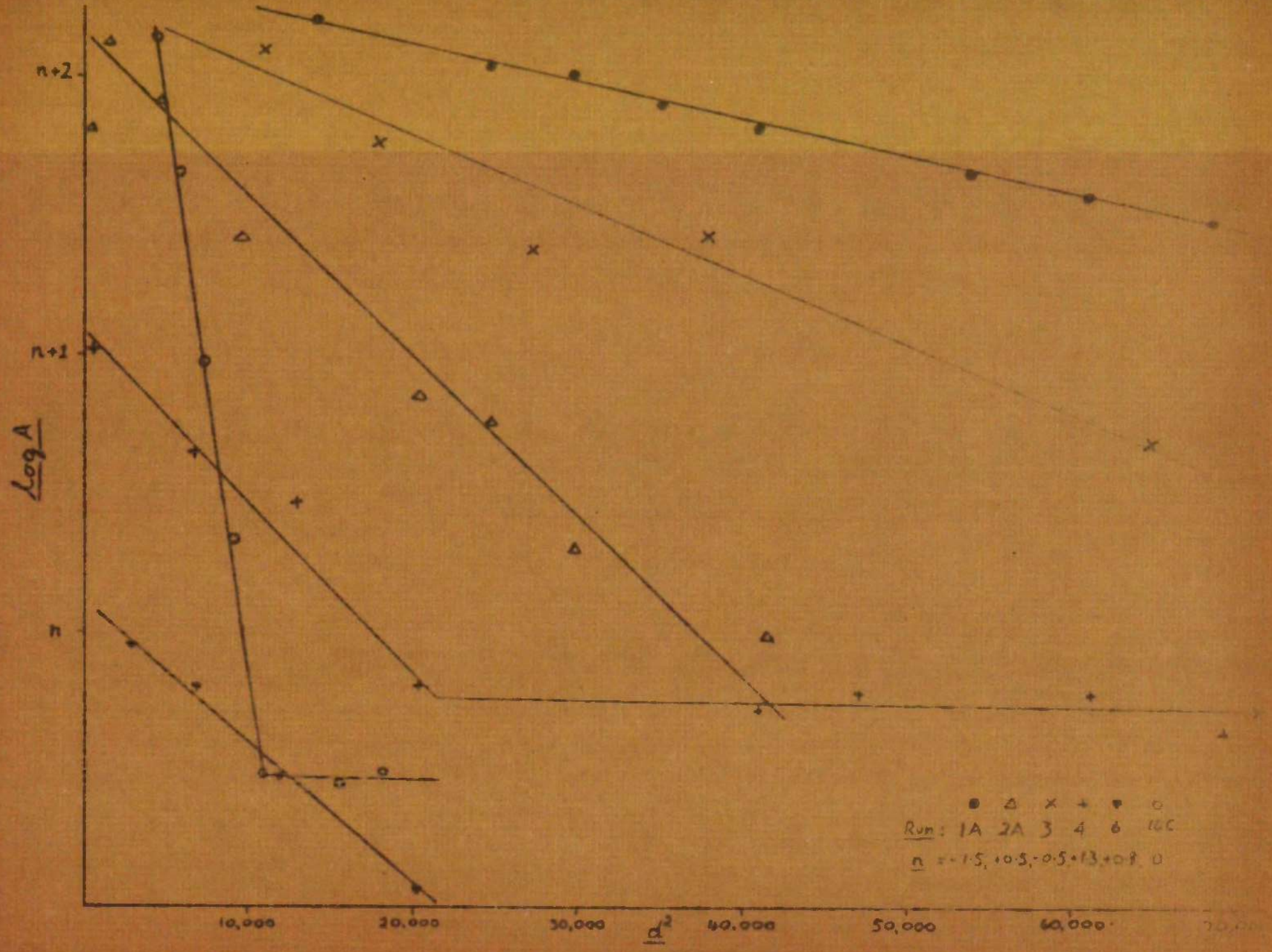

Fig. 3.1(a): Naphthalene - Diffusion Perpendicular to "ab" Plane

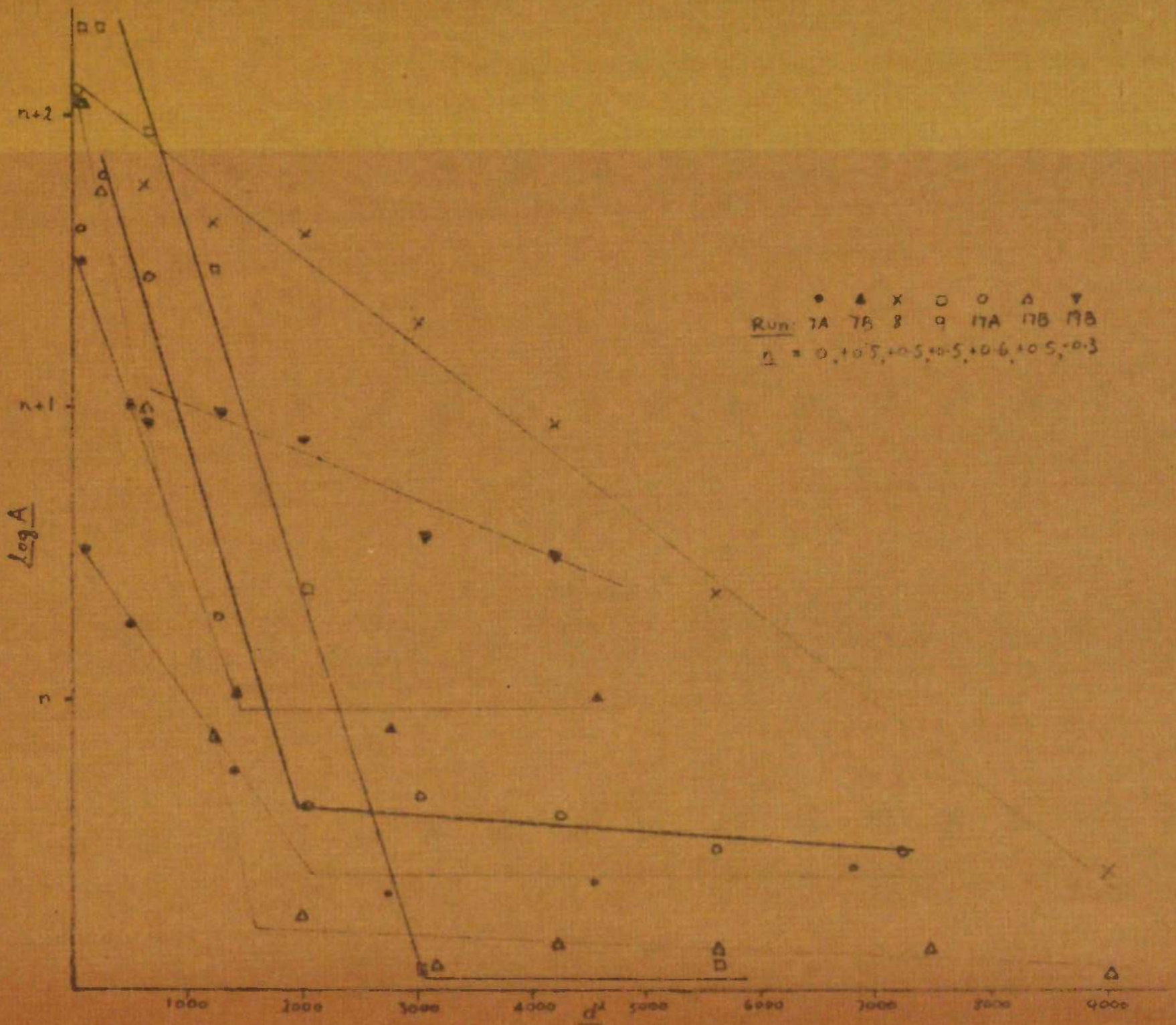

Fig. 3.1 (b): Naphthalene - Diffusion Perpendicular to "ab" Plane

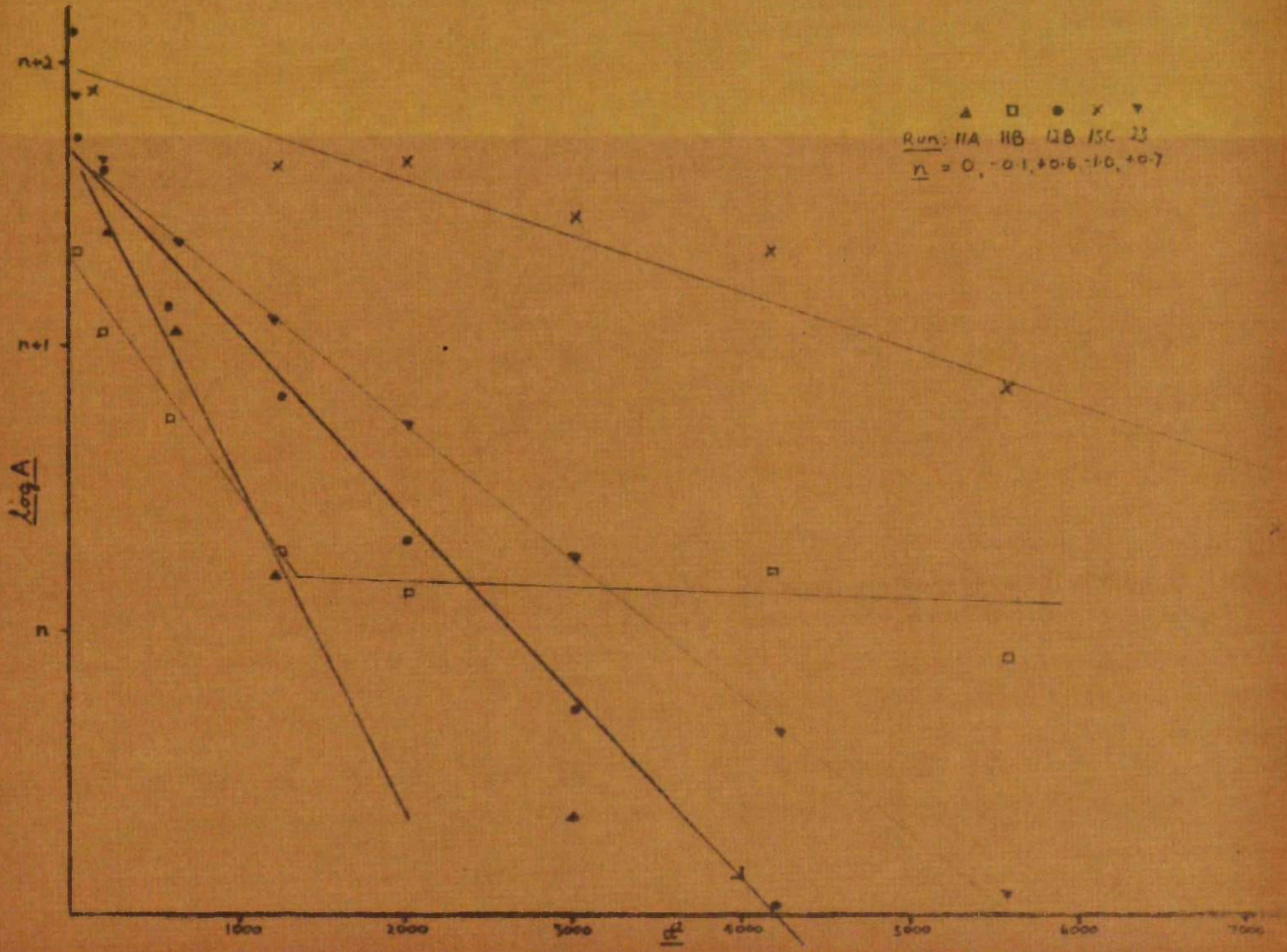

Fig. 3.1 (c): Naphthalene - Diffusion Perpendicular to "ab" Plane.

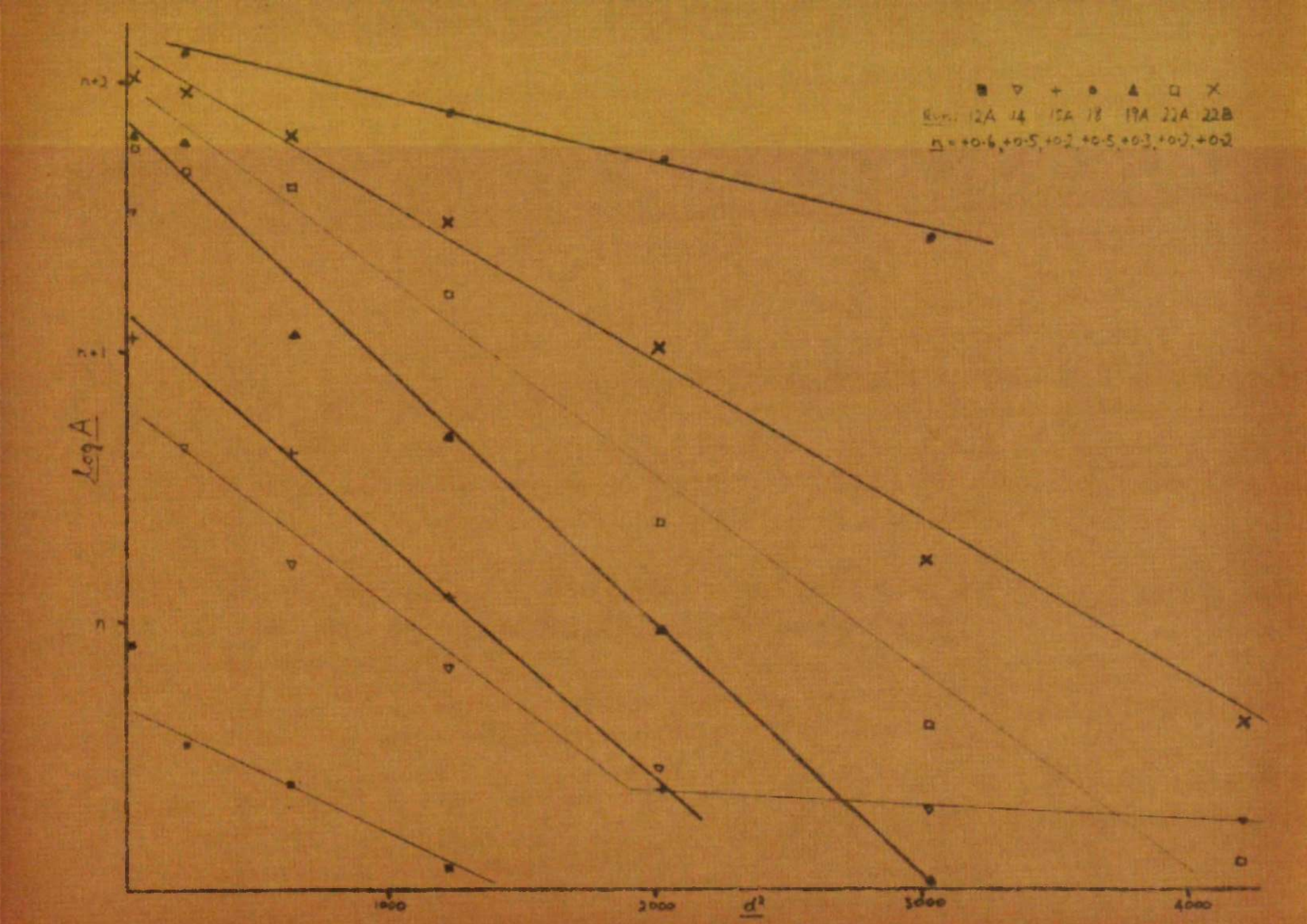

Fig. 3.1 (d): Naphthalene - Diffusion Perpendicular to "ab" Plane.

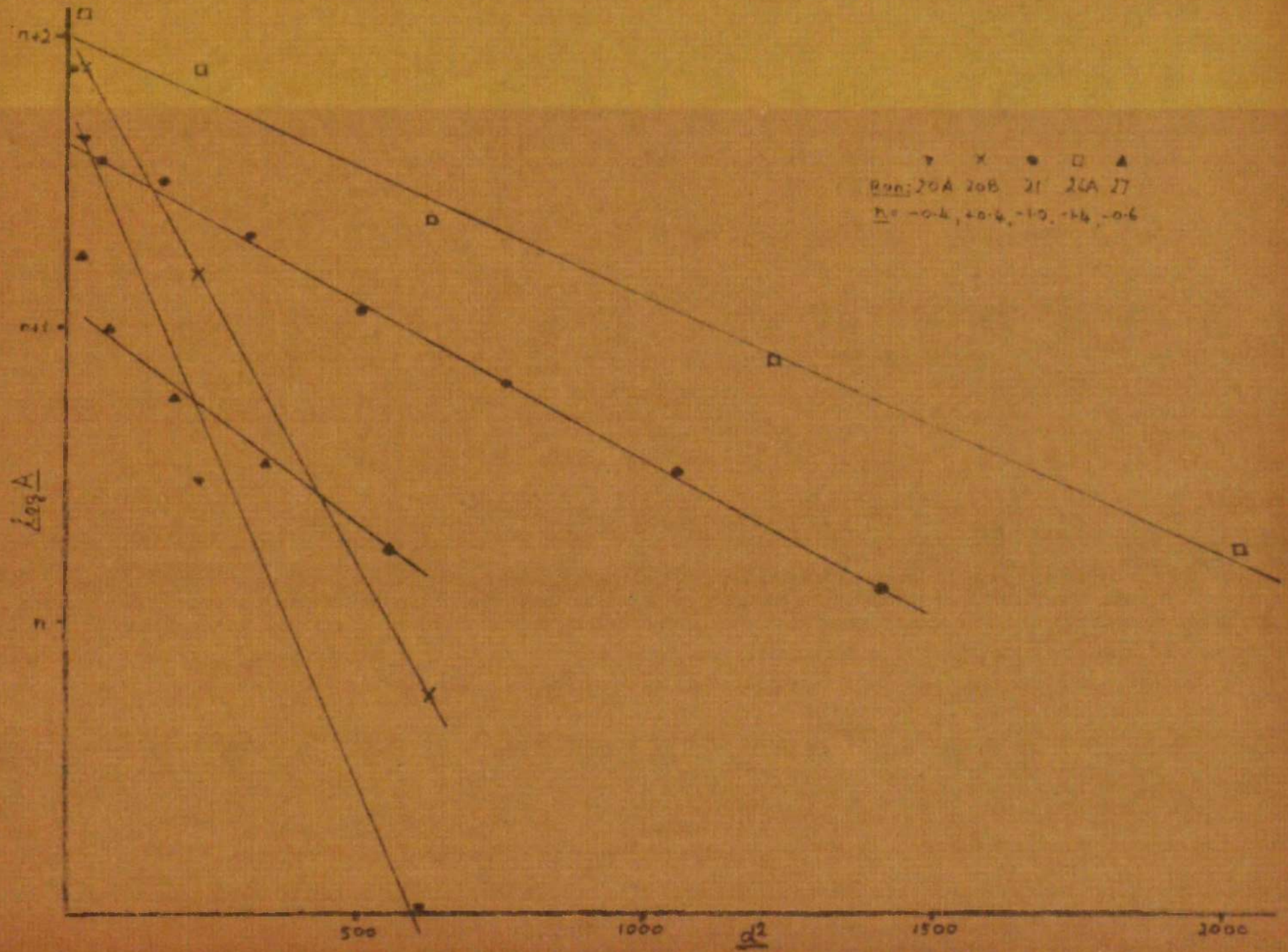

Fig. 3.1 (e): Naphthalene - Diffusion Perpendicular to "ab" Plane.

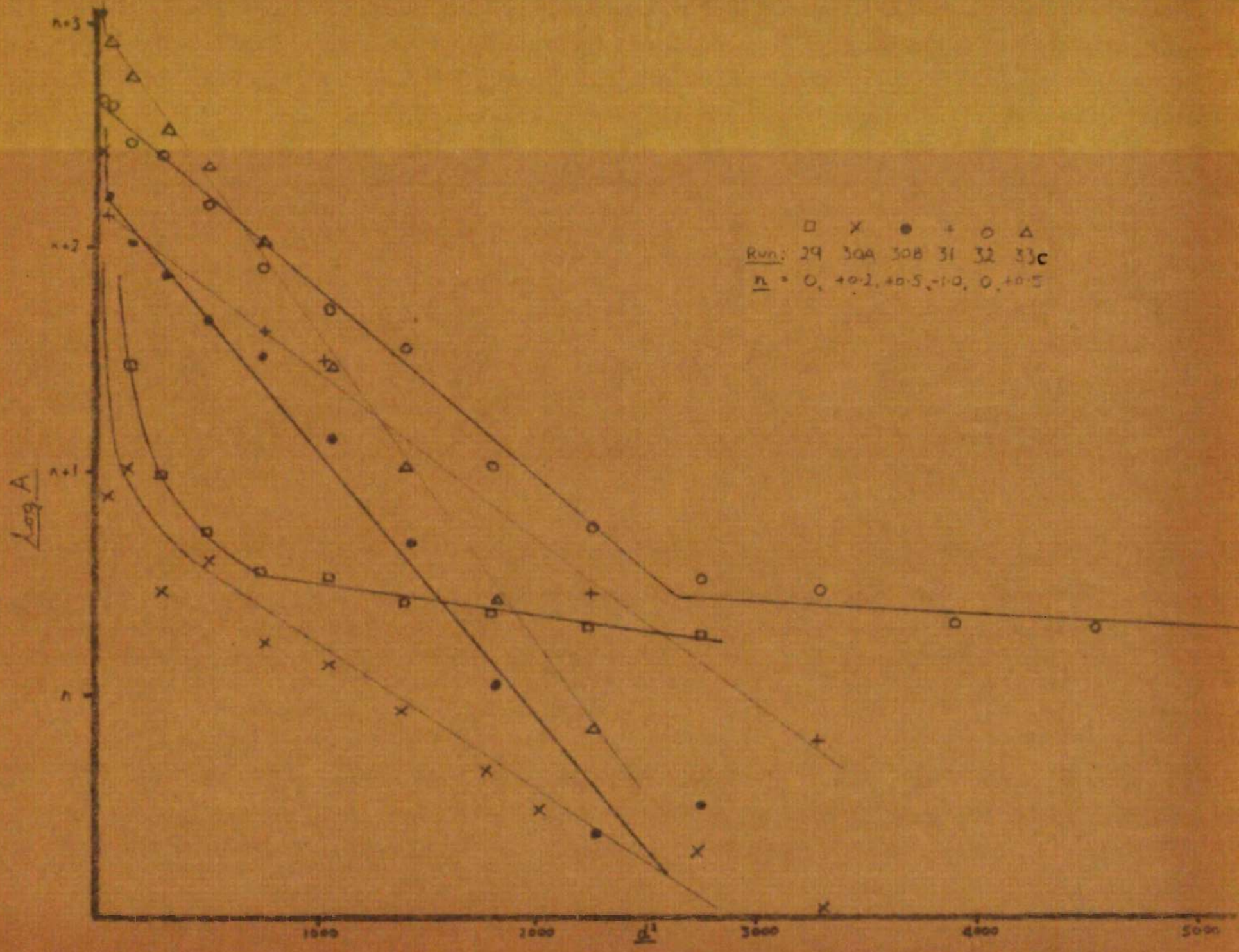

Fig. 3.1 (f): Naphthalene - Diffusion Perpendicular to "ab" Plane.

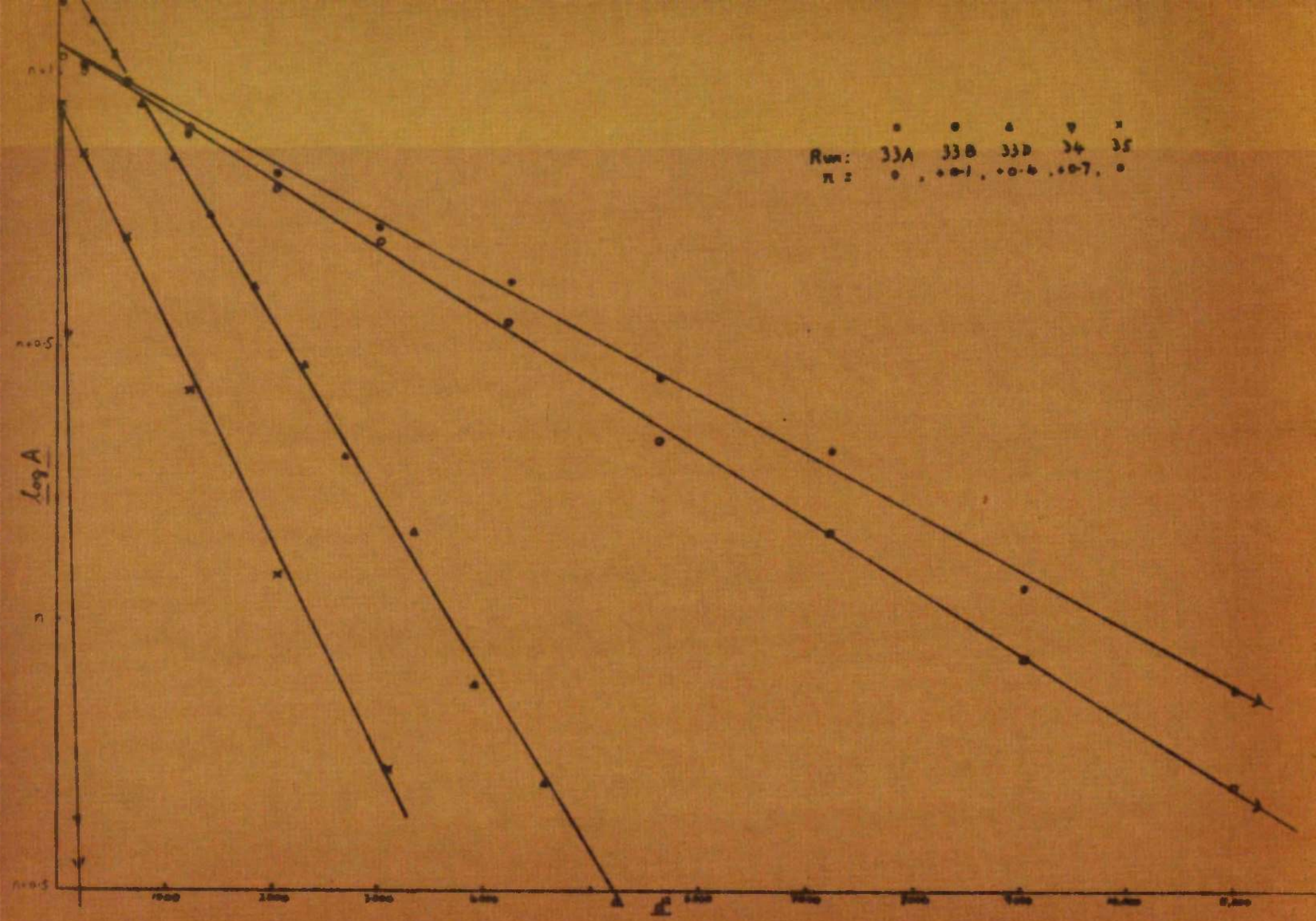

Fig. 3.1(g): Naphthalene - Diffusion Perpendicular to "ab" Plane).

Table 3.2: Diffusion of Tritiated Naphthalene.
(Tracer-sectioning method, perpendicular to "ab" plane.)

Run	t (hrs.)	Slice	d	A	d^2	log A
T1	119.2	1	5	3.23	25	0.509
		2	15	2.82	225	0.450
		3	25	2.01	625	0.303
		4	35	1.46	1,225	0.164
T2	346.1	1	5	4.28	25	0.631
		2	15	3.61	225	0.558
		3	25	2.28	625	0.358
		4	35	1.35	1,225	0.130

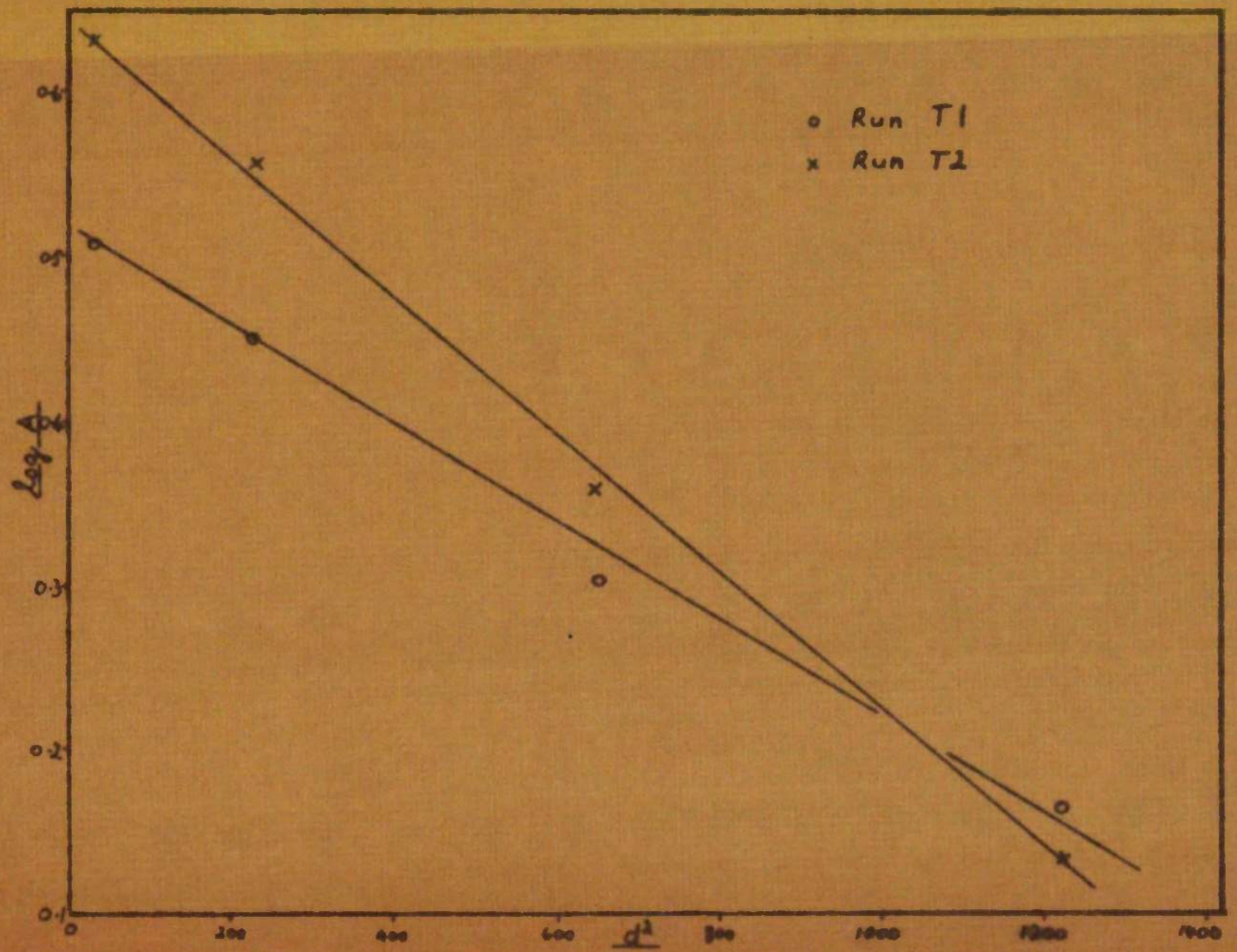

Fig. 3.2: Diffusion of Tritiated Naphthalene.

Table 3.3 Naphthalene - Diffusion Parallel to "a" Axis.
(Tracer-sectioning method, using Naphthalene-1-C14 as tracer)

Run	t (hrs.)	Slice	d	A	d^2	logA
A1	89.0	1	5	82.29	25	1.915
		2	15	50.81	225	1.706
		3	25	69.09	625	1.839
		4	35	22.80	1,225	1.358
		5	45	13.20	2,025	1.121
		6	55	6.00	3,025	0.778
		9	85	0.14	7,225	-0.854
		10	95	0.12	9,025	-0.921
A2	546.2	1	5	276.7	25	2.442
		3	25	183.2	625	2.263
		5	45	120.2	2,025	2.080
		7	65	28.7	4,225	1.458
		9	85	9.95	7,225	0.998
		11	105	1.45	11,025	0.161
		12	115	0.63	13,225	-0.201
A3	40.0	1	5	143.3	25	2.156
		3	25	70.8	625	1.850
		4	35	54.0	1,225	1.732
		6	55	23.9	3,025	1.378
		7	65	10.7	4,225	1.029
		8	75	2.82	5,625	0.450

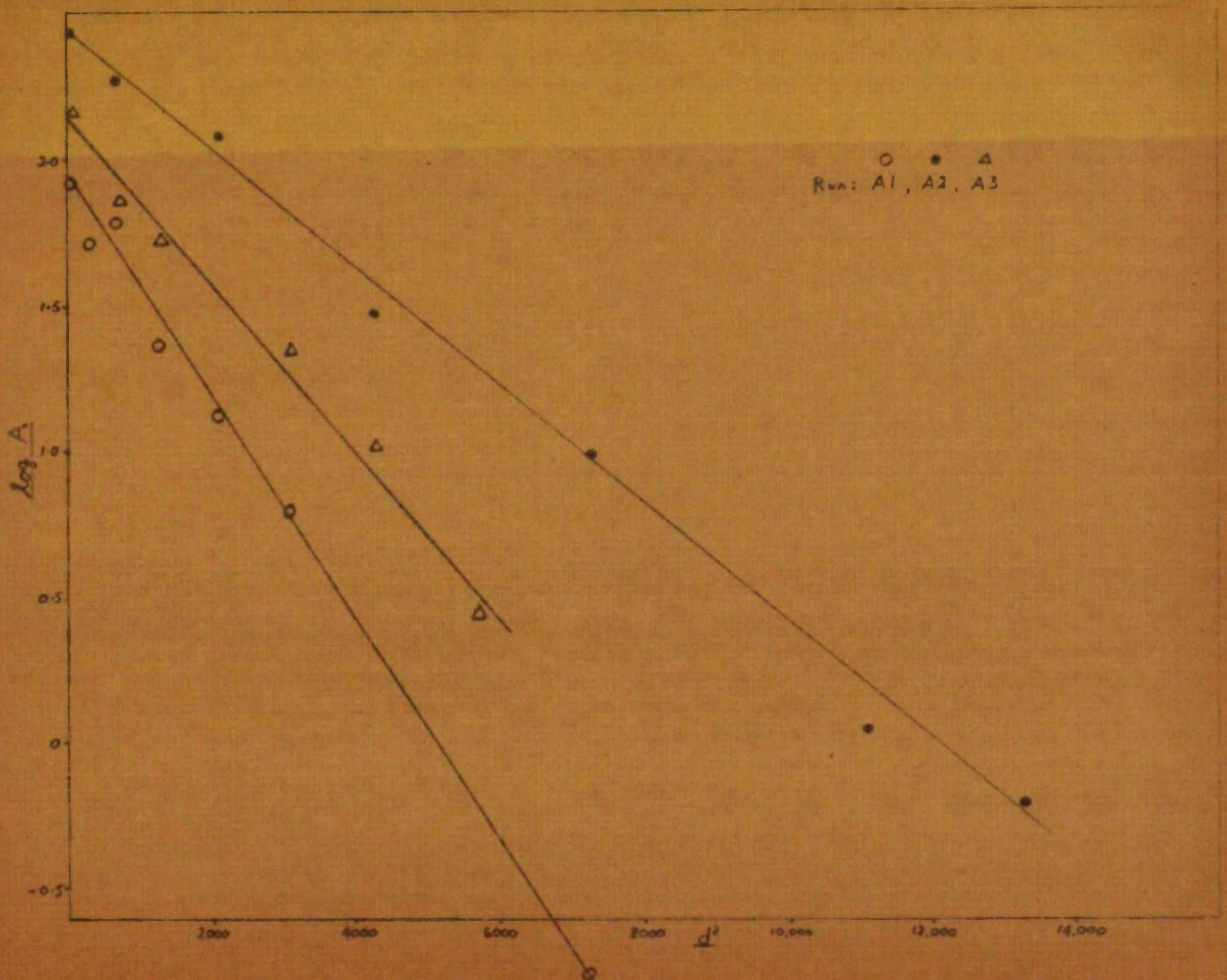

Fig 3.3: Naphthalene - Diffusion Parallel to "a" Axis.

Table 3.4 Naphthalene - Diffusion Parallel to "b" Axis.

(Tracersectioning method, using Naphthalene-1-C14 as tracer)

Run	t (hrs.)	Slice	d	A	d^2	logA
B1	65.0	3	25	86.13	625	1.935
		4	35	49.06	1,225	1.691
		5	45	33.60	2,025	1.526
		6	55	15.13	3,025	1.180
		7	65	3.75	4,225	0.574
		8	75	2.85	5,625	0.455
		9	85	3.54	7,225	0.549
		10	95	3.55	9,025	0.550
B2	89.0	1	5	52.5	25	1.720
		2	15	44.9	225	1.652
		3	25	36.3	625	1.560
		4	35	15.9	1,225	1.201
		5	45	7.87	2,025	0.896
		6	55	3.16	3,025	0.500
		7	65	1.01	4,225	0.004
		8	75	0.25	5,625	-0.600
B3	546.2	1	5	502.4	25	2.701
		3	25	450.0	625	2.653
		5	45	251.7	2,025	2.401
		6	55	190.6	3,025	2.280
		8	75	55.5	5,625	1.744
		10	95	21.1	9,025	1.324
		12	115	2.53	13,225	0.403
		13	125	0.99	15,625	-0.004

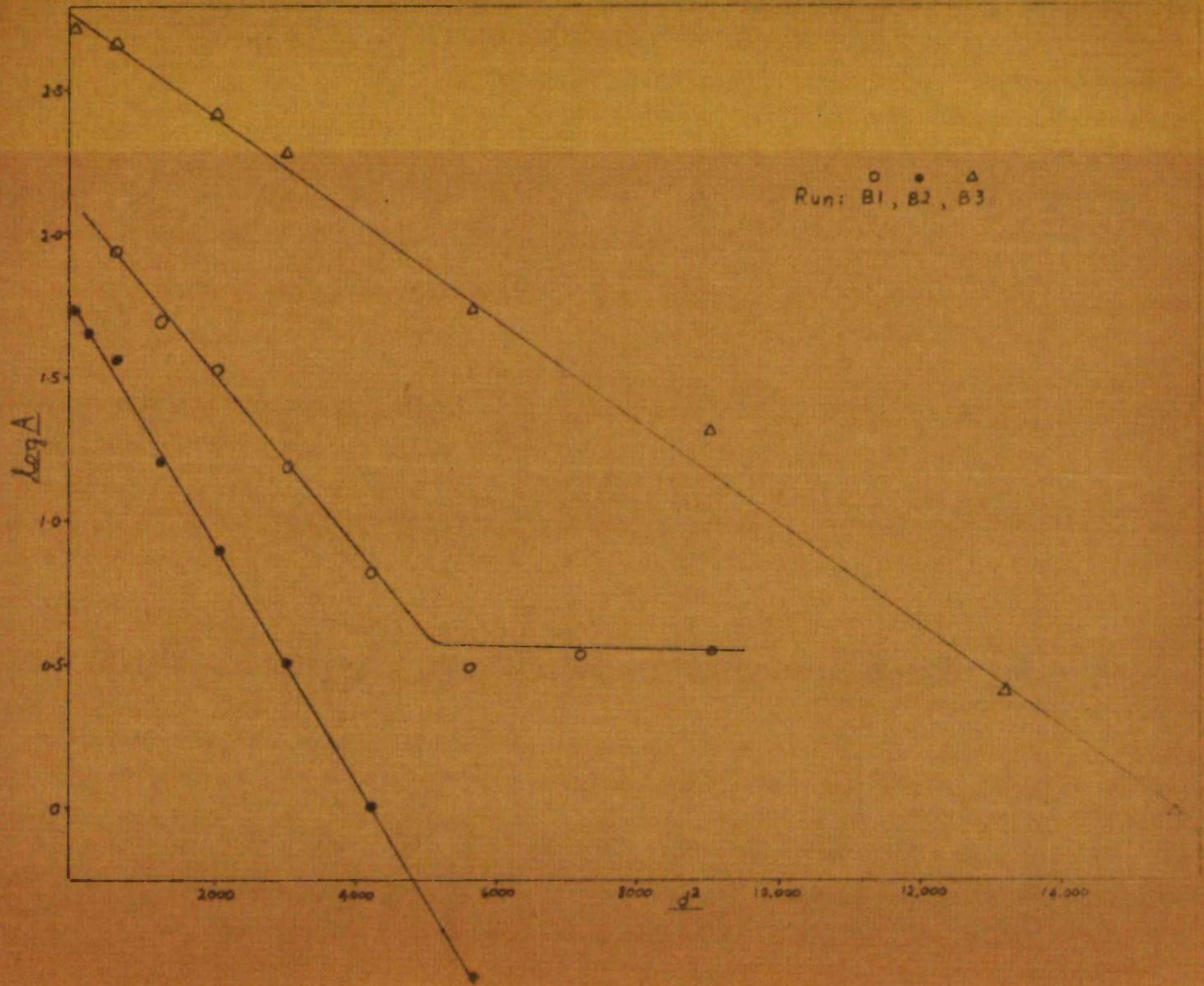

Fig. 3.4: Naphthalene - Diffusion Parallel to "b" Axis.

Table 3.5 Diffusion in Doped Naphthalene.
(Tracer-sectioning method, using Naphthalene-1-C14 as tracer - Diffusion perpendicular to "ab" plane.

Run	t (hrs.)	Slice	d	A	d^2	logA
D1	65.0	2	15	43.89	225	1.642
		3	25	34.19	625	1.534
		4	35	22.99	1,225	1.362
		5	45	21.87	2,025	1.340
		6	55	13.15	3,025	1.118
		7	65	9.12	4,225	0.960
		8	75	5.41	5,625	0.733
		9	85	2.21	7,225	0.344
		10	95	0.64	9,025	-0.194
		12	115	0.91	13,225	-0.041
		13	125	0.39	15,625	-0.409
D2	89.0	4	35	209.9	1,225	2.322
		5	45	68.75	2,025	1.837
		6	55	11.31	3,025	1.054
		7	65	1.77	4,225	0.248
		8	75	1.31	5,625	0.117
		9	85	0.64	7,225	-0.194
		10	95	0.65	9,025	-0.187
		11	105	0.55	11,025	(-0.260)
D3	449.0	1	5	227.4	25	2.357
		2	15	65.73	225	1.818
		3	25	23.34	625	1.368
		4	35	7.81	1,225	0.893
		5	45	4.12	2,025	0.615
		6	55	1.44	3,025	0.158
		7	65	0.46	4,225	-0.337
		8	75	0.20	5,625	-0.699
		9	85	0.11	7,225	(-0.959)
D4	396.0	1	5	7.78	25	0.891
		2	15	6.61	225	0.820
		3	25	4.97	625	0.696
		4	35	3.13	1,225	0.496
		5	45	1.71	2,025	0.233
		6	55	0.79	3,025	-0.102

Table 3.5 (cont/d.)

Run	t(hrs.)	Slice	d	A	d^2	logA
D5	396.0	1	5	7.08	25	0.850
		2	15	5.82	225	0.765
		3	25	3.96	625	0.598
		4	35	2.50	1,225	0.398
		5	45	1.16	2,025	0.065
		6	55	0.49	3,025	-0.310
D6	89.0	1	5	320.9	25	2.506
		2	15	28.75	225	1.459
		3	25	2.28	625	0.358
		4	35	0.29	1,225	-0.538
		5	45	(0.04)	2,025	-

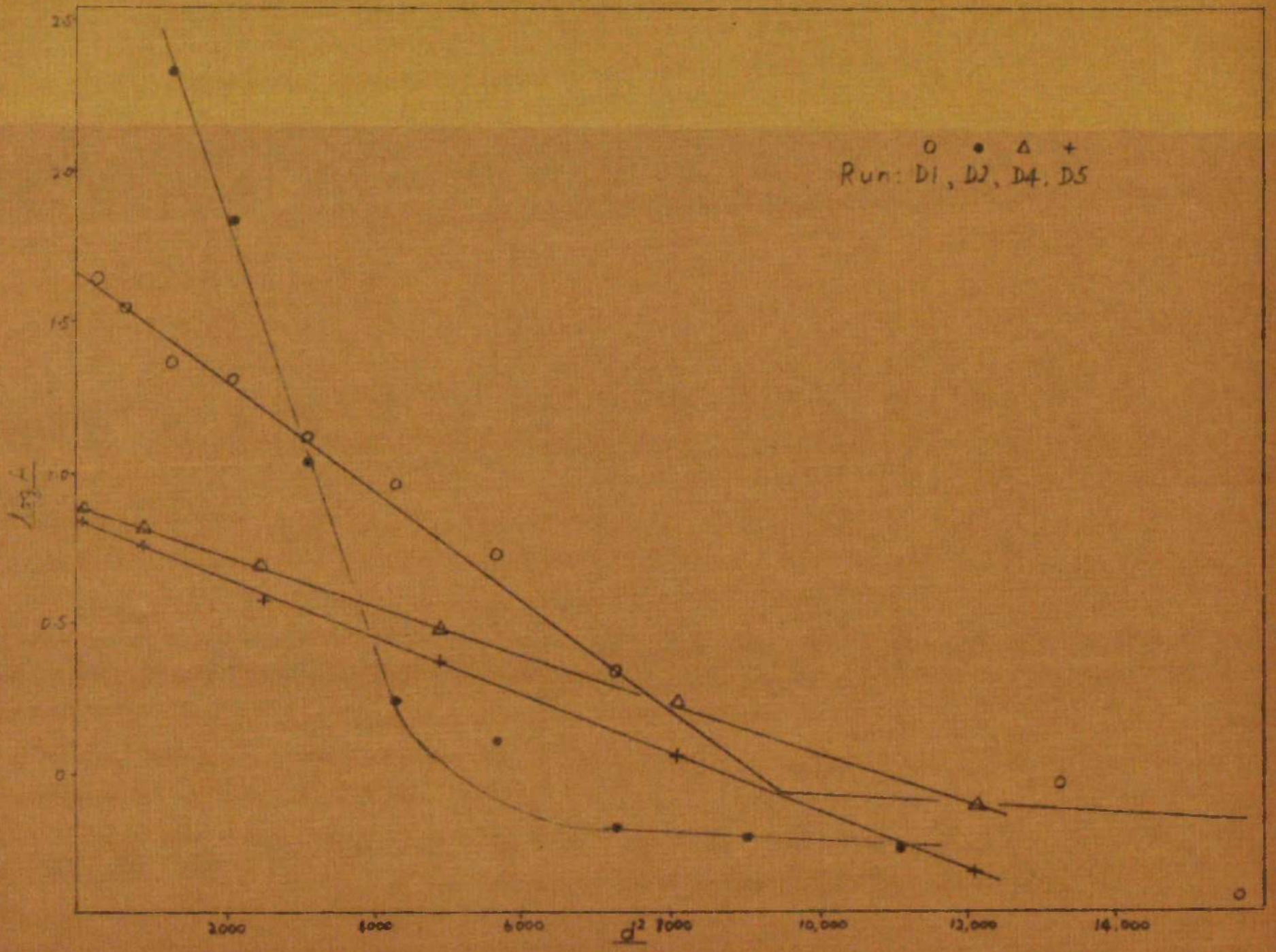

Fig 3.5(a): Diffusion in Doped Naphthalene.

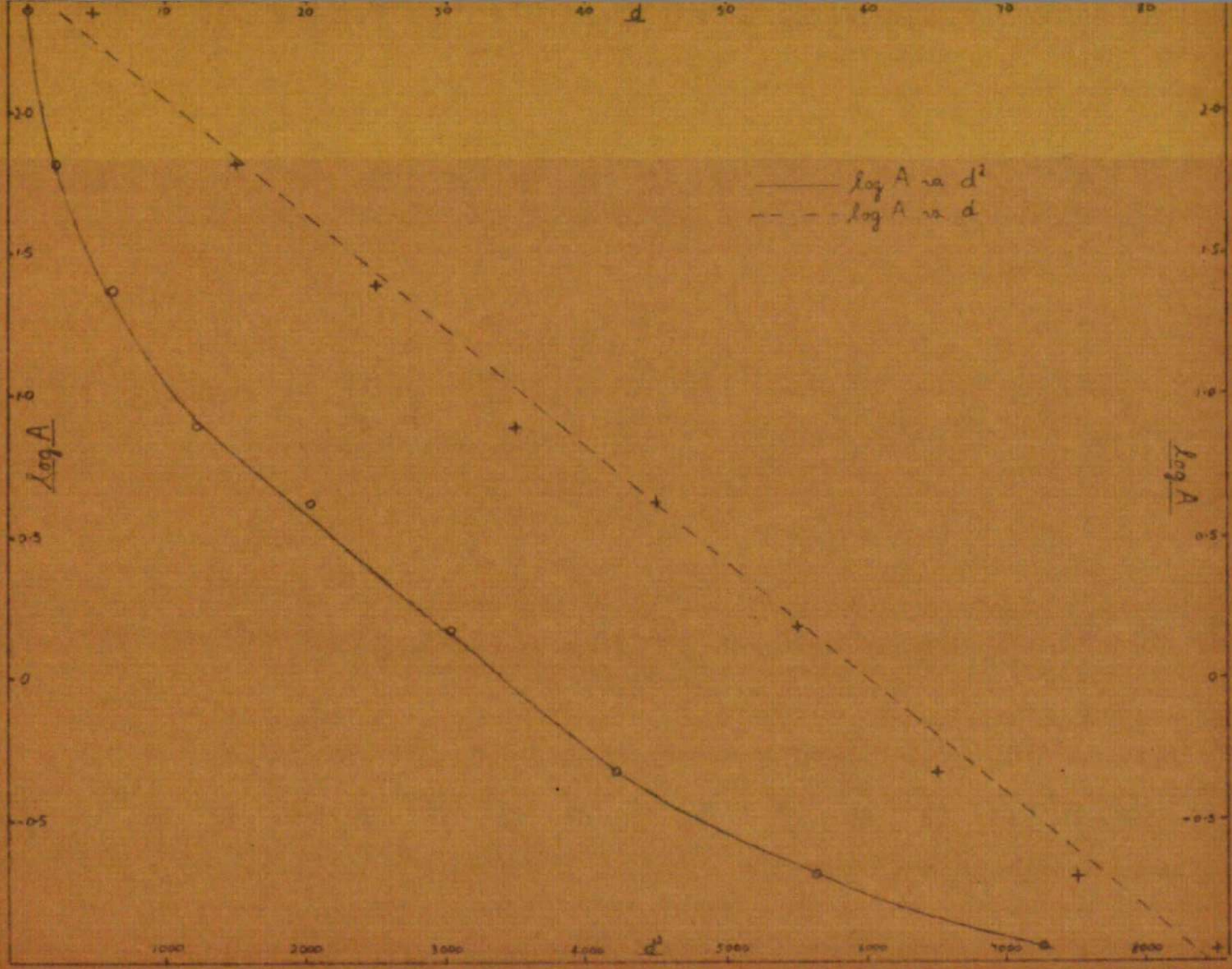

Fig. 3.5(b): Diffusion in Doped Naphthalene - Run D3

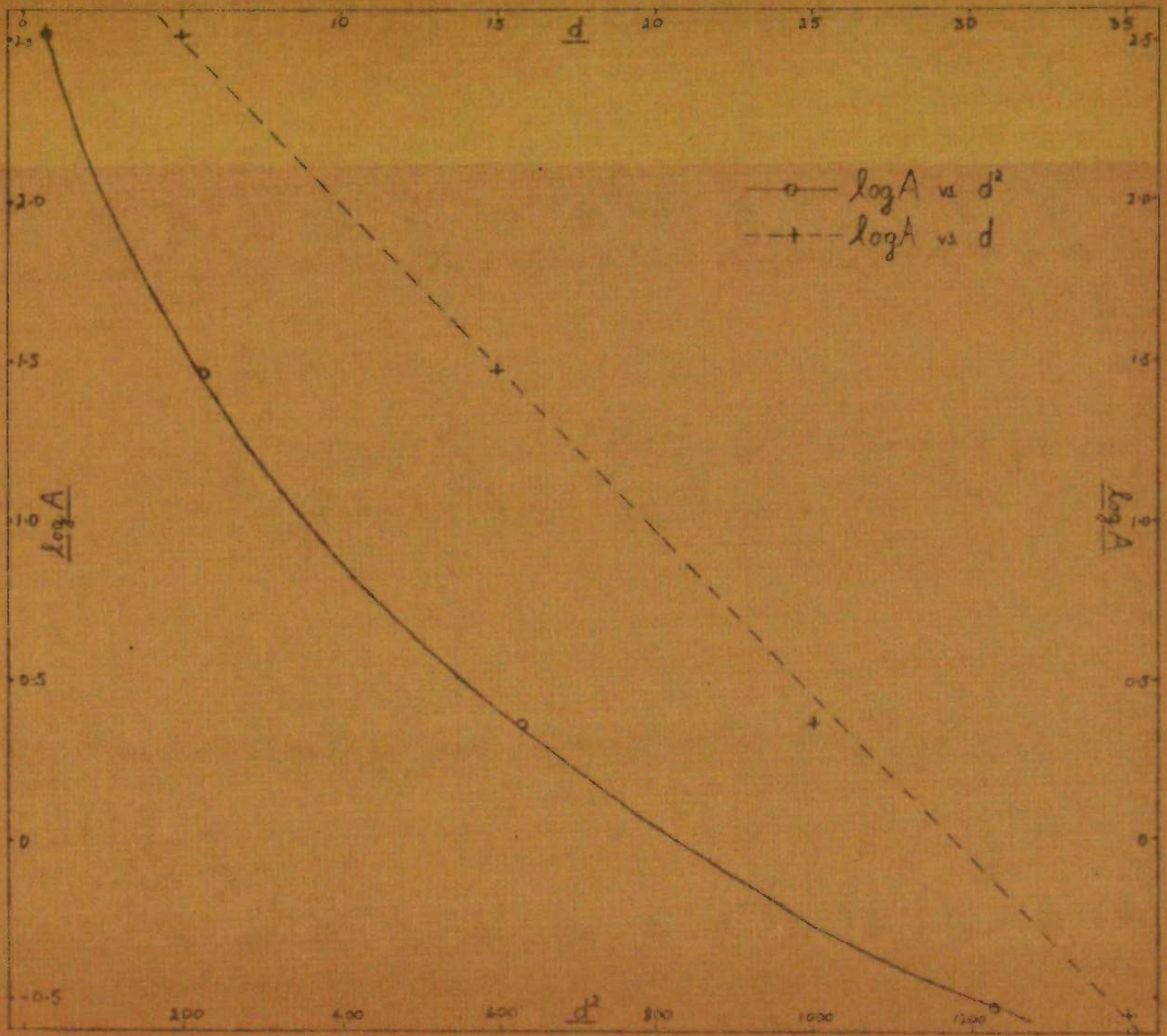

Fig. 3.5(a): Diffusion in Doped Naphthalene - Run D6

Table 3.6 Naphthalene - Diffusion in Polycrystalline Compacts.

(Tracer-sectioning method, using Naphthalene-1-C14 as tracer)

Run	t(hrs.)	Slice	d	Δ	d^2	logΔ
C1	48.0	8,9	120.0	494.5	14,400	2.694
		12,13	180.0	301.9	32,400	2.480
		16,17	240.0	112.6	57,600	2.052
		20,21	300.0	120.2	90,000	2.080
		24,25	360.0	28.2	129,600	1.450
		28,29	420.0	15.0	176,400	1.176
		32,33	480.0	4.87	230,400	0.688
		36,37	540.0	2.80	291,600	0.447
		40,41	600.0	1.63	360,000	0.212
		44,45	660.0	1.28	435,600	0.107
C2	72.0	13,14	195.0	21.6	38,030	1.335
		18,19	270.0	17.4	72,900	1.241
		23,24	345.0	1.20	119,000	0.079
		27,28	405.0	1.32	164,000	0.121
		31,32	465.0	0.50	216,200	-0.301
		35,36	525.0	0.43	275,600	-0.367
		39,40	585.0	0.32	342,200	-0.495
		43,44	645.0	0.28	416,000	-0.553
C3	26.17	6	82.5	291.7	6,808	2.465
		8	112.5	119.4	12,660	2.077
		10	142.5	60.7	20,310	1.783
		12	172.5	40.0	29,750	1.602
		13	187.5	39.4	35,160	1.595
		14	202.5	20.4	41,020	1.310
		15	217.5	9.98	47,320	0.999
		22	322.5	6.50	104,000	0.813
C4	43.25	1	5	85.35	25	1.931
		2	15	71.89	225	1.857
		5	45	81.27	2,025	1.910
		6	55	88.69	3,025	1.948
		8	75	47.56	5,625	1.677
		9	85	29.63	7,225	1.472
		10	95	27.35	9,025	1.437
		12	115	22.20	13,225	1.346
		15	145	13.20	21,025	1.121

Table 3.6 (cont/d.)

Run	t(hrs.)	Slice	d	A	d^2	logA
C5	24.0	1,2	10	221.1	100	2.345
		3	25	85.48	625	1.932
		4	35	52.60	1,225	1.722
		5	45	28.83	2,025	1.460
		6	55	32.02	3,025	1.505
		8,9	80	20.82	6,400	1.319
		10,11	100	14.25	10,000	1.154
		14,15	140	9.38	19,600	0.972
		18,19	180	6.18	32,400	0.791
		22,23	220	4.21	48,400	0.624
		26,27	260	2.32	67,600	0.366
		30,31	300	2.09	90,000	0.320
		34,35	340	1.19	115,600	0.076
		40,41	400	1.01	160,000	0.004
		47,48	470	0.74	220,900	-0.131
		49,50	490	0.56	240,100	-0.252
		55,56	550	0.52	302,500	-0.284
		60,61	600	0.44	360,000	-0.356
		65,66	650	0.36	422,500	-0.444
		70,71	700	0.33	490,000	-0.481
C6	21.0	1	5	889.5	25	2.949
		3	25	184.9	625	2.267
		5	45	29.64	2,025	1.472
		6	55	16.19	3,025	1.209
		7	65	11.63	4,225	1.066
		8	75	9.89	5,625	0.995
		9	85	7.14	7,225	0.854
		10	95	6.68	9,025	0.825
		12	115	5.42	13,225	0.734
		13	125	3.89	15,625	0.590
		14	135	5.15	18,225	0.712
		15	145	4.19	21,025	0.622
		16	155	2.76	24,025	0.441
		17	165	2.44	27,225	0.387
		18	175	2.79	30,625	0.446
		19	185	2.41	34,225	0.382
		20	195	2.23	38,025	0.348

Table 3.6 (cont/d.)

Run	t(hrs.)	Slice	d	A	d^2	logA
C7	21.0	1	5	373.9	25	2.573
		2	15	14.6	225	1.164
		3	25	49.4	625	1.694
		4	35	12.3	1,225	1.089
		5	45	7.35	2,025	0.866
		6	55	5.31	3,025	0.725
		7	65	3.51	4,225	0.545
		8	75	3.27	5,625	0.515
		9	85	2.39	7,225	0.378
		10	95	2.21	9,025	0.344
		11	105	2.68	11,025	0.428
		12	115	1.48	13,225	0.170
		13	125	1.59	15,625	0.201
		14	135	1.24	18,225	0.093
		15	145	1.13	21,025	0.053
		16	155	1.05	24,025	0.021
		17	165	0.97	27,225	-0.013
		18	175	0.76	30,625	-0.119
		19	185	0.67	34,225	-0.174
		20	195	0.62	38,025	-0.208
		21	205	0.60	42,025	-0.222
		22	215	0.42	46,225	-0.377
		23	225	0.40	50,625	-0.398
		24	235	0.40	55,225	-0.398
		25	245	0.44	60,025	-0.356

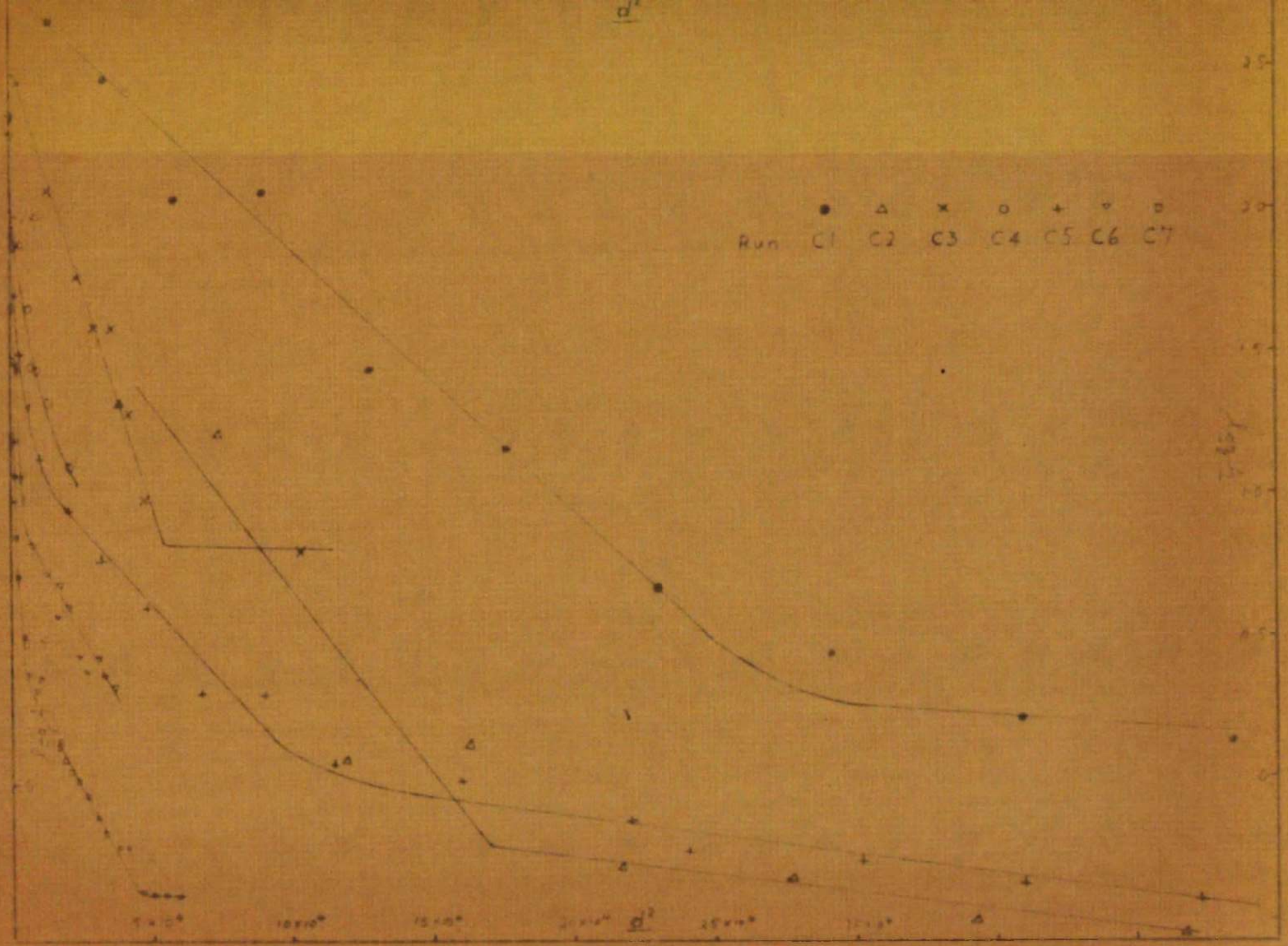

Fig. 3.6; Naphthalene-Diffusion in Polycrystalline Compacts.

Table 3.7: Surface-Decrease Method.

(Self-Diffusion in Naphthalene Perpendicular to the "ab" Plane)

(a) Run S.D.1. T = 52.5°C.; background count = 0.5 c.p.s.; Boule B

t (mins)	Count-Rate (c.p.s.)	I/I_o	log t	t (mins)	Count-Rate (c.p.s.)	I/I_o	log t
0	74	1	-	55	63	0.850	1.740
5	71	0.959	0.699	60	62.5	0.843	1.778
15	69	0.931	1.176	70	61	0.823	1.848
20	68	0.918	1.301	75	60.5	0.816	1.875
25	67	0.905	1.398	89	59.5	0.803	1.949
30	66	0.891	1.477	101	59.0	0.796	2.004
35	65	0.878	1.544	108	58.5	0.789	2.033
40	64.5	0.871	1.602	135	57	0.769	2.130

(b) Run S.D.2. T = 70.0°C.; background count = 0.4 c.p.s.; Boule D

t (secs.)	Count-Rate (c.p.s.)	I/I_o	log t	t (secs.)	Count-Rate (c.p.s.)	I/I_o	log t
0	83.3	1	-	4600	71.5	0.861	3.663
340	79.0	0.948	2.532	4900	72.0	0.864	3.690
580	78.0	0.936	2.763	5200	72.2	0.866	3.716
880	77.2	0.926	2.945	5550	71.9	0.862	3.744
120	76.0	0.912	3.049	6100	71.3	0.855	3.785
360	75.8	0.910	3.134	6400	70.7	0.848	3.806
600	74.9	0.899	3.204	6700	72.4	0.868	3.826
840	75.0	0.900	3.265	7300	70.9	0.850	3.863
080	75.3	0.904	3.318	8200	71.9	0.862	3.914
320	73.2	0.878	3.366	8500	72.0	0.864	3.929
560	73.2	0.878	3.408	8800	71.9	0.862	3.945
800	73.4	0.880	3.447	9700	70.1	0.841	3.987
040	73.6	0.883	3.483	10,000	71.5	0.858	4.000
280	73.6	0.883	3.516	10,300	70.8	0.849	4.013
700	71.9	0.862	3.568	10,600	71.3	0.855	4.025
000	73.3	0.879	3.602	10,900	70.2	0.842	4.037
300	72.1	0.865	3.634	11,200	69.7	0.836	4.049

(c) Run S.D.3. T = 60.8°C.; background count = 0.4 c.p.s.; Boule E

t (hrs.)	Count-Rate (c.p.s.)	I/I_o	log t	t (hrs.)	Count-Rate (c.p.s.)	I/I_o	log t
0	22.4	1	-	9.25	19.5	0.868	0.966
1.04	22.3	0.996	0.017	9.92	19.7	0.877	0.997
1.32	21.7	0.968	0.121	22.60	18.4	0.818	1.354
1.63	22.0	0.982	0.212	22.70	18.3	0.814	1.356
2.17	21.2	0.945	0.337	23.89	18.2	0.809	1.378
2.75	21.1	0.941	0.439	25.07	18.1	0.805	1.399
2.99	21.3	0.950	0.476	32.20	17.9	0.795	1.508
320	20.8	0.927	0.505	34.83	17.8	0.791	1.542
3.40	20.9	0.932	0.532	47.07	17.5	0.777	1.673
3.98	20.5	0.914	0.600	50.12	17.3	0.768	1.700
4.16	20.7	0.923	0.619	51.51	17.3	0.768	1.712
4.32	20.4	0.909	0.636	54.92	17.2	0.764	1.740
4.58	20.6	0.918	0.661	56.97	17.1	0.759	1.756
5.50	20.3	0.905	0.740	58.09	17.1	0.759	1.764
6.26	20.0	0.891	0.797	71.50	16.9	0.750	1.854
6.65	20.2	0.900	0.823	72.70	16.7	0.741	1.862
7.33	19.9	0.886	0.865	74.40	16.8	0.745	1.872
8.09	19.9	0.886	0.908	98.60	16.6	0.736	1.994
8.50	19.6	0.873	0.929	144.1	16.1	0.714	2.159

(d) Run S.D.4. T = 78.6°C.; background count = 0.6 c.p.s.; Boule H

0	267.0	1	-	7.300	195.3	0.730	0.863
0.267	255.1	0.955	-0.573	7.567	195.5	0.731	0.879
1.767	228.1	0.854	0.247	22.47	163.2	0.610	1.352
1.850	224.6	0.841	0.267	22.53	162.3	0.606	1.353
2.073	224.8	0.842	0.317	22.63	163.0	0.610	1.355
2.700	218.9	0.820	0.431	24.00	160.6	0.601	1.380
2.775	218.7	0.818	0.443	24.07	161.3	0.603	1382
2.900	218.9	0.820	0.462	26.90	158.0	0.591	1.430
3.167	217.9	0.815	0.501	26.97	157.2	0.588	1.431
3.567	213.4	0.799	0.552	28.00	157.0	0.587	1.447
3.667	211.5	0.792	0.564	28.18	158.2	0.592	1.450
3.867	210.9	0.790	0.587	28.67	157.7	0.590	1.457
4.267	209.9	0.785	0.630	29.00	156.8	0.586	1.462
4.733	207.5	0.777	0.675	48.00	143.4	0.536	1.681
4.833	207.2	0.776	0.684	48.07	143.2	0.535	1.682
5.067	204.2	0.764	0.705	49.00	142.8	0.534	1.690

cont/d...

(d) cont/d.....

t (hrs.)	Count Rate (c.p.s.)	I/I_o	log t	t (hrs.)	Count Rate (c.p.s.)	I/I_o	log t
5.433	203.2	0.761	0.735	52.42	140.8	0.526	1.720
5.567	203.9	0.763	0.746	52.50	140.3	0.524	1.720
6.067	202.3	0.756	0.783	52.63	141.3	0.528	1.721
6.133	200.8	0.752	0.788	52.85	140.7	0.526	1.723
6.200	200.6	0.751	0.792	93.83	122.8	0.458	1.972
7.100	197.8	0.740	0.851	94.00	121.5	0.454	1.973
7.167	197.1	0.737	0.855	95.08	122.2	0.456	1.978

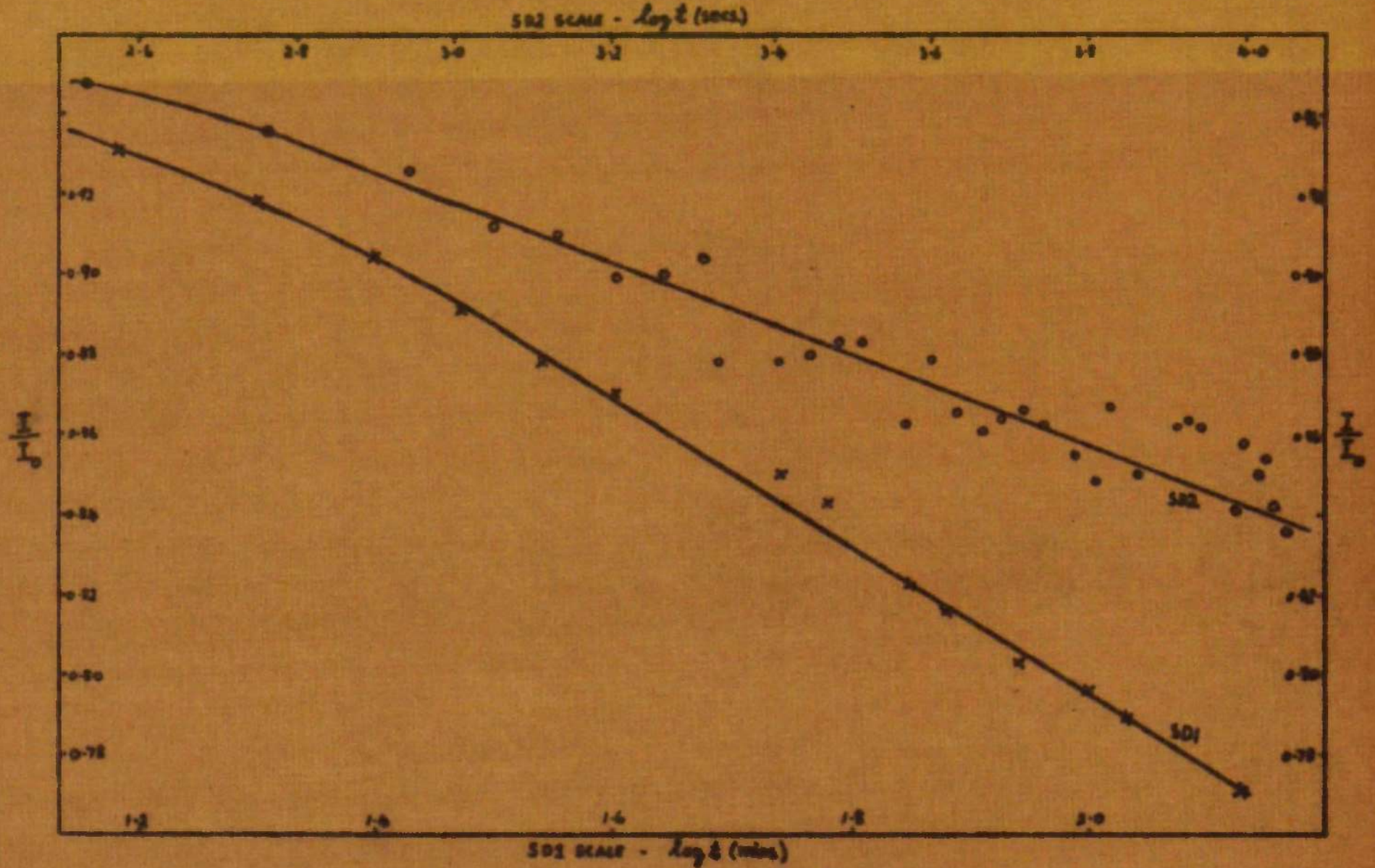

Fig. 3.7(a): Surface-Decrease Results, SD1 and SD2.

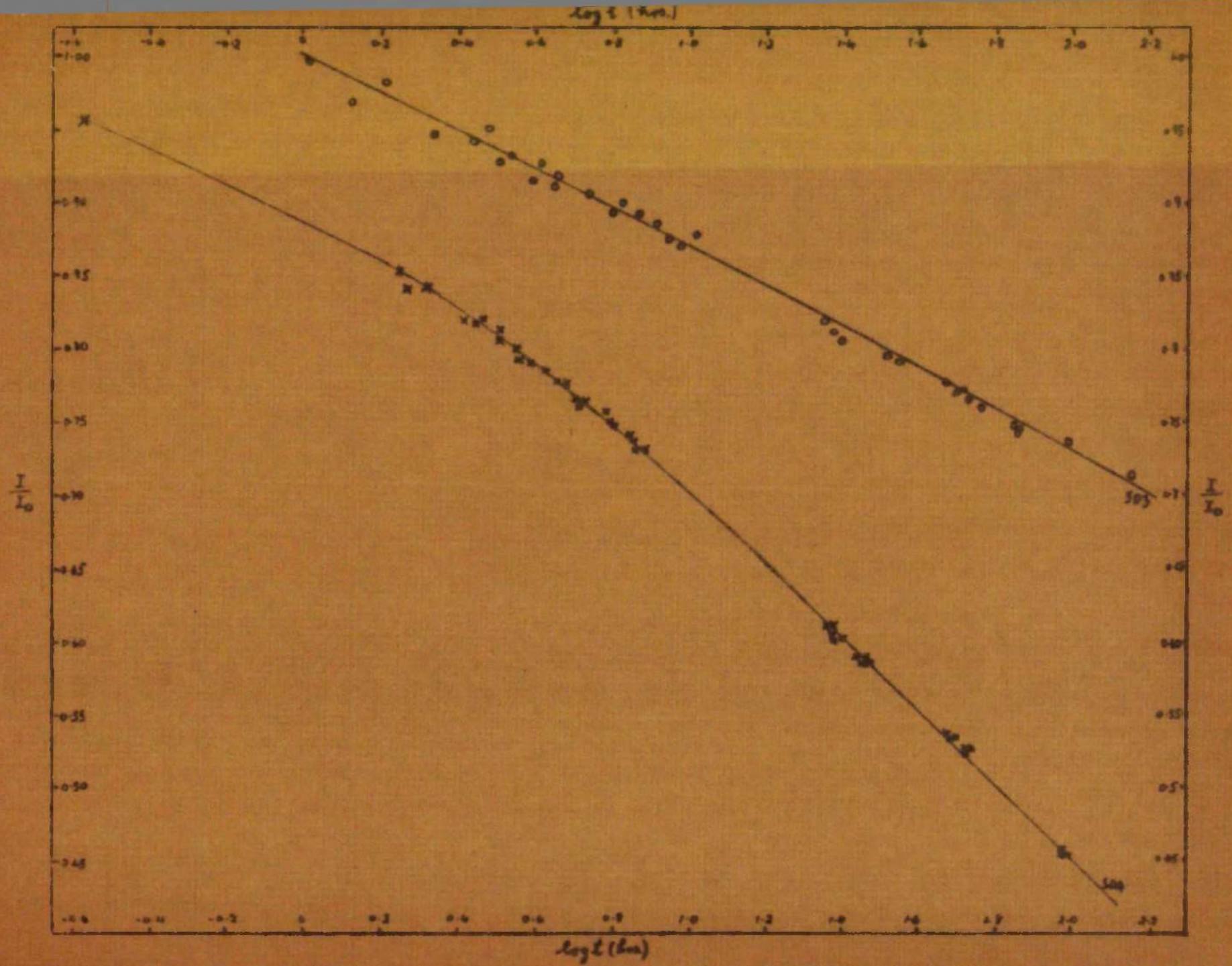

Fig. 3.7(b): Surface-Decrease Results, SD3 and SD4

Table 3.8: Calculation of D from Surface-Decrease Results.
(Diffusion Perpendicular to "ab" Plane in Naphthalene)

(a) Run S.D.1; T = 52.5 °C.; Boule B.

I/I_o	log t (mins.)	$\mu(Dt)^{\frac{1}{2}}$	$D \times 10^{11}$
0.92	1.280	0.075	4.61
0.90	1.426	0.096	5.40
0.88	1.569	0.117	6.50
0.86	1.645	0.139	6.82
0.84	1.752	0.162	7.28
0.82	1.858	0.186	7.52
0.80	1.966	0.211	7.52
0.78	2.073	0.237	7.41
0.76	2.180	0.264	7.21

Final value, $D = 6.83 \times 10^{-11}$

(b) Run S.D.2; T = 70.0 °C.; Boule D.

I/I_o	log t (secs.)	$\mu(Dt)^{\frac{1}{2}}$	$D \times 10^{11}$
0.93	2.84	0.065	5.73
0.92	2.97	0.075	5.65
0.91	3.10	0.086	5.52
0.90	3.23	0.096	5.08
0.89	3.36	0.106	4.59
0.88	3.50	0.117	4.06
0.87	3.63	0.128	3.60
0.86	3.76	0.139	3.15
0.85	3.89	0.150	2.72
0.84	4.02	0.162	2.36

Final value, $D = 4.25 \times 10^{-11}$

(c) Run S.D.3; T = 60.8 °C.; Boule E.

I/I_o	log t (hrs.)	$\mu(Dt)^{\frac{1}{2}}$	$D \times 10^{12}$
0.96	0.30	0.036	1.69
0.94	0.46	0.055	2.73
0.92	0.60	0.075	3.68
0.90	0.75	0.096	4.27
0.88	0.90	0.117	4.49
0.86	1.04	0.139	4.59
0.84	1.19	0.162	4.23
0.82	1.34	0.186	4.13

(c) Run S.D. 3: (Cont/d.)

I/I_o	log t (hrs.)	$\mu(Dt)^{\frac{1}{2}}$	$D \times 10^{12}$
0.80	1.49	0.211	3.75
0.78	1.64	0.237	3.36
0.76	1.78	0.264	3.02
0.74	1.94	0.293	2.57
0.72	2.17	0.322	1.83

Final value, $D = 4.06 \times 10^{-12}$

(d) Run S.D.4: T = 78.6 °C.; Boule H.

I/I_o	log t (hrs.)	$\mu(Dt)^{\frac{1}{2}}$	$D \times 10^{11}$
0.95	-0.52	0.046	1.83
0.90	-0.08	0.096	2.88
0.85	0.27	0.150	3.15
0.80	0.56	0.211	3.19
0.75	0.79	0.278	3.27
0.70	1.00	0.352	3.24
0.65	1.20	0.435	2.84
0.60	1.40	0.532	2.94
0.55	1.61	0.641	2.63
0.50	1.81	0.768	2.38
0.45	2.02	0.923	2.12

Final value, $D = 3.04 \times 10^{-11}$

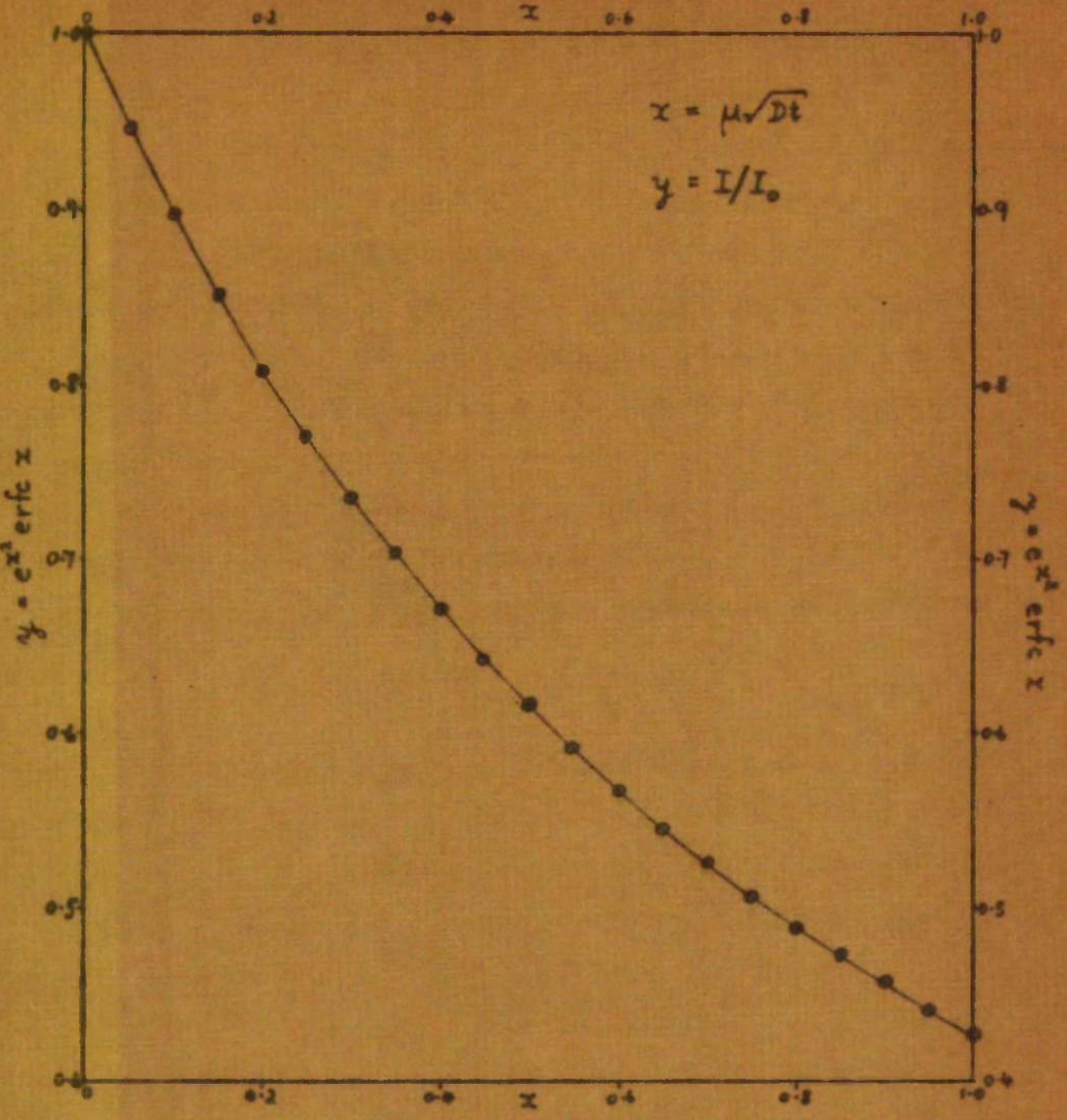

Fig. 3.8: The Function $y = \exp(x^2)\ \mathrm{erfc}\ x$

(ii) Solution of Fick's Equation.

Diffusion is governed by Fick's Second Equation, viz.

$$\frac{dc}{dt} = D\frac{d^2c}{dx^2} \qquad \text{Eqn. 3.1}$$

where c is the concentration of diffusant at a distance x after time t. D is the diffusion coefficient and is usually given in cm^2 per sec. Fick's equations are discussed more fully in the introduction to this thesis.

The solution of Fick's Second Equation depends on the boundary conditions of the particular experiment. In all the tracer-sectioning results reported here the source of the diffusant is an active deposit 2 to 6 microns thick from which diffusion takes place to depths much greater than the deposit thickness into a crystal whose dimension in the diffusion direction is very much greater than the penetration of diffusant. These experimental conditions approximate to that of diffusion from an infinitely thin source into a semi-infinite solid. The appropriate solution[31,32] of Fick's equation for these boundary conditions is

$$c = \frac{Q}{(\pi Dt)^{\frac{1}{2}}} \exp\left(\frac{-d^2}{4Dt}\right) \qquad \text{Eqn. 3.2}$$

where c is the concentration of radioactive tracer at a distance d from the deposit after time t. (In this equation d is used in place of x). Q is the total activity deposited at the surface; D is the diffusion coefficient. Thus a plot of $\log_{10}c$ against d^2 should give a straight line of slope (m) given by

$$m = -1/(2.303 \times 4Dt). \qquad \text{Eqn. 3.3}$$

The linearity of such a plot is usually taken as being diagnostic of bulk diffusion. Thus, if the boundary conditions have been chosen correctly, a plot of the logarithms of the specific activities, A (used as a measure of c), against the corresponding values of d^2 should be a straight line of negative slope, m, from which the diffusion coefficient may be obtained by the calculation

$$D = -1/(2.303 \times 4mt).$$

(iii) Tracer-Sectioning Results for Naphthalene Monocrystals.

The tracer-sectioning results for single crystals of naphthalene are shown in Figs. 3.1 to 3.5 and Tables 3.1 to 3.5. The plots of log A vs d^2 are almost all linear indicating that the correct boundary conditions are present and that bulk diffusion is taking place. From these plots which are linear and show none of the peculiarities outlined below, the diffusion coefficients were calculated using Eqn. 3.4. The gradients were computed by the method of least squares using the Sirius computer at the Colville's Computing Laboratory, University of Strathclyde. The calculated bulk self-diffusion coefficients are given in Table 3.9 along with the corresponding diffusion temperatures and details of the crystals studied.

Some of the plots show one or more of the following departures from simple linearity/-

(a) An intial high point.

An initial high point occurs in the following naphthalene runs: 12A, 12B, 14, 16C, 21, 23, 27, 30B, 31 and 33C. No explanation could be found why these runs, rather than others, should have high initial points. There is no correlation between the existence of a high point and the absolute activity at the surface, the diffusion coefficient, or the diffusion time or temperature.

High initial points have been found in many diffusion studies, including both the published studies on anthracene. Labes and his co-workers found[2] that the first two or three sections gave anomalously high specific activities but do not say how high. Sherwood and Thomson[1] found initial high points in all their crystals. The activities of their first sections were at least three times greater than that of the second slices and in six crystals out of eight studied the first slice was more than ten times more active than the second slice. In contrast, the results on naphthalene reported here show only ten crystals with high initial points out of more than 50 studied, and of these ten, only two (Runs 30B and 31

have initial activities greater than about ten times the activities of the second sections.

The practice adopted by previous workers who found anomalously high initial activities was to discount the first point and calculate D from the remainder of the slope. However, Mortlock[37] has cast doubt on this procedure and has shown how the diffusion coefficient calculated from a slope with high initial point can be corrected. Applying Mortlock's correction to the two worst cases (30B and 31) in the results reported here, it can be shown that the calculated diffusion coefficients are from 10 to 20% too low. Taking a 20% increase as being correct, the diffusion coefficient for Run 30B becomes 9.08×10^{-13} instead of 7.56×10^{-13} as calculated directly from the log A vs. d^2 plot. Similarly Run 31 gives $D = 2.24 \times 10^{-11}$ instead of 1.87×10^{-11}. In all other cases the increase is smaller.

The differences made to the Arrhenius plots by applying these corrections to the diffusion coefficients is well within the standard deviations of the gradients of the plots, hence, it was decided to follow the example of previous workers and calculate the diffusion coefficients directly from the plot of log A against d^2 since the corrections required by the initial high points are not significant in the present case.

(b) An initial upward hook.

This occurs in Runs 29 and 30A where the first few slices have anomalously high activities. In both these crystals the activity at the surface was considerably greater than average and the first few slices may have been contaminated from the initial slice despite the great care taken to prevent this. Other workers[2,36] have reported the presence of a pronounced upward hook at small penetrations and attributed it to deformation of the surface layer during preparation of the crystals for deposition. However, contamination is a more likely reason in the present case.

In calculating the diffusion coefficients from these two plots, the upward hook was ignored and D calculated from the linear part of the plot. Application of Mortlock's correction does not alter the diffusion coefficients appreciably.

(c) A diffusion "tail".

Typical diffusion "tails" were found in many of the crystals studied. Such tails have been reported[1,2] by many workers and attributed to rapid diffusion down dislocations or block walls resulting in a levelling out of tail activity through the crystal. This secondary diffusion, although rapid, carries only a small fraction (a reported 1% in anthracene) of the mass transported and hence diffusion coefficients calculated from the main part of the plot and ignoring the tail are not much in error. However, the tail is easily corrected for and this was done in the present case.

The method of correction used was to extrapolate the tail backwards to cut the log A axis and read off the activity due to the tail at each point on the main part of the plot. These values were then subtracted from the measured activities and the logarithms of the corrected activities re-plotted against d^2. This procedure invariably gave a linear plot from which D was calculated. An example of a tail correction is given in the Appendix.

The reasons for the diffusion tail in naphthalene will be discussed in a later section.

(d) Non-linear plots.

In Runs D3 and D6 the plots of log A against d^2 do not give straight lines (see Figs. 3.5 (b) and 3.5 (c). Run D6 is completely non-linear in d^2, however, Run D3 could be treated as linear if the final point is interpreted as a tail and the initial points as an upward hook. A diffusion coefficient was calculated from the remaining linear part but must be treated with caution. It is quoted in the Table of Diffusion Coefficients. These two plots, which are apparently linear in d rather than d^2, will be

reconsidered later.

The results from the tracer-sectioning experiments on naphthalene monocrystals are given in Table 3.9 and discussed in relation to the Arrhenius parameters in a later section.

(iv) Results for Polycrystalline Compacts of Naphthalene.

The same boundary conditions apply to the tracer-sectioning results on the compacts as in the monocrystals on the assumption that bulk diffusion is taking place. The results are given in Table 3.6 and log A plotted against d^2 in Fig. 3.6. A is in c.p.s. per mg., d in microns, and d^2 in square microns.

Several differences from the results on single crystals are immediately apparent. Penetrations are much deeper in the compacts than in the monocrystals. Tails are much more in evidence and some of them have an apparent slope; upward hooks at smaller penetrations occur in the majority of the results. However, a large central portion of the plot is linear in d^2 (except Run C4 which was not sectioned deep enough).

Discounting the initial upward hooks and subtracting the tails as is the practice in other diffusion studies, diffusion coefficients can be calculated from the remainder of the plot using Eqn. 3.4. The gradients were determined by the method of least mean squares as in the monocrystal results. The apparent bulk diffusion coefficients so calculated are given in Table 3.9 and discussed later, in relation to the results on single crystals and the Arrhenius parameters.

The possibility of the compact results not being validly analysed in terms of lattice diffusion is discussed in a later section.

(v) Surface-Decrease Results for Naphthalene Monocrystals.

Mathematical Treatment.

In the surface-decrease experiments the diffusant was a thin layer

of radioactive naphthalene deposited on the cleavage plane of a naphthalene monocrystal. The thickness of the crystal in the diffusion direction was about 4 mm. These conditions approximate to diffusion from an infinitely thin layer into a semi-infinite solid. The solution of Fick's equation for these boundary conditions (see section (ii) above) is

$$C = \frac{Q}{(\pi Dt)^{\frac{1}{2}}} \exp\left(\frac{-x^2}{4Dt}\right) \qquad \text{Eqn. 3.2}$$

In the tracer-sectioning method the activities due to individual crystal sections are measured, activity in other parts of the crystal not "interfering" in the measurements. However, in the surface-decrease method the activity detected at the crystal surface is due not only to active material on the surface but also to activity in deeper layers of the crystal some of the emissions from which penetrate the intervening layers and reach the detector. Allowance must be made for this. In the present case the emitted rays are weak beta particles which are not very penetrating (see Table 2.3.1 on page 45).

The absorption of radiation in matter can be found by measuring the activity of a source behind increasing thicknesses of material. The absorption of electromagnetic radiation is found to obey Lambert's Law,

$$I = I_0 e^{-\mu x}, \qquad \text{Eqn. 3.5}$$

where I is the intensity of the radiation after traversing a thickness x of absorber, and I_0 is the intensity of the radiation in the absence of absorber. This equation defines the linear coefficient of absorption, μ. Since beta rays are not undulatory there is no apparent reason why they should obey Eqn. 3.5, however, it is usually found that the rays do, in fact, follow Lambert's Law.[14] Thus the coefficient of absorption as defined by Eqn. 3.5 can be found although the concept has only a dubious and probably limited application to beta particles.

Assuming that Eqns. 3.2 and 3.5 are applicable, the total activity, I, measured at the surface of the crystal after time t will be[15,104]

$$I = \frac{I_0}{(\pi Dt)^{\frac{1}{2}}} \int_0^{\infty} \exp\left(\frac{-x^2}{4Dt} - \mu x\right) dx,$$

where I_0 is the activity at $t = 0$.

Introducing the error function in the form

$$\text{erf } \mu (Dt)^{\frac{1}{2}} = \frac{2}{(\pi)^{\frac{1}{2}}} \int_0^{\mu(Dt)^{\frac{1}{2}}} \exp(-y^2)\, dy,$$

where

$$y = \frac{x}{2(Dt)^{\frac{1}{2}}} + \mu (Dt)^{\frac{1}{2}},$$

it can be shown that[15,31,104]

$$I = I_0 \exp(\mu^2 Dt)(1 - \text{erf } \mu(Dt)^{\frac{1}{2}})$$

or, writing

$$\text{erfc } x = 1 - \text{erf } x,$$

$$I = I_0 \exp(\mu^2 Dt)\ \text{erfc } \mu(Dt)^{\frac{1}{2}} \qquad \text{Eqn. 3.6}$$

Thus, since I, I_0 and t can be measured, $x = \mu(Dt)^{\frac{1}{2}}$ can be found if the function

$$y = \exp(x^2)\ \text{erfc } x$$

can be evaluated. This function has been used by previous workers[15,10] and tabulated. It is shown graphically in Fig. 3.8. Therefore, by measuring the decrease of surface activity of the crystal with time, $\mu (Dt)^{\frac{1}{2}} = x$ can be evaluated from Fig. 3.8. The only problem remaining is the evaluation of μ.

Evaluation of the Absorption Coefficient, μ

Because of the doubtful validity of Eqn. 3.5 the absorption coefficient should be determined experimentally for each absorber and the range of application of Lambert's Law found. However, it is found in practice that the mass absorption coefficient, μ_m cm.^{2} per g., is nearly independent of the nature of the absorber[105] so that if μ_m is known by

measurement in one absorber it can be assumed to apply to other absorbers at least approximately. Since the experimental evaluation of μ for naphthalene would be a difficult undertaking and the results were required only as a check on the tracer-sectioning experiments, it was decided not to re-determine μ but to utilise published figures to calculate the absorption coefficient for C-14 beta rays in naphthalene.

The mass absorption coefficient, μ_m cm.^{2} per g., is defined by the relation[105]

$$\mu_m = \mu / \rho \qquad \text{Eqn. 3.8}$$

where μ is the absolute absorption coefficient in cm.$^{-1}$ and ρ is the density of the absorber in g. per cm.^{3} The mass absorption coefficient can be calculated from the half-thickness, $d_{\frac{1}{2}}$ g. per cm.^{2}, thus

$$\mu_m = 0.693/d_{\frac{1}{2}} \qquad \text{Eqn. 3.9}$$

Combining Eqns. 3.8 and 3.9 to obtain the absolute absorption coefficient, μ, we obtain

$$\mu = 0.693 \rho / d_{\frac{1}{2}} \qquad \text{Eqn. 3.10}$$

Inserting the published values: for C14 beta's[105], $d_{\frac{1}{2}} = 2.43$ mg./cm.^{2}, and for naphthalene[106], $\rho = 1.145$g./cm.^{3} Eqn. 3.10 gives

$$\mu = (0.693 \times 1.145)/ (2.43 \times 10^{-3}), \qquad \text{Eqn. 3.11}$$

i.e., $\mu = 326.5$ cm.$^{-1}$

This was the value used in the present work for the absorption coefficient of C-14 beta rays in naphthalene.

Calculation of the Diffusion Coefficients.

Diffusion coefficients were calculated from the surface-decrease results (Table 3.7) by the following procedure:-

1. I/I_o was plotted against log t. The resulting graph is almost linear and a smooth curve was drawn through the points (Fig. 3.7). I_o is the initial surface activity, and I the activity after time t.

2. The function $y = \exp(x)^2 \operatorname{erfc} x$ was plotted and a smooth curve

drawn (Fig. 3.8).

3. Convenient values of I/I_o were selected and the corresponding values of log t read off from Fig. 3.7.

4. Using the same values of I/I_o as in 3., corresponding values of $\mu(Dt)^{\frac{1}{2}}$ were read off from Fig. 3.8. $I/I_o = y$, and $\mu(Dt)^{\frac{1}{2}} = x$. Thus corresponding values of log t and $\mu(Dt)^{\frac{1}{2}}$ were obtained. These are shown in Table 3.8.

5. $\mu(D)^{\frac{1}{2}}$ was calculated from the values of $\mu(Dt)^{\frac{1}{2}}$ and log t. The time, t, must be converted to seconds.

6. The diffusion coefficient, D, was calculated from the values of $\mu(D)^{\frac{1}{2}}$ using $\mu = 326.5\ cm.^{-1}$ as given in Eqn. 3.11.

By this procedure several values of D were obtained for each surface-decrease experiment. Ideally these values should all be equal, however, as can be seen in Table 3.8, a narrow range of values was obtained in each experiment. Values calculated from very long t's or very short t's (where the I/I_o vs. log t plot is non-linear) deviate farthest from the average and these were rejected before averaging the remaining values to obtain a final value of the diffusion coefficient for the experiment. These values are included in Table 3.9.

Table 3.9: Bulk Self-Diffusion Coefficients for Naphthalene.

Run	D(cm.^{2} per sec.)	T(°C.)	$\frac{1}{T}\times10^3$(°K.$^{-1}$)	log (D×10^{12})
Boule A (Perpendicular to "ab" Plane) Line A				
1A	$(4.52\pm0.11)\times10^{-10}$	50.0	3.094	2.655
2A	$(7.97\pm0.44)\times10^{-11}$	40.5	3.188	1.901
3	$(2.00\pm0.26)\times10^{-10}$	45.7	3.137	2.301
4	$(1.93\pm0.18)\times10^{-10}$	45.1	3.142	2.286
Boule B (Perpendicular to "ab" Plane) Line B				
SD1	6.83×10^{-11}	52.5	3.071	1.834
Boule D (Perpendicular to "ab" Plane) Line D				
SD2	4.25×10^{-11}	70.0	2.914	1.628
Boule E (Perpendicular to "ab" Plane) Line G',H',J', (Symbol ▲)				
SD3	4.06×10^{-12}	60.8	2.994	0.609
Boule G, Annealed (Perpendicular to "ab" Plane) Line G',H',J', (Symbol o)				
8	$(2.53\pm0.07)\times10^{-11}$	70.4	2.914	1.404
9	$(5.71\pm0.28)\times10^{-12}$	60.0	3.001	0.757
11A	$(1.22\pm0.11)\times10^{-11}$	76.2	2.862	1.086
11B	$(1.29\pm0.14)\times10^{-11}$	76.2	2.862	1.111
12B	$(1.07\pm0.01)\times10^{-11}$	66.3	2.945	1.029
Boule H, Annealed (Perpendicular to "ab" Plane) Line G',H',J', (Symbol ▲)				
12A	$(1.36\pm0.08)\times10^{-11}$	66.3	2.945	1.132
14	$(3.18\pm0.69)\times10^{-11}$	78.6	2.843	1.502
5D4	3.04×10^{-11}	78.6	2.843	1.483
Boule J, Annealed (Perpendicular to "ab" Plane) Line G',H',J', (Symbol ●)				
15C	$(2.15\pm0.16)\times10^{-11}$	68.0	2.930	1.332
16C	$(8.58\pm0.15)\times10^{-12}$	61.5	2.988	0.934
18	$(2.30\pm0.12)\times10^{-12}$	57.3	3.026	0.362
19B	$(1.08\pm0.18)\times10^{-11}$	64.2	2.963	1.032
29	$(3.74\pm0.38)\times10^{-11}$	74.9	2.873	1.573
33D	$(2.56\pm0.01)\times10^{-12}$	56.2	3.036	0.408

Table 3.9 (Cont/d.)

Run	$D(cm^2 per sec.)$	$T(^oC.)$	$\frac{1}{T} \times 10^3 (^oK^{-1})$	$\log (D \times 10^{12})$
Boule J, Annealed (Parallel to "a" Axis) Line G',H',J', (Symbol x)				
A1	$(8.89 \pm 0.24) \times 10^{-12}$	61.5	2.988	0.949
A2	$(2.75 \pm 0.05) \times 10^{-12}$	57.3	3.026	0.439
A3	$(2.71 \pm 0.14) \times 10^{-11}$	70.9	2.906	1.433
Boule J,Annealed (Parallel to "b" Axis) Line G',H',J', (Symbol +)				
B1	$(1.62 \pm 0.18) \times 10^{-11}$	68.0	2.930	1.209
B2	$(8.13 \pm 0.09) \times 10^{-12}$	61.5	2.988	0.910
B3	$(3.16 \pm 0.06) \times 10^{-12}$	57.3	3.026	0.499
Boule J, Specially Annealed (Perpendicular to "ab" Plane) Line J"				
15A	$(5.52 \pm 0.13) \times 10^{-12}$	68.0	2.930	0.742
17A	$(5.14 \pm 0.29) \times 10^{-13}$	52.5	3.070	-0.289
17B	$(3.58 \pm 0.03) \times 10^{-13}$	52.5	3.070	-0.447
19A	$(2.80 \pm 0.11) \times 10^{-12}$	64.2	2.963	0.447
20A	$(1.77 \pm 0.16) \times 10^{-13}$	51.3	3.082	-0.753
20B	$(2.11 \pm 0.02) \times 10^{-13}$	51.3	3.082	-0.675
21	$(5.00 \pm 0.05) \times 10^{-13}$	51.4	3.081	-0.301
22A	$(8.87 \pm 0.51) \times 10^{-12}$	72.5	2.893	0.940
22B	$(1.11 \pm 0.03) \times 10^{-11}$	72.5	2.893	1.043
23	$(1.91 \pm 0.03) \times 10^{-12}$	60.9	2.993	0.280
33C	$(5.96 \pm 0.69) \times 10^{-13}$	56.2	3.036	-0.225
Boule L, Specially Annealed, (Perpendicular to "ab" Plane) Line L"				
26A	$(5.25 \pm 0.20) \times 10^{-12}$	74.35	2.877	0.720
27	$(1.90 \pm 0.01) \times 10^{-12}$	69.67	2.916	0.278
30A	$(1.84 \pm 0.15) \times 10^{-12}$	78.2	2.846	0.264
30B	$(7.56 \pm 0.35) \times 10^{-13}$	78.2	2.846	-0.121
34	$(2.77 \pm 0.03) \times 10^{-13}$	56.8	3.030	-0.723
Boule N, (Perpendicular to "ab" Plane) Line N				
31	$(1.87 \pm 0.05) \times 10^{-11}$	56.0	3.038	1.271
32	$(4.62 \pm 0.08) \times 10^{-12}$	48.8	3.106	0.664

Table 3.9 (Cont/d.)

Run	D(cm²per sec.)	T(°C.)	$\frac{1}{T}\times10^{3}$(°K.$^{-1}$)	log(D$\times10^{12}$)
Boule N, Annealed (Perpendicular to "ab" Plane) Line N' (Symbol x)				
33A	$(7.92\pm0.05)\times10^{-12}$	56.2	3.036	0.899
33B	$(7.76\pm0.11)\times10^{-12}$	56.2	3.036	0.889
35	$(2.11\pm0.03)\times10^{-12}$	48.9	3.105	0.313
Boule N, Annealed (Triiodated Naphthalene as Tracer) (Perp. to "ab" Plane Line N' (Symbol +)				
T1	$(8.69\pm0.05)\times10^{-12}$	56.8	3.030	0.939
T2	$(2.06\pm0.06)\times10^{-12}$	48.9	3.105	0.313
Boule AD2, Annealed (Anthracene Doped) (Perp. to "ab" Plane) Line G',H',J', (Symbol △)				
D3	$(1.80\pm0.07)\times10^{-12}$ (?)	52.9	3.070	0.255
Boule AD3, Annealed (Anthracene Doped) (Perp. to "ab" Plane) Line G',H',J', (Symbol □)				
D1	$(2.21\pm0.11)\times10^{-11}$	68.0	2.930	1.345
D2	$(5.70\pm0.37)\times10^{-12}$	61.5	2.988	0.756
D4	$(2.10\pm0.21)\times10^{-12}$	51.3	3.082	0.323
Boule MD, Annealed (2-Methyl Naphthalene Doped) (Perp. to "ab" Plane) Line G',H',J', (Symbol ▫)				
D5	$(1.98\pm0.02)\times10^{-12}$	51.3	3.082	0.296
Polycrystalline Compacts. Line Comp				
C1	$(6.50\pm0.22)\times10^{-10}$	50.0	3.094	2.813
C2	$(3.16\pm0.93)\times10^{-10}$	40.5	3.188	2.500
C3	$(3.66\pm0.27)\times10^{-10}$	45.1	3.142	2.563
C5	$(9.13\pm0.44)\times10^{-10}$	60.9	2.993	2.961
C6	$(8.33\pm0.72)\times10^{-10}$	54.6	3.051	2.920
C7	$(9.040\pm0.47)\times10^{-10}$	54.6	3.051	2.956

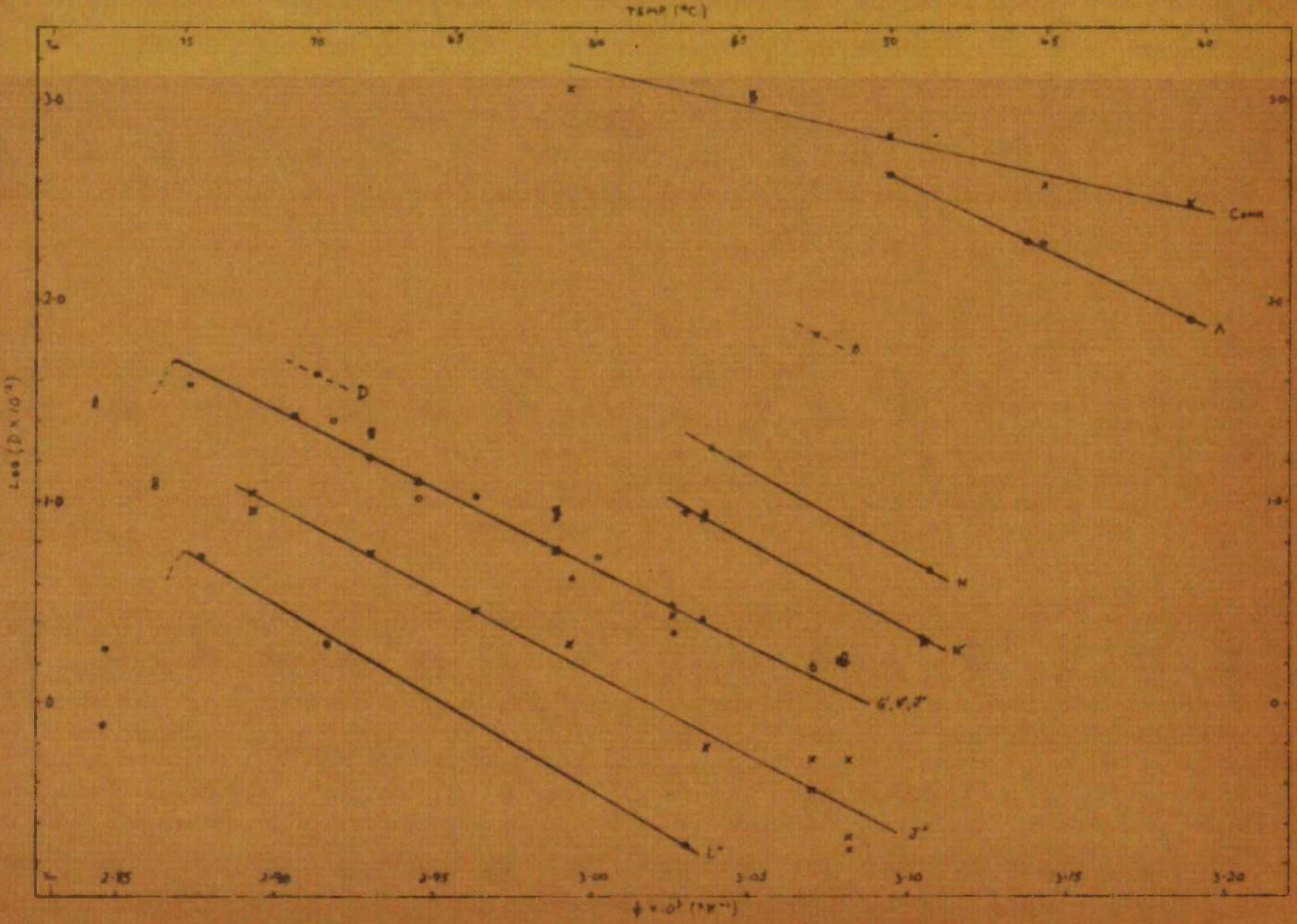

Fig. 3.9; Naphthalene-Arrhenius Plot.

Table 3.10: The Arrhenius Parameters for Naphthalene.

Boule	E (k cal.)	$\log D_o$ ($cm.^2 sec.^{-1}$)
A	36.85±0.60	15.44±0.41
G'	32.79±5.79	10.11±3.72
J' (perp."ab"plane)	35.45±2.79	11.81±1.80
J' (par."a"axis)	36.37±5.58	12.44±3.61
J' (par."b"axis)	33.20±4.78	10.38±3.10
J' (all J' results)	35.24±1.76	11.69±1.13
G',H',J' (all points on line)	34.87±1.47	11.45±0.95
J"	37.96±1.69	12.88±1.10
L"	42.73±1.61	15.40±1.03
N' (C14 tracer)	38.77±0.39	14.46±0.26
N' (C14 and H3 results)	38.62±0.19	14.36±0.13
AD3	30.01±4.61	8.37±3.00
All doped crystals	30.66±2.42	8.78±1.60
Compacts	12.74±1.42	-0.64±0.95

(vi) The Arrhenius Equation for Naphthalene.

In diffusion studies the integrated form of the Arrhenius equation is usually given in the form

$$D = D_o \exp(-E/RT) \qquad \text{Eqn. 3.12}$$

from which it can be seen that a plot of $\log_{10} D$ against $1/T$ should be a straight line of negative slope $E/(2.303R)$ and intercept $\log D_o$. The meanings of the terms are explained in Part I of this thesis. The Arrhenius equation has been found to be almost universally applicable to diffusion coefficients.

Table 3.9 lists the bulk self-diffusion coefficients for naphthalene found in the present work. The origin of the crystals used in the measurements is also given, along with the temperatures of measurement and the reciprocal temperatures. The logarithms of the diffusion coefficients are plotted against $1/T$ in Fig. 3.9. In the Figure and Table a prime (') is used to indicate an annealed crystal, and a double prime (") to indicate specially annealed crystals.

It is immediately obvious from Fig. 3.9 that the results do not fall on any one Arrhenius line. A series of lines is found, the particular line on which a diffusion measurement falls depending on the history of the crystal on which the measurement was made. This conclusion was completely unexpected. The line on which a result falls is indicated in both the Table and the Figure.

The highest line in the Arrhenius plot is formed by diffusion measurements made on compacts (line Comp. in Fig. 3.9). The next line (line A) results from measurements made on crystal A, which was the first crystal grown and which was of very poor quality. Results on the (annealed) boules G',H', and J' all appear to fall on one line, but a line which is much lower than A. Crystals G',H', and J' were of very good quality. It would appear from this that the better the quality

of a crystal the lower is its diffusion coefficient at a particular temperature. The purity of the crystal may also have an affect since boules G,H, and J were made from purer material than previous boules.

These conclusions are borne out by the surface-decrease measurements. Diffusion coefficients found for boules B and D lie lower than those for boule A but higher than those from G. Surface-decrease results from subsequent boules lie very close to line G',H',J'; the result from Run BD4 on boule H being in excellent agreement with the tracer-sectioning result on the same crystal at the same temperature.

To test if annealing was a factor in reducing the diffusion coefficient, crystals from the annealed boule J were "specially annealed" (see page 47) and their diffusion coefficients measured. An even lower Arrhenius line (line J") resulted. To find the effect of impurities, crystals were grown exactly as for boule J' but with impurities added. It was found that annealed crystals from these doped boules fell close to line J'.

To test the matter further, diffusion coefficients were measured on specially annealed crystals from boule L (this was one of the most optically perfect boules grown) and on unannealed crystals from boule N (which was grown from unpurified material at twice the usual rate). The diffusion coefficients from the former gave an Arrhenius plot (line L") lower than line J" whereas the latter gave a plot (line N) higher than line J'. Annealing of boule N reduced its diffusion coefficients to line N'.

That the effect is not spurious can be seen particularly clearly from Run 33 in which the diffusion coefficients of 4 crystals were measured, two from boule N (annealed)(Runs 33A and B), one from boule J (annealed)(Run 33D), and one from boule J (specially annealed)(Run 33C) Runs 33B,C, and D were diffused for the same time at the same temperature but gave different diffusion coefficients showing clearly that the diffusion coefficient varies with the crystal. Runs 33A and B were

on crystals treated exactly alike except for the diffusion time. These two runs gave the same coefficient within the experimental error.

In the experiments to test for anisotropy (carried out on annealed boule J) it was found that the diffusion coefficients parallel to the "a" axis, and parallel to the "b" axis fell on the same Arrhenius line as coefficients measured perpendicular to the "ab" plane. It can be concluded that if diffusion anisotropy exists in naphthalene it is very slight. Tracer experiments using tritiated naphthalene gave the same results as those using naphthalene-1-C14 as tracer. Hence proton diffusion does not occur in naphthalene.

From Fig. 3.9 it can be concluded that diffusion in single crystals of naphthalene is an extrinsic property of the crystal and depends on the perfection of the crystal. To a first approximation the different Arrhenius lines for monocrystals are parallel. The Arrhenius line resulting from polycrystalline material is higher than that for single crystals and is less steep.

The results close to the melting-point are anomalous in that the Arrhenius plot dips downwards at high temperatures.

It can be seen from Eqn. 3.12 that the activation energy of diffusion can be calculated from the slope of the Arrhenius plot and the pre-exponential factor from the intercept. The gradients and intercepts of the various Arrhenius lines were calculated by the method of least squares using the Sirius computer. The pre-exponential factors and activation energies so found are given in Table 3.10. The high temperature points were omitted from the calculation.

Examination of Table 3.10 shows the following:-

1. Aasuming that bulk diffusion is being measured in the compacts, diffusion in polycrystalline naphthalene can be described by the equation

$$D = 0.2 \exp(-12,700/RT), \qquad \text{Eqn. 3.13}$$

The error in E is ±1.42 kcal. The error in $\log D_o$ indicates that D_o

lies between 0.02 and 1.88 $cm.^2/sec.$, the most probable value being 0.21. The activation energy for polycrystals is about three times smaller than that found for monocrystals and D_o is about 10^{12} smaller.

2. Annealed boules G' and J' have the same activation energy and frequency factor within experimental error.

3. Within experimental error diffusion measurements parallel to the "a" axis, parallel to the "b" axis, and perpendicular to the "ab" plane of naphthalene do not show anisotropy.

4. Bulk diffusion in annealed single crystals of naphthalene follows the equation

$$D = 2.8 \times 10^{11} \exp(-34{,}900/RT) \qquad \text{Eqn. 3.14}$$

The error in E is ±1,47kcal. D_o lies between 3.18×10^{10} and 2.50×10^{12} $cm.^2/sec.$ Eqn. 3.14 was calculated from diffusion coefficients measured on boules G', H', and J'.

5. Specially annealed crystals from boule J give the equation

$$D = 7.6 \times 10^{12} \exp(-38{,}000/RT) \qquad \text{Eqn. 3.15}$$

and specially annealed crystals from boule L give

$$D = 2.5 \times 10^{15} \exp(-42{,}700/RT) \qquad \text{Eqn. 3.16}$$

6. The differences in E between boules A, G',J', and J" are of doubtful significance, but E could be interpreted as increasing with increasing perfection of the crystal (i.e. the lower the Arrhenius line in Fig. 3.9, the higher the energy). E for boule L" (which gave the lowest line) is significantly higher than the others. However, boule N' does not agree with the conclusion that E is higher the lower the Arrhenius line.

7. D_o increases from J', to J", to L". However, the results on A and N' do not agree with the interpretation that D_o increases as the Arrhenius line is lowered.

Despite these discrepancies it may be the case that both E and D_o

do increase with perfection of the crystal. This seems the most likely pattern assuming that the diffusion coefficients vary with the crystal: the overall results leave little doubt that D is in fact an extrinsic property of the solid. That no absolutely regular change in D_o and E was found could be attributed to the difficulties in the experimental technique.

8. The results on doped crystals obey the equation

$$D = 6.1 \times 10^{8} \exp(-30{,}700/RT) \qquad \text{Eqn. 3.17}$$

The differences in E and D_o between doped and undoped crystals are significant.

In summary, the results for naphthalene show that diffusion is an extrinsic property of the crystal. The Arrhenius pre-exponential factor and activation energy for diffusion probably increase with increasing perfection of the crystal; the value of the diffusion coefficient at a given temperature definitely decreases with increasing perfection. Diffusion anisotropy is not found. The energy of diffusion in monocrystals is approximately 35 kcal. and D_o is approximately 10^{12} cm2 $sec.^{-1}$ Dopants reduce both E and D_o. The pre-exponential factor in polycrystals is $0.2 cm.^{2} sec.^{-1}$, and E in polycrystals is about one-third of that found in single crystals. The interpretation of the results on polycrystals depends on the assumption that bulk diffusion is being measured in the compacts.

(vii) Annealing Experiment.

The experiment is described on page 60. Four identical crystals were annealed at 79.64±0.02 °C. for varying times, t_a, after which their diffusion coefficients were measured by the tracer-sectioning method. The diffusion temperature, T_d, and diffusion time, t_d, were the same for all four crystals. T_d = 68.0 °C.; t_d = 399 hours. The results are shown in Fig. 3.10(a). A is the specific activity at a distance d microns from the deposit after time t_d. A_o is the specific activity at d = o after time t_d (as found from the intercept of the least mean squares

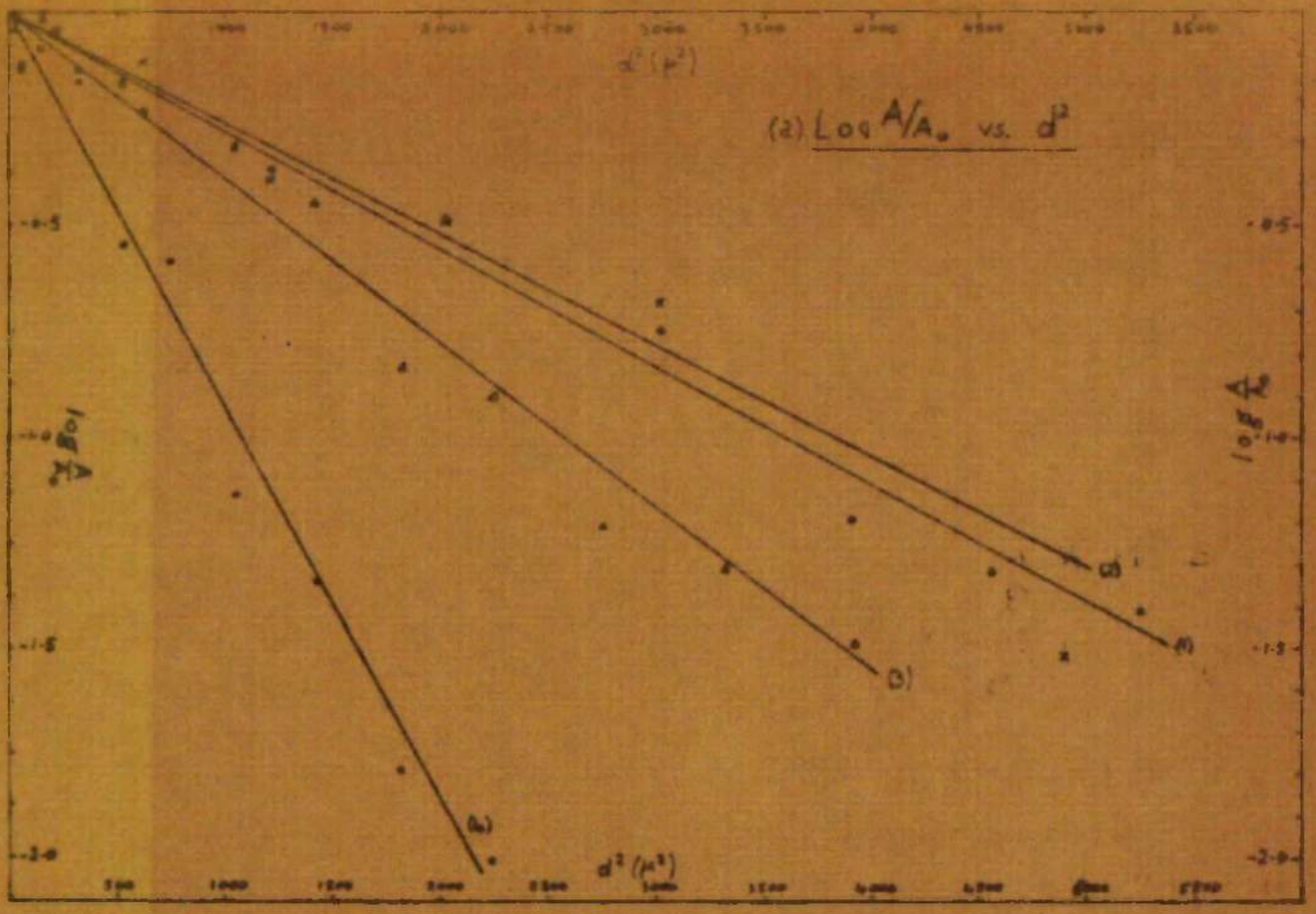

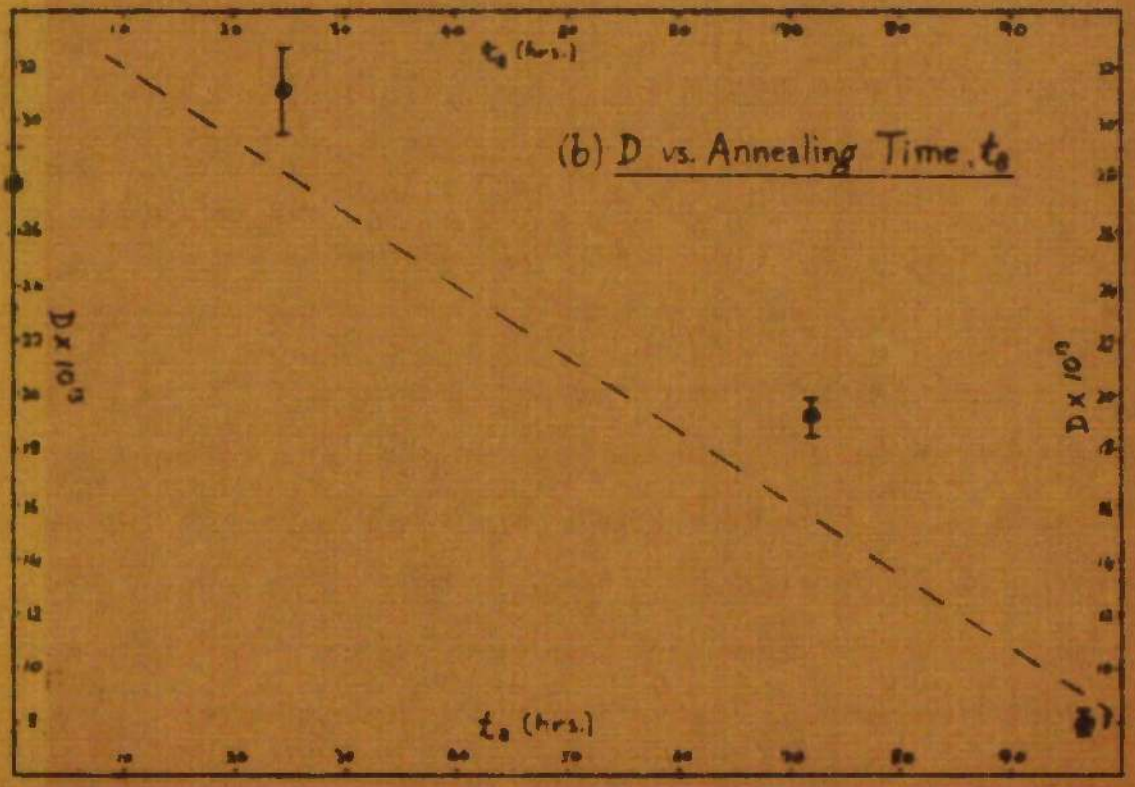

Fig. 3.10: Reduction of D on Annealing

plot of log A versus d^2). From the slopes of the curves it can be seen that the diffusion coefficients of the crystals have changed after annealing. Table 3.11 gives the diffusion coefficients calculated by the method of least squares, and the annealing time, t_a, at 79.64 °. The diffusion coefficients are plotted against t_a in Fig. 3.10(b).

Table 3.11: Change of D on Annealing at 79.64°C.

Crystal	t_a (hrs.)	$Dx10^{13}$ (cm.^{2} sec.$^{-1}$
1	0	27.41±1.50
2	24.25	30.95±1.55
3	72.00	19.08±0.68
4	96.25	8.05±0.34

After annealing for 24 hours the diffusion coefficient is unchanged. After a further two days' anneal D has dropped to approximately two-thirds of its original value, and after another day's annealing (96 hours in all), D has fallen to just over one-quarter of its value before annealing. Thus annealing at a high temperature undoubtedly decreases the diffusion coefficient.

Assuming that the decrease in diffusion coefficient is due to the annealing out of defects, it might be expected that the change in D would follow an exponential law such as

$$\Delta D = \Delta D_o \exp(-t_a/K) \qquad \text{Eqn. 3.18}$$

where ΔD is the change in D after annealing for time t_a; ΔD_o and K are constants. Equations similar to 3.18 have been found to hold for annealing out of quenched-in resistivity[108,109] in some metals. However, a plot of $\log \Delta D$ vs. t_a is not linear in the present case so the exponential law apparently does not hold.

It has been found in some annealing studies on metals that quenched-in resistivity does not decay exponentially. The resistivity (ρ) may

decrease only slowly at the beginning of the anneal, followed by a period during which $\Delta\rho/\Delta\rho_o$ decreases more rapidly, slowing up at longer t_a's to approach an asymptotic value. When $\Delta\rho/\Delta\rho_o$ is plotted against t_a an S-shaped curve results. Such a curve has been found for high temperature quenches in gold.[110] It has been suggested that this behaviour results when high concentrations of quenched-in defects are present in crystals of low dislocation content. In such cases the interaction of point defects becomes important.

Unfortunately it is not possible to measure diffusion coefficients in a short-time experiment at temperatures well below the annealing temperature, so that experiments strictly analagous to quenching experiments in metals cannot be performed. Although the results of the present experiment show clearly that annealing reduces the diffusion coefficient it is not possible to say with any confidence what simple law, if any, the annealing process obeys.

(viii) Diffusion "Tails" in Naphthalene.

As discussed in Part I. of this thesis, diffusion "tails" have been found in many diffusion studies (including anthracene[1,2]) and been attributed to rapid diffusion down short-circuiting paths. The tail manifests itself in tracer experiments as small activities within the specimen at depths much greater than the bulk diffusion penetration. It has been suggested that penetration of the crystal is complete. In some crystals tested by the author the tail extended as far into the crystal as it was possible to section (3-4mm.). However, tails were not present in all crystals, and in almost all cases where a tail was found the activity was very low and hence of doubtful significance.

Table 3.12: The Incidence of Diffusion Tails in Naphthalene.

See Over.

Table 3.12: The Incidence of Diffusion Tails in Naphthalene

Crystal	Run	t(hrs.)	T(°C.)	R_T(c.p.s.)	R_T/R_S
A	4	26.17	45.1	20.0	4.4
G'	9	48.0	60.0	0.4	0.8
G'	11A	20.0	76.2	N.D.	Nil
G'	11B	20.0	76.2	1.4	2.8
G'	12B	48.0	66.3	N.D.	Nil
H'	14	96.0	78.6	0.9	3.0
J'	16C	89.0	61.5	0.3	1.0
J'	19B	113.0	64.2	1.6	5.3
J'	33D	360.0	56.2	N.D.	Nil
J'(par."a")	A1,A2	89.0,546.2	61.5,57.3	N.D.	Nil
J'(par."b")	B1	65.0	68.0	3.5	14.0
J'(par."b")	B2	89.0	61.5	N.D.	Nil
J"	17A	449.0	52.5	0.5	2.5
J"	17B	449.0	52.5	0.5	2.5
J"	(19A,20A,20B, 21,22A,22B, 23, 33C	48.0 to 396.0	51.3) to 72.5)	N.D.	Nil
L"	(26A, 27, 30A, 34	63.1 to 356.0	56.8) to 78.2)	N.D.	Nil
N	31	21.5	56.0	N.D.	Nil
N	32	70.0	48.8	2.0	1.7
N'	(33A, 33B 35,T1,T2	119.2 to 360.0	48.9) to 56.8)	N.D.	Nil
AD3	D1	65.0	68.0	0.6	2.4
AD3	D2	89.0	61.5	0.6	3.0
AD3	D4	396.0	51.3	N.D.	Nil
MD	D5	396.0	51.3	N.D.	Nil
Compact	C1	48.0	50.0	2.0	0.5
Compact	C2	72.0	40.5	0.5	0.13
Compact	C3	26.17	45.1	6.5	1.0
Compact	C5	24.0	60.9	1.0	8.3
Compact	C7	21.0	54.6	0.4	0.3

Table 3.14: Tail Experiments.

	Expt. 1 T=26±1°C.; t=165 hrs. R_B=1.08c.p.s.		Expt. 2 T=60±1°C.; t=72 hrs. R_B=1.22c.p.s.		Expt. 3 T=70±2°C.; t=15 hrs R_B=1.15c.p.s.	
Xtal	R_s (c.p.s.)	A (c.p.s/mg.)	R_s (c.p.s.)	A (c.p.s/mg.)	do	do
J	-	-	Nil	Nil	1.28	0.010
L	1.75	0.010	0.76	0.005	1.21	0.033
L'	0.39	0.002	-	-	0.17	0.003*
N	0.04	0.0004*	0.47	0.002	Nil	Nil
AD2	0.26	0.001*	Nil	Nil	0.69	0.005
AD3	0.14	0.001*	Nil	Nil	-	-
MD	0.07	0.0005*	2.22	0.023	Nil	Nil
ID	0.31	0.003*	Nil	Nil	Nil	Nil
Comp.	-	-	5.77	0.071	13.6	0.136

Table 3.12 lists all the tracer-sectioning experiments on naphthalene in which a tail was found or would have been found if present. Those experiments are omitted in which the crystal was not sectioned deep enough to find the tail or in which, for some other reason, no definite decision could be made about its presence or absence. The diffusion time and temperature are included in the Table. R_T is the count-rate found in the tail minus the background count, R_B. N.D. indicates the absence of a tail. The ratio R_T/R_B is given as a measure of the significance of the count. Table 3.12 is summarized in Table 3.13. The total number of runs carried out on each crystal boule is listed together with the number of runs in which a tail was detected. Doubtful experiments are omitted.

Table 3.13: Summary of Diffusion Tails in Naphthalene.

Crystal :	A	G'	H'	J'	J''	L''	N	N'	Doped	Comps.
No. of Runs:	1	4	1	7	10	4	2	5	4	5
No. of Tails:	1	2	1	3	2	Nil	1	Nil	2	5

It is difficult to generalise from Tables 3.12 and 3.13 because of the low activities involved and the small number of experiments carried out on some of the crystal boules. However, it could be concluded that as the crystal becomes more perfect the tails become fewer. For example, tails were found in all of the compacts, in half of the doped crystals, in half of the annealed crystals (G',H',J'), in one-fifth of crystals from specially annealed boule J'', and in none of the crystals from specially annealed boule L''. This is the expected pattern if the tails are caused by dislocations and block walls. Nevertheless, the results are inconclusive.

To obtain more definite results the experiments described on page 61 were carried out. By this means comparatively large weights of crystal were obtained and so, if tails were levelled through the crystals,

comparatively large (and significant) counts could be expected. The results are given in Table 3.14. R_s is the count-rate of the sample minus the background count, R_B. A is the specific activity in c.p.s./mg. ($=R_s$/wt. of sample). R_s = Nil indicates that the sample count-rate was within one standard deviation of the background count. Any R_s less than about 0.3 c.p.s. is highly dubious and results from such counts are marked with an asterisk.

The following conclusions can be drawn from the tail experiments:-

(a) Boule N and doped boules AD2, AD3, and ID do not have tails;

(b) Boule J (unannealed) and L'(Annealed), and doped boule MD probably do not have tails, or at best have only very small tails;

(c) Boule L (unannealed) has a very small tail; and

(d) The compacts have diffusion tails.

Apart from the results on compacts the incidence of tails found by these experiments is not the one expected if the tails are due to short-circuiting paths such as dislocations and block walls. Certainly the tails are not levelled through the crystal. Even where a tail was found in these experiments the specific activities are at least a factor of 10 smaller than would be predicted from the tracer-sectioning results.

The author is of the opinion that the evidence indicates strongly that diffusion tails found by the tracer-sectioning method (in naphthalene) are not "real", but are attributable to the experimental technique.

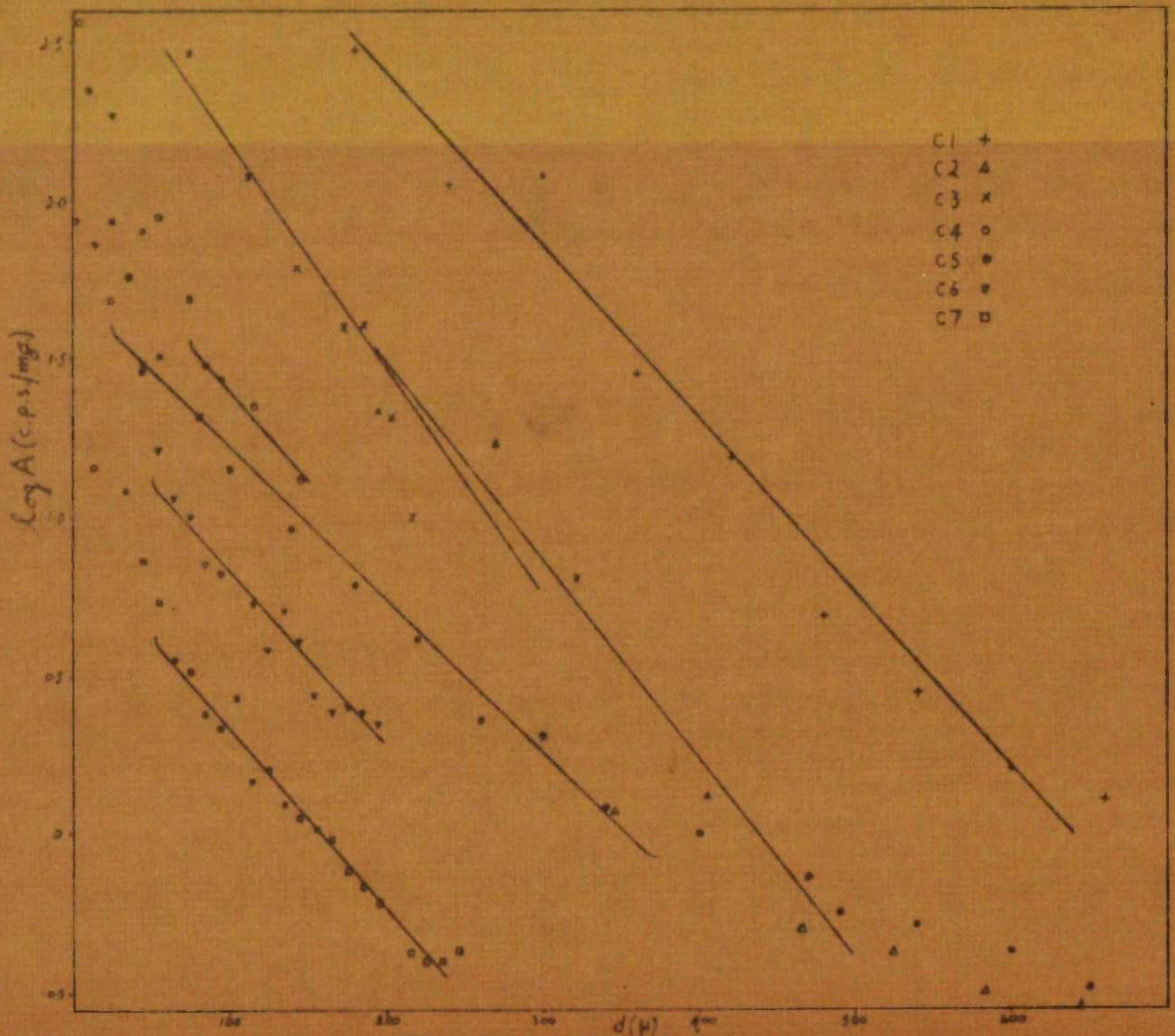

Fig. 3.11: Log A vs. d for Compacts.

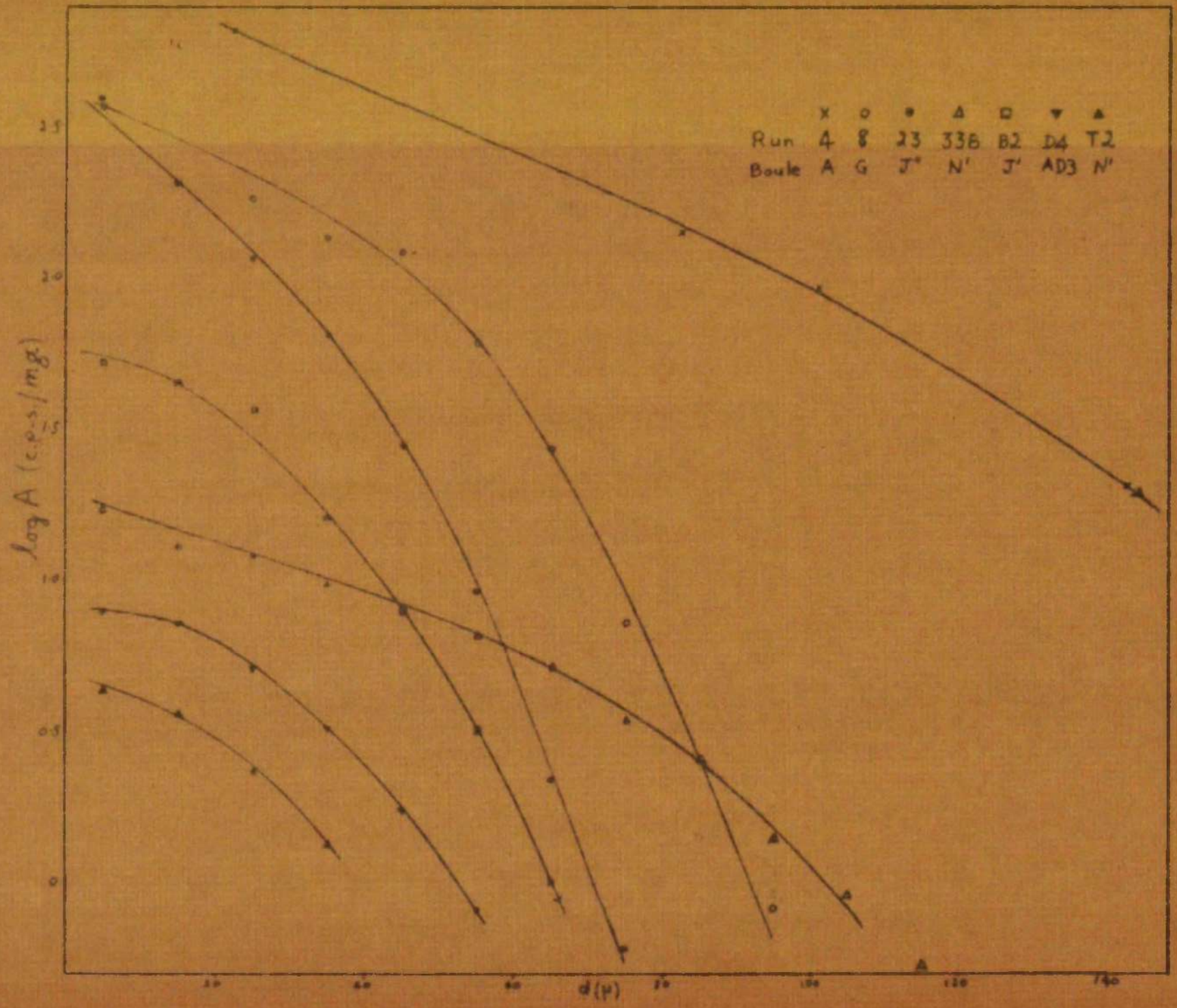

Fig. 3.12: Log A vs. d for Monocrystals.

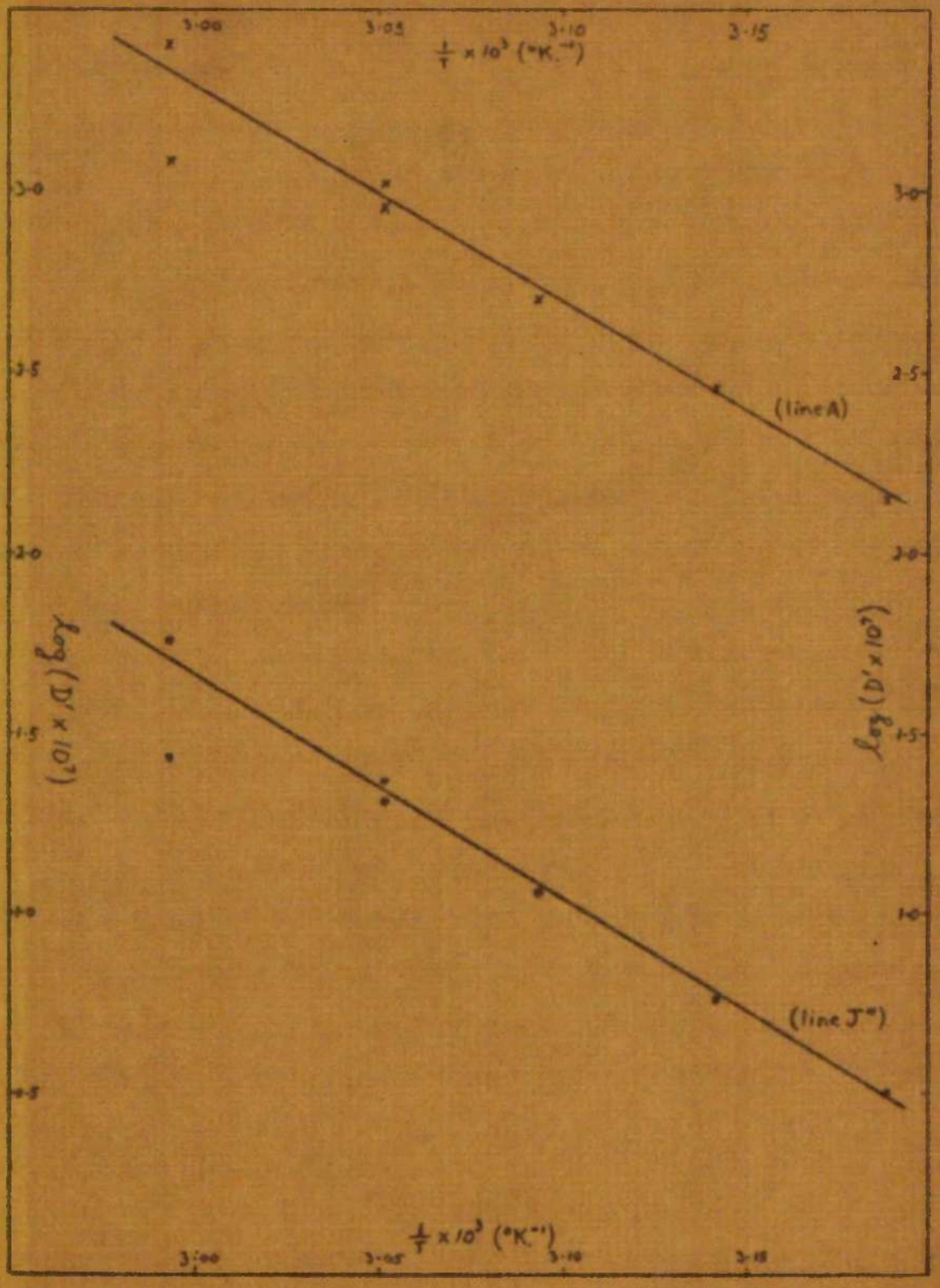

Fig. 3.13: Arrhenius Plot - Grain-Boundary Diffusion.

(ix) Grain-Boundary Diffusion in Naphthalene

(ix) Grain-Boundary Diffusion in Naphthalene

In the former sections results on polycrystalline naphthalene and on Runs D3 and D6 (doped monocrystals) doubts were expressed whether diffusion in these cases could be legitimately treated as bulk diffusion. Figs. 3.5(b) and (c) show Runs D3 and D6 plotted against both d and d^2. The plots against d are more nearly linear than the plots against d^2. Linearity in d is typical of grain-boundary diffusion.

The results from naphthalene compacts are given in Table 3.6 (page 82) and plotted against d^2 in Fig. 3.6. They are discussed in terms of bulk diffusion on page 94. In Fig. 3.11 the same results are plotted against d, and, for comparison, a selection of results from monocrystals are shown plotted against d in Fig. 3.12. The monocrystals show the downward curvature expected, but in the compacts downward curvature is absent and fairly linear plots are obtained except near the surface of the crystal and in some cases at deep penetrations. It seemed worthwhile, therefore, to carry out a Fisher analysis on these results to find if they were consistent with grain-boundary diffusion.

In grain-boundary diffusion[111] material is usually considered to diffuse from a source of constant concentration down a uniform boundary of width δ, the boundary being perpendicular to the surface. Fick's laws are assumed to be obeyed with the diffusion coefficient (D') in the boundary very much greater than the bulk diffusion coefficient, D. Several solutions to the grain-boundary diffusion problem have been published, the simplest to apply being that of Fisher,[112] viz.

$$C = C_o \exp(-\pi^{\frac{1}{4}} \eta \beta^{-\frac{1}{2}}) \operatorname{erfc} \tfrac{1}{2}\xi \qquad \text{Eqn. 3.19}$$

where $\eta = y/(Dt)^{\frac{1}{2}}$, $\beta = D'/D.\frac{1}{2}\delta/(Dt)^{\frac{1}{2}}$, and $\xi = (x-\frac{1}{2}\delta)/(Dt)^{\frac{1}{2}}$. y is the direction of diffusion down the boundary, and x the direction normal to it. The solution is approximate only, but is the principle one used for measuring D'.

It can be shown[108,111] that, in the sectioning method where sections are taken parallel to the free surface and perpendicular to the boundary, Fisher's solution gives

$$m = d \log c/dy = -2^{\frac{1}{2}}/(2.303(\pi Dt)^{\frac{1}{4}} (D'\delta/D)^{\frac{1}{2}} \quad \text{Eqn. 3.20}$$

where c is the concentration of diffusant at a distance y, and t is the diffusion time. That is, a plot of log c against y (or d) should be a straight line of slope, m, given by equation 3.20.

The least mean squares (l.m.s.) slopes of the linear portions in Figs. 3.5(b), 3.5(c), and 3.11 were calculated and D' found from Eqn. 3.20 by the rearrangement

$$D'\delta = \frac{1}{(2.303)^2} \cdot \left(\frac{d \log c}{dy}\right)^{-2} \cdot \frac{2D}{(\pi Dt)^{\frac{1}{2}}} \quad \text{Eqn. 3.21}$$

δ was assumed to be 8 Angstrom units. D' was calculated taking the lattice diffusion coefficient, D, from line A in Fig. 3.9 and also from line J". The results are shown in Table 3.15, both calculated values of D' being given.

Table 3.15: Grain-Boundary Diffusion Coefficients in Naphthalene-A

Run	Slope(cm.$^{-1}$)	t(hrs)	T($^{\circ}$C.)	D'(lineA)	D'(lineJ")
C1	-52.2±1.8	48.0	50.0	4.99×10^{-5}	1.15×10^{-6}
C2	-57.7±6.9	72.0	40.5	1.40×10^{-5}	3.13×10^{-7}
C3	-70.0±6.6	26.17	45.1	2.90×10^{-5}	5.73×10^{-7}
C4	-55.6±1.3	43.25	60.9	1.20×10^{-4}	2.71×10^{-6}
C5	-44.5±1.4	24.0	60.9	2.51×10^{-4}	5.69×10^{-6}
C6	-54.5±2.8	21.0	54.6	1.04×10^{-4}	2.36×10^{-6}
C7	-58.6±1.6	21.0	54.6	8.97×10^{-5}	2.03×10^{-6}
D3	-429±7	449.0	52.9	3.01×10^{-7}	6.81×10^{-9}
D6	-1023±20	89.0	60.9	2.47×10^{-7}	5.59×10^{-9}

Grain-boundary diffusion obeys an Arrhenius relationship in the form

$$D' = D'_o \exp(-E'/RT) \quad \text{Eqn. 3.22}$$

where E' is the activation energy for grain-boundary diffusion, T is the absolute temperature, and D'_o is the pre-exponential factor. Log D' is

shown plotted against 1/T in Fig. 3.13. A good straight line is obtained (with the possible exception of Run C4) irrespective of whether the bulk diffusion coefficient from line A or line J" (Fig. 3.9) is used in the calculation. Runs D3 and D6 are not shown since they give a positive slope.

The Arrhenius parameters calculated from the l.m.s. slopes and intercepts of Fig. 3.13 are tabulated below.

Table 3.16: Arrhenius Parameters for Grain-Boundary Diffusion

	E(kcal.)	$\log D'_o$ ($cm^2.sec.^{-1}$)	Notes
(a)	25.6±1.9	12.91±1.27	D from line A
(b)	26.3±1.9	11.69±1.27	D from line J"
(c)	28.9±0.8	15.15±0.51	D from line A; Run C4 omitted.
(d)	29.6±0.6	13.97±0.43	D from line J"; Run C4 omitted.

It can be seen from Table 3.16 that the activation energies calculated from the two lines of Fig. 3.13 are in good agreement. Therefore, although the absolute value of D' depends on which value of D is used in the calculation, the activation energy obtained is not sensitive to the choice of D as long as a consistent set of D values is used.

It is of interest to compare the Arrhenius parameters of Table 3.16 with the parameters obtained for bulk diffusion in single crystals. Such comparison shows $E' = 0.7E$ and $D'_o = D_o$.

Another question arises from these results and from the variability of the bulk diffusion coefficient with the crystal: Is it possible that some of the results on monocrystals could be interpreted as grain-boundary diffusion? Plots of log A versus d for monocrystals are, however, not linear, except possibly for Runs 1A, 2A, and 3 on boule A. A Fisher analysis was carried out on these results together with Run 4 (also boule A). The results are shown in Table 3.17. Bulk diffusion coefficients taken from line J" (Fig. 3.9) were used in the calculation.

Table 3.17: Fisher Analysis of Results from Boule A.

Run	T(°C)	1/T(°K^{-1})	D'(cm^2.s.$^{-1}$)	log D'
1A	50.0	3.094×10^{-3}	1.09×10^{-6}	-5.96
2A	40.5	3.186×10^{-3}	5.02×10^{-6}	-5.30
3	45.7	3.136×10^{-3}	1.95×10^{-7}	-6.71
4	45.1	3.142×10^{-3}	8.93×10^{-7}	-6.05

An Arrhenius plot constructed from Table 3.17 does not give a straight line; indeed, no three results fall on a straight line. This is strong evidence that the tracer-sectioning results on boule A cannot be interpreted as grain-boundary diffusion and have already been correctly interpreted as bulk diffusion.

Before accepting the results on polycrystals as being due to grain-boundary diffusion it would be useful to have a comparison between the results obtained by the Fisher analysis and results obtained by a more exact solution. Whipple[113] has published a solution to the grain-boundary diffusion problem which avoids the approximations made by Fisher, but which is much more difficult to apply in its original form to experimental results. However, Le Claire[111] has made comparisons between the solutions of Fisher and Whipple and shown how the former may be "corrected".

The grain-boundary diffusion coefficient can be expressed in the form

$$D'\delta = \frac{1}{(2.303)^2} \cdot \frac{(d\log c)^{-2}}{(dy)} \cdot \left(\frac{4D}{t}\right)^{\frac{1}{2}} \cdot A^2 \qquad \text{Eqn. 3.23}$$

where $A = d\log c/d(\eta\beta^{-\frac{1}{2}})$.

Comparison with equation 3.21 shows that this is equivalent to Fisher's solution when $A = \pi^{-\frac{1}{2}}$. Therefore, if A can be evaluated using a more exact solution than Fisher's, a direct comparison can be made between the two solutions. Le Claire has evaluated A as a function of $\eta\beta^{-\frac{1}{2}}$ at various β's using Whipple's exact solution.

Table 3.18 shows values of β, and $\eta\beta^{-\frac{1}{2}}$ calculated from the results

on polycrystalline compacts of naphthalene. Values of y near the mid-point of the diffusion penetration were used and D values were taken from line J"(Fig. 3.9). Corresponding values of A were found from Le Claire's analysis and inserted in Eqn. 3.23 to give "corrected" (Whipple) values of the grain-boundary diffusion coefficients. These are shown in the Table.

Table 3.18: Grain-Boundary Diffusion Coefficients in Naphthalene-B

Run	y(cm.)	β	$\eta\beta^{-\frac{1}{2}}$	A	$D'(cm.^2.sec.^{-1})$
C1	0.04	940	6.41	1.317	3.53×10^{-6}
C2	0.04	3098	9.29	1.445	1.16×10^{-6}
C3	0.02	2203	4.29	1.220	1.51×10^{-6}
C4	0.01	143	3.65	1.200	6.92×10^{-6}
C5	0.03	402	4.09	1.225	1.51×10^{-5}
C6	0.01	901	1.67	1.085	4.92×10^{-6}
C7	0.01	778	1.80	1.095	4.33×10^{-6}

The "corrected" values of D' are about a factor of 3 higher than the Fisher values. An Arrhenius plot of the "corrected" values gives E = 24.2kcal., and $D'_o = 6\times10^{10} cm.^2.sec.^{-1}$ D_o is in fair agreement with the Fisher analysis; the activation energies are in remarkably good agreement.

In deciding whether the polycrystal results should be interpreted as grain-boundary diffusion or as bulk diffusion, the following points were considered:-

1. Log A can be interpreted as being linear in either d or d^2. The standard deviations of the plots are as follows

Run	C1	C2	C3	C4	C5	C6	C7
d^2 plot	3.4%	30%	7.4%	-	4.8%	8.6%	5.2%
d plot	3.4%	12%	9.4%	2.3%	3.2%	5.1%	2.8%

Since the more truly linear the plot the smaller will be its standard deviation these figures indicate that the plots are more linear in d than in d^2. This favours an interpretation as grain-boundary diffusion, however, the differences are marginal.

2. The number of points on those portions used to calculate D or D' are as follows

Run	C1	C2	C3	C4	C5	C6	C7
d^2 plot	8	4	7	Nil	7	11	13
d plot	9	6	8	6	11	13	17

This favours the grain-boundary interpretation in all cases.

3. The standard deviations of the Arrhenius plots are

(a) Assuming bulk diffusion : for E, 11.1% ; for log D_o, 141%

(b) Assuming grain-boundary diffusion: for E', 7.2% for log D'_o, 11%.

Again this favours the grain-boundary interpretation.

4. The assumption of bulk diffusion in the polycrystalline compacts gives the equation

$$D = 0.2 \exp(-12{,}700/RT).$$

There is nothing intrinsically unlikely about this equation, indeed its parameters are of approximately the same order as those reported by Labes and his co-workers[2] for bulk diffusion in anthracene. The assumption of grain-boundary diffusion in the compacts gives

$$D' = 5\times10^{11} \exp(-26{,}000/RT). \qquad \text{Eqn. 3.24}$$

which is remarkably similar to the results reported here for bulk diffusion in naphthalene ($D'_o = D_o$; $E' = 0.7E$). Again there is nothing intrinsically unlikely about this.

In summary, the results on polycrystals can be interpreted either as bulk diffusion or as grain-boundary diffusion. The evidence for bulk diffusion is that the log A versus d^2 plots are reasonably linear and give consistent results. The evidence for grain-boundary diffusion is that the plots are marginally more linear in d than in d^2. The monocrystal results cannot be considered as linear in d. The Fisher and Whipple analyses of the polycrystals are in good agreement. In addition, it is more likely than not that polycrystals would show evidence of grain-boundary diffusion. On balance, therefore, the available evidence favours the grain-boundary interpretation.

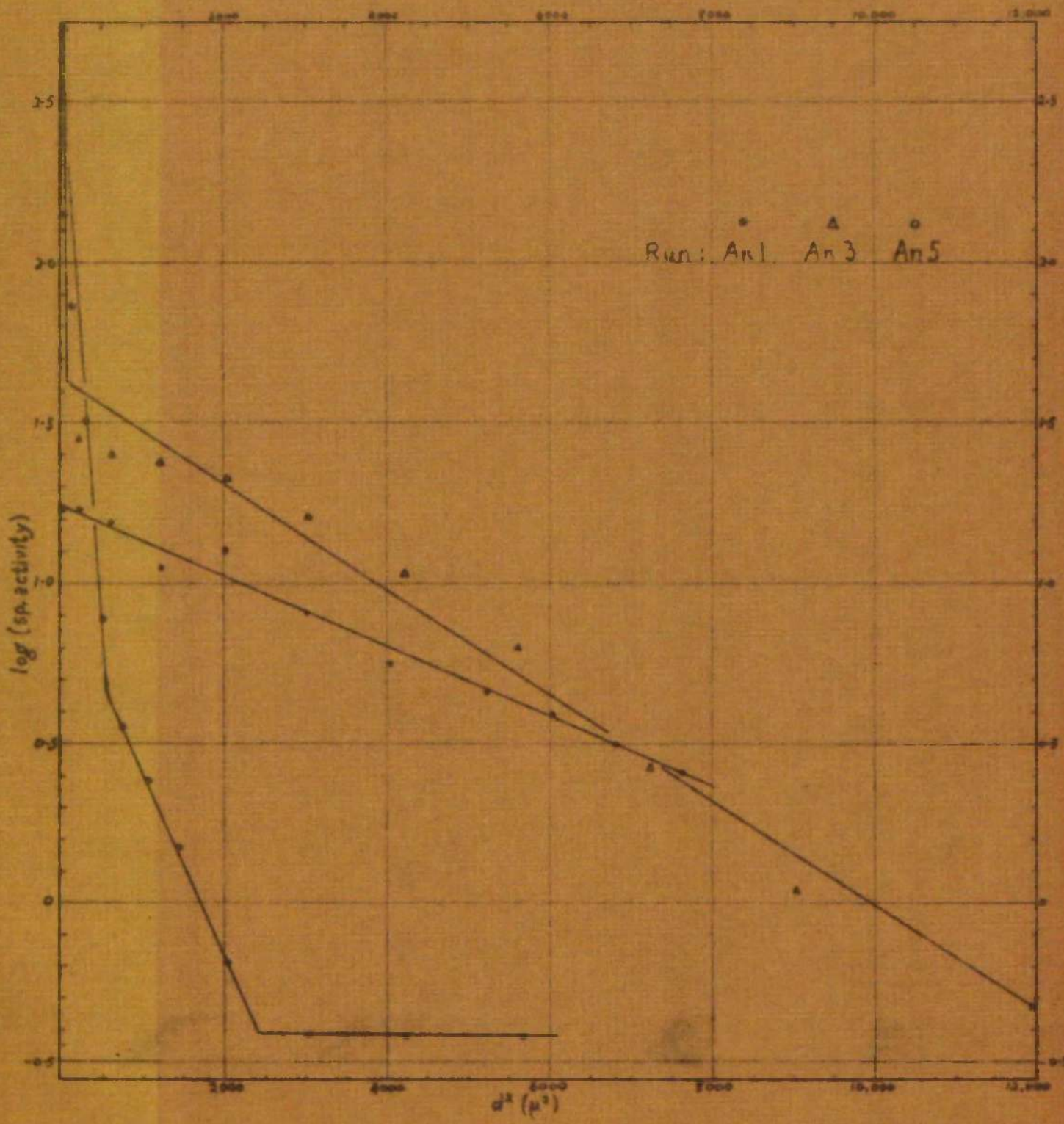

Fig. 3.14: (a) : Bulk Diffusion in Anthracene.

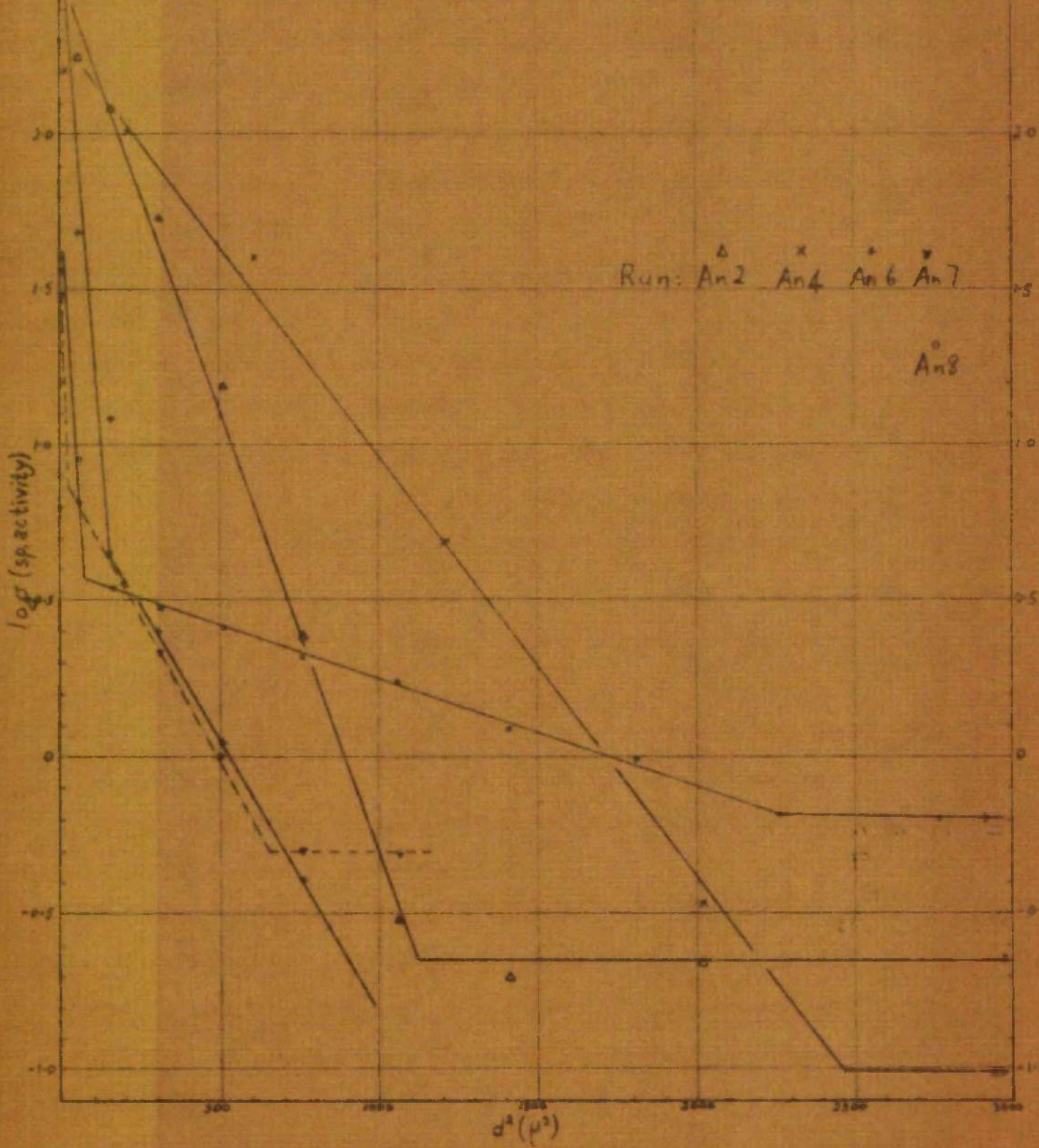

Fig. 3.14:(b): Bulk Diffusion in Anthracene.

(x) Bulk Diffusion in Anthracene.

The tracer-sectioning results on anthracene are shown in Figs. 3.14(a) and (b). The plots of log A against d^2 show the following features:-

Run An 1: The plot is a good straight line showing neither an initial high point nor a tail. D was calculated directly from the l.m.s. slope using all the points in the calculation.

Run An 2: The plot is a good straight line with no high point but with a typical diffusion tail. The diffusion coefficient was calculated from the l.m.s. slope after subtracting the tail.

Run An 3: There is an initial high point but no tail. The plot shows a slight curvature. The diffusion coefficient was calculated from the l.m.s. slope omitting the first point.

Run An 4: Gives a line with no initial high point but with a diffusion tail. D was calculated from the l.m.s. slope after correcting for the tail.

Run An 5: The plot against d^2 falls into three regions, (a) An initial, steep portion; (b) A middle region less steep than (a); (c) A diffusion tail. This was the behaviour found by Labes and his co-workers[2] in their sectioning experiments. The diffusion coefficient was calculated from the middle region, (b), after correcting for the tail, (c).

Run An 6: Gives regions (a) and (b) described under Run An 5, but does not have a tail. D was calculated from region (b).

Run An 7: Gives three regions similar to An 5. D calculated from the middle region after correcting for the tail.

Run An 8: Similar to An 5 and An 7. D calculated as before.

Reasons for the diffusion tail in anthracene have been discussed by Jarnagin and Sherwood[114] who have demonstrated that tail activity increases with increasing impurity content. Short-circuiting paths induced by the presence of impurity molecules are presumed responsible so that it would be expected that the higher the dislocation density in a crystal the

greater would be the mass transported by the diffusion tail. In the present work, too few anthracene crystals were examined to contribute anything further to our knowledge of diffusion tails.

The near-surface region of high activity and steep gradient found in Runs An 5,6,7 and 8 appears to be similar to that found by Labes and his co-workers in their tracer-sectioning measurements on anthracene. These workers discounted the initial high points because the levelling for sectioning and the flatness of the surface were not always ideal. In the present work it was found that the crystal surface was planar to within 5 microns after the diffusion anneal so that complete sections could be removed even very close to the surface. Some explanation must be found for the high region other than uneveness at the surface.

It is possible that the initial steep region is due to bulk self-diffusion. However, diffusion coefficients calculated from this region are small, and the results obtained from different crystals are not self-consistent. Nevertheless, the accuracy of the technique is such that this possibility cannot be ruled out completely. Another possibility is that the high region is caused by diffusion of an impurity present at the surface. For example if anthraquinone were formed at the surface from active anthracene it would be expected to diffuse inwards. At 195 °C. the ratio of the diffusion coefficient of anthraquinone in anthracene to that of anthracene in anthracene is [114] approximately 0.22. The diffusion coefficients calculated from the near-surface regions in Runs An 5,6,7 and 8 are respectively 0.25,0.14, 0.03, and 0.13 times the coefficients calculated from the second portions of the same plots. The respective temperatures are 189.5°, 180.5°, 187.6°, and 187.6°. Since the activation energy for diffusion of anthraquinone in anthracene is greater than the energy of self-diffusion in anthracene[114], and the diffusion coefficients in the near-surface region were measured only inaccurately, it is possible that the near-surface regions found in Runs An 5,6,7, and 8 are attributable to diffusion of

anthraquinone. A further possibility is that the near-surface region has an anomalously low self-diffusion coefficient compared with the bulk. Such behaviour has been observed in other materials.[38]

Whatever the cause of the initial steep portion in Runs An 5 - 8, it was decided to use the second portion of the log A vs.d^2 plots to calculate the diffusion coefficients. This is in accord with the practice adopted by other workers[2,36] and gives reasonably consistent results. Inclusion of the initial parts of the plots leads to inconsistencies in the results and difficulties in explaining the second (main) portion of the diffusion profiles.

The boundary conditions in the tracer-sectioning experiments on anthracene are the same as in the experiments on naphthalene. The appropriate solution of Fick's equation for these conditions is (see page 90)

$$c = \frac{Q}{(\pi Dt)^{\frac{1}{2}}} \exp\left(\frac{-d^2}{4Dt}\right),$$

where c is the concentration of diffusant at distance d after time t. Hence the diffusion coefficient is given by

$$D = -1/(2.303 \times 4mt),$$

where m is the gradient of the log c vs.d^2 plot. The plots are shown in Figs. 3.14(a) and (b). Experimental details and the calculated diffusion coefficients are given in Table 3.19.

Table 3.19: Bulk Self-Diffusion Coefficients for Anthracene.

Run	Xtal	t(hrs.)	D(cm^2/sec.)	log ($D \times 10^{14}$)	T°C)	$1/T°K^{-1} \times 10^3$)
An1	2	561.6	$(4.93 \pm 0.12) \times 10^{-12}$	2.693	196.0	2.131
An2	2	308.0	$(3.47 \pm 0.09) \times 10^{-13}$	1.535	185.0	2.183
An3	1	30.5	$(6.23 \pm 0.21) \times 10^{-11}$	3.794	204.0	2.096
An4	2	30.5	$(7.31 \pm 0.22) \times 10^{-12}$	2.864	204.0	2.096
An5	1	24.0	$(1.47 \pm 0.03) \times 10^{-11}$	3.169	189.5	2.162
An6	2	379.0	$(4.53 \pm 0.01) \times 10^{-13}$	1.656	180.5	2.205
An7	2	187.5	$(8.89 \pm 0.23) \times 10^{-13}$	1.949	187.6	2.171
An8	1	187.5	$(4.74 \pm 0.22) \times 10^{-12}$	2.676	187.6	2.171

As can be seen from the Table crystals originating from two boules

were used in the diffusion experiments. Details of the boules are as follows:

Boule 1: This was grown by the author as described in Part II A of this thesis. It is designated Boule An 1 in Table 2.1 (page 44). The crystal was of fairly good quality but was slightly yellow.

Boule 2: This was grown and annealed by Sherwood (1964) who made diffusion measurements[94,114] on similarly grown boules. This unpublished work of Sherwood will be referred to later. The boule was grown by the Bridgmann-Stockbarger method[88]; it was water-white and of good quality.

An Arrhenius plot (log Dvs. 1/T) of the results in Table 3.19 does not give a single line but gives two lines, one for each crystal boule. By analogy with the naphthalene results this behaviour is not surprising but has not previously been reported. The Arrhenius parameters obtained from the two lines are

Crystal 1: $E = 59.3 \pm 14.4$kcal., $\log D_o(cm^2/sec.) = 16.80 \pm 6.70$

Crystal 2: $E = 60.89 \pm 7.75$kcal., $\log D_o(cm^2/sec.) = 16.68 \pm 3.63$

There is considerable scatter about the Arrhenius lines but there is no doubt that the results fall into two different groups, one for each crystal boule.

The Arrhenius plots of the above results are shown in Fig. 3.15 along with results obtained by other workers. All the lines drawn in the Figure are least mean square lines. Full lines and circles are used for the Arrhenius plots from this work, and broken lines for the published results of Sherwood and Thomson, and of Labes and co-workers. Sherwood's unpublished measurements referred to above are shown by a broken line and crosses. The Arrhenius parameters found from these lines are collected in Table 3.20.

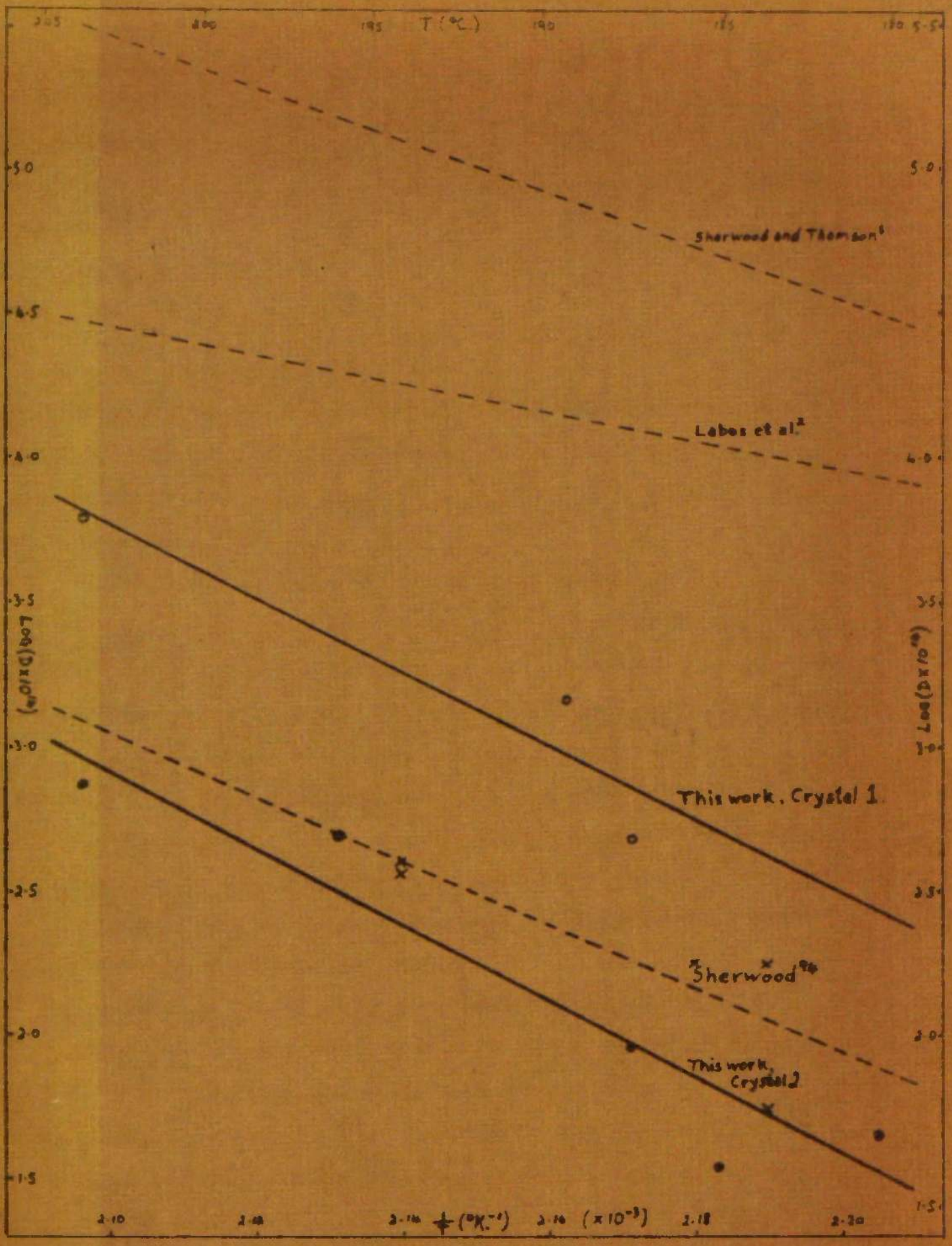

Fig. 3.15: Anthracene-Arrhenius Plots.

Table 3.20: The Arrhenius Parameters for Anthracene.

Reference	E(kcal.)	D_o($cm^2.sec.^{-1}$)
Sherwood and Thomson[1]	42.4	6.5×10^{10}
Labes et al.[2]	22.0	3
Sherwood[94]	51.0	2.8×10^{12}
This work, crystal 1	59.0	6.3×10^{16}
This work, crystal 2	61.0	4.8×10^{16}

All the results given in Table 3.20 were made by the tracer-sectioning technique perpendicular to the cleavage (ab) plane of anthracene. Labes and co-workers also report slight anisotropy: In measurements perpendicular to the ac plane they obtained E = 24kcal., and D_o = 16$cm^2.sec.^{-1}$

The results obtained in the present work are in fairly good agreement with Sherwood's unpublished results.[94] They agree less well with the original measurements of Sherwood and Thomson[1], but D_o and E have similar magnitudes in both studies. The results reported here disagree with Labes' findings[2]: Labes' diffusion coefficients are between one and two orders of magnitude greater than the ones found by the present writer. The Arrhenius parameters reported by Labes are smaller than the ones reported here.

The two sets of results obtained by the present author and the data of Sherwood and Thomson, and Sherwood can be reconciled in the light of the results on naphthalene reported in this thesis. According to these, the measured diffusion coefficient at a given temperature will be lower the greater the perfection of the crystal, and D_o and E will increase with increasing perfection. The anthracene results clearly fit this pattern if Sherwood and Thomson's crystals were inferior to the crystals subsequen ly grown by Sherwood, and if these latter are of better quality than the

crystals grown by the present writer. It is too late to pronounce on the crystals used by Sherwood and Thomson, but the crystals more recently grown by Sherwood are optically more perfect than the anthracene crystals grown in this work.

However, the anthracene results obtained by Labes and co-workers cannot readily be made to fit this pattern. Labes reports that he was aware that the presence of fissures and other imperfections in the crystal could lead to inconsistencies in experimental results. He made two sets of measurements on two different grades of crystal to ensure that this type of error did not occur. Fissures or other gross imperfections are not believed by the present writer to be responsible for the variable coefficients found in naphthalene and anthracene. Many of the crystals used were of very good quality and the values of E and D_o obtained in different crystals were of similar magnitudes, much higher than Labes'. At all temperatures the absolute values of the diffusion coefficients found by the author were considerably smaller than those found by Labes.

A possible explanation of the discrepancies between the anthracene results reported here and those reported by Labes and his co-workers may lie in a comparison between Labes' results and those on polycrystalline naphthalene. If the measurements on polycrystals are interpreted as bulk diffusion it is found that D_o is approximately 0.2 with an upper limit of about 1.9 $cm.^2 sec.^{-1}$ (cf. page 105). The activation energy is 12,700cals. Labes finds for his results on anthracene $D_o = 3$, and E = 22,000 cals. If the latent heat of sublimation (ΔH_s) is assumed to be related to the activation energy for diffusion, then Labes finds $E = 1.0 \times \Delta H_s$ for anthracene, and the present author $E = 0.7 \times \Delta H_s$ for polycrystalline naphthalene. Obviously D_o and E in both studies are of comparable magnitudes.

Another empirical similarity between naphthalene polycrystals and

Labes' anthracene results can be found in terms of the melting-point (T_m). All the result on pure monocrystals of naphthalene and anthracene reported in this thesis fit the relationship

$$E = 113T_m$$

to within 12 per cent. However, Labes' results give $E = 45Tm$ and the results on polycrystalline naphthalene give $E = 36T_m$. It has already been pointed out (section (ix) above) how difficult it can be to distinguish between grain-boundary and bulk diffusion under certain circumstances. This, together with the similarities outlined above, suggest to the writer that Labes may have been measuring grain-boundary or dislocation diffusion in his crystals.

PART IV. - DISCUSSION.

DISCUSSION.

(i) Summary of Previous Work - Direct Measurements.

Direct measurements of diffusion in organic solids have been made on anthracene, Cyclohexane, and pivalic acid. In all cases single crystals were used. Diffusion has also been measured in the molecular solids, hydrogen, phosphorus, sulphur and argon.

Self-diffusion in solid hydrogen was measured by Cremer (1938)[25] following his studies of the bimolecular transformation of para-hydrogen in the solid state. The rate of self-diffusion becomes an important factor in the conversion when only isolated para-hydrogen molecules remain in the solid. From his experiments Cremer was able to measure the coefficient of self-diffusion between 11.3° and 13.6°K., from which he calculated the activation energy of diffusion was 790±130cal. per mole. This value is consistent with a vacancy mechanism.[31]

Measurements of self-diffusion perpendicular to the (111) plane of orthorhombic sulphur were made by Cuddeback and Driokamer[51] by a tracer technique. They found two diffusion processes, one predominating at lower temperatures and one at temperatures closer to the transition point (95.5°C.). On the assumption that the two processes were the result of diffusion anisotropy it was deduced that the measured diffusion coefficient, D, perpendicular to the (111) plane was the resultant of two processes, one, of coefficient $D_{par.}$, parallel to the c-axis of the crystal, and the other, of coefficient $D_{perp.}$, perpendicular to the c-axis. From the geometry of the lattice they proposed that the coefficients were related by the equation

$$D = 0.099D_{par.} + 0.901D_{perp.}$$

This equation fitted their experimental data with

$$D_{par.} = 1.78\times10^{36} \exp(-78{,}000/RT), \qquad \text{Eqn. 4.1}$$

and

$$D_{perp.} = 8.32\times10^{12} \exp(-3000/RT), \qquad \text{Eqn. 4.2}$$

Thus, diffusion parallel to the c-axis controls at high temperatures, and perpendicular diffusion at low temperatures. However, this interpretation of the data is open to some doubt, and it has been suggested[39] that the high energy and pre-exponential factor found near the transition point is in fact due to the formation and diffusion of disordered or premelted regions in the lattice.

Cuddeback and Drickamer also carried out some measurements in sulphur at temperatures beyond the transition point to the monoclinic phase. Under the conditions of their experiments the sulphur would be polycrystalline. At 101°C. they found $D = 4\times10^{-12}$ cm.^{2} sec.$^{-1}$

Self-diffusion in monoclinic sulphur has been measured by Hauffe[115] who found

$$D = 2.8\times10^{13} \exp(-46{,}800/RT). \qquad \text{Eqn. 4.3}$$

These little-discussed measurements are of particular interest because of the high pre-exponential factor and energy. At 101°C., the diffusion coefficient calculated from this equation is $D = 2\times10^{-14}$ which does not agree with the above value of Cuddeback and Drickamer.

Measurements of diffusion in alpha-white phosphorus were made by Nachtrieb and Handler[39] who found two processes similar to those found in rhombic sulphur. Between 0° and 30°C. (Range I.) they found that diffusion satisfied the equation

$$D_I = 1.07\times10^{-3} \exp(-9400/RT), \qquad \text{Eqn. 4.4}$$

the probable mechanism of diffusion in this range being that of the random walk of relaxed P_4 vacancies. Between 30° and the melting-point, 44° (Range II.) a rapid increase in the diffusion coefficient, D, was observed

such that

$$D = D_{I.} + D_{II.}$$

with

$$D_{II.} = 2\times10^{46} \exp(-80{,}600/RT), \qquad \text{Eqn. 4.5}$$

predominating above 30°. Phosphorus consists of P_4 tetrahedra in a cubic lattice so that diffusion anisotropy is unlikely. Dissociation of P_4 is also unlikely for energetic reasons. The authors concluded that in Range II. diffusion takes place via pre-melted clusters; the mean number of molecules per cluster was calculated to be about 150.

N.M.R. measurements[40] have failed to confirm the existence of Range II. in phosphorus. Nachtrieb and Handler's theory of diffusion via "liquid" microphase regions must remain in doubt until measurements have been made on pure monocrystals. Only then will it be possible to decide whether Range II. in phosphorus is the result of a true bulk property or of grain-boundaries in the specimens used by the authors.

Diffusion measurements in solid argon were carried out[48] by measuring the rate of disappearance of A-36 from vapour in contact with the crystal. Measurements were in the range 76.2 to 81.8°K. on both polycrystals and single crystals grown by the Bridgmann method. The vapour decrease method as used for argon suffered from large uncertainties due both to experimental difficulties in handling the material and to lack of knowledge of the effective surface area for exchange. Despite these difficulties the authors were able to measure D_o and E to a reasonable accuracy. They found $D_o = 0.3^{+2.7}_{-0.27}$ cm.^{2}sec.$^{-1}$ and E = 3930±400cals. per mole. In monocrystals the experimental D_o was 36^{+300}_{-30} cm.^{2}sec.$^{-1}$, but this figure was thought to be less reliable than the one previously quoted.

The D_o and E values found in the tracer experiments on argon are in satisfactory agreement with the values calculated from n.m.r. data on xenon using the theorem of corresponding states.[48,49] Unfortunately the

experimental values do not agree well with the values calculated from absolute rate theory.[45] The discrepancy between the observed and calculated values of the Arrhenius parameters in such a "simple" crystal as argon does not bode well for theoretical calculations in more complex systems.

The first direct measurement of diffusion in an organic solid was made by Sherwood and Thomson[1] on anthracene. They found

$$D = 6.5 \times 10^{10} \exp(-42{,}400/RT), \qquad \text{Eqn. 4.6}$$

Recent measurements by Labes[2] in the same solid gave

$$D = 3 \exp(-22{,}000/RT), \qquad \text{Eqn. 4.7}$$

Possible reasons for the discrepancy between these studies have already been discussed (page 123).

Self-diffusion in single crystals of cyclohexane have been found to obey the relationship[24,101]

$$D = 6.3 \times 10^{6} \exp(-16{,}500/RT), \qquad \text{Eqn. 4.8}$$

and in single crystals of pivalic acid self-diffusion gives[101]

$$D = (2.25 \pm 1.25)\exp(-10{,}000 \pm 300/RT), \qquad \text{Eqn. 4.9}$$

The former was measured by a tracer-sectioning method using cyclohexane C14 as tracer and has been confirmed by surface-decrease and vapour exchange measurements.[24] The measurements on pivalic acid were made by the tracer-sectioning method using pivalic acid tritiated at the acid hydrogen.

From the high D_o and E values found in cyclohexane the authors concluded that diffusion takes place by the random walk of relaxed vacancies with about 20 molecules per "relaxion". The corresponding number in pivalic acid is 7.

The n.m.r.[116] and tracer results on pivalic acid are in reasonable agreement, but it is possible that diffusion in this solid is complicated by proton movement. The tracer-sectioning results on cyclohexane are not in agreement with n.m.r. measurements[19] (E_{nmr} = 8kcal.). They are,

however, in reasonable agreement with the activation energy found by an E.S.R. method in which the rate of anihilation of radiation induced radicals is measured. This method[117] gives an activation energy of 20kcal.

(ii) Summary of Previous Work - N.M.R. Measurements.

Nuclear magnetic resonance measurements of self-diffusion have been made on phosphorus[40], xenon,[49] hydrogen,[118] and a number of organic solids.[20] In addition the n.m.r. results on xenon have been used to calculate the energy of diffusion in argon.[48] N.M.R. failed to detect diffusion in benzene, naphthalene, and anthracene,[119,120] but it has been suggested[120] that the width of the nuclear magnetic resonance line will decrease as a result of diffusion only when the molecules are moving through the lattice more rapidly than the line width expressed as a frequency. Thus, slow moving species will not be detected. Radical diffusion has been observed in benzene below the melting-point.[121]

The solids in which diffusion has been measured by the n.m.r. method fall into that group known as plastic crystals. These are characterised by the globular shape of their molecules and by low entropies of melting. For example, cyclohexane is a globular molecule and the solid undergoes a transition at 186°K. to a plastic, cubic phase. The entropy change at the transition is 8.6 e.u. whereas the entropy of fusion is 2.2 e.u. This low melting entropy indicates that, on melting, the molecules have little to gain (except translation) in freedom of movement and have considerable motional freedom in the cubic phase. Such solids would be expected to exhibit rapid diffusion. Extrapolation of Hood and Sherwood's data[24] to the melting-point gives $D = 4 \times 10^{-5}$ cm.^{2} sec.$^{-1}$ which is of the same order as diffusion in the liquid. Diffusion in more rigid lattices would be much slower.

The n.m.r. results on molecular solids give an activation energy (E) somewhat less than the latent heat of sublimation (ΔH_s)(Camphor[122] gives E slightly greater than ΔH_s). The latent heat of sublimation is

approximately equal to the theoretical energy for the creation of a vacant lattice site,[31] so that the correlation between ΔH_s and E as found by n.m.r. has lead to the suggestion[119] that diffusion in molecular solids takes place by a vacancy mechanism. The agreement of n.m.r. and tracer measurements on alkali metals[123] has given some force to this argument. However, the energy for diffusion in xenon as measured by n.m.r. is approximately twice the latent of sublimation, and no organic solid has been measured using both the n.m.r. method and a C14 tracer technique.

Molecular solids in which diffusion has been measured by more than one method are shown in Table 4.1.

Table 4.1: Comparison of NMR and Other Measurements.

Solid	Method	ΔH_s (kcal)	E (kcal)	$E/\Delta H_s$	Ref.
Hydrogen	o-p-conv.	0.49*	0.79	1.6	25
Hydrogen	NMR	0.49*	0.38	0.8	118
Phosphorus	tracer	14	9.4	0.7	39
Phosphorus	NMR	14	12.1	0.9	40
Argon	tracer	1.8	3.93	2.2	48
Argon	NMR**	1.8	3.83	2.1	48
Pivalic acid	tracer(H3)	10	10	1.0	101
Pivalic acid	NMR	10	8	0.8	116
Cyclohexane	tracer(C14)	8.5	16.5	1.9	24
Cyclohexane	NMR	8.5	8	0.9	19
Cyclohexane	ESR	8.5	20	2.4	117

* includes zero-point energy[31]; ** calculated from n.m.r. data[49] on Xe.

It can be seen that the tracer and n.m.r. results are in reasonable agreement in the cases of phosphorus (Range I.), argon, and pivalic acid, but in disagreement in the cases of hydrogen and cyclohexane. Tracer and E.S.R. measurements on cyclohexane are in fair agreement. In all cases, except argon and xenon, E is found by n.m.r. to be approximately equal to ΔH_s. In argon and xenon n.m.r. finds $E = 2\Delta H_s$. Tracer and E.S.R. results on cyclohexane also give $E = 2\Delta H_s$. The

position is very difficult to resolve, but it is perhaps significant that where n.m.r. and tracer results agree each method "sees" the same element (e.g. hydrogen in pivalic acid, phosphorus in phosphorus), whereas in cyclohexane n.m.r. "sees" hydrogen, but the tracer measurements "see" carbon. In addition, the presence of grain-boundaries and impurities may have a profound affect on the measurements.[39,120]

Our knowledge of diffusion in molecular solids is in an unsatisfactory state. Agreement between different methods is seldom good and in some cases experiments have been performed on polycrystalline specimens or on materials of questionable purity. Various diffusion mechanisms have been proposed but none satisfactorily established. The number of materials investigated is very small and so far no unifying principle has emerged.

(iii) Measurements on Naphthalene and Anthracene.

In the present investigations various expressions were found for bulk self-diffusion in naphthalene and anthracene depending on the state of the single crystal used for the measurements. Although the diffusion coefficien at a particular temperature varied greatly from crystal to crystal, the Arrhenius expressions showed less variability. Both D_o and E appeared to increase with increasing perfection of the crystal. The results may be summarised as follows (cf. pages 103 and 124):-

(a) In annealed single crystals of naphthalene diffusion follows the equation

$$D = 2.8 \times 10^{11} \exp(-34{,}900/RT).$$

(b) In highly pure, well-annealed single crystals of naphthalene, diffusion takes place according to the relationship

$$D = 2.5 \times 10^{15} \exp(-42{,}700/RT).$$

(c) In annealed monocrystals of naphthalene containing dopant, diffusion follows the equation

$$D = 6.1 \times 10^{8} \exp(-30{,}700/RT).$$

(d) In polycrystalline naphthalene diffusion follows

$$D = 0.2 \exp(-12,700/RT),$$

if diffusion is considered to take place via the lattice, or

$$D = 5 \times 10^{11} \exp(-29,600/RT)$$

if diffusion takes place by a grain-boundary mechanism. The latter interpretation is favoured (see page 118).

(e) Anisotropic diffusion was not observed in naphthalene.

(f) Diffusion in single crystals of anthracene is found to obey the equation

$$D = 5 \times 10^{16} \exp(-60,000/RT).$$

As in naphthalene, D_o and E appear to increase with increasing perfection of the crystal, while D decreases with increasing perfection.

The high activation energies and pre-exponential factors in the present work are more in agreement with the values found for the high temperature ranges in sulphur and phosphorus, and with the tracer results on cyclohexane, than with the n.m.r. measurements on organic solids. How the present values for anthracene can be reconciled with earlier results on the same solid has already been discussed (page 124).

(iv) The Pre-Exponentail Factors in Naphthalene and Anthracene.

Many expressions for D_o and E have been derived from various models of the diffusion process, the quantities entering into the theoretical expressions depending on the particular model. For example, Le Claire[44] has related the energy of diffusion to the elastic strain energy of the lattice with very useful results; others[6,42] have stressed the relationship between self-diffusion and the anharmonicity of the vibrations of the lattice particles. By comparison of the predicted and experimental values of the parameters a choice can be made between the various theories. Unfortunately, the theoretical expressions require a knowledge of physical properties which have not as yet been measured in organic solids.

In metals, D_o usually, but not always, falls within the range 0.1 to

$10cm^2/sec$. Many of the theoretical expressions for D_o correctly predict this order or less. It is clear that the values for D_o found in the present study are much too large to be explained by such theories. In any case, the theories have been derived from a consideration of diffusion in metals and it is highly questionable if they can be applied correctly to an extrinsic process in molecular solids.

Diffusion in organic solids is unlikely to take place either by an interstitial mechanism or by direct interchange of molecules on neighbouring sites. The close-packed structure of organic solids precludes the former; energetic considerations the latter. Zener's ring mechanism is unlikely since it can be shown that this mechanism does not predict[44] a large value for D_o. From structural considerations a vacancy mechanism seems the most likely, but the size of D_o and E suggest that it will not be simple vacancy diffusion.

In a vacancy mechanism diffusion is the nett result of a large number of random jumps made by molecules between successive equilibrium positions. If n is the average number of such jumps made in unit time by each molecule, then the diffusion coefficient will be proportional to n. In isotropic crystals it can be shown that

$$D = ga^2n \qquad \text{Eqn. 4.10}$$

where a is the jump distance and g a geometrical factor, depending on the number of neighbouring sites into which the molecule may jump.

The number of jumps, n per sec., is the product of two probabilities: p_m, the probability that the molecule will move by a sufficient distance to detach itself from the original site; and p_v, the probability that such a molecule has a vacancy as a nearest neighbour. If n_v is the fractional concentration of vacancies and z the co-ordination number, then $p_v = zn_v$. The fraction of vacancies is given by $\exp(-\Delta G_F/RT)$, where ΔG_F is the free energy of formation of a vacancy, i.e. $p_v = z \exp(-\Delta G_F/RT)$. The probability, p_m, is given by $p_m = \nu \exp(-\Delta G_M/RT)$, where ν is

the number of times the molecule attempts to surmount the potential barrier separating it from the vacancy and the Boltzmann factor is the probability that it has enough energy to do so. ΔG_M is the free energy of migration. Combining the geometrical factors to give γ we obtain from equation 4.10

$$D = ga^2 p_v . p_m$$

i.e. $$D = \gamma a^2 v \exp(-\Delta G_F/RT) . \exp(-\Delta G_M/RT)$$

For organic solids it can be shown that γ is unity or nearly so, therefore

$$D = a^2 v \exp(-\Delta G/RT),$$

where $\Delta G = \Delta G_F + \Delta G_M$. Expanding ΔG in the usual fashion we obtain

$$D = a^2 v \exp(\Delta S/R) . \exp(-\Delta H/RT). \quad \text{Eqn. 4.11}$$

Equating ΔH with the activation energy for diffusion, comparison of equation 4.11 with the Arrhenius relationship, $D = D_o \exp(-\Delta H/RT)$, gives

$$D_o = a^2 v \exp(\Delta S/R) \quad \text{Eqn. 4.12}$$

where ΔS, the diffusion entropy, is the sum of the entropies of migration and vacancy formation. Equation 4.12 can be derived more rigidly[44,50] and from different considerations.[31,42]

The frequency, v, is usually taken as the Debye frequency which can be calculated from

$$\theta = e^{4/3} . \frac{h}{k} . v$$

where θ is the appropriate Debye temperature. The lattice parameter is used for a. Taking $\theta = 108^\circ$ and 89°, a = 11.16Å and 8.66Å for anthracene[124,125] and naphthalene[125,126] respectively we can obtain a value for ΔS., the entropy of diffusion, from equation 4.12 and the experimental value for D_o. Values of ΔS so obtained are shown in Table 4.2. They are not sensitive to the factor $\gamma a^2 v$, so that despite inaccuracies in this factor ΔS should be a fair estimate of the diffusion entropy.

Table 4.2: Experimental Entropies of Diffusion.

	ΔS (cal./mole)	$\Delta S/\Delta S_m$
Naphthalene.-		
Crystal A	80.2	6.2
Crystals G',H',J'	61.8	4.8
Crystal J"	68.4	5.3
Crystal L"	80.0	6.2
Doped Xtals.	49.5	3.8
Compacts*	6.2	0.5
Compacts**	62.8	4.8
Anthracene.-		
This work, Xtl.1	84.9	6.1
This work, Xtl.2	84.3	6.0
Sherwood and Thomson[1]	57.3	4.1
Labes et al.[2]	9.8	0.7
Sherwood[94]	64.9	4.6

* Assuming bulk diffusion; ** Assuming grain-boundary diffusion.

It can be seen from the Table that the entropies of diffusion are large which suggests that more then one molecule is involved. The entropy of melting, ΔS_m, for anthracene is 14 cals. per mole, and for naphthalene, 13 cals. per mole. The final column in the Table gives the ratio of the entropy of diffusion to that of melting. For pure naphthalene the ratio varies from 4.8 to 6.2, and for anthracene is equal to 6.

From the correlation found in some solids between the activation energy for diffusion and the latent heat of melting, Nachtrieb and Handler proposed[127] a mechanism of diffusion in which the rate-limiting movements occur within small regions of disorder in the crystal. They suggest that the disordered region consists of 12 to 14 molecules which have relaxed inwards around a lattice vacancy and have an energy content about the same as the equivalent number of molecules in the liquid. They use the term "relaxion" to describe the resulting defect. The above values of the entropies of diffusion suggest that in naphthalene and anthracene, relaxions of 5 to 6 molecules may be the diffusing species.

(v) The Activation Energy of Diffusion.

For a simple vacancy the energy of formation is approximately equal to the latent heat of sublimation.[31] However, in the present work, E was found to be approximately equal to twice ΔH_s, which suggests that the diffusing species may be a divacancy. Detailed calculations on metals have shown that clusters of vacancies are stable and that in copper the energy of migration of a divacancy is much less than the energy of migration of a monovacancy.[109] In organic crystals no detailed theoretical calculations of this nature have been made so that no conclusion can be drawn about divacancy formation and migration.

In calculations on argon,[128] the formation energy of a vacancy was found to be approximately equal to the latent heat of sublimation. The energy of diffusion must therefore be greater than this, as was found experimentally.[48] For other systems the energies of formation and migration are often approximately equal, so that E could very well be equal to twice ΔH_s for molecular solids.

However, there is strong evidence in favour of the view that there is considerable relaxation of the surrounding molecules into a vacancy. The free volume of the vacancy after relaxation has been variously estimated[129,130] at between 25% and 75% of the volume before relaxation. Relaxation will reduce the free energy of formation of the vacancy, but in molecular solids the reduction will be small. Diffusion will then take place by a co-operative mechanism involving several molecules. This type of defect is rather similar to a "relaxion".

In their mechanism of diffusion by relaxions, Nachtrieb and Handler[39,12] suggested that the formation energy of a relaxion was related to the latent heat of melting, ΔH_m, by

$$\Delta G_F = n \Delta H_m \ (1 - T/T_m),$$

where T_m is the melting-point, n the number of molecules per relaxion, and

ΔG_F the free energy of formation of a relaxion. The diffusion coefficient due to relaxions is then

$$D = K \exp\left(\frac{-n\Delta H_m (T_m - T)}{RTT_m}\right),$$

where K is a constant. Separation of terms in the above equation and comparison with the Arrhenius relationship gives

$$D_o = K \exp\left(n\Delta H_m / RT_m\right),$$

and

$$E = n\Delta H_m, \qquad \text{Eqn. 4.13}$$

thus n can be calculated. For naphthalene, ΔH_m = 4,570 cal./mole, and for anthracene, ΔH_m = 6,890 cal./mole. Using the experimental values for the diffusion energy, n, the number of molecules per relaxion, was calculated. This is shown in Table 4.3. The number of molecules per relaxion was found to be 8 or 9 for pure naphthalene and 9 for anthracene. Considering the approximations inherent in the derivation of equation 4.13 the agreement with the figure (5 or 6) found from the pre-exponential factor is good.

Table 4.3: Number of Molecules per "Relaxion".

	E (kcal./mole)	$n = E/\Delta H_m$
Naphthalene.-		
Crystal A	36.85	8.1
Crystals G',H',J'	34.87	7.6
Crystal J''	37.96	8.3
Cryatal L''	42.73	9.3
Doped Xtals.	30.66	6.7
Compacts*	12.74	2.8
Compacts**	29.59	6.4
Anthracene.-		
This work, Xtal.1	59.0	8.6
This work, Xtal.2	61.0	8.8
Shorwood and Thomson[1]	42.4	6.2
Labes et al.[2]	22	3.2
Sherwood[94]	51.0	7.5

* Assuming bulk diffusion; ** Assuming grain-boundary diffusion.

Nachtrieb and Handler's analysis may be taken a stage further. $n\Delta H_m$ is the energy of formation of the defect whereas E is the energy of formation plus migration. If the pre-exponential figure of n = 6 is accepted as the number of molecules per relaxion then the energy of formation is $6\Delta H_m$. But $E = 9\Delta H_m$, which gives $3\Delta H_m$ for the energy of migration. However, because of the many approximations and assumptions made in its derivation, this figure cannot be accepted as any more than an indication.

The important fact of the variation of diffusion coefficient with perfection of the crystal has not so far been taken into account. In other solids where the defect concentration is controlled by impurities or deformation, the formation energy drops out of the activation energy leaving E equal to the energy of migration alone.[131] If the same applies to extrinsic diffusion in organic solids, the diffusion energies reported here are energies of migration and not energies of formation plus migration. Therefore, for true intrinsic diffusion in these solids, E must be even larg than $2\Delta H_s$. No such process was found in the present investigations.

(vi) Comparison of Results on Molecular Crystals.

To obtain a graphical comparison between the results on naphthalene and those on anthracene, the diffusion coefficients at the melting temperature and at equal fractions of the melting-point were calculated from the respective Arrhenius equations for the crystals. These are shown in Fig. 4.1 as a plot of log D against T_m/T, where T_m is the melting-point Least mean square lines are drawn for a selection of naphthalene crystals and for the anthracene results from this work and previous studies. The l.m.s. lines are drawn over the range $T = T_m$ to $T = T_m/1.2$ although, of course, this range was not completely covered by the measurements.

It can be seen from the Figure that there is a rough parallelism between all the results on naphthalene and anthracene with the exception of

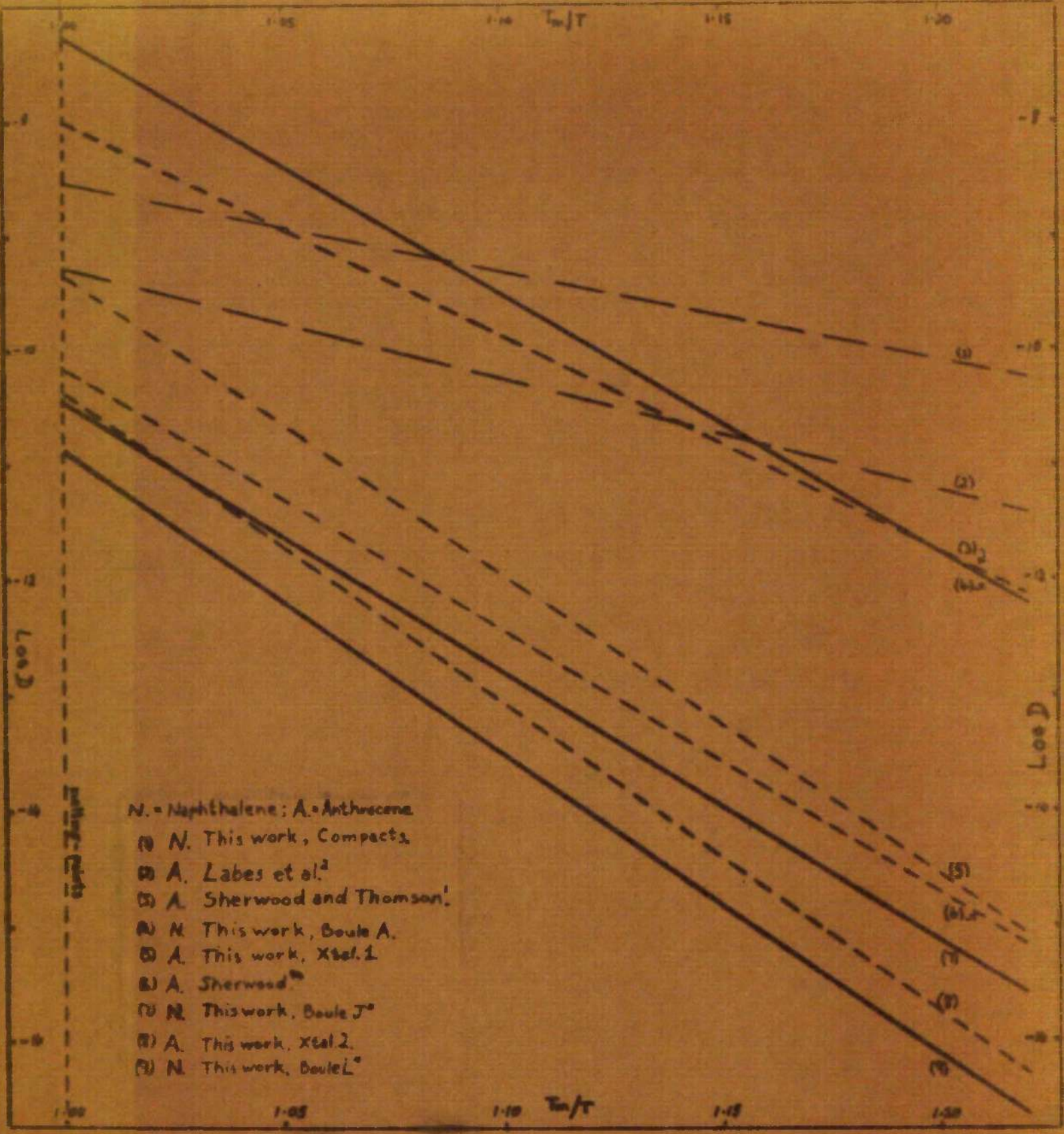

Fig. 4.1: Comparison of Naphthalene and Anthracene.

naphthalene polycrystals and the anthracene results of Labes and his co-workers. Labes' anthracene results and the present results on polycrystalline naphthalene are very nearly parallel.

The findings reported in this thesis suggest that the lower the line in Fig. 4.1, the more perfect the crystal. If the anthracene and naphthalene results can be compared in this way (and such a comparison does not seem unreasonable), the first naphthalene crystal grown in this work (boule A) was of approximately the same degree of perfection as Sherwood and Thomson's original anthracene crystals. Similarly naphthalene boule J'' was of about the same perfection as Sherwood's later anthracene crystals.

Comparisons with other molecular crystals are less close. The n.m.r. measurements on organic crystals show no resemblances with the results reported here. However, the direct measurements on hydrogen, argon, cyclohexane, monoclinic sulphur, and the high temperature ranges in orthorhombic sulphur and phosphorus, together with the n.m.r. results on xenon (and, by the theorem of corresponding states, argon) do show resemblances to the present work in that they have large Arrhenius parameters. These resemblances shall be developed in the next section.

(vii) Empirical Relationships.

Empirical relationships between the activation energy of diffusion and other physical constants have been found in metals.[47] The best known of these is the equation $E \approx 16.5 \Delta H_m$ which is found to hold for some face-centred cubic and body-centred cubic metals and also for the low temperature range of phosphorus. It was the existence of this relationship which suggested to Nachtrieb and Handler[39] that there might be a connection between diffusion and melting. Although results on molecular crystals are not nearly as numerous as in metals it seemed worthwhile to search for similar empirical relationships in the substances mentioned in the previous section.

Table 4.4: Empirical Relationships.

	$E/\Delta H_m$	$E/\Delta H_s$	E/T_m
Naphthalene.-			
Crystal A	8	2.2	104
Crystals G', H', J'	8	2.1	99
Crystal J"	8	2.2	107
Crystal L"	9	2.5	121
Anthracene.-			
This work, Xtl.1	9	2.6	121
This work, Xtl2	9	2.6	124
Sherwood and Thomson[1]	6	1.8	87
Sherwood [94]	8	2.2	105
Sulphur (S_8).[115]			
Monoclinic	20	2.0	120
Hydrogen[25]	25	1.7	57
Argon[48]	14	2.2	49
Xenon[49]	14	1.9	46
Cyclohexane[24]	26	1.9	46
Phosphorus (P_4).[39]			
Range II.	134	6.8	250
Sulphur (S_8).[51]			
Rhombic, Range II.	32	3.2	480

Table 4.4. shows the ratio of the diffusion energy to other physical constants. E is the experimental activation energy for diffusion, ΔH_s and ΔH_m are the latent heats of sublimation and melting respectively, and T_m is the melting-point in degrees Kelvin. It is seen that the high temperature ranges in phosphorus and orthorhombic sulphur do not correlat with any of the others. In naphthalene and anthracene E is $8-9x\Delta H_m$, but none of the other materials fits this formula even approximately.

However, except for phosphorus and orthorhombic sulphur, there are interesting correlations between E and ΔH_s, and also between E and

T_m. The results from this thesis fit the relationship $E = 2.3\Delta H_s$ to within about 13%, and the others are close to this figure also. In the E/T_m column it can be seen that in pure substances $E = 113\ T_m$ for monoclinic crystals, and for cubic crystals $E = 53T_m$. Although these correlations are not exact, they are as good as is found in the empirical relationships for metals.

(viii) Nature of the Diffusion Process in Naphthalene and Anthracene.

The two main features of the diffusion study reported here are (a) the decrease in diffusion coefficient with increasing perfection of the crystal, and (b) the large values of the Arrhenius parameters. A theory of diffusion in naphthalene and anthracene must attempt to explain both of these facts.

Alteration of diffusion coefficients with the state of the specimen has been reported in alkali halides[18,132,133], metals,[131] and semiconductors[6,13]. Good correlations between diffusion enhancement, strain,[131] and dislocation density[18] have been found. Despite the demonstrable influence of dislocations, bulk kinetics may be followed.[18,131,132].

Harrison[135] has shown how dislocations may act to increase the measured diffusion coefficient without altering the dependence on bulk kinetics. Where the scale of the dislocation network is small compared to the diffusion distance, the diffusing particles will have wandered sufficiently far to have migrated in and left a large number of dislocations. The particles will "see" a single diffusion coefficient representing the combined effects of bulk and dislocation diffusion. There will be no marked concentration differences between bulk and dislocations, and Fick's law will appear to be obeyed.

Another possibility is that the concentration of lattice imperfections is disturbed by the presence of a dislocation. In that case, where the number of bulk defects is altered but not their nature, the rate of diffusion may be changed without altering the activation energy.

There is some evidence in molecular solids for enhancement of mobility in dislocations.[136,137] Jarnagin and Sherwood[114] have shown that there is rapid diffusion down dislocations in anthracene, but that the mass transported by this method is very small in pure, annealed crystals. In the present work it has been demonstrated that this rapid diffusion process is extremely small, perhaps absent, in naphthalene, from which it seems unlikely that dislocation diffusion is playing a major role in single crystal diffusion in this substance.

Conductivity studies on anthracene and naphthalene have shown that various types of defect may be present.[8,138,139] Defects of a physical type, primarily introduced during growth of the crystal, have been found;[140] these defects are annealable. Other non-annealable defects have been postulated. Mechanical and other imperfections play an important role in processes involving excited states in naphthalene single crystals,[141] and studies[142] of the fluorescence spectrum of naphthalene has led to the recognition of characteristically disturbed regions of the crystal. There is thus considerable evidence of a defect structure in naphthalene and anthracene possibly consisting of "disturbed" regions in the lattice and possibly introduced during growth.

The organic crystals used in this study were grown from the melt by the Bridgmann method, a technique which requires a sharp temperatur gradient. It is possible, therefore, that defects present on solidification are trapped. These quenched-in defects would be annealable resulting in a diminution of the diffusion coefficient in an annealed crystal compared with the same crystal unannealed. This was exactly the behaviour observed. The energy for diffusion found in such crystals would probably be the energy for migration alone, but in well-annealed crystals the energy of formation may become a factor. If this is the case E should increase with annealing. The presence of dopant would by the same reasoning lead to an increase in the number of imperfections and a decrease in E. Although the evidence in this investigation is not decisive it is possible that

some such mechanism is operative. It is also possible that two kinds of defect are responsible for diffusion, one frozen-in, and a second intrinsic to the lattice and present in equilibrium concentrations. The annealing-out of the former would lead to a decrease in D with the latter's role increasing as the concentration of non-equilibrium defects decreased. Both the decrease in D and the probable increase in E then become understandable. A decrease in E in doped crystals is also explainable on this basis but D in doped crystals would be expected to be higher than was in fact found.

The changes in D from crystal to crystal are believed by the author to be caused by some such process as described above. It does not, however, explain why D_o and E should be so large. This matter has already been partially dealt with in discussion of the Arrhenius parameters but it is worthwhile considering whether it is likely that some large-scale defect of a cluster-type may be either frozen into the crystal, or present as an equilibrium defect, or both. From studies[143] of "premonitory" phenomena (i.e., pre-melting and pre-freezing effects) it has been suggested that lattice flaws may re-group into a co-operative system, a theory which has received some support from X-ray scattering measurements on naphthalene.[144] This is somewhat different from either a relaxon or a relaxed vacancy but is a phenomenon of a similar type. Large entropy contributions are likely from any of these imperfections. It is also possible that disordered clusters of molecules will be trapped into the solid on rapid freezing. Such clusters are known to be present in many melts and to increase in concentration as the freezing-point is approached.[145,146] These "non-crystallisable clusters"[146] in the solid could be considered either as molten regions or as disordered regions. If the defects were molten regions the entropy term would be expected to be even higher than was found. If the disordered region involves more

than two or three molecules it will appear isotropic to the lattice and diffusion anisotropy will be small or absent.

Both the variability of D and the high values of D_o and E are understandable in the light of this explanation. It is not possible as yet to decide whether the defect is a relaxion, or a disordered region, or a relaxed vacancy involving nearest and next-nearest neighbours. In any case, it appears to the writer that the three terms are not describing unrelated phenomena but merely different degrees of lattice disorder. The term "disordered region" can be used to cover all three possibilities. Such a disordered region will have a high entropy content and hence a high D_o and diffusion will occur by co-operative movements of more than one molecule leading to a high value of E.

(ix) Conclusion.

Aromatic hydrocarbons can be purified by the methods described and good single crystals of the material grown. The diffusion coefficients of the crystals can be measured and their variation with temperature determined.

Diffusion in naphthalene and anthracene is an extrinsic process with high values of the Arrhenius parameters. The diffusion coefficient decreases with increasing perfection of the crystal, and the Arrhenius parameters increase with increasing perfection. Dopants decrease both D_o and E. Diffusion anisotropy is either very small or absent. A Fisher analysis of diffusion in polycrystalline naphthalene also gives high values for the Arrhenius parameters.

The diffusion results can be explained in terms of lattice defects consisting of disordered regions of about 8 - 9 molecules. The defects may be frozen in during crystal growth.

(x) Future Work.

The two chief requirements for an understanding of the diffusion processes in organic solids are (a) more data, and (b) identification of the defect responsible for diffusion.

To obtain data on a wide variety of solids a rapid method of measuring diffusion coefficients would be a great advantage. The author believes that development of the vapour exchange method may lead to its more ready application to organic solids. With this method, not only would measurements be quicker and easier, but it would be possible to measure smaller diffusion coefficients than is possible with the tracer-sectioning technique. This would be a very important advantage since diffusion coefficients in highly perfect organic crystals are probably very small. Only when a large number of measurements have been made will it be possible to generalise about the defect nature of molecular solids.

Several types of measurement are likely to yield information about the nature of the defect responsible for diffusion. If the defect is a fairly extensive disordered region direct observation by an X-ray or allied technique may be possible. Light-scattering experiments should also be useful. Accurate measurements of density, expansivity, and other physical properties should reveal differences between highly imperfect and highly perfect crystals of the same material. The variation of these properties with temperature and comparison with the "ideal" value of the properties should help to establish the size and physical nature of the defect. Further annealing experiments should also help. If the imperfection is quenched in, variations of diffusion coefficient with crystal growth rate and temperature gradient should be apparent.

Once sufficient data have been collected and the defect identified it will be profitable to investigate the finer details of the defect structure of organic solids.

REFERENCES.

REFERENCES.

1. J.N. Sherwood and S.J. Thomson, Trans. Faraday Soc., 56, 1443 (1960).
2. C.H. Lee, H.K. Kevorkian, P.J. Reucroft, and M.M. Labes, J. Chem. Phys., 42, 1406 (1965).
3. K. Lark-Horovitz and V.A. Johnson (Eds.), "Solid State Physics" (Academic Press, N.Y., 1959).
4. H. Morawetz, "Physics and Chemistry of the Organic Solid State", Eds. D. Fox, M.M. Labes, and A Weissberger (Interscience, N.Y., 1963).
5. R.A.W. Hill, "Reactivity of Solids", Ed. J.H. de Boer (Elsevier, Amsterdam, 1961).
6. B.I. Boltaks, "Diffusion in Semiconductors" (Infosearch, Ltd., London, 1963).
7. H. Kallman and M. Silver (Eds.), "Symposium on Electrical Conductivity of Organic Solids" (Interscience, N.Y., 1961).
8. A.A. Kazzaz and A.B. Zahlan, Phys. Rev., 124, 90 (1961).
9. H. Morawetz, J. Poly. Sci., Part C, No. 1, 1963.
10. A.I. Kitaigorodskii, "Organic Chemical Crystallography", (Consultants Bureau, N.Y., 1961).
11. A.I. Kitaigorodskii, and R.M. Myasnikova, Soviet Physics - Crystallography, 5, 230 (1960).
12. Roberts-Austen, Phil. Trans, 187A, 393 (1896).
13. D. Lazarus, and B. Okkerse, Phys. Rev., 105, 1677 (1957).
14. C. Leymonie, "Les Traceurs Radioactifs en Metallurgie Physique" (Dunod, Paris, 1960).
15. J. Steigman, W. Shockley, and F.C. Nix, Phys. Rev., 56, 13 (19
16. R.A.W. Haul and L.H. Stein, Trans. Faraday Soc., 51, 1280 (1955).
17. W.J. Klimecki and J.N. Sherwood, Unpublished work, University of Strathclyde, 1964.
18. L.W. Barr, I.M. Hoodless, J.A. Morrison, and R. Rudham, Trans. Faraday Soc., 56, 697 (1960).

19. E.R. Andrew, "Report on the Conference on Defects in Crystalline Solids, Univ. of Bristol, 1954" (The Physical Soc. London, 1955).

20. E.R. Andrew and P. Allen, Paris Conference on Motion and Phase Changes in Molecular Solids, 1965. (To be published in J. Chimie Physique).

21. J.G. Aston, "Physics and Chemistry of the Organic Solid State", Eds. D. Fox, M.M. Labes, and A. Weissberger (Interscience, N.Y 1963).

22. N.H. Nachtrieb, E. Catalano, and J.A. Weil, J. Chem. Phys., 20, 1185 (1952).

23. C.P. Slichter, "Defects in Crystalline Solids" (The Physical Society, London, 1955).

24. G.M. Hood and J.N. Sherwood, Paris Conference on Motion and Phase Changes in Molecular Solids, 1965 (To be published in J. Chimie Physique).

25. E. Cremer, Z. Phys. Chem., B39, 445 (1938) (Quoted in Ref. 31)

26. L.A.K. Stavely, "Ann. Rev. Phys. Chem. 1962", 13, 351.

27. R. Marx, Paris Conference, 1965 (See Ref. 24, above.).

28. A. Ascoli, M. Asdente, E. Germagnoli, and A. Manara, J. Phys. Chem. Solids, 6, 59 (1958).

29. R.E. Larsen and A.C. Damask, Acta Metallurgica, 12, 1131 (1964)

30. A. Glasner and R. Reisfeld, J. Phys. Chem. Solids, 18, 345 (1961

31. W. Jost, "Diffusion" (Academic Press, N.Y., 1960).

32. J. Crank, "Mathematics of Diffusion" (Clarendon Press, Oxford, 1956

33. W.E. Garner, "Chem. of the Solid State" (Butterworths, London, 1955).

34. C.S. Fuller and J.M. Whelan, J. Phys. Chem. Solids, 6, 173 (195

35. Ling Y. Wei, J. Phys. Chem. Solids, 18, 162(1961).

36. J.D. Keys and H.M. Dutton, J. Phys. Chem. Solids, 24, 563 (196

37. A.J. Mortlock, Acta Metallurgica, 12, 675 (1964).

38. W. Biermann, F.R. Winslow, and T.S. Lundy, Acta Metallurgica, 12, 328 (1964).

39. N.H. Nachtrieb and G.S. Handler, J. Chem. Phys., 23, 1187 (195

40. H.A. Resing, J. Chem. Phys., 37, 2575 (1962).

41. L.A. Girifalco, "Atomic Migration in Crystals" (Blaisdell Publ. Co., N.Y., 1964).

42. A.W. Lawson, S.A. Rice, R.D. Corneliussen, and N.H. Nachtrieb J. Chem. Phys., 32, 447 (1960).

43. C. Coston and N.H. Nachtrieb, J. Phys. Chem., 68, 2219 (1964).

44. A.D. Le Claire, Acta Metallurgica, 1, 438 (1953).

45. R. Fieschi, G. Nardelli, and A Repanai, Phys. Rev., 123, 141(196

46. G. Nardelli et al., Nuovo Cimento, 18, 1053 (1960).

47. A.D. Le Claire, Brit. J. Appl. Phys., 13, 433 (1962).

48. A. Borne, G. Boato, and M. De Paz, Il Nuovo Cimento, 24, 1179 (1962).

49. W.M. Yen and R.E. Norberg, J. Chem. Phys., 131, 269 (1963).

50. C. Zener, J. Appl. Phys., 22, 372 (1951).

51. R.B. Cuddeback and H.G. Drickamer, J. Chem. Phys., 19, 790 (1951).

52. J.R. Hulett, Quarterly Reviews, 18, 227 (1964).

53. R.H. Doremus, J. Chem. Phys., 34, 2186 (1961).

54. C. Zener, "Imperfections in Nearly Perfect Crystals" (John Wiley and Sons, N.Y., 1952).

55. R.H. Hochstrasser, Radiation Research, 20, 107 (1963).

56. R.E. Hoffman, D. Turnbull, and E.W. Hart, Acta Metallurgica, 3, 417 (1955).

57. E.W. Hart, Bull. Amer. Phys. Soc., ser.II., 2, 145 (1957).

58. H.W. Schamp and E. Katz, Phys. Rev., 94, 828 (1954).

59. Naboikin et al., "Growth of Crystals", Vol. 3, Eds. A.V. Shubniko and N.N. Sheftal (Consultants Bureau, N.Y., 1962).

60. G.B. Belikova and L.M. Belyaev, "Growth of Crystals"(see Ref. 5

61. V.G. Formin et al., Soviet Physics-Crystallography, 2, 172, 178 (1964).

62. G.J. Sloan, "Phys. and Chem. of the Organic Solid State" (see Ref. 21, above).

63. C.D. Thurmond, "Methods of Experimental Physics", 6A, Eds. K. Lark-Horovitz and V.A. Johnson (Academic Press, N.Y., 1959)

64. P.H. Egli, L.R. Johnson, and W. Zimmerman, "Methods of Experimental Physics" (see Ref. 63).

65. N.L. Parr, "Zone Refining" (Royal Institute of Chemistry Monograph No. 3, 1957).

66. W.G. Pfann, J. Metals, 4, 747 (1952).

67. E.F.G. Herrington, R. Handley, and A.J. Cook, Chem. and Ind., 1956, 292.

68. W.R. Wilcox, R. Friedenberg, and N. Black, Chem. Revs., 64, 187 (1964).

69. J.A. Burton, R.C. Prim, and W.P. Slichter, J. Chem. Phys., 21, 1987 (1953).

70. P. Sorensen, Chem. and Ind., 1959, 1593.

71. G.J. Sloane and N.H. McGowan, Rev. Sci. Instr., 34, 60 (1963).

72. E.T. Knypland K. Zielenski, J. Chem. Ed., 40, 352 (1963).

73. A.R. McGhie, University of Strathclyde, Private communication.

74. H.M. Hawthorn, University of Strathclyde, Private communication.

75. J.H. Beynon and R.A. Saunders, Brit. J. Appl. Phys., 11, 128 (1960).

76. R.A. Friedel and M. Orchin, "Ultraviolet Spectra of Aromatic Hydrocarbons" (John Wiley and Sons, Inc., N.Y., 1951).

77. J. N. Sherwood, Private communication.

78. G.J. Sloan, "Physics and Chemistry of the Organic Solid State", Vol. 1 (see Ref. 4 above).

79. G.F. Reynold, "Phys. and Chem. of the Organic Solid State" (see Ref. 4 above).

80. B. Honigmann, Z. fur Elektrochem., 58, 322 (1954).

81. H.E. Buckley, "Crystal Growth" (John Wiley and Sons, Inc., N.Y 1951).

82. G.H. Nancollas and N. Purdie, Quarterly Reviews, 18, 1 (1964).

83. R. Handley and E.F.G. Herrington, Chem. and Ind., 1956, 304.

84. H.M. Hawthorn, A.R. McGhie, and J.N. Sherwood, University of Strathclyde, To be published.

85. P.W. Bridgmann, Proc. Am. Acad. Arts Sci., 60, 305 (1905).

86. D.C. Stockbarger, Rev. Sci. Instr., 7, 133 (1936).

87. M. Tanenbaum, "Methods of Experimental Physics", 6A (see Ref. 63 above).

88. J.N. Sherwood and S.J. Thomson, J. Sci. Instr., 37, 242 (1960).

89. I.V. Stepanov and M.A. Vasileva, "Growth of Crystals", Vol. 3 (see Ref. 59, above).

90. E. Billig, Proc. Roy. Soc., A235, 37 (1956).

91. A.A. Petrauskas and F. Gaudry, J. Appl. Phys., 20, 1257 (1949).

92. G. Tammann, "Lehrbuch der Metallographie" (Voss, Leipzig, 1923).

93. G.M. Hood and J.N. Sherwood, Brit. J. Appl. Phys., 14, 215 (1963).

94. J.N. Sherwood, University of Strathclyde, Unpublished work.

95. K.T.B. Scott, S.K. Hutchison, and R. Lapage, Report No. 0-4/53, U.K. Atomic Energy Authority, 1953.

96. S. Kyropoulos, Z. Anorg.U. Allgen. Chem., 154, 308 (1926).

97. F.R. Lipsett, Can. J. Phys., 35, 284 (1957).

98. V.R. Matejec, Berichte der Bunsengesellschaft fur Phys. Chem., 68, 964 (1964).

99. C. Montescu and A.T. Balaban, Canadian J. Chem., 41, 2120 (1963).

100. A.N. Winchell "The Optical Properties of Organic Compounds", (The University of Wisconsin Press, 1943).

101. G.M. Hood, Ph.D. Thesis, University of Glasgow, 1963.

102. C.T. Tomizuka, "Methods of Experimental Physics", Vol. 6A (see Ref. 63 above).

103. G.A. Shirn, E.S. Wadja, and H.B. Huntington, Acta Metallurgica, 1, 513 (1953).

104. J.-P. Renouf, Theses, L'Universite de Lyon, 1964.

105. G. Friedlander and J.W. Kennedy, "Introduction to Radiochemistry" (Chapman and Hall, London, 1949).

106. Handbook of Chemistry and Physics, 43rd Edition, (Chemical Rubber Publ. Coy., Cleveland, Ohio, 1961).

107. D.S. Tannhauser, J. Appl. Phys., 27, 662 (1956).

108. P.G. Shewmon, "Diffusion in Solids" (McGraw-Hill, N.Y., 1963).

109. A.C. Damask and G.J. Dienes, "Point Defects in Metals" (Gordon and Breach, London, 1963).

110. J. E. Bauerle and J.S. Koehler, Phys. Rev., 107, 1493 (1957).

111. A.D. Le Claire, Conf. on Diffusion and Mass Transport in Solids, Reading, 1962, Paper 9. Brit. J. Appl. Phys., 13, 433 (1962).

112. J.C. Fisher, J. Appl. Phys., 22, 74 (1951).

113. R.T. Whipple, Phil. Mag. 45, 1225 (1954).

114. R.C. Jarnagin and J.N. Sherwood, Organic Crystal Symposium, Univ. of Chicago, 1965.

115. K. Hauffe, "Realktionem in und an festen Stoffen" (Berlin, 1955). Quoted in Ref. 6.

116. Suga and Syuzo, J. Phys. Chem. Solids, 24, 330 (1963).

117. H. Sware and R. Marx, J. Chim. Phys., 57, 680 (1960).

118. M. Bloom, Physica, 23, 767 (1957).

119. E.R. Andrew and R.G. Eades, Proc. Roy. Soc., 216A, 398 (19

120. F.A. Rushworth, J. Phys. Chem. Solids, 18, 77 (1960).

121. N.N. Semenov, Pure and Appl. Chem., 5, 350 (1962).

122. J.E. Anderson and W.P. Slichter, J. Chem. Phys., 41, 1922 (19

123. D.F. Holcomb and R.E. Norberg, Phys. Rev., 98, 1074 (1955).

124. J.M. Robertson, Rev. Mod. Phys., 30, 155 (1958).

125. D.W.J. Cruickshank, Rev. Mod. Phys., 30, 163 (1958).

126. S.C. Abrahams, J.M. Robertson and J.G. White, Acta Cryst, 2, 133 (1949).

127. N.H. Nachtrieb and G.S. Handler, Acta Met., 2, 797 (1954).

128. P.Flubacher, A.J' Leadbetter, and J.S. Morrison, Proc. Phys. Soc., 78, 1449 (1961).

129. A.J.E. Foreman and A.B. Lidiard, Phil. Mag., 8, 97 (1963).

130. R.H. Beaumont, H. Chihara, and J.A. Morrison, Proc. Phys.So 78, 1462 (1961).

131. C.H. Lee and R. Maddin, Trans AIMME, 215, 397 (1959).

132. J.F. Laurent and J. Benard, J. Phys. Chem. Solids, 7, 218 (19

133. J. Cabane, J. Chim. Phys., 59, 1135 (1962)

134. H. Widmer, Phys. Rev., 125, 30 (1962).

135. L.G. Harrison, Trans Faraday Soc., 57, 1191 (1961).

136. P.H. Geil, "Polymer Single Crystals" (Interscience, N.Y., 1963).

137. R. Bensasson, A. Dworkin, and R. Marx, J. Poly. Sci., Part C No. 4, 1963, p.881.

138. J.J. Brophy and J.W. Buttrey (Eds.), "Organic Semiconductors" (Macmillan, N.Y., 1962).

139. R.C. Jarnagin, J. Gilliland, J.S. Kim, and M. Silver, J. Chem. Phys., 39, 573 (1963).

140. S.Z. Weisz, R.C. Jarnagin, M. Silver, M. Simhony, and J. Balberg, J. Chem. Phys., 40, 3365 (1964).

141. S.Z. Weisz, A.B. Zahlan, J. Gilreath, R.C. Jarnagin and M. Silver, J. Chem. Phys., 41, 3491 (1964).

142. R. Schnaithmann and H.C. Wolf, Organic Crystal Symposium, Univ. of Chicago, 1965.

143. J.W.H. Oldham and A.R. Ubbelohde, Proc. Roy. Soc., A176, 50 (1940).

144. M.L. Canut, and J.L. Amaros, J. Phys. Chem. Solids, 21, 146, (1961).

145. E. McLaughlin and A.R. Ubbelohde, Trans Faraday Soc., 56, 988 (1960).

146. A.R. Ubbelohde, "Liquids", Ed. by T.J. Hughel (Elsevier, Amsterdam, 1965).

147. M.J. Moroney, "Facts from Figures", (Penguin Books, Harmondsworth, Middlesex, 1960).

APPENDIX.

Calculation of Diffusion Coefficients.

APPENDIX

Calculation of Diffusion Coefficients.

The count-rate is the number of counts divided by the time of observation. If R_t is the count-rate of the sample including background, and R_B the background count-rate alone, then $R_s = R_t - R_B$ is the count-rate for the sample alone. The specific activity, A, is R_s divided by W, where W is the weight of sample. The standard deviation, S, is given by $S_s = (S_t^2 + S_B^2)^{\frac{1}{2}}$, where $S = (R/t)^{\frac{1}{2}}$. Subscripts have the same meaning as before; t is the time of observation of the count.

Run 17B is taken as an example. All slices are 10 microns thick. W is in mg., time in secs., R and S in counts per sec., and A in c.p.s per mg. The distance, d, from the centre of the slice to the surface is quoted in microns and d^2 in square microns. K is used as an abbreviation for 1,000.

Background count = 8027 in 50Ksecs., therefore R_B = 0.161c.p.s.

Slice	W	Count	time	R_t	S_s	A	log A	d^2
1	0.850	10K	31.8	314.5	3.1	366.3	2.564	25
2	0.613	10K	94.5	105.8	1.1	172.3	2.236	225
3	0.759	10K	419.5	23.84	0.24	31.20	1.495	625
4	0.786	10K	5059	1.98	0.02	2.32	0.366	1,226
5	0.561	6.7K	13636	0.49	0.01	0.59	-0.229	2,025
6	1.136	2.3K	3915	0.59	0.01	0.38	-0.420	3,025
7	0.854	5.3K	9522	0.56	0.01	0.47	-0.328	4,225
8	0.973	2K	3449	0.58	0.01	0.43	-0.366	5,625
9	0.768	2K	4181	0.48	0.01	0.42	-0.377	7,225
10	0.951	1K	1944	0.51	0.02	0.37	-0.432	9,025

Log A was plotted against d^2. A straight line with a typical diffusion tail was obtained. The tail, consisting of slices 6 - 10, was

extrapolated backwards to cut the logA axis and values of log A_T read off at values of d^2 corresponding to slices 1 - 5. A_T is the activity due to the tail. A_T was subtracted from A to give corrected values of the specific activity due to bulk diffusion alone, as follws

Slice	A_T	$A-A_T$	log $(A-A)_T$
1	0.57	365.7	2.563
2	0.56	171.7	2.235
3	0.55	30.65	1.486
4	0.54	1.78	0.250
5	0.52	0.07	-1.155

Log $(A-A_T)$ was re-plotted against d^2. A straight line was 147
obtained whose slope, m, was determined by the method of least squares. The diffusion coefficient was calculated from the time of diffusion and m $cm.^{-2}$ as described on page 90.